SESSION VI

OFF-GAS TREATMENT

Tuesday, August 8, 1978
CHAIRMEN: R. R. Bellamy, R. Brown

OPENING REMARKS OF SESSION CHAIRMAN:

BELLAMY: We will be hearing papers in this session concerning the treatment of offgases from fuel reprocessing plants. We expect the use of fuel reprocessing plants to become larger as the nuclear industry expands. We hope that will be the case for the future. The contaminants of concern that we will hear about this afternoon include gaseous fission products (iodine-129, tritium, carbon-14), gaseous NO_x compounds, carbon-14 as CO_2, tributyl phosphate and tributyl phosphate vapors. We will also hear a paper that will discuss a technique for the measurement of these offgas pollutants.

BURNER AND DISSOLVER OFF-GAS TREATMENT IN HTR FUEL REPROCESSING

H. Barnert-Wiemer
M. Heidendael
H. Kirchner
E. Merz
G. Schröder
H. Vygen
Kernforschungsanlage Jülich GmbH
Jülich/Germany

Abstract

In the reprocessing of HTR fuel essentially all of the gaseous fission products are released during the head-end treatment, which includes burning of the graphite matrix and dissolving of the heavy metallic residues in THOREX reagent.

Three facilities for off-gas cleaning are described, the status of the facility development and test results are reported.

Hot tests with a continuous dissolver for HTR-type fuel (throughput 2 kg HM/d) with a closed helium purge loop have been carried out. The goals of these experiments were two-fold:

- the complete dissolver unit was to be tested before a similar one is built into the JUPITER facility
- the composition and some steps of an off-gas cleaning system were to be checked.

Preliminary results of these experiments are reported.

I. Facility development

In the Institute for Chemical Technology of KFA Jülich three facilities for off-gas cleaning during reprocessing of HTR-fuel are being developed:

- the AKUT II-facility for the burner off-gas
- the KRYOSEP I-facility for the off-gas from a discontinuous dissolver
- the KRYOSEP II-facility for the off-gas from a continuous dissolver with a closed purge gas loop.

The AKUT II-facility

The flowsheet of the AKUT II-facility (Fig. 1), consisting of the consecutive steps

filtering
catalytic burning
tritium removal
compression and liquefaction
distillation

has already been described previously [1].

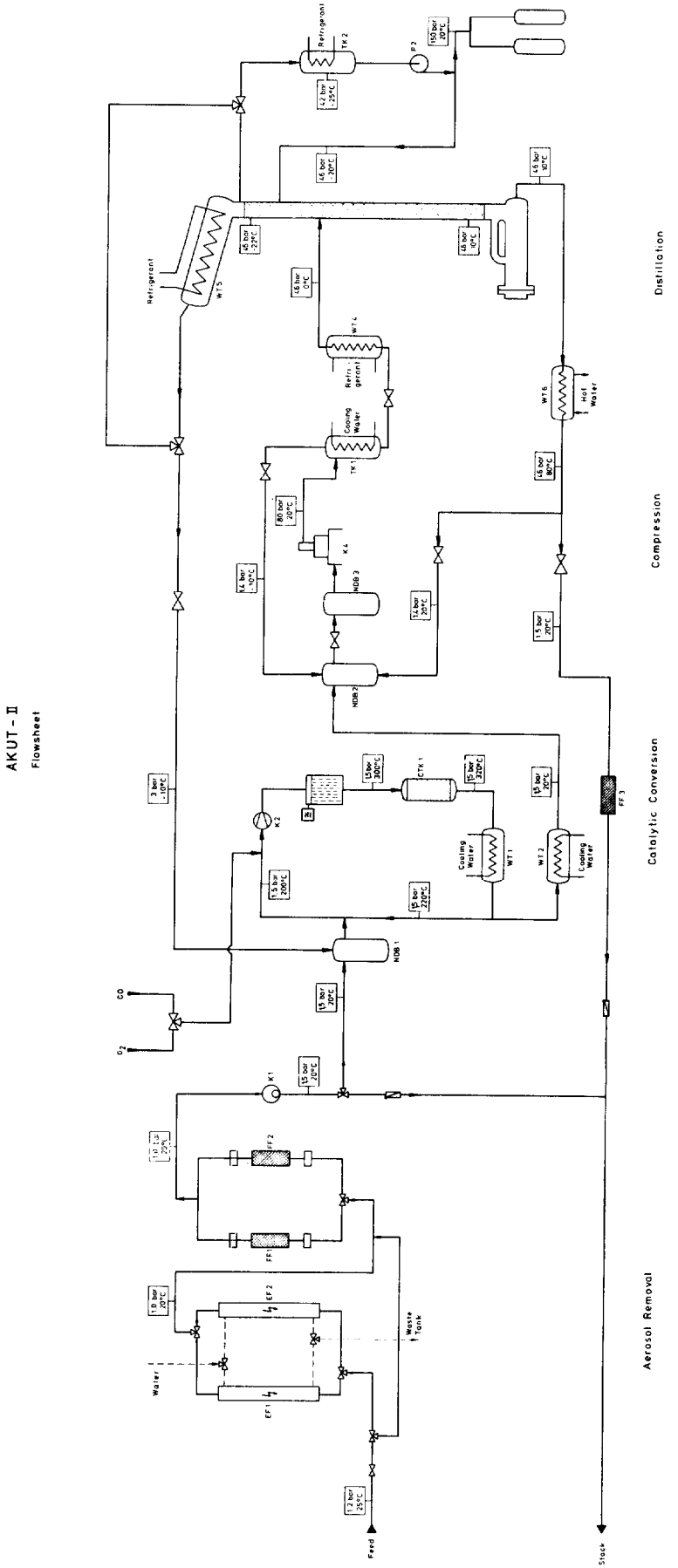

Fig. 1: Flowsheet of the AKUT II-facility

One of the electrostatic precipitators [1] is at this time being tested in the laboratory to check the influence of the Kr-85 concentration on the efficiency. The throughput is varied between 5 and 40 m^3/h and the Kr-85 concentration between 0,5 and 25 Ci/m^3. The efficiency of the filter is determined by adding cesium aerosols with Cs-137 as tracer to the gas stream. In further experiments graphite dust (particle size < 5 µm) in varying amounts (1 to 10 g/m^3) is to be fed into the gas and the efficiency for graphite dust removal is to be evaluated.

The catalytic burning equipment (Fig. 2) has undergrone preliminary testing.

The off-gas from the JUPITER fluidized bed burner is at steady state expected to be 7,5 m^3/h consisting of CO_2 with 20 % CO. The maximum capacity of the catalytic burner is 10 m^3/h off-gas consisting of 100 % CO. To handle the wide range of possible off-gas compositions the off-gas is fed into a recycled gas stream whose throughput can be varied by means of a blower between 75 and 325 m^3/h according to the conditions of the off-gas. The catalyst bed contains 15,4 l of a palladium catalyst (0,1 % Pd on Al_2O_3) distributed in two 40 mm high layers. The catalyst can be operated at temperatures between 200 °C and 650 °C and space velocities up to 30 m^3/h per liter catalyst.

In the tests the CO-concentration was increased to 14 % in the feed gas of 5 m^3/h which resulted in a temperature increase in the catalyst bed from 250 °C to 281 °C, the recycle gas flow being 150 m^3/h. Behind the catalyst no CO was detected, but the O_2-concentration was 0,25 %. The tests were discontinued because of a leak in the blower. In future tests the main task will be to improve the facility control, mainly the response of the O_2 supply valves to the CO concentration.

No data are available on iodine poisoning of the catalyst. But since the J_2 concentration in the off-gas is below 1 ppm the supplier of the catalyst expects no difficulties.

The AKUT II-facility (Fig. 3) as a whole is expected to be ready for preliminary testing in late fall, with the exception of the tritium removal system for which laboratory testing still needs to be done.

The KRYOSEP I-facility

During the dissolution of the heavy metal ash the remainder of the gaseous fission products is released into the off-gas.

Since only 20 l/h dissolver off-gas are produced by the JUPITER reprocessing pilot plant, this off-gas is compressed and filled in gas cylinders till enough gas has been collected to operate the KRYOSEP I-facility which has a throughput of 5 m^3/h. KRYOSEP I consists of a pretreatment unit, a O_2/NO_x removal system and a cryogenic separation unit.

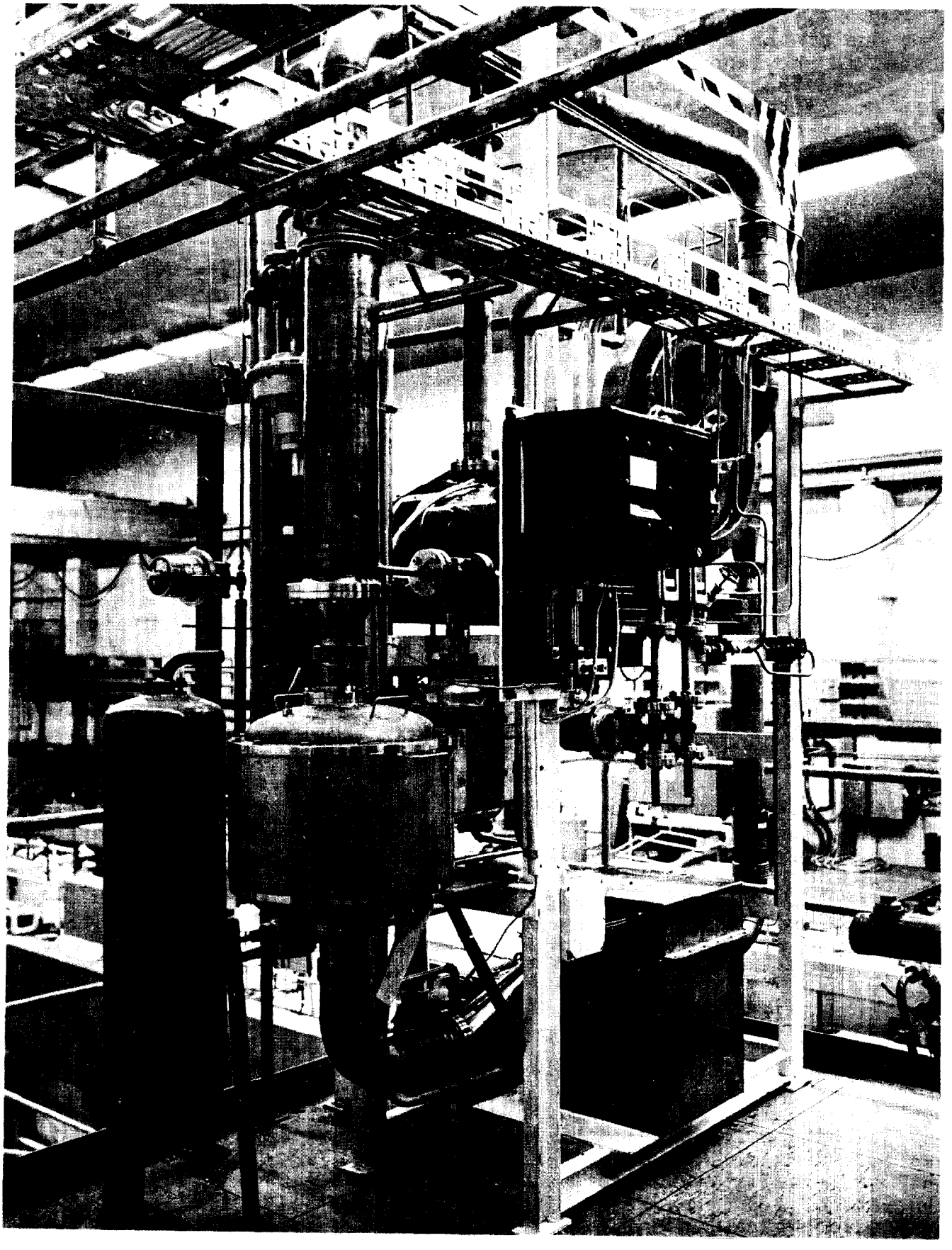

Fig. 2: The catalytic burning equipment of the AKUT II-facility

Fig. 3: View of the AKUT II-facility during assembly

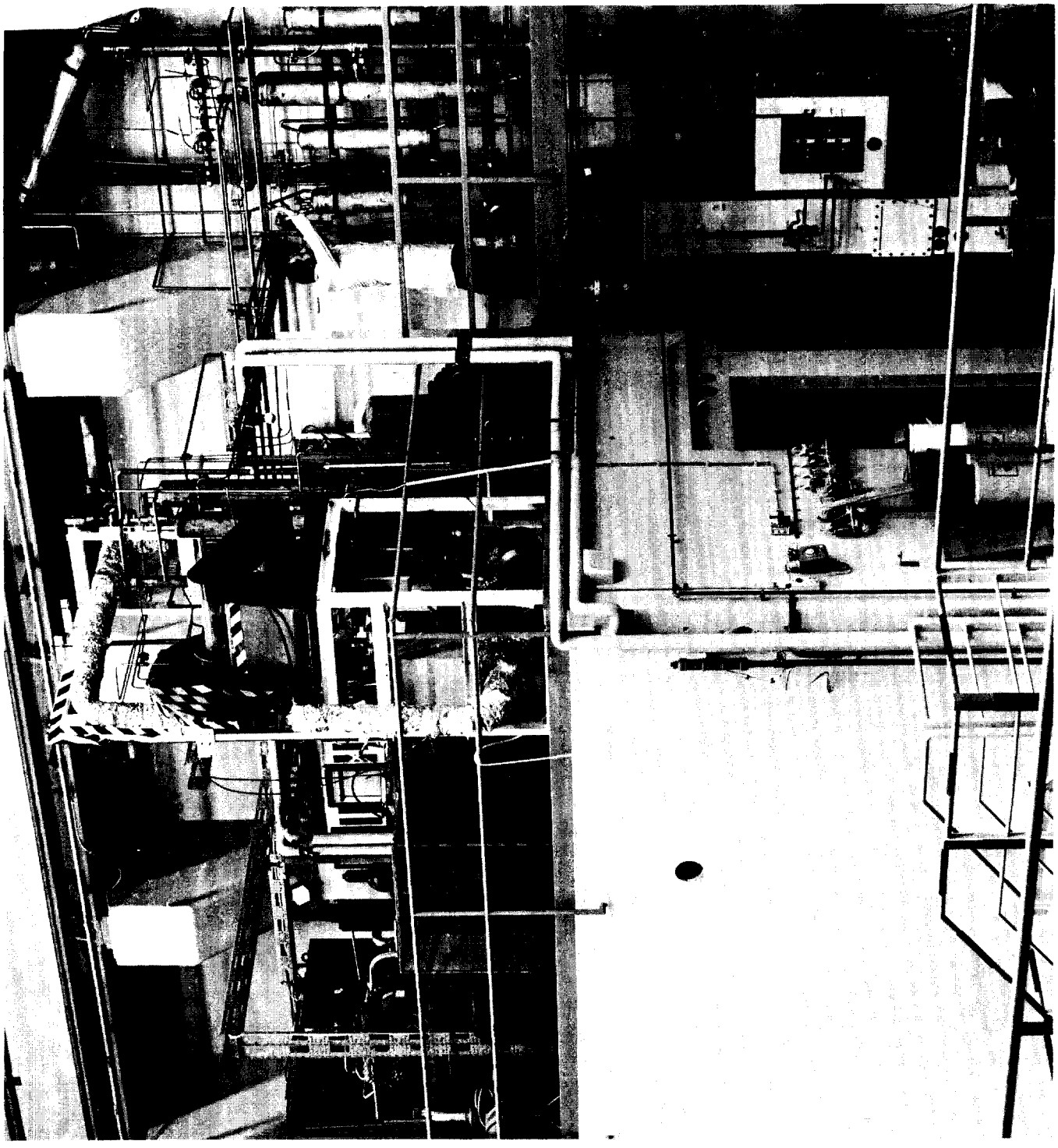

To prevent poisoning of the catalyst in the O_2/NO_x separation system iodine is removed quantitatively before the gas enters said system. This is achieved by fixation in two alternately operated filters filled with the sorption material AC-6120, an Ag-impregnated product on the basis of amorphous silicic acid.

The gas entering the O_2/NO_x removal system (Fig. 4) consists mainly of the following components:

N_2	:	76,5 %
O_2	:	20,6 %
NO_x	:	1,0 %
Ar	:	0,9 %
Xe	:	0,7 %
Kr	:	0,1 %.

To avoid the formation of ozone ($3\ O_2 \xrightarrow{h\nu} 2\ O_3$) in presence of a γ-radiation field and to exclude the latent risk of explosion when distilling liquid noble gas - oxygen mixtures, oxygen and nitrogen oxides are eliminated by reaction with hydrogen in the presence of a catalyst, whereby oxygen and nitrogen oxides are converted to elemental nitrogen, water and traces of ammonia. While direct conversion results in elevated temperatures of about 1100 °C, the same reaction takes place on precious metal catalyst at a temperature range of 200 - 300 °C. To operate outside the explosion limits, the relative high oxygen-content is lowered by feeding the off-gas into a recycle of oxygen free gas. Moreover, this dilution is necessary to avoid overheating of the catalyst, because each vol-% O_2 induces a rise of temperature in the catalyst bed of ~ 150 °C. A flow-sheet is shown in figure 5: NO_x-containing dissolver off-gas (5 m^3/h) is diluted by nitrogen which is recycled by a blower (K1) with a throughput of 65 m^3/h. Thereby the oxygen-content of the gas stream is decreased to about 2 vol-% O_2. The O_2-concentration given by a paramagnetic O_2-analyser, and the flow-rate given by a flow-meter control the hydrogen feed. Behind the catalyst bed (K.B.) the gas stream, primarily N_2, passes through a water-cooled condenser (WT1) to remove the water formed by the H_2-O_2-reaction. The surplus hydrogen (~ 2000 ppm) is subsequently removed by reaction with activated copper oxide (CuO-B1 or CuO-B2) and the water from that reaction is removed in a water-cooled heat exchanger (WT4). Before leaving the O_2/NO_x removal system the gas is dried by molecular sieves (MS-B1 or MS-B2) which also adsorb traces of impurities like CO_2, NO_2 and NH_3.

During cold tests it was found that the platinum catalyst caused nearly all of the NO_x to react with the hydrogen to form ammonia. Therefore laboraty tests are under way to find a catalyst suitable for O_2 and NO_x removal at the same time. Two ruthenium and one nickel catalyst are being tested at present.

The gas entering the cryogenic distillation unit (Fig. 6) where the separation of krypton and xenon from the gas stream and further purification of the xenon fraction is achieved, consists mainly of N_2, Ar, Xe and Kr.

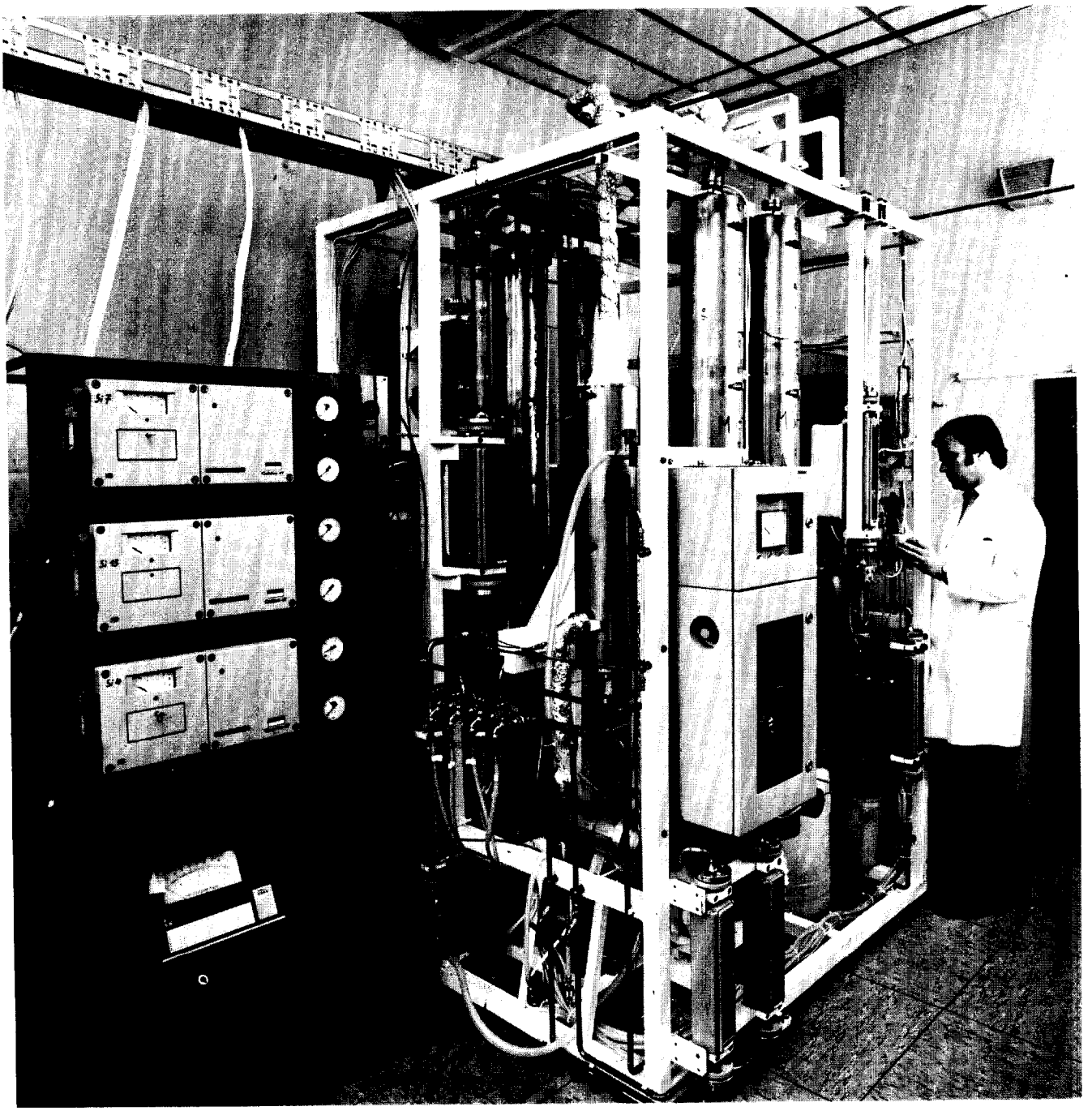

Fig. 4: View of the O_2/NO_x removal system

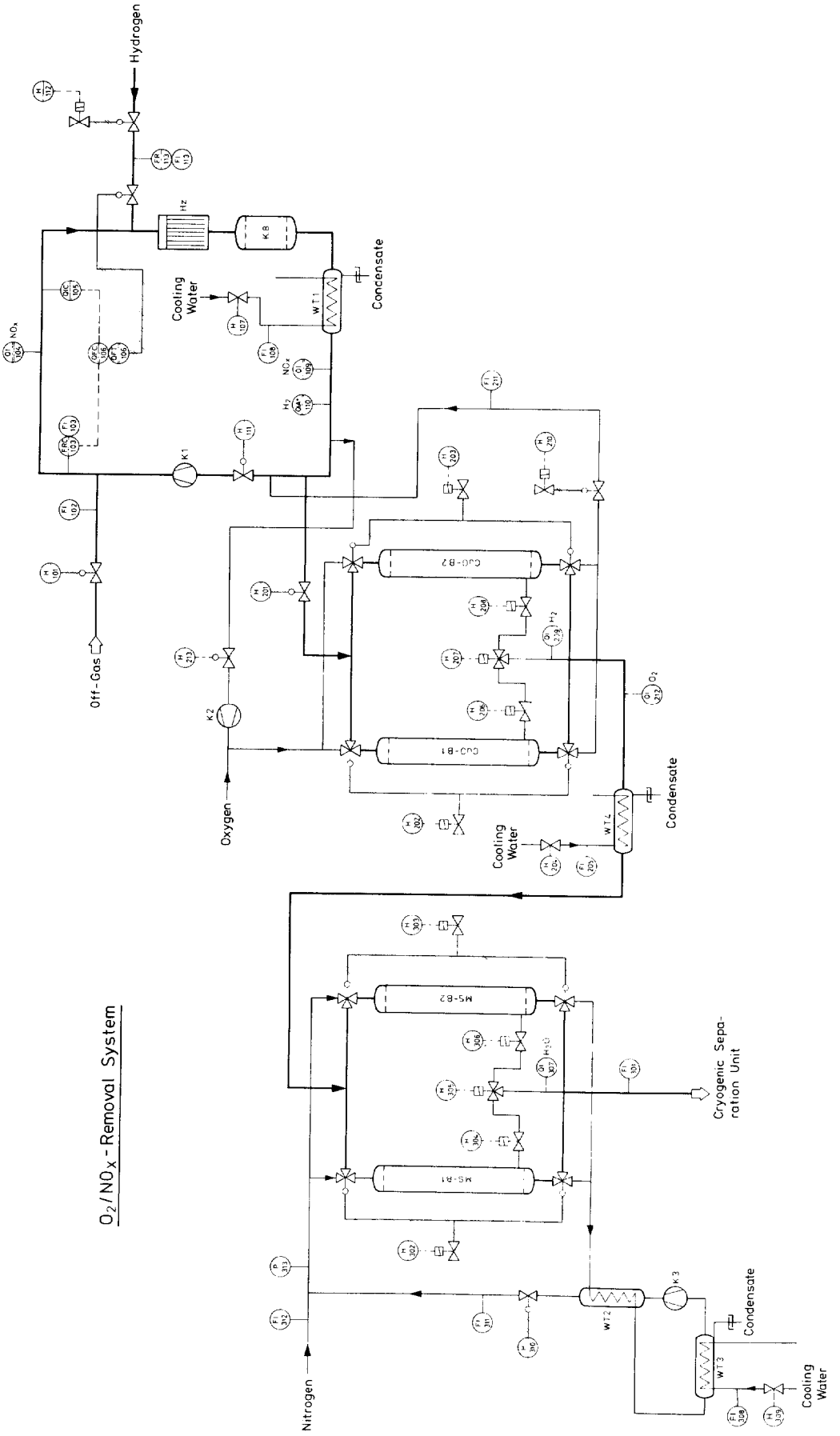

Fig. 5: Flowsheet of the O_2/NO_x removal system

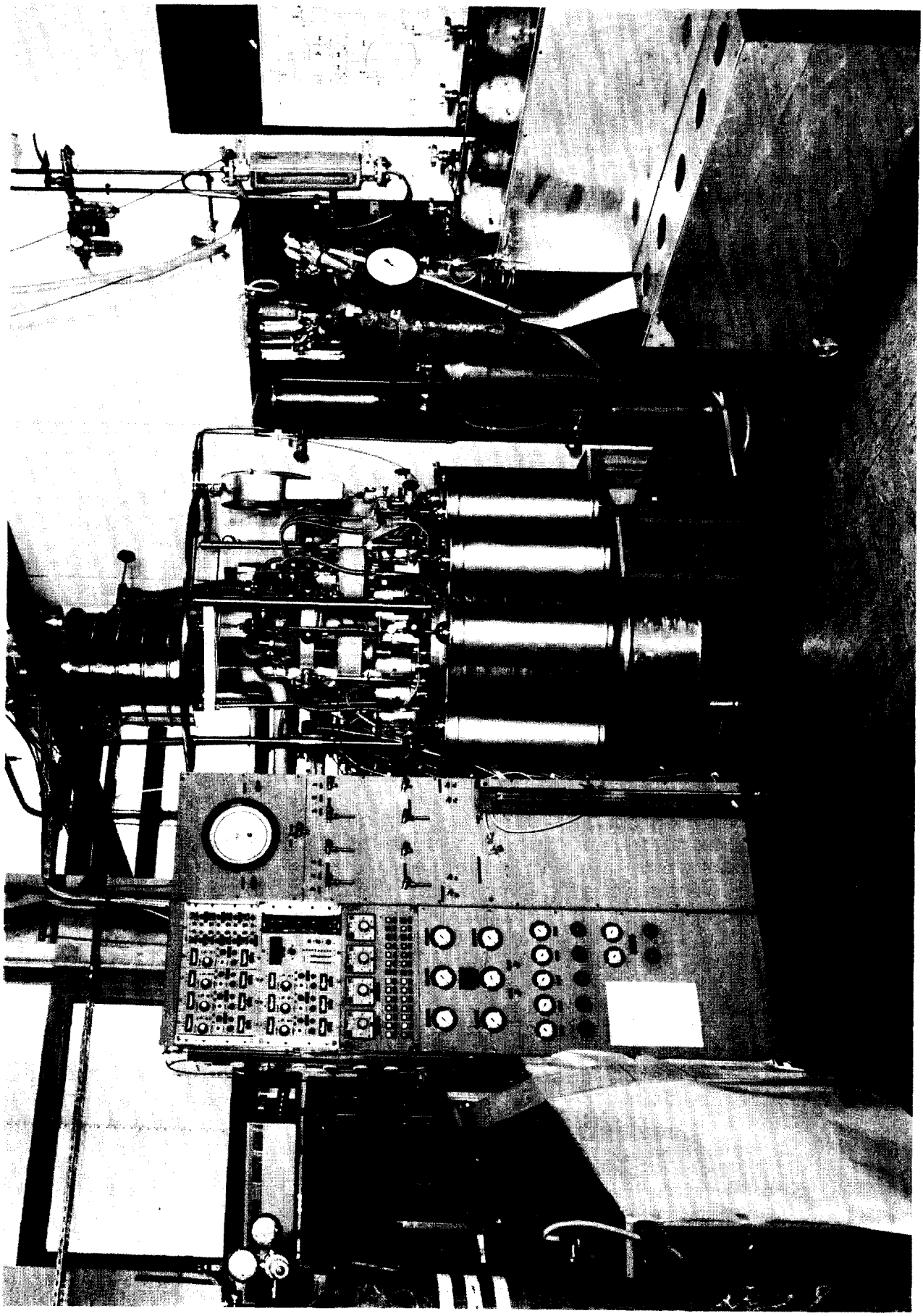

Fig. 6: View of the KRYOSEP I-facility

The components of the system are placed in a vacuum container (height: 3 m, diameter: 1 m) where a vacuum of 10^{-5} Torr is maintained.

Fig. 7 shows the flowsheet: Entering the cryogenic part of the separation unit the preconditioned gas stream passes a countercurrent heat-exchanger where it is precooled to 160 - 180 K by the effluent cold gas from the cooling system of the cold-traps.

In the upper part of two alternately operated cold-traps xenon is deposited at about 80 K in solid form adsorbing about 0,5 vol-% krypton. Simultaneously, the remaining gas components are liquified in the lower part of the Xe-separator and flow to a 200 l storage tank.

The liquified gas-mixture is fed by overpressure from the storage tank to the still. The column (height: 1600 mm, diameter: 38 mm) is packed with "Knitmesh Multifil" wire mesh which is similar in structure to Goodloe packing. At operating conditions the system pressure is 1,2 bar. The liquid levels in the reboiler and the 200 l storage tank are controlled by level indicators on the basis of capacity metering devices. Thermometry is achieved by resistance thermometers.

During operation an average rate of about 6 liters/h liquid enters the column. The decontaminated gas stream, primarily nitrogen, is discharged at the top of the column, while krypton is enriched in the bottom of the still. During the last two campaigns decontamination factors of $2 \cdot 10^3$ and $8 \cdot 10^3$ were achieved for krypton. The Kr-fraction, containing about 10 - 40 vol-% krypton is withdrawn batchwise from the bottom and filled in high-pressure steel cylinders.

To reduce the ultimate storage volume of the fission product noble gases or to get an extremely pure xenon for eventual industrial utilization Kr-85 contaminated xenon, previously deposited in the cold traps must be refined. This is done by batch distillation in the second column with the aim to obtain a Kr-85 content of < 3 µ Ci Kr-85 / m^3 xenon. Therefore 4,5 kg xenon-charges bottled in high-pressure steel cylinders are transferred periodically to the still (volume: 1,5 l liquid xenon) to remove the contaminant by boiling under total reflux. Krypton and small amounts of xenon discharged from the top of the column are recycled to the primary process gas stream. Decontaminated xenon is withdrawn from the bottom to be bottled in steel cylinders for further use.

Up to now the batch distillation has rendered only unsatisfactory decontamination factors of 10^6. To meet the specification of the purified xenon a decontamination factor better than $3 \cdot 10^8$ is necessary.

To reach this goal it is intended to add inactive Kr to the Xe-batch and repeat the distillation.

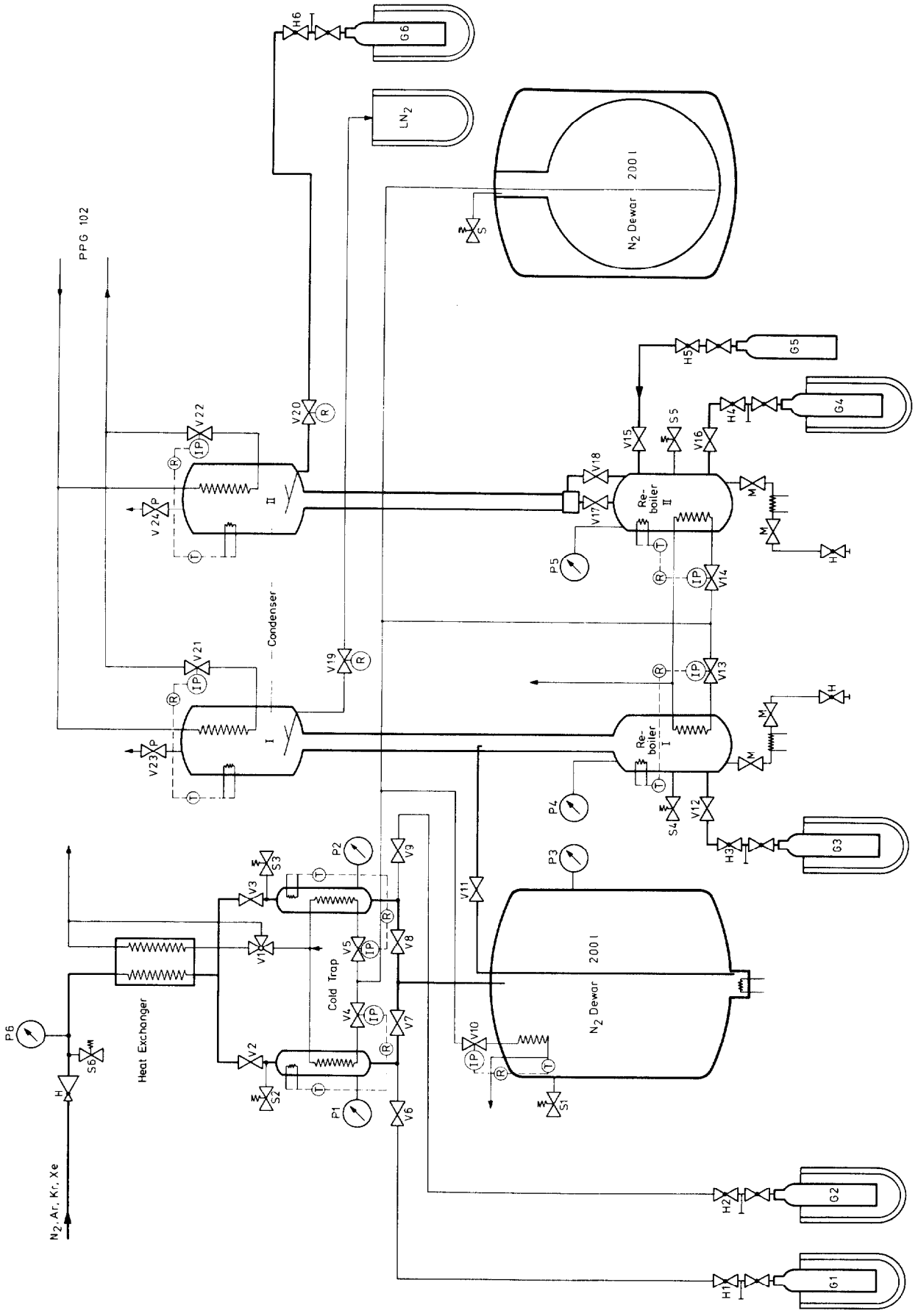

Fig. 7: Flowsheet of the KRYOSEP I-facility

The KRYOSEP II-facility

The KRYOSEP II-facility (Fig. 8) for cryogenic separation of Xe and Kr from the off-gas of a continuous dissolver with a closed helium-purge loop has the same pretreatment steps as the KRYOSEP I-facility, with the difference that only traces of O_2 (from inleaking air) have to be removed together with the NO_x. The facility has been described previously [2].

The KRYOSEP II-facility which is not intended for hot operation is at present being repaired and improved and is expected to be ready for start up in late fall.

II. Hot dissolver experiments

The dissolver (Fig. 9) is a round-bottomed in the lower part cylindrical, in the upper part conical stainless steel vessel with jackets for steam heating. The throughput is 2 kg HM/d.

The heavy metal ash is brought into the continuously operating dissolver (D 301) by an auger. The THOREX reagent is fed in near the bottom of the vessel. The fuel solution leaves the dissolver near the top and flows into the intermediate storage tank F 101. The concentration and the liquid level in the dissolver are measured by dip tubes. The helium from these measurements leaves the dissolver transporting the fission gases and the remainder of the NO_x and the water vapor which are not condensed in the heat exchanger D 201 to the off-gas cleaning facility (Fig. 10).

The radioactive components are semicontinuously monitored at four points (MS 1 - 4) by multichannel analysers. Gas samples can be taken before (GM - 1) and after (GM - 2) the off-gas clean-up. The gas first enters absorber columns to remove J_2 and NO_x. It is scrubbed with a 0,5 M HNO_3 / 0,1 % H_2O_2 solution in the first column (WK 1) and with a 5 M NaOH / 0,1 M $Na_2S_2O_3$ solution in the second column (WK 2). The NO_x concentration is measured before and after the absorber columns. The absorber columns are followed by demisters (DM WT 1 and 2) for water aerosol removal. Heated absolute filters (AF 1 and 2) are passed before the gas reaches the membrane gas pumps (GP 1 and 2). After adsorption of water and impurities like NO_x or CO_2 on molecular sieves (MSP 1 and 2) the oxygen is removed by reaction with copper catalysts (BTS 1 and 2) before the remainder of the iodine is removed by silver impregnated silica gel type AC 6120 (JOF 1 and 2). Xenon and part of the krypton are frozen out in the liquid nitrogen cooled cold traps (GF 1 and 2). Before the helium leaves the clean-up system the remainder of the impurities is separated in a liquid nitrogen cooled active charcoal bed.

In two runs 3,7 kg heavy metal ash have been dissolved. The U/Th ratio of the mixed oxide particles was 1 : 5. The burnup was 45 % fifa and the cooling time 4 years. Assuming that 7 % of the fission gases had been released during the burning step, the particles still contained 2,7 Ci H-3 and 73 Ci Kr-85. To gain information on iodine removal newly irradiated particles were added to the ash.

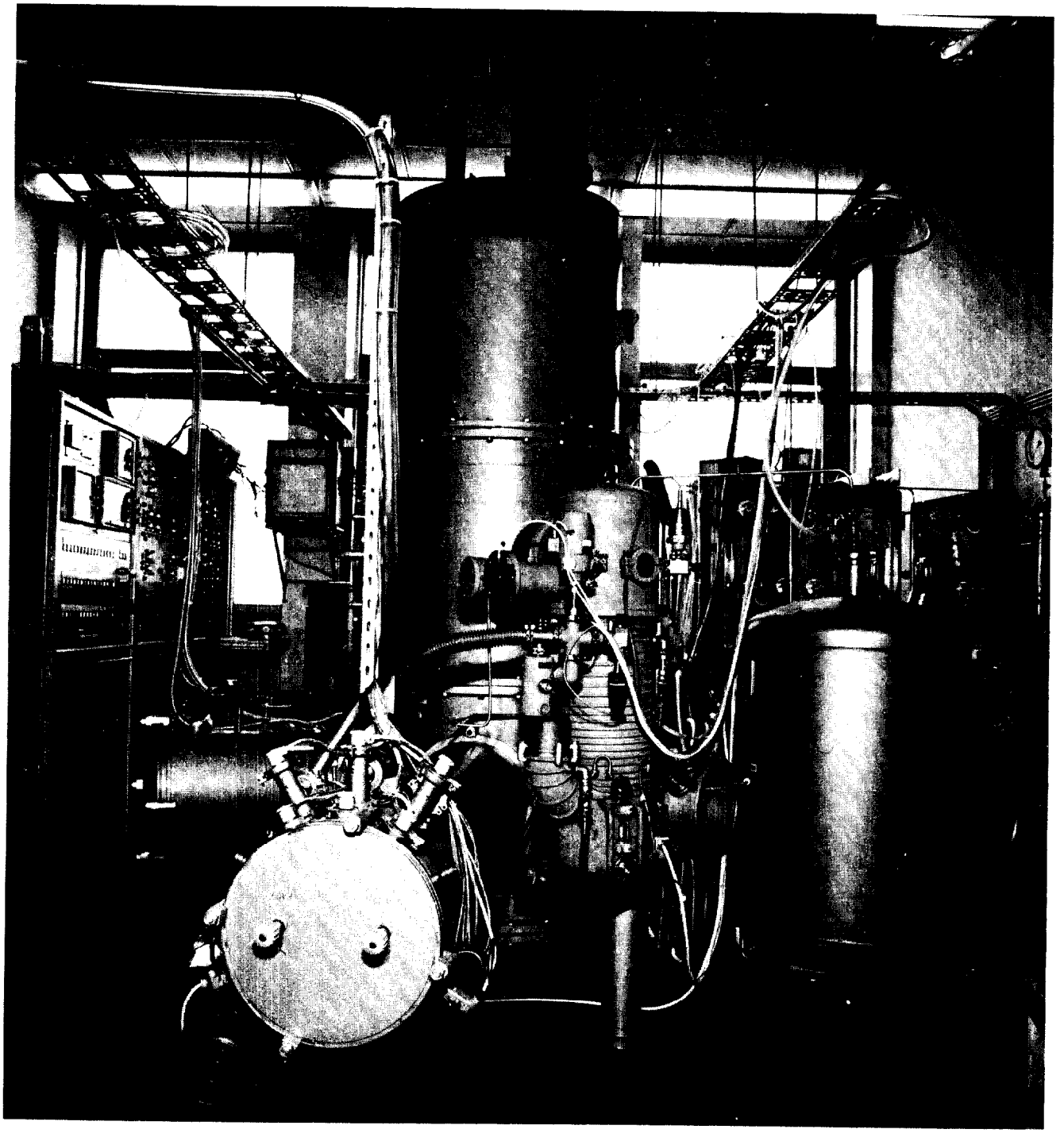

Fig. 8: View of the KRYOSEP II-facility

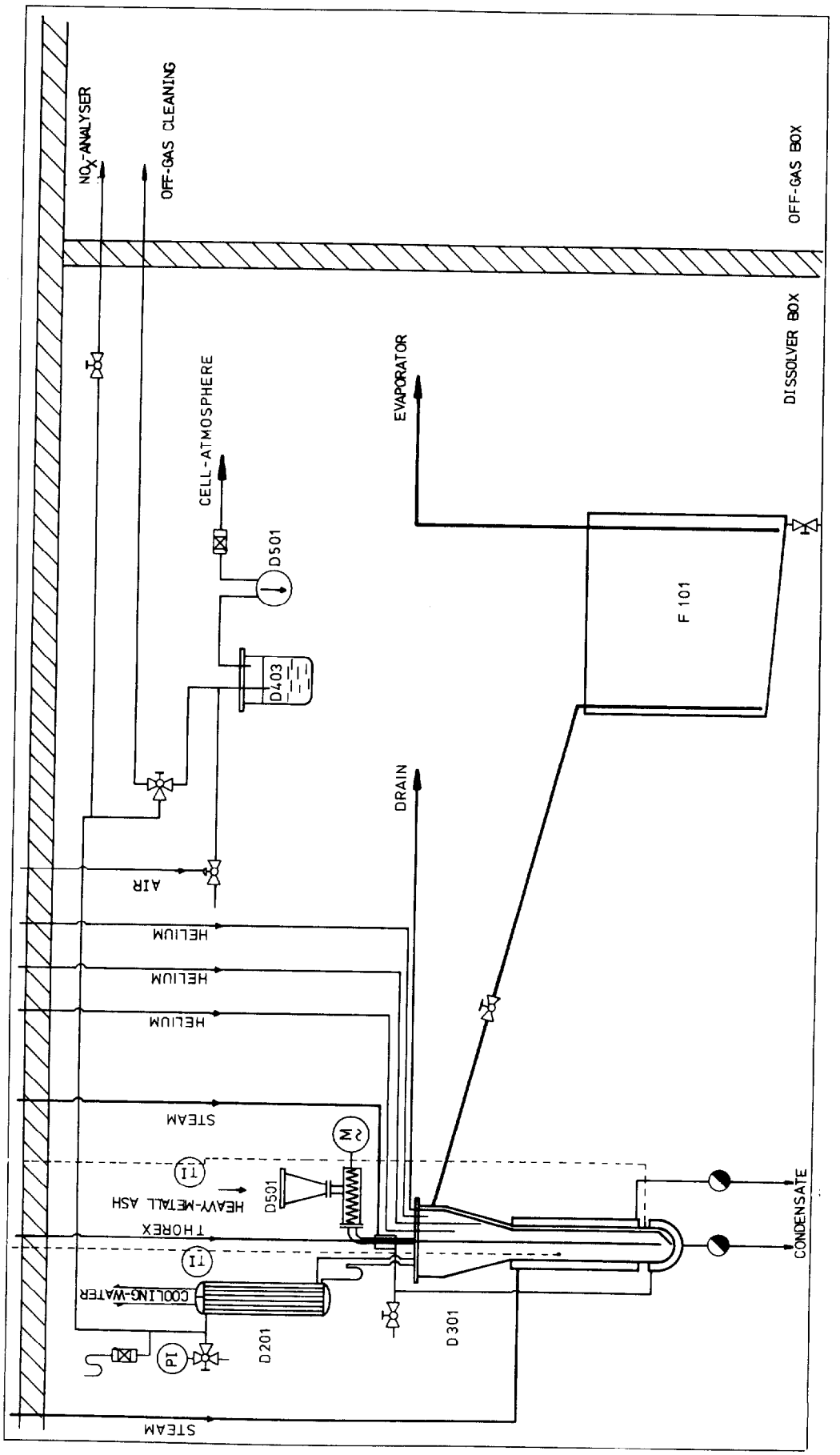

Fig. 9: Flowsheet of the dissolver equipment used for hot tests

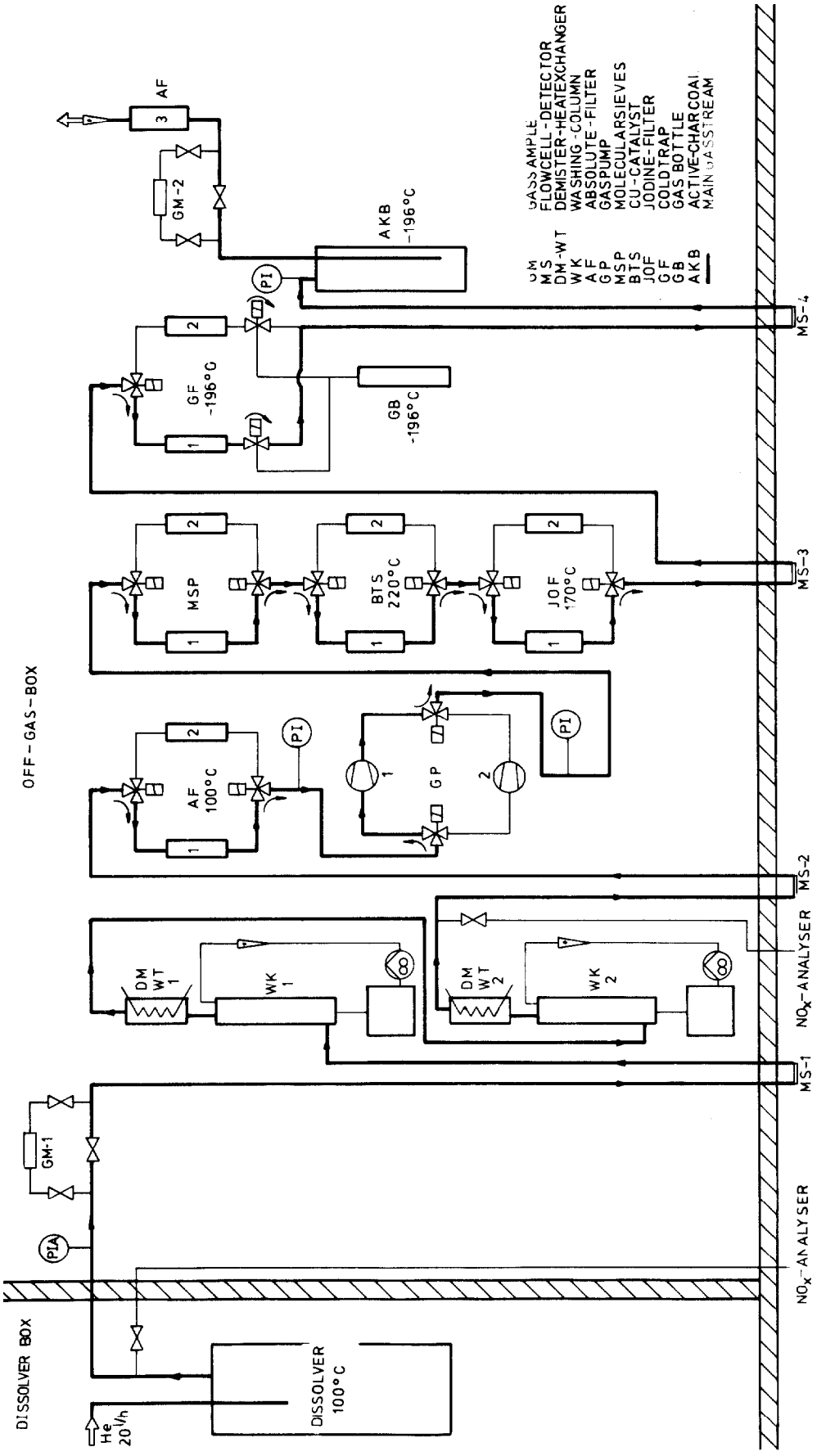

Fig. 10: Flowsheet of the off-gas equipment for the hot dissolver tests

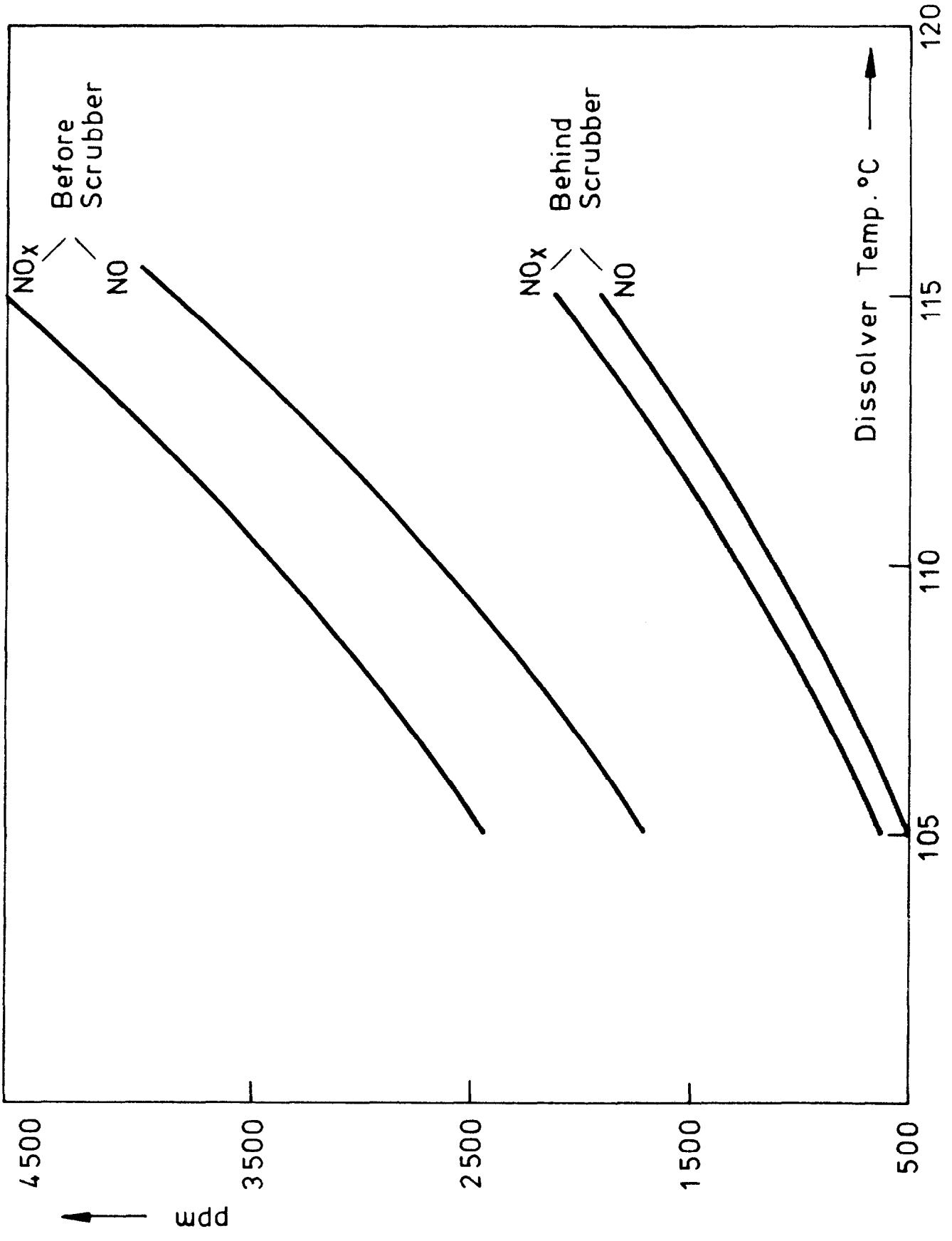

Fig. 11: NO_x concentration in the dissolver off-gas

The NO_x concentration in the off-gas was found to be dependent mainly on the dissolver temperature (Fig. 11). The NO_x concentration ranged between 2400 ppm and 4700 ppm for dissolver temperature between 105 °C and 115 °C. The main component of the off-gas being helium with only traces of oxygen present, the greater part of the NO_x was NO (~ 80 %). The efficiency of the scrubbers for NO_x was only 65 %, a fact that could be expected from the data in literature 3). For iodine the efficiency of the scrubbers was 99,7 %. 75 % of the absorbed iodine were found in the scrub solution of column WK 1 and 25 % in the solution of column WK 2.

2 % of the tritium inventory of the particles was found in the off-gas, 98,5 % of which were retained in the off-gas clean-up system, indicating that ~ 1,5 % of the tritium in the off-gas existed as 3 H_2. No ruthenium was found in the off-gas. The decontamination factors for Kr and Xe have not been determined yet.

References

1. H. Barnert-Wiemer, H. Beaujean, M. Laser, E. Merz, H. Vygen
   14 th ERDA Air Cleaning Conf., Sun Valley, Idaho, Aug. 2 - 4, 1976

2. J. Bohnenstingl, S.H. Djoa, M. Laser, St. Mastera, E. Merz P. Morschl
   14 th ERDA Air Cleaning Conf., Sun Valley, Idaho, Aug. 2 - 4, 1976

3. ERDA - 76 - 43 V. 2 (1976) p. 13.44

AEROSOL AND IODINE REMOVAL SYSTEM FOR THE DISSOLVER OFF-GAS IN A LARGE FUEL REPROCESSING PLANT

J. Furrer, J. G. Wilhelm [+], *K. Jannakos* [++]

[+] Laboratorium für Aerosolphysik und Filtertechnik

[++] Abteilung Reaktorbetrieb und Technik

Kernforschungszentrum Karlsruhe GmbH
Postfach 3640, D-7500 Karlsruhe 1, Germany

Abstract

A newly developed filter combination for the dissolver off-gas in a reprocessing plant with a throughput of 1400 t/yr of heavy metal is presented and single filter components are described. The design principle chosen provides for remote handling and direct disposal in waste drums of 200 l volume. The optimization of housings and filter units is studied on true scale components in the simulated dissolver off-gas of a test facility named PASSAT. This facility will be described. PASSAT will be also used for final testing of the SORPTEX process which is under development. Its concept is included in the paper. The design and function of the new multiway sorption filter providing for complete loading of the iodine sorption material and maintaining continuously high decontamination factors will also be given.

Removal efficiencies measured for aerosols and iodine in an existing reprocessing plant are indicated.

I. Introduction

The risk potential of a reprocessing plant as regards its environment is based almost exclusively on the inventory of radioactive materials, especially fission products and actinides. Part of these materials is converted into off-gas and exhaust air by evaporation and further aerosol generating processes; the radionuclides present as gases in the fuel are immediately released into the off-gas during the process of fuel dissolution.

By several filter barriers the release of radioactive materials into the environment is reduced. In case of operation of a reprocessing plant according to the specifications the highest gas borne activity occurs in the dissolver off-gas. In this paper processes and equipment will be described for dissolver off-gas cleaning from iodine and from solid and liquid aerosols, which are being developed and tested, respectively, with a view to a planned German reprocessing plant.

II. Requirements to Off-Gas Cleaning

The requirements to the off-gas cleaning of the large German reprocessing plant are a result of recommendations prepared jointly in 1977 by the Reactor Safety Commission and the Radiation Protection Commission on behalf of the German Federal Minister of the Interior (1). It was specified that the emissions of ^{129}I should be limited to 0.2 Ci/yr, of α-aerosols to 0.05 Ci/yr, and of β-aerosols to 5 Ci/yr. Based on these values and on the emission values for T, C-14 and Kr-85 and applying the "bases of calculation for the determination of radiation exposure

through emission of radioactive substances with the exhaust air" presently valid in the Federal Republic of Germany, maximum radiation exposures of 4 mrem/yr for the whole body and of 18 mrem/yr for the thyroid are received at the most unfavorable point of exposure.

For an I-129 throughput of 57 Ci/yr in the planned reprocessing plant this implies for the removal of iodine practically completely present in the off-gas that a total removal efficiency of 99.65 % is required. Since iodine released with the vessel off-gas as well as released due to unforeseen handling operations and bypassing the removal devices have also to be taken into account, it is the objective of the work described to reliably guarantee a decontamination factor $\geq$ 99.9 % of the iodine sorption filter in the dissolver off-gas filter train during the service life of the facility.

The requirements to aerosol filtering depend on the activity concentration of the off-gases which are not only a function of the activity inventory of the plant but decisively of the type, design and number of aerosol generating components and of the way the process is run. As a rule, removal efficiencies $\geq$ 99.9 % are required.

III. Setup and Layout of the Filter Train for the Dissolver Off-Gas

Prior to the removal of solid particulates by HEPA filters and before iodine removal the off-gas must undergo preliminary treatment. This preliminary off-gas treatment serves the following purposes:

(1) Reduction of the content of water vapor.
(2) Removal of droplet aerosols, preliminary removal of solid particulates.
(3) Reduction of the relative humidity and concentration of corrosive media to tolerable values such that the performance of HEPA filters is not impaired.

The task indicated under (1) is fulfilled by lowering the dew point temperature, possibly by a condenser. To achieve (2), special droplet separators have to be used which guarantee a high removal efficiency also for small droplets (< 10 µm diameter) as well as particulates. To be able to manage variable mass concentrations as well as a broad spectrum of droplets, a distinction must be made between coarse and fine droplet separators. To achieve (3) heaters are provided in the off-gas stream downstream of droplet separators, the temperatur rise must ensure the destruction of residual droplet aerosols or transformation into solid aerosols by evaporation.

The eligible corrosive media are above all those nitric oxides whose concentrations are usually reduced by a preceding scrubber (NO_2 absorption). Previous experience will not be sufficient to make statements about the longterm behavior of the HEPA filters at high NO_x concentrations. The planned iodine sorption filters can be conveniently used at a higher nitric oxide concentration.

The layout of the filter train for dissolver off-gas purification can be seen from Fig. 1. The filter train consists of a wave plate separator for coarse droplet removal, a packed-fiber mist eliminator for fine droplet removal, a heater, two HEPA and iodine sorption filters each connected in series, an additional HEPA filter following the iodine sorption filters, a cooler, and the off-gas ventilator. If appropriate, an additional heater is installed between the two first HEPA filters and the iodine sorption filters in order to be able to set the operating temperature of the HEPA filters sufficiently above the dew point temperature of the off-gas so as to avoid damage, although below the iodine sorption filter operating temperature

(130 - 150°C). Accordingly, a cooler should be provided upstream of the HEPA filter following the iodine sorption filters.

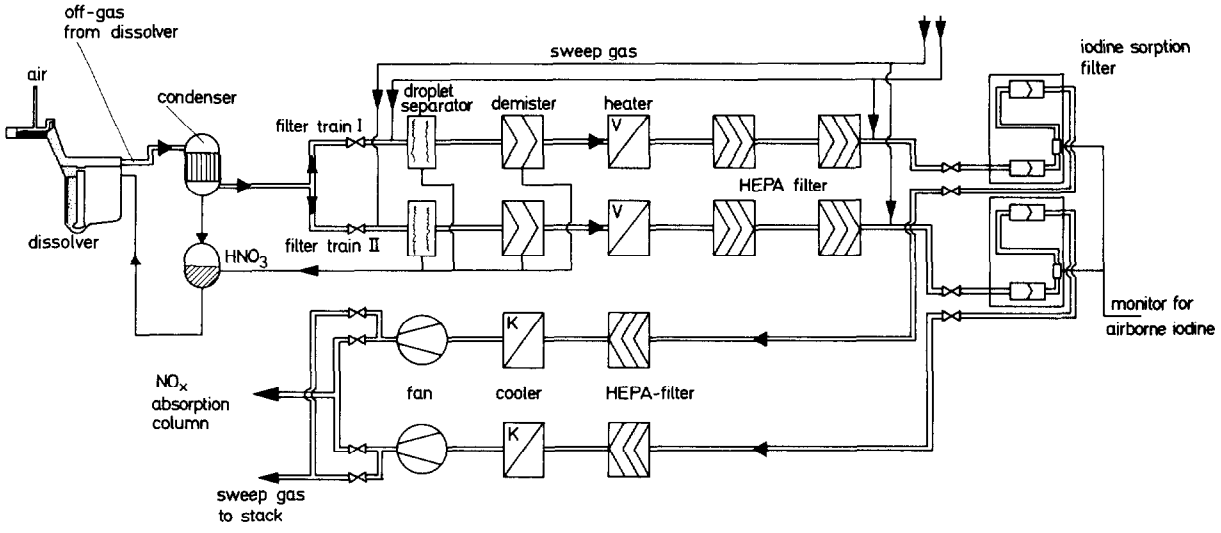

FIGURE 1 SORPTEX-process for head end iodine removal in a reprocessing plant.

The whole filter train is presently still planned for installation downstream of an NO_2 absorption and an I_2 desorption column in the dissolver off-gas. With this configuration a major portion of the fission product iodine already present as vapor in the off-gas stream is absorbed by the acid recovered in the NO_2 absorption column. Via a downstream desorption column it has to be returned into the off-gas stream to be finally removed in the iodine sorption filters.

Installation of the whole filter train immediately downstream of the dissolver (with a preceding condenser so as to reduce the vapor content in the off-gas) would allow a much simplified flowsheet since the expenditure in terms of process engineering needed to release fission product iodine from the recombined acid can be avoided. The development of this so-called SORPTEX process will be the subject of future R&D activities. The higher activity and acid concentrations in the upstream gas preceding the filter train (due to the lack of removal efficiency of the columns with respect to aerosols) as well as the reduction of the pressure acting in the NO_2 column due to the pressure reduction in the preceding filter train, have to be regarded as drawbacks of this technique. On account of the pressure loss either a fan placed in-between or a greater number of trays in the NO_2 absorption column is required.

IV. Criteria of Selection and Requirements to the Filter Components

For the filter train only passive components are chosen which require little maintenance work and are characterized by a high removal efficiency. In case that a regular replacement was foreseeable during operation, only remotely handled

filters were eligible which fulfil the following requirements regarding this characteristic:

- Remotely handled filter replacement has to be carried out as far as possible without contaminating the joint room of installation.
- One single, easy to operate remote handling system (hoist unit) must be sufficient for replacement of all filter elements provided in the filter train.
- The filter elements must be capable of being remoteley packed into 200 l waste drums without reduction of volume.
- The leaktightness of the filter seats must be capable of being continuously monitored during operation.
- The filter vessels must be capable of being decontaminated.
- The lids of the filter vessels should have the same outer dimensions and be equipped with identical closing systems.
- Provisions must be made that the lids can be closed and opened by the remotely handled hoist unit (in case of failure of the hydraulic closing system) which is also used for the replacement of filter elements (emergency handling).
- Independent lid locking devices must be available which prevent the filter vessels from opening in case of pressure pulses resulting from an incident.
- The lid openings of the filter vessels have to be provided at one level in a straight line of the room of installation in order to be able to perform all necessary work using a hoist unit.

V. Filter Components for Aerosol Removal

Fig. 2 shows the coarse droplet separator. A wave plate separator was designed which is equipped with a self-cleaning system and does not call for any maintenance work. For droplets > 10 µm a removal efficiency $\geq$ 90 % is required. The design of the separator allows flanged connection to the off-gas line; on account of previous operating experience a remotely handled design proved to be superfluous. In case salt crusts are formed, diluted nitric acid is sprayed in by short spraying periods via a nozzle system provided at the gas inlet so that the crusts formed get detached again.

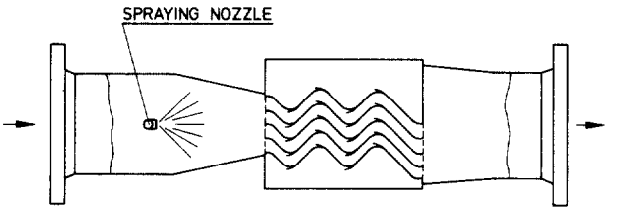

Fig.2 Wave-plate separator, component I, droplet removal > 10 µm

Fig. 3 shows the remotely handled packed-fiber mist eliminator provided in the exhaust air of the wave plate separator. It is intended to remove liquid droplets < 10 µm with a removal efficiency ≥ 99 %. Moreover, it is to be used as a prefilter for particulates so as to increase the service life of the following HEPA filter. Since a greater surface is offered on the upstream gas side of the fiber package, flow from outside to inside is preferred.

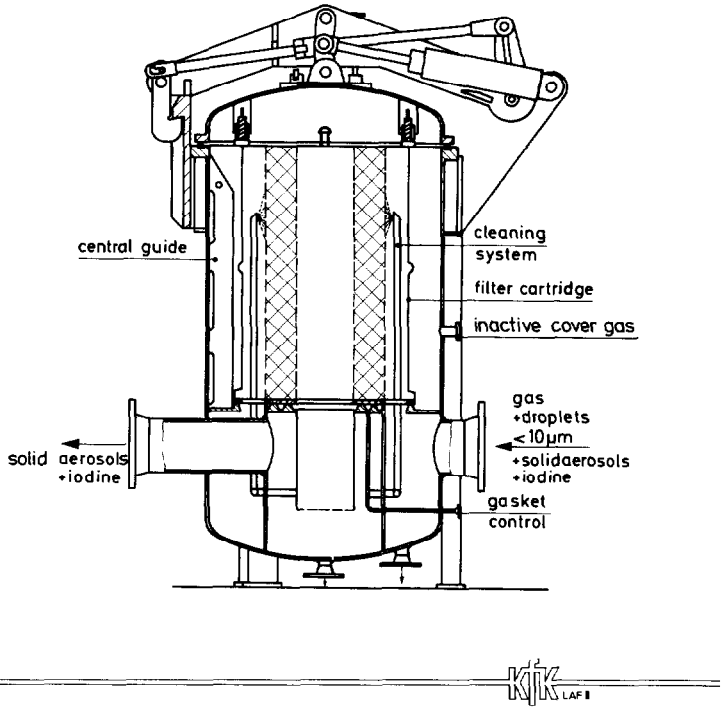

Fig.3 Passat packed fiber mist eliminator,- high efficiency element,-component II, for droplet removal<10µm

The demister consists of packed glass fibers of about 20 µm diameter with a statistically vertical orientation. Impinging droplets are retained by the fibers, combine into larger droplets, and due to gravity and pressure difference they migrate from top to bottom in the fiber layer to reach ultimately the sump in the filter vessel.

The fiber layer is placed in a sheet metal case open on the bottom and is replaced together with this case. The upstream and downstream gases are routed within this sheet metal case. Plating out of radioactive salts on the outer side of the case in the upper part of the filter vessel and on the inner side of the lid is prevented by sealing and an inactive cover gas. The leaktightness can be monitored continuously, as will be described for the HEPA filter. As soon as an unacceptable high pressure difference over the fiber layer is obtained, a spraying device is actuated which consists of a spray ring with six nozzles surrounding the fiber layer so as to wash out with diluted nitric acid the crystallized salts and the solid aerosols deposited. Steam condensate can possibly be formed by reducing the off gas temperature below the dew point temperature in front of the packed-fiber mist eliminator, which will result in continuous self-cleaning of the fiber layer.

Preliminary tests were made on a Brink packed-fiber mist eliminator supplied by Monsanto which was not yet delivered as a demister capable of remote handling as described above. The fiber layer was 150 mm deep and had a high packing density. For droplets between 3 and 10 µm a decontamination factor of > 75.000 was obtained which was calculated via the detection limit and with the mass concentration known. The packed-fiber mist eliminator yielded a removal efficiency > 99 % for solid aerosols with particle diameters between 0.1 and 1 µm (uranine test)[2].

In the PASSAT technical-scale facility described at the end of this paper tests are planned for optimizing the remotely handled packed-fiber mist eliminator with a view to pressure reduction, depth of the fiber layer, and packing density for given removal efficiencies. Moreover, studies relate to the deterioration of the removal efficiency by loading with soluble and insoluble salts, to the effect of continuous and batchwise spraying with diluted nitric acid for clean up and to the self-cleaning behavior.

Fig. 4 shows the HEPA filter installed behind a heater in the off-gas stream. The filter vessel also complies with the requirements mentioned above. The filter element is exposed to internal flow so as to keep low the outside contamination with a view to filter replacement. Also in this case continuous monitoring of the leaktightness of the filter seat is possible during operation, inclusive of both the top and the bottom surfaces of the gasket between the filter element and the mounting frame in the filter vessel.

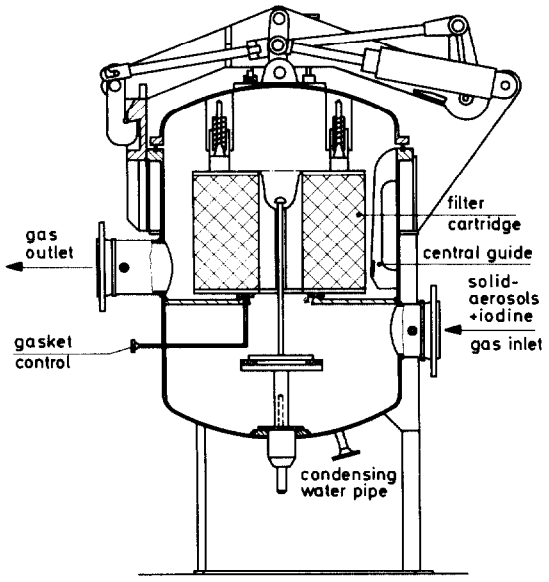

Fig.4 Passat HEPA - filter, component III, removal of solid aerosols η≥99.9%

A new HEPA filter element is presently developed. For the time being, an earlier design is used which allows replacement by means of a proven remote handling system. Attempts are made to simplify the design and to increase the temperature resistance to 150°C continuous temperature.

Measurement of the removal efficiencies of filter papers used in HEPA filter elements in the dissolver off-gases (Table I) of two reprocessing plants show that the standards for HEPA filters so far assumed with removal efficiencies > 99.97 % for aerosols in the dissolver off-gas of reprocessing plants are not observed. Removal efficiencies between 99 and 99.4 % were obtained in short-term and long-term investigations. Therefore, several HEPA filters were series connected in both plants.

In the off-gases of the Karlsruhe reprocessing pilot plant (WAK) still different filter papers are investigated. The best suited papers will be installed in newly conceived filter elements which can be bagged out into a 200 l standard waste drum.

In PASSAT an integral in-place filter testing method is to be tested by use of a uranyl nitrate test aerosol so that the safe use of aerosol filters can be ensured in the dissolver off-gases.

VI. Fission Product Iodine Removal

On account of excellent experience obtained with iodine sorption filters [3], using the AC 6120 iodine sorption material [4, 5] in WAK during 2.5 years of operation until now, removal of the total fission product iodine from the dissolver off-gas is planned to be achieved on the AC 6120 solid iodine sorption material. A multitude of measurements of the removal efficiency performed in the course of dissolving and standstill periods showed that with the help of the iodine sorption filter installed in WAK, which does not yet comply with the design described in the subsequent text, removal efficiencies of at least > 99.9 %, usually > 99.99 %, were achieved.

With this method silver in the amount of about 10 kg $Ag/GW_{el} \cdot yr$ is used. Due to the relatively low consumption of silver, conversion is not planned of the silver iodide obtained in the sorption material while recovering the silver although would be quite feasible in additional process steps.

The iodine sorption filters, Figs. 5, 6 and 7, presented here were designed and built for removal of about 400 kg/yr of fission product iodine in filter elements, which can be transferred into the usual 200 l waste drums for radioactive waste without further conditioning or loss of drum volume.

This led to the selection of a filter element having the shape of a cylindrical deep bed filter with a diameter of the iodine sorption material layer of 50 cm and a bed depth of 69 cm. This bed depth is solely determined by the highest possible loading capacity, whilst the required removal efficiency is achieved already with a much lower bed depth (and residence time, respectively) [5].

Table I Removal Efficiencies of HEPA-Filters in Dissolver Off Gases of Nuclear Fuel Reprocessing Plants (NFRP).

Operating conditions at the filter paper:

	NFRP I	NFRP II
type of filter paper	SS 6	Astrocel
temperature	150°C	130°C
NO_x-concentration	< 10 Vol.%	< 10 Vol.%
linear gas velocity	2,2 cm/s	4,2 cm/s

	NFRP 1					NFRP II
Test-No.	1	2	3	4	5	6
sampling place in relation to absorption column	up-stream	down-stream	down-stream	down-stream	up-stream	down-stream
sampling time (h)	6,5	6,25	8,5	8,5	6,75	960
removal efficiency (%)	99,3	99,03	99,27	99,23	99,0	99,24
decontamination factor	143	103	137	130	100	132

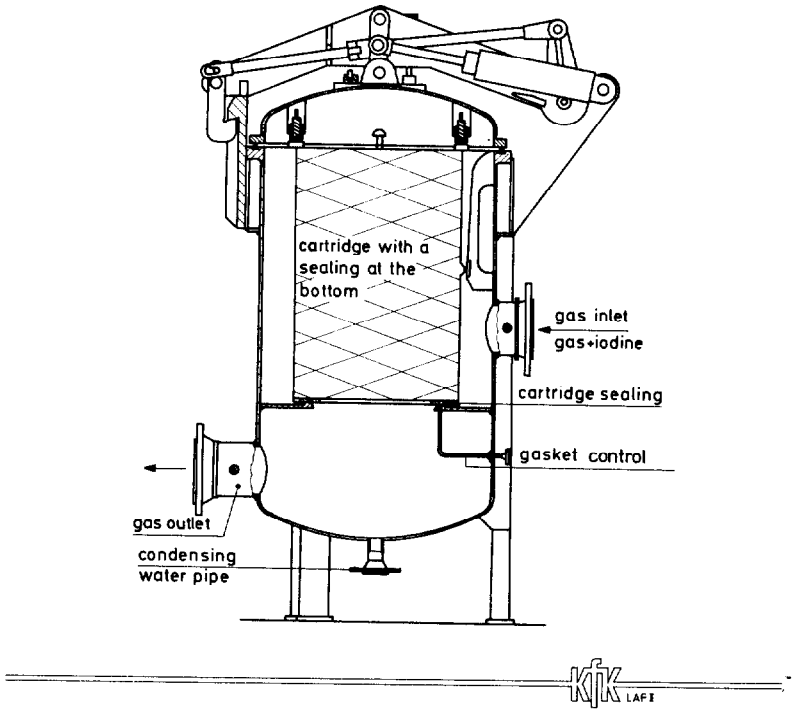

Fig.5 Passat iodine filters, components IV+V, removal of gaseous iodine compounds $\eta \approx 99.9\%$

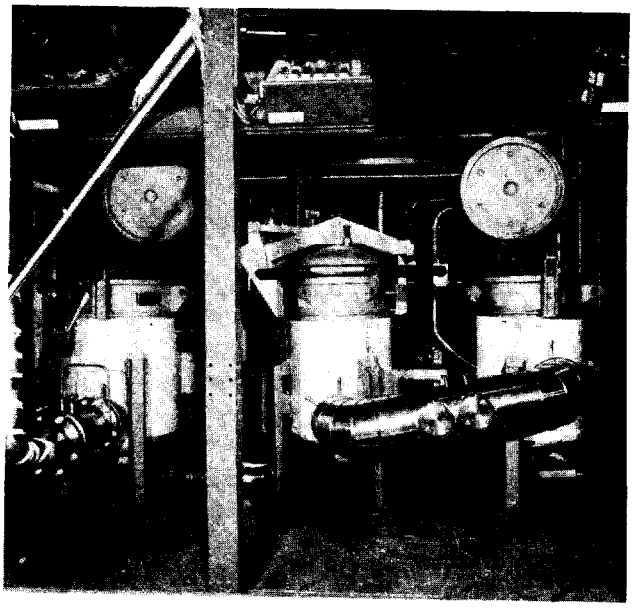

Fig. 6 Filter housings of mist eliminator (left) and two iodine sorption filters (right)

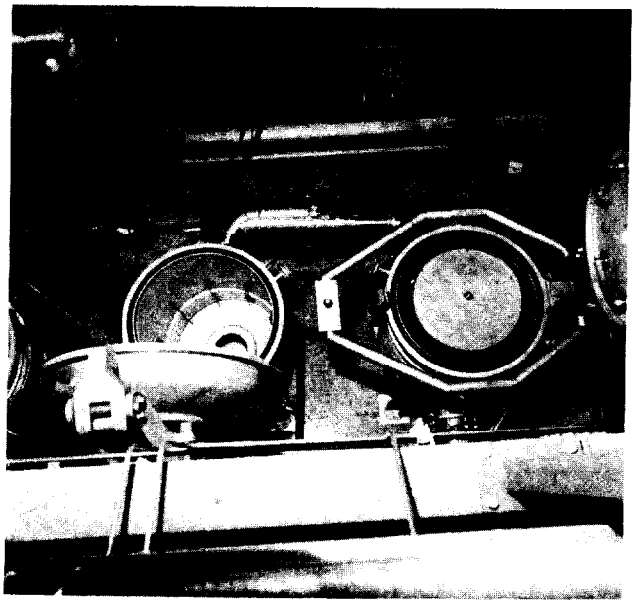

Fig. 7 Filter housings of iodine sorption filters, one cartridge loaded (right)

Although the design described causes a higher pressure loss during operation as compared with a ring layer of the sorption material, advantages were decisive, such as

- simple design,
- guaranteed leaktightness of the sorption layer (if the flow is directed from top),
- maximum quantity of sorption material filling, and
- complete utilization of the sorption material.

The service life of a filter element in the dissolver off-gas is limited by the maximum iodine load of 11.8 kg. This means that the filter element has to be replaced after about 10 days of filter operation, assuming a daily capacity of about 4 t of uranium. Therefore, a very stable design had to be chosen for the filter vessel in order to avoid tolerances occurring after many replacements. Due to the frequency of filter element replacements resulting from operation, the replacement itself must be an easy and fast process and, moreover, the tight seal of the filter element in the filter vessel must be inspected continuously. Therefore a design was selected which allows to apply a test pressure (compressed air) to the whole circumference of the gasket. The gasket (between the filter element and the mounting frame of the vessel) was attached as usual at the filter element and is replaced with the latter. If a filter element is used twice (in the first and second vessel of a two-stage filter) care was taken by use of a staggered arrangement of the sealing edges in the filter vessels that the sealing of the filter unit after relocation is achieved by a part of the gasket not previously compressed.

The already described high degree of preliminary aerosol removal is intended to avoid as much as possible contamination of the filter vessel and filter element by fission product aerosols (including hard γ-emitters). Nevertheless, plating out of radioactive aerosols in pipings, valves and filter vessels cannot be safely excluded for extended operation. Therefore, the design chosen for the iodine sorption filter allows remote filter replacement and remote packing of the filter element into the waste drum as well as bagging out.

To be able to fully use the iodine sorption material containing silver, two iodine sorption filters connected in series will be provided. The filter element located in the first vessel in the direction of flow is exhaustively loaded (Fig. 1), whilst the filter element in the second vessel is used only to remove the iodine occurring in the exhaust air stream of the first filter. This filter element is exhaustively loaded only after its relocation into the first vessel in flow direction. At the end of this period of use the relocated filter element shows practically no residual removal efficiency and the required total removal efficiency of ≥ 99.9 % must be obtained solely by the second iodine sorption filter. At this time any leak of the second filter can fully impair the removal efficiency achievable.

Since at the end of the service life of the filter element in the first vessel the iodine concentration in the downstream air is practically equal to that in the upstream filter air, the clean air side of this filter as well as the whole zone up to the sorption layer of the second filter element are contaminated by off-gas with a high iodine concentration. Prior to replacing the filter elements this contamination has to be removed by scavenging with air free from iodine or, if applicable, iodine release into the clean air must be avoided by flow reversal or sealing. Therefore, in the design of the filter vessel, the flow was routed such that dead spaces are largely excluded which cannot be flushed.

In addition to the relocation of filter elements for complete loading a piping is in discussion which allows alternate loading of the filter vessel (Fig. 8). An appropriate method involves the use of at least 7 valves which have to be controlled by a program and locked in order to avoid wrong connections. Besides, on account of unavoidable contamination of the "clean air side" of each of the two series connected filters in the course of switching over, loss of the removal efficiency must be expected, the more so since scavenging by filtered air is possible only during operating phases strictly limited in duration.

A major portion of the PASSAT test program will be devoted to testing the relocation and switching operation under realistic operating conditions, especially with a view to the iodine partial vapor pressure and the off-gas condition. For the quantitative determination of clean air contamination possibly occurring during filter replacement radioactively labeled iodine is used.

As an alternative to iodine removal by the assembly described the use of a multi-way sorption filter (MWS filter) is considered (6). However, use of this filter calls for a perfect flow behavior of the iodine sorption material, which can be proved only by several years of operating experience. The newly developed MWS filter offers the advantages of a countercurrent filter. The size of the surface and the filter bed depth can be broadly varied as opposed to the countercurrent filter; the influence of the sorption material pouring cone on the bed depth of the sorption material was completely eliminated (Fig. 9).

Fresh sorption material is introduced batchwise from top into the MWS filter and withdrawn at the bottom after passage through two or more filter chambers and complete loading. The off-gas stream to be cleaned is passed several times (at least twice) through the sorption material in the horizontal direction. In case of plane parallel withdrawal and appropriate design of the zone between the two filter chambers the sorption material can be completely loaded while maintaining a given removal efficiency. Mechanical leaks via the sorption layer can be excluded without requiring additional sorption material.

VII. Description of the PASSAT Technical Scale Test Facility

The performance of the filter train described calls for cooperation of quite a number of single units with no experience available on their performance and reliability under the conditions prevailing in the dissolver off-gas of a reprocessing plant. Due to its importance in safety technology the availability of the dissolver off-gas section directly influences the availability of the reprocessing plant. To avoid hazards in terms of safety and economy, extensive testing in cold and hot operation is therefore required. For cold testing of the whole filter train and for optimizing individual components the technical scale PASSAT facility was built which allows to simulate the dissolver off-gas of a reprocessing plant.

PASSAT consists of a room for filter installation, accommodating the entire filter train, the remote handling devices for filter replacement and packing, and the equipment for the production and circulation of the simulated dissolver off-gas.

Fig. 10 shows the block diagram for PASSAT. The volume flow of the simulated dissolver off-gas can be freely set between 50 an 250 Nm^3/h and so includes the off-gas flows under discussion for the dissolver off-gas train of a reprocessing plant having a daily capacity of about 4 t of heavy metal.

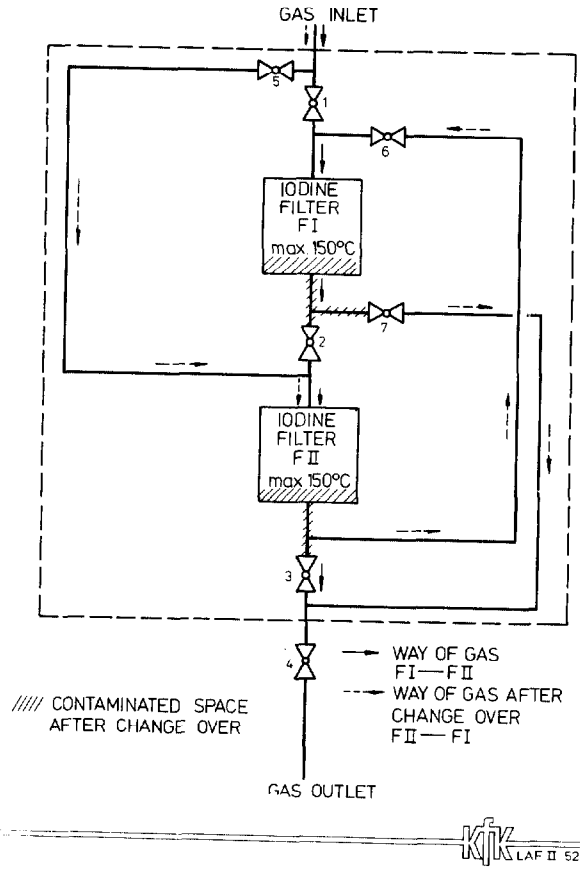

Fig. 8 Iodine filter switching system

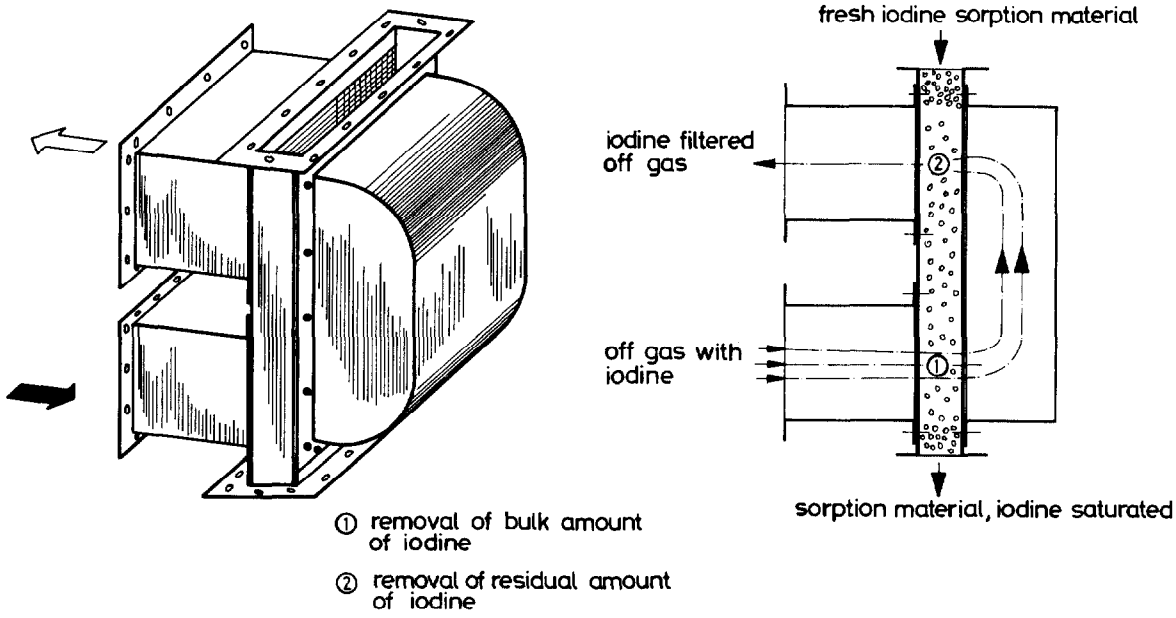

Fig. 9 Multiway iodine sorption-filter

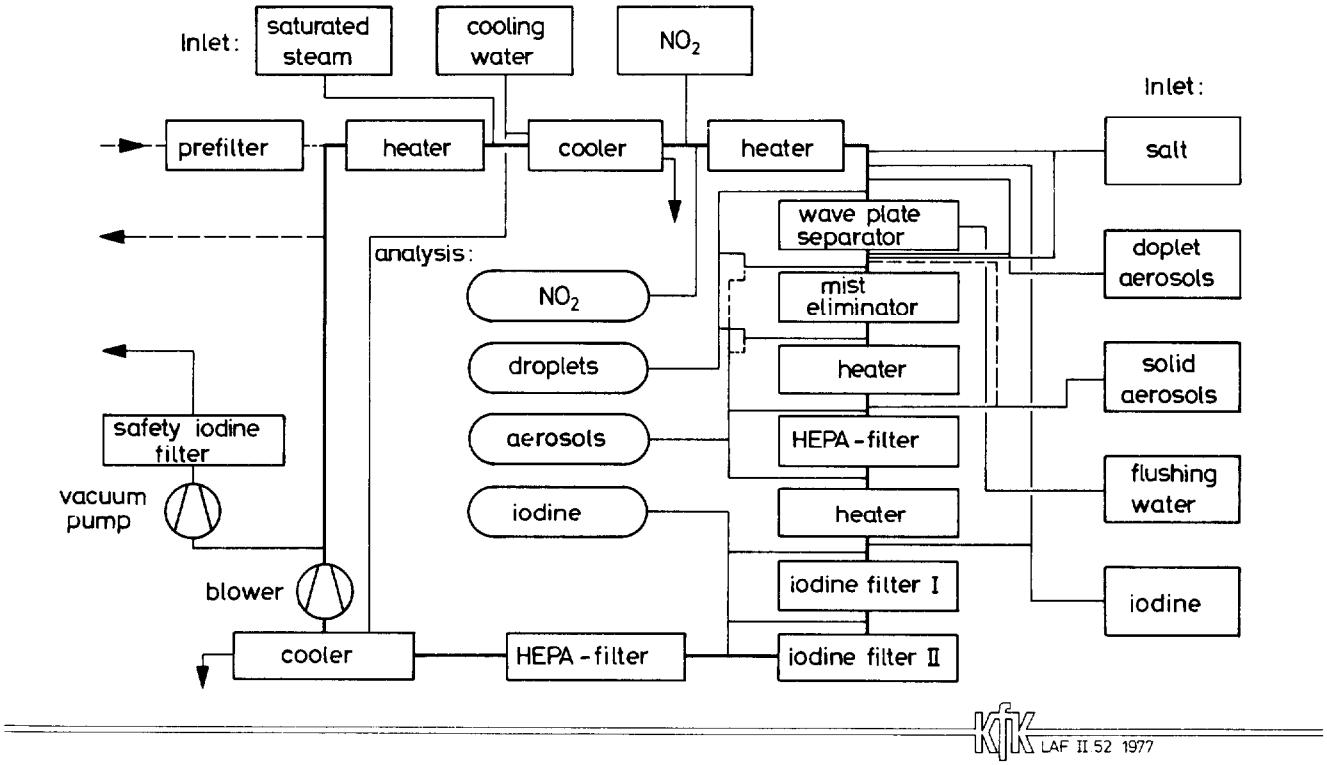

Fig.10 Process flowsheet of the Passat test facilities

For reasons of safety and supply PASSAT can be operated with fresh gas or recycled gas depending on the operating conditions. Recycling is intended especially at higher nitric oxide concentrations and in cases where radioactively labeled iodine is fed into the system.

Upstream of the filter train an operating pressure of about 80 mbar below atmospheric pressure is set in order to simulate the specified inlet pressure of the filter train of a reprocessing plant. This pressure is determined by the pressure difference over the dissolver and the subsequent columns.

The gas upstream of the filter train may consist of an air-water vapor mixture of 30 - 100 % relative humidity kept within the temperature range from 30°C to 75°C. The temperature of the gas flow may be increased up to 160°C upstream of the HEPA and iodine filters. The NO_2 content in the upstream gas may reach up to 10 vol.%. The maximum pressure difference permitted over the whole facility is 0.5 bar.

Test droplet aerosols are fed into the droplet separators and measured according to the flowchart represented in Fig. 10, with droplet sizes > 10 µm attained with a single-component nozzle at the wave plate separator and droplet sizes of 1 - 10 µm attained with a two-component nozzle at the packed-fiber mist eliminator. Sampling and measurement are performed isokinetically at a constant pressure of the plant by use of a light scattering instrument calibrated with respect to droplets.

With respect to the HEPA filter, the removal of particulates with a diameter of about 0.1 µm will be tested. They are generated by an aerosol generator spraying a 1 % sodium fluoresceine solution (uranine) into the homogenizer where the droplets are dried. Sampling is made isokinetically upstream and downstream of the filter.

A partial gas stream is drawn through a measuring filter. The filters are evaluated with a spectral fluorimeter determining the mass concentration. The distribution of aerosol particle sizes is determined by pictures taken with the X-ray electron microscope; subsequently the particles are classified and counted.

The iodine released during dissolution of spent fuel elements mainly occurs as elemental iodine. Organic iodides are formed only at low concentrations by the recycled and recombined acid.

Fig. 11 shows the gas chromatogram of the dissolver off-gases of the WAK during a dissolution period (7). As compared with the iodine inventory of the dissolver of about 18 g and an off-gas throughput of 100 m^3/h, the concentration of organic components was less than 0.05 % of the total inventory.

In Fig. 12 the iodine concentration curve has been plotted which is typical of a dissolution period in WAK. The iodine concentration was monitored with an iodine detector. The respective plots are obtained during Kr-85 measurement. The wet chemical method according to Duflos which is used in PASSAT and which relies on the reaction of an alkali iodide with ammonium ferric sulfate in sulfuric acid solution allows the momentaneous increase of iodine production by addition of the alkali iodide and thus the simulation of the iodine concentration curve in the dissolver off-gas (8).

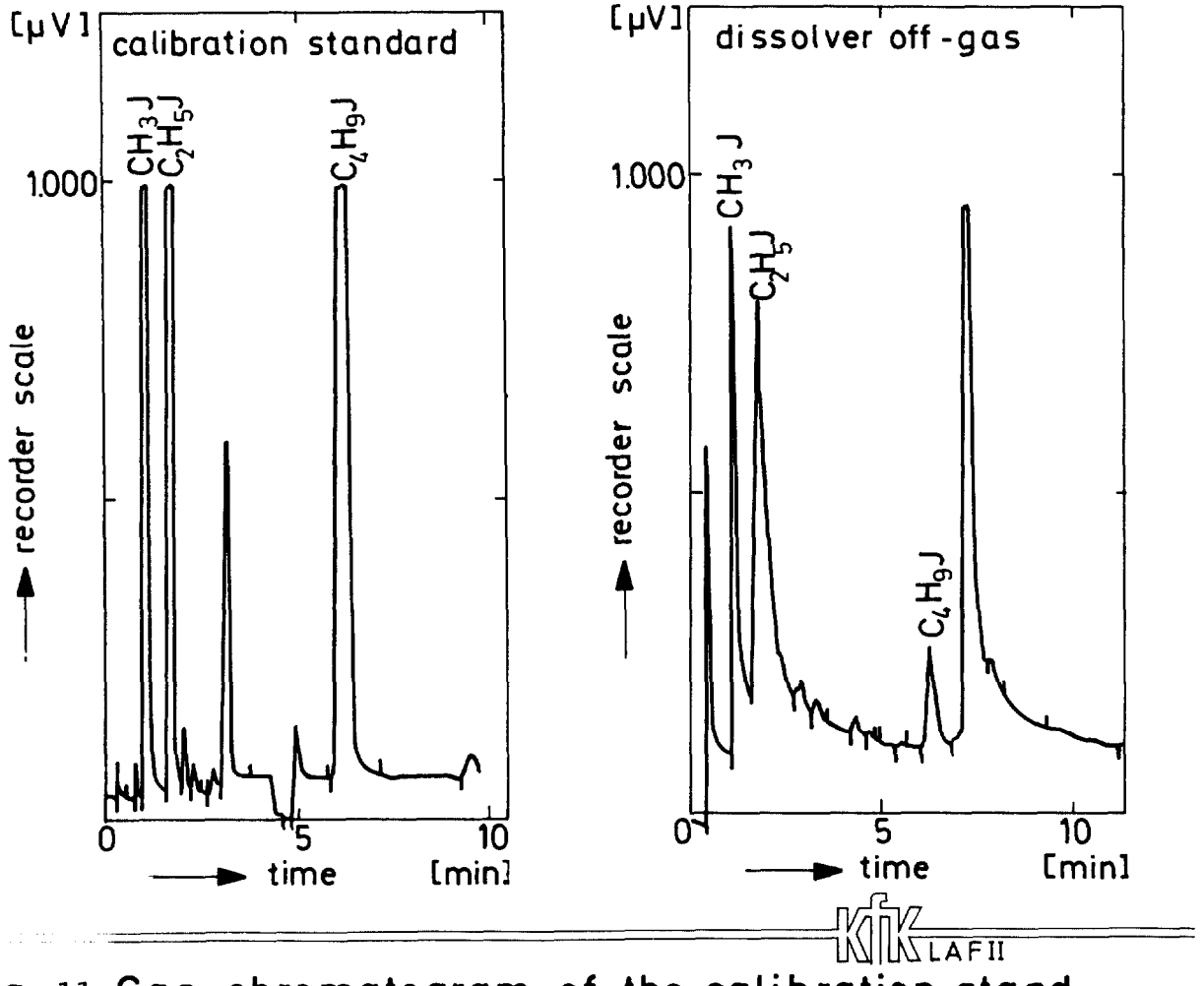

Fig. 11 Gas-chromatogram of the calibration standard in toluene and of the dissolver off-gas

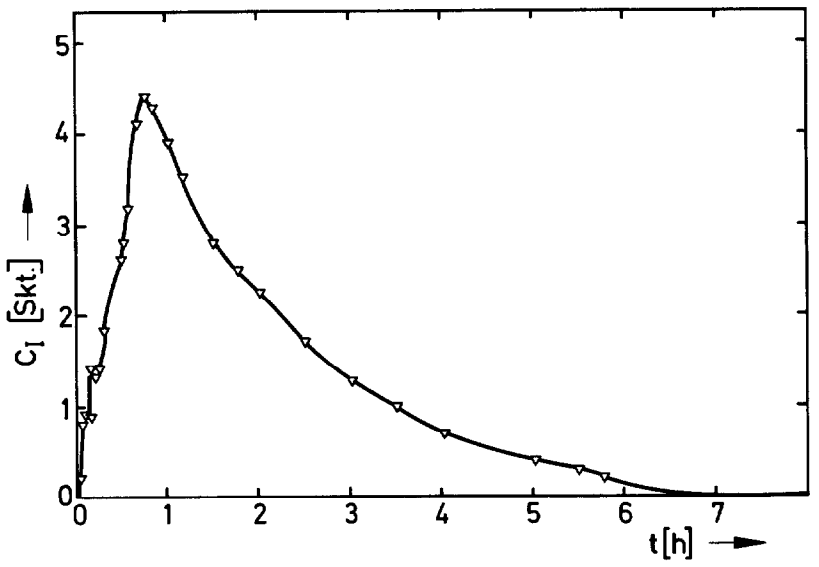

KfK LAF II 52 1977

Fig. 12 **Iodine distribution in the WAK dissolver off-gas during dissolution**

The decontamination factors of the individual filter stages are determined by gas sampling upstream of, between and downstream of the filters, accompanied by chemisorption of iodine on impregnated iodine sorption material and measurement of the ^{131}I activity added as a tracer.

Loading of the first filter stage is indicated by measurement of the iodine concentration after iodine penetration, using an iodine detector. After a given concentration has been reached, a signal is released for filter replacement.

The investigation program performed at PASSAT includes the development and testing of remotely handled devices for the replacement and bagging out of filter units (Fig. 13). In this program a remote handling device was developed and tested which includes a single track trolley and a hoist allowing easy performance of all manipulations without spreading the contamination into the filter cell. All the filter vessels were arranged in one line so that both replacement of the filter elements and emergency handling of the filter vessels can be performed with the same hoisting equipment.

One of the main problems during reloading is the contamination free transport of filter elements out of the cell of the filter train. A simple double lid lock was conceived which allows bagging in and bagging out of the filter elements with the help of the waste drum. For coupling the waste drum on the lock a lifting-swiveling mechanism was used instead of the previously employed coupling vehicle. These are the advantages of this mechanism:

- no tracks and track drive,
- no cable takeup reel and cables,
- no emergency handling of the vehicle drive,
- accurate positioning possible by manual operation.

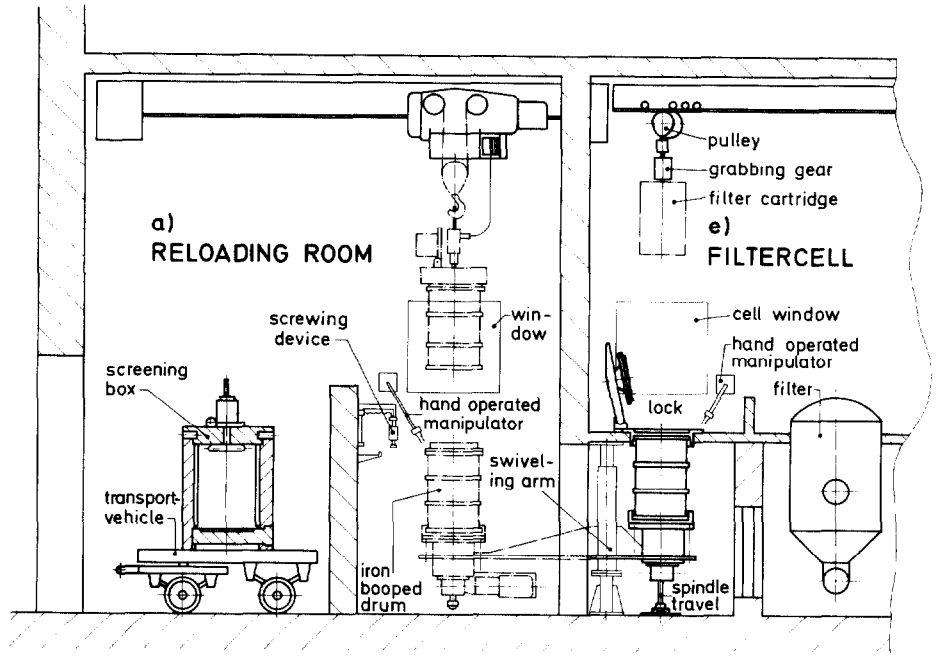

FIG.13 Lock for contaminated filter cartridges

The first true-scale cold tests with the cell lock have performed statisfactorily.

Acknowledgments

The authors express their gratitude to all the cooperators in the PASSAT project and particularly to Messrs. H.-G. Dillmann, R. Herrmann, R. Kaempffer, H. Mock, G. Potgeter, and M. Tuczek.

References

1) GRS: Grundsätzliche sicherheitstechnische Realisierbarkeit des Entsorgungszentrums. Beurteilung und Empfehlungen der Reaktorsicherheitskommission (RSK) und der Strahlenschutzkommission (SSK); (1977).

2) A. Briand, J. Dupoux: Mesure en laboratoire et en usine l'efficacité des éléments filtrantes et du papier filtre par la méthode à l'aérosol de fluorescéine sodée (uranine). Norme AFNOR NFX 44 011, V/835/77, p. 249.

3) V. Böhmer, G. Herrmann, H.-P. Wichmann: Messungen zur Bestimmung der Rückhaltung und Ableitung von I-129 bei der WAK, Conference paper of Reaktortagung 1977, p. 393.

4) J.G. Wilhelm, H. Schüttelkopf, An Inorganic Adsorber Material for Off-Gas Cleaning in Fuel Reprocessing Plants, CONF-720 823, p. 540 (1972).

5) J.G. Wilhelm, J. Furrer, E. Schultes, Head-end Iodine Removal from a Reprocessing Plant with a Solid Sorbent. CONF-760 822, p. 447 (1976).

6) M. Ohlmeyer, J.G. Wilhelm: Filteranlage zum Reinigen von Gas- oder Luftströmen, DT/OS 2540141, March 10, 1977.

7) J. Furrer, R. Kaempffer, R. Gerhard: Messung von Iodverbindungen im Abgas der WAK. KFK 2500, p. 121 (1977).

DISCUSSION

BURCHSTED: What fiber was used in your demister?

FURRER: We used in our demister packed glass fibers of about 20 μm diameter with a statistically vertical orientation.

BURCHSTED: What was the air temperature at the HEPA filter?

FURRER: At the HEPA filter, we work at 120°C up to 150°C.

BURCHSTED: I'd be interested in knowing the construction of that filter.

FURRER: A new HEPA filter element is presently developed. For the time being, an earlier design is used which allows replacement by means of a proven remote handling system. Attempts are made to simplify the design and to increase the temperature resistance to 150°C continuous temperature.

BELLAMY: I have a question along the same lines for the silver zeolite used. Could you tell us what the level of silver was on the silver zeolite and if there are plans to recover or regenerate that material?

FURRER: We don't want to regenerate. We don't think that the silver price for iodine removal is too high. With this method, silver in the amount of about 10 kg $Ag/GW_{el}.yr$ is used. Due to the relatively low consumption of silver, conversion of the silver iodate obtained in the sorption material is not planned. Nevertheless, recovering the silver would be quite feasible by additional steps.

GRADY: Would you explain a little more about the reason for putting HEPA filters before the iodine bed and, again, after the iodine bed but before the NO_x adsorber? Why do you need that much filtration in that part of the process?

FURRER: There may be aerosol generation in the filter beds; for example loss of silver nitrate impregnant. Therefore, we set a second HEPA filter behind the iodine filters as a safety filter for the following sand.

GRADY: I see, so you're saying that the particulates that are getting through the mist eliminator possibly will cause some problems in your iodine bed or downstream?

FURRER: Yes.

T. R. THOMAS: Did you mention that you would like to try the iodine adsorbent before the nitric acid scrubber?

FURRER: Yes.

T. R. THOMAS: What are the advantages?

FURRER: The advantages are: a) no iodine loading of the scrubber solutions; b) no contamination by aerosols of the scrubber solution; c) no further iodine desorption process.

T. R. THOMAS: Would you expect to have problems with nitric acid, NO_x, or particulates? Would you still remove particulates before the iodine adsorbent?

FURRER: Although we haven't tried it yet, we will try this material at very high concentrations because we expect concentrations up to 30 volume percent of NO_2.

T. R. THOMAS: Is there an advantage to keeping iodine out of the nitric acid scrubber?

FURRER: We tried this method in the DOG of the French reprocessing plant in Marcoule with great success and high removal efficiencies.

T. R. THOMAS: Can you heat AC/6120 to a high enough temperature to regenerate (i.e., 400-500°C)? Doesn't the silver nitrate run off?

FURRER: The silver nitrate does not run off. We ran it up to 500°C and also some melting occurred on the surface, but the silver nitrate did not evaporate.

T. R. THOMAS: It doesn't melt or change the structure?

FURRER: It melts normally at 210°C, but it doesn't change the structure or removal efficiency.

T. R. THOMAS: From your experience with the WAK, how long have you had an AC/6120 bed in service and what is the iodine loading obtained?

FURRER: The sorption material was in for one year of continuous operation in a ring layer-filter. We reached a capacity of about 80% of iodine loading and had a removal efficiency of more than 99.9%.

NOBLE GAS SEPARATION WITH THE USE OF INORGANIC ADSORBENTS*

D. T. Pence, C. C. Chou, J. D. Christian, and W. J. Paplawsky
Science Applications, Inc.
4030 Sorrento Valley Boulevard
San Diego, California 92121

Abstract

A noble gas separation process is proposed for application to airborne nuclear fuel reprocessing plant effluents. The process involves the use of inorganic adsorbents for the removal of contaminant gases and noble gas separation through selective adsorption. Water and carbon dioxide are removed with selected zeolites that do not appreciably adsorb the noble gases. Xenon is essentially quantitatively removed with a specially developed adsorbent using conventional adsorption-desorption techniques. Oxygen is removed to low ppm levels with the use of a rapid cycle adsorption technique on a special adsorbent leaving a krypton-nitrogen mixture. Krypton is separated from nitrogen with a special adsorbent operated at about -80 ^{o}C. Because the separation process does not require high pressures and oxygen is readily removed to sufficiently limit ozone formation to insignificant levels, appreciable capital and operating cost savings with this process are possible compared with other proposed processes. In addition, the proposed process is safer to operate.

I. Introduction

A number of techniques have been proposed for noble gas separation from airborne nuclear fuel reprocessing plant effluents. Cryogenic distillation has received the most attention because the required equipment is similar to that used in air separation technology. Also, a cryogenic distillation process for separating krypton and xenon from a reprocessing plant off-gas stream has been demonstrated at the Idaho Chemical Reprocessing Plant;[1,2] however, the original design was intended for partial rather than complete removal of the noble gases.

A process is under development at Oak Ridge National Laboratory that involves the use of fluorocarbon absorption and selective distillation for product separation. This process has been described and discussed in several previous Air Cleaning Conference papers[3,4] and requires some pressurization and low-temperature operation.

Several processes have been proposed that involve a pressure-swing technique using charcoal adsorbents for noble gas separation, but have not been developed for reprocessing plant application.[5,6]

The process reported in this paper is being supported under a DOE-sponsored program for the development of an integrated off-gas treatment process for nuclear fuel reprocessing facilities. Because

*Work performed under USDOE (SRO) Contract EY-77-C-09-0979

the complete process scheme has only been recently developed and the patent application is still in progress, only a general description of the proposed process will be provided.

II. General Process Description

A schematic process flow diagram is shown in Figure 1.

NO_x and Semivolatile Removal

The dissolver off-gas is first passed through an NO_x adsorption tower and condenser where most of the NO_2 is converted to nitric acid for recycle to the dissolver. The remaining NO_2 and NO are then directed through an interchanger and a heater prior to entering an NO_x destructor.

The NO_x (primarily NO and NO_2) entering the destructor is catalytically reduced to nitrogen and water on a bed of hydrogen-form synthetic mordenite using ammonia as the reducing gas.[7,8,9] The catalyst bed temperature is maintained at about 400 °C. Most of the semivolatile compounds, such as ruthenium, are expected to plate-out on the NO_x destructor catalyst. In our laboratory tests, it has been observed that volatilized ruthenium can be removed on the catalyst bed with a decontamination factor (DF) of greater than 200 at airborne ruthenium concentrations equivalent to 0.01% volatility of the ruthenium present in the dissolver solution. This amount of ruthenium is probably an order of magnitude or so higher than that which will actually become volatilized, so it is a conservative estimate.

The attainable semivolatile DF has not yet been defined because of the sensitivity of our analytical techniques. These techniques are being improved to increase the attainable sensitivities.

After the NO_x destructor, the off-gas flows through the interchanger where it is cooled to about 150 °C while it is heating the feed gas to the NO_x destructor. The cooled gas then enters the iodine adsorbent bed where the iodine is removed. The iodine adsorbent will either be the German-developed, silver nitrate-impregnated, amorphous silicic acid catalyst material, AC 6120,[10] or silver-exchanged synthetic mordenite.[11] These materials, and others are being evaluated for this application in another recently initiated task of this DOE-sponsored program, and the results will be reported at a later meeting. Two iodine removal beds will be placed in parallel so one can be in service while the other can be replaced or regenerated.

It should be noted that the proposed component arrangement is conceptual and subject to change pending the results of the iodine adsorbent evaluation studies. There is some evidence[10] indicating AC 6120 material may perform better if it is located prior to the NO_x absorption column. Also, the affect of iodine on the NO_x destructor catalyst has not yet been determined.

Water Removal

After the iodine adsorbent bed, the off-gas is cooled to near ambient temperature, and the bulk of the water removed with a

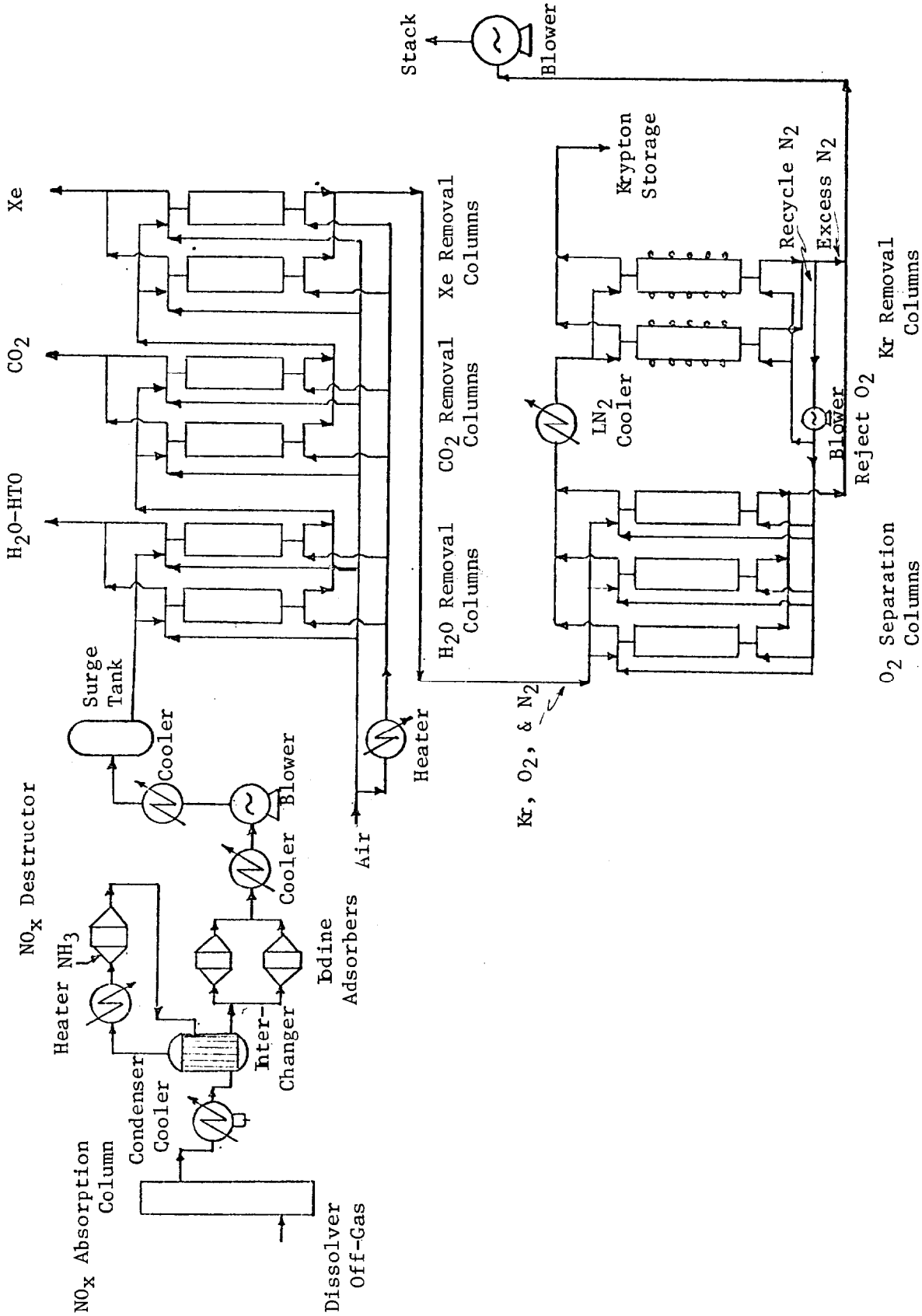

Figure 1. Schematic Flow Sheet For Noble Gas Separation With The Use Of Selective Inorganic Adsorbents

condenser. Type 3A zeolite is then used to remove the remaining water to about 1 ppm. The Type 3A zeolite is used because it will not appreciably coadsorb any of the other remaining gaseous species. Two water removal columns will be operated in parallel so that one can be regenerated while the other is in service. Before the water is removed, the water-laden column is given a short purge of air in the feed direction to ensure no residual contaminant gases other than water remain in the column.

Carbon Dioxide Removal

Following water removal, carbon-14 containing carbon dioxide is then selectively removed with Type 4A zeolite. The physical arrangement using two parallel adsorption beds is similar to that of the water removal step. The other remaining gaseous species, nitrogen, oxygen, xenon, and krypton, do not appreciably coadsorb with the carbon dioxide and are readily purged from the CO_2-loaded column with air prior to the regeneration step; the purged gas is added to the feed to the xenon removal column. Carbon dioxide DFs of greater than 100 have been demonstrated in laboratory tests.

Xenon Removal

Xenon is selectively removed from the remaining gases with a specially developed adsorbent in the same parallel bed arrangement as that for water and carbon dioxide. The xenon-adsorbent interaction is strong enough at ambient temperature and pressure to allow adsorption of up to several weight percent before xenon breaks through the column. This allows the xenon adsorption column to be in service many hours before regeneration becomes necessary. DFs for xenon separation of greater than 10^3 have been obtained using this technique. Unlike the water and carbon dioxide regeneration steps that require temperatures of about 250 ^{o}C and a gas stream purge for several hours, xenon can be readily desorbed from the adsorbent at a temperature of about 100 ^{o}C with a smaller gas purge. The size of the adsorbent bed is essentially the same as that for water and carbon dioxide.

Oxygen Separation

The next separation is oxygen from krypton and nitrogen which is also done by selective adsorption on a specially developed adsorbent material. Because the krypton-adsorbent interaction is stronger than the oxygen-adsorbent interaction, the krypton remains adsorbed on the column while oxygen passes through. Some of the nitrogen coadsorbs with the krypton limiting the loading capacity of the krypton on the adsorbent causing krypton breakthrough after a few minutes. Therefore, the separation is performed using a rapid adsorption-desorption technique. The best cycle time will depend on the selected operating conditions and adsorbent bed size. Preliminary results indicate the best cycle time is about 6 minutes while operating the bed near ambient temperature and pressure. A typical cycle would be feed for 3 minutes, forward purge with recycle nitrogen for 0.5-minute, and back-purge for about 2.5 minutes. To ensure adequate recovery of the adsorbed krypton, the back purge flow rate is about twice that of the feed. This will result in about a 67% dilution of the krypton, but it will reduce the oxygen content in the krypton-nitrogen mixture

to concentrations that limit ozone formation from oxygen radiolysis to an insignificant level. Oxygen concentrations in the krypton-nitrogen mixture on the order of 40 ppm and krypton DFs greater than 150 have been obtained using this technique through 15 cycles of operation without a measurable change in krypton DF or increase in oxygen concentration in the effluent. Because the cycle times are so short, accurate DFs are difficult to determine; and they may be considerably better than 150, but they are at least this great. A three-adsorbent bed arrangement is used for this separation to allow adequate purge of the krypton prior to being returned to service.

Krypton Removal

The separation of krypton from nitrogen is performed with the same adsorbent but operated at sub-ambient temperature and ambient pressure. Decontamination factors greater than 10^3 for the separation of krypton from nitrogen have been obtained with the adsorbent cooled to about -80 °C. A dual bed arrangement is used to allow recovery of the krypton-rich fraction while the other adsorbent bed is in service. Loading times of several hours of continuous operation are obtainable with the adsorbent bed at -80 °C. By heating the adsorbent bed to about ambient temperature with a slow purge, krypton concentration factors on the order of 10^4 are expected. Nitrogen is used as the purge gas for the krypton recovery beds; and after krypton is removed from the gas stream in the krypton removal beds, some of the nitrogen is recycled for desorption of the adsorbed krypton from the oxygen separation step. The cooled nitrogen will not be reheated prior to its use as a purge gas for krypton, and the oxygen separation beds will be cooled slightly. This procedure is expected to enhance the oxygen separation from the krypton.

If desired, the krypton can be purified further by collecting the desorbed krypton from the krypton removal beds with a liquid nitrogen-cooled krypton collection trap in a closed recirculating system.

III. Status Of Development

Initial evaluations for component-selective adsorption on various adsorbents were performed with the use of a modified gas chromatograph (GC). Small adsorption beds, 0.6-cm dia by 20-cm long columns, packed with adsorbents ground to 40-60 mesh were used. For the more promising adsorbents, the evaluations were performed with the same diameter but longer beds, 90-cm long columns. The GC was modified with additional switching valves so that several adsorption-desorption cycles could be performed.

Additional adsorbent evaluations were performed using 4.6-cm dia by 90-cm long columns packed with 10-20 mesh granular or beaded adsorbent materials. The flow rates used with the large columns were generally about 1 to 2 m^3/h. A test apparatus was constructed that allowed either single cycle or multicycle operation. Each of the separations has been demonstrated with the use of the large columns except the krypton-nitrogen separation at sub-ambient temperatures. A quadrupole mass spectrometer was used to verify the DFs. The feed gas composition used for the gaseous separations tests was as follows:

water, 40 °C dew point; carbon dioxide, about 300 ppm; oxygen, about 20%; xenon, 2500 ppm; krypton, 200 ppm; and the balance, nitrogen.

A small-scale engineering system is being designed that will provide integrated operation for the separation of water, carbon dioxide, xenon, oxygen, and krypton. The rapid cycle separation of the oxygen will be performed using microprocessor control of electronically operated valves.

IV. Comparison Of Proposed Separation Technique With Alternatives

The two main advantages of the proposed noble gas separation technique compared with alternative techniques are improved safety of operation and reduced capital and operating costs.

Improved safety of operation is obtained because none of the separation steps require high-pressure systems. The only pressures involved in the separations are the pressure drops across the adsorbent beds to maintain adequate flow. The only steps requiring pressurization in the process are: (1) the slight pressure buildup of the krypton recovery bed prior to venting and purging as it warms from sub-ambient to ambient temperature; and (2) pressurization for krypton storage, assuming steel cylinder storage.

Another, and perhaps the most important, improved safety feature of the proposed process, is the reduced ozone formation hazard. Because nearly all of the oxygen is removed from the feed stream before krypton is concentrated, the probability of ozone formation from radiolysis of oxygen by krypton-85 is reduced to essentially zero. This design would eliminate the need for including the oxygen recombiner currently being incorporated in many of the present designs to remove the oxygen prior to the cryogenic distillation unit.

The proposed noble gas separation process offers a number of economic advantages compared with other proposed processes:

1. Because high pressures are not required for the separations, considerable capital and operating cost savings can be realized by eliminating the need for pressure vessels and compressors.

2. The need for including an oxygen recombiner in the off-gas pretreatment train would be eliminated resulting in a substantial capital and operating cost savings.

3. Sub-ambient cooling is necessary for only one step in the process, and the lowest temperature required is about -80 °C, therefore reduced operating costs are expected compared with conventional cryogenic separation techniques.

4. Although a number of switching valves are involved, the separation columns are relatively simple in design and size and will have lower capital costs.

5. The separations process is readily amenable to remote operation and maintenance and requires less cell space. High maintenance

valves can be located for easy accessibility in a secondary containment-maintenance corridor.

At the completion of the small engineering-scale tests, the overall proposed system can be more clearly defined, and a more detailed cost analysis comparison will be performed.

V. References

1. C.L. Bendixsen and G.F. Offutt, Rare Gas Recovery Facility At The Idaho Cehmical Reprocessing Plant, IN-1221, (April 1969).

2. C.L. Bendixsen and F.O. German, 1974 Operation Of The ICPP Rare Gas Recovery Facility, ICP-1057 (March 1975).

3. M.J. Stephenson, et al., "Absorption Process For Removing Krypton From Off-Gas From An LMFBR Fuel Processing Plant," Proceedings, 13th AEC Air Cleaning Conference, CONF 740807, p. 263 (August 1974).

4. M.J. Stephenson and R.S. Eby, "Development Of The FASTER Process For Removing Krypton-85, Carbon-14, And Other Contaminants From The Off-Gas Of Fuel Reprocessing Plants," Proceedings, 14th ERDA Air Cleaning Conference, CONF 760822, p. 1017 (August 1976).

5. T. Kanazawa, et al., "Development Of The Cryogenic Selective Adsorption-Desorption Process On Removal Of Radioactive Noble Gases," Proceedings, 14th ERDA Air Cleaning Conference, CONF 760822, p. 964 (August 1976).

6. Y. Yuasa, et al., "Selective Adsorption-Desorption Method For The Enrichment Of Krypton," Proceedings, 13th AEC Air Cleaning Conference, CONF 740807, p. 177 (August 1974).

7. D.T. Pence and T.R. Thomas, "NO_x Abatement Using Ammonia With Zeolite Catalyst," Proceedings Of The AEC Pollution Control Conference, CONF 721030, p. 115 (October 25, 1972).

8. D.T. Pence and T.R. Thomas, "NO_x Abatement At Nuclear Processing Plants," Proceedings Of The 2nd AEC Environmental Protection Conference, WASH-1332(74) (April 16, 1974).

9. T.R. Thomas and D.H. Munger, An Evaluation Of NO_x Abatement By NH_3 Over Hydrogen Mordenite For Nuclear Fuel Reprocessing Plants, ICP-1133 (January 1978).

10. J.G. Wilhelm and J. Furrer, "Head-End Iodine Removal From A Reprocessing Plant With A Solid Adsorbent," Proceedings, 14th ERDA Air Cleaning Conference, CONF 760822, p. 447 (August 1976).

11. T.R. Thomas, et al., Airborne Elemental Iodine Loading Capacities Of Metal Zeolites And A Method For Recycling Silver Zeolite, ICP-1119 (July 1977).

DISCUSSION

STEVENSON: You indicated that your equipment is small. Could you give us an idea of column diameter for a typical 5 to 10 ton per day reprocessing plant?

PENCE: The size of the columns depends, of course, on the flow rate of the offgas to be treated. Assuming a dissolver offgas flow rate of 200 m^3/hr for a 5 MTHM/d reprocessing plant, the size of the columns would be on the order of 60 cm (2 ft) in diameter.

STEVENSON: Barnwell's flow rate is about 500 cfm.

PENCE: I know, but Barnwell's design is a little bit different from most of the proposed plants. I think the Exxon plant was 200 cfm and I think the European plants are normally in this range.

STEVENSON: What sort of velocity does this represent?

PENCE: Face velocities between 25 and 40 feet per minute.

STEVENSON: I was wondering then about heat transfer as heat transfer characteristics of packed beds are not very good and beds that size and larger don't do as well as small beds. You have only two traps shown. How fast can you cool down and heat up those traps in the krypton regeneration cycle? Is it feasible to cycle with only two traps?

PENCE: The desorption cycle time for water, carbon dioxide, and xenon removal steps are all shorter than the adsorption or leading times so that only two columns are required for separation. The desorption cycle for krypton during the oxygen separation step is nearly equal to that of the adsorption cycle so three adsorption beds will probably be required. We do not have enough information at this point to determine whether two or three beds will be required for the krypton recovery step.

STEVENSON: Your process is based on chromatographic separation. Have you considered the effect of radioactive heat of decay on the sorption-desorption characteristics of the solid sorbent?

PENCE: We do not expect the decay heat to significantly affect any of the removal or separation steps except the final concentration step because the adsorbed krypton concentration will always be quite low. In the final concentration step, the incoming gas and adsorption column will be cooled sufficiently to compensate for the decay heat.

STEVENSON: You indicated that your system does not require a process gas compressor. What is the difference between your "blower" and a gas compressor? What do you define as a high pressure process?

PENCE: I do not care to get into a discussion regarding the differences between a blower and a compressor, but in the presentation, I used the term "blower" rather than "compressor" to indicate the pressure drops in the system are on the order of cm (in.) of water rather than thousands of Pascals (tens to hundreds of psi). I would consider anything over about 10 KPa ($\sim$70 psi) as high pressure with regard to this discussion. Of course, this is an arbitrary definition on my part.

STEVENSON: Fluorocarbon-based systems have been running at an absorber pressure

of only 100 psig for the last two years, whereas the cryogenic process operates in the neighborhood of 60 pounds. These are not high pressure processes so I was wondering what you were comparing them against.

PENCE: Operating costs and the need for high pressure. If you have to compress, that's one of the biggest energy users we have. That's the point I was trying to make.

STEVENSON: We ran into the effect where you have radiation heat in a gas chromatograph that effects the loading characteristics of the components and the way the curves come off the chromatographic beds. I know your system is based primarily on the operation of a chromatograph. You've worked with cold krypton. Have you assessed the effect of hot krypton on the elution of the various peaks through the columns?

PENCE: I don't understand where there would be such an effect. The only time there would be a heating effect would be when krypton is concentrated and we don't concentrate the krypton until the final bed. Up to that point, the krypton is still around 200-250 ppm and we don't expect the heating of that to be significant because it's not absorbing. It's just a pass-through system.

STEVENSON: Where you hold the krypton on the bed, you can have a heat effect. It can warm it up and it can affect the desorption characteristics of the bed.

PENCE: It's possible this could occur on the final bed, but we don't load it at any step other than the oxygen separation. That could become a problem except that the enrichment factor is very small and it's very rapid.

STEVENSON: You cite low pressure as being a safety feature and yet you point out that your process requires a high pressure bottling step for final storage of the Kr-85. This step is the largest hazard normally associated with the other krypton removal processes, as it is for yours, also. Yet, you say your process is low pressure and is therefore safer than the others. Why?

PENCE: With regard to storage pressures, I assumed storage would be in high-pressure steel cylinders, but this does not really have anything to do with the separation and recovery processes used.

VON AMMON: I'm sure you are aware of the German development of the company Bachbahlforschen in Issen which developed an adsorbent material for the separation of nitrogen and oxygen on the basis of coal with molecular sieve properties. Now, my question is, could you give us a small hint concerning your adsorbent? Has it something to do with this coal based molecular sieve?

PENCE: The adsorbent material we use for the oxygen separation step is completely inorganic in nature.

CHENG: It wasn't clear to me from the flow charts how you plan to regenerate the oxygen removal beds.

PENCE: During the oxygen separation step, the adsorbent adsorbs krypton and nitrogen, and the oxygen is not significantly adsorbed, but passes on through the column. The krypton is recovered by back-purging with nitrogen. The back-purge flow rate is twice that of the column feed, and this increased flow strips the krypton from the oxygen separation column. The entire oxygen separation process cycle is performed near ambient pressure.

CHENG: Do you expect much carry-over of radioactive material from the purge stream?

PENCE: No, we don't.

WILHELM: How many valves do you need for this process?

PENCE: Five valves per column on the rapid cycle adsorption and, for the others, about the same, or maybe six. Five for each column and for most operations six. We have five in each column for the test setup we're using. We are only doing single column studies now.

WILHELM: That's what I'd like to comment on. I assume you need a total of about 100 valves. Each has to be leak tight and have a high reliability. I think that might be a problem for this process.

PENCE: There is only one place where trouble may occur and you need that many valves no matter what process you use. There are five valves per column and at this lower point you're down to krypton and nothing else. Since krypton doesn't contaminate anything permanently, if you have a defective valve you can back-purge it, bring it out, and do hands-on maintenance. I would expect a reasonable failure rate. I don't know what this is, but if the valves are easy to get at and repair, I think it would be acceptable.

WILHELM: I would expect some corrosion. Also, rubidium comes from the krypton and this will work on the valves, too.

VAN BRUNT: What about temperature effects and the effects of rapid recycling on the metal in the high radiation field? I assume that a large number of recycles might affect the wells and cause problems. Have you assessed that? I'm beginning to think you might have reliability problems that you might not otherwise have in a process that remains either cold or warm.

PENCE: I don't think we will have a materials problem because we don't concentrate the krypton until the last step. Until then, the columns operate under atmospheric conditions. We have not yet made an in-depth evaluation of this at this time. Because the temperature swing will only be about 120°C, we do not expect the problems to be unsolvable, though. Therefore, I don't see where this process will be any different than any of the others.

VAN BRUNT: I was referring to where you have temperature differences, because you're cycling so many times from -100 to room temperature.

BROWN: Will you be using the sensible heat of your very low purge in the krypton concentration system to heat up that system from -100 to room temperature or will you be using external heat transfer?

PENCE: Desorption of the krypton during the oxygen separation step is accomplished primarily by the change in partial pressure of the krypton-free purge gas rather than in the use of external heat.

BROWN: The combined time for the heating and cooling must be equal to or less than the time of your adsorption. Have you worked out what the energy balance is and the times required?

PENCE: No, we haven't gone to that detail for several reasons. First, we don't know for certain how long our cycle time will be. It may be anywhere from

1-3 hr. We're not certain at this point whether we'll have to use a third column or can work with two.

ALEXANDER: I was interested in the fact that you said you expected the ruthenium to plate out on your catalyst. Do you expect that to affect the performance of the catalyst adversely and do you have large quantities of ruthenium?

PENCE: Considering the expected amount of volatile ruthenium, we do not expect the catalyst material to lose its activity. However, we have observed some variation in the NO_x catalyst efficiency with increasing ruthenium plate-out. Unfortunately, we also experienced operational difficulties with our NO_x analyzer. We will repeat these experiments to verify the effect, if any, of the ruthenium plate-out on the catalyst material. In our initial experiments, we also used 10-to-100 times greater ruthenium concentrations than we expect in an actual reprocessing plant off-gas in order to ensure adequate sensitivities in our ruthenium analyses. We believe that we have refined the ruthenium analytical technique sufficiently so that we can use lower ruthenium concentrations in the off-gas.

DIETZ: I'd just like to point out that flake mineralological graphite is a very good trap for rubidium and could be used to localize the krypton decay product. You can clean up your gas mixture if you have a little bit of powdered graphite in there. I have some evidence for it.

PENCE: Many of the zeolites would serve the same purpose and would probably be less expensive.

NITROGEN OXIDE ABSORPTION INTO WATER AND DILUTE NITRIC ACID IN AN ENGINEERING-SCALE SIEVE-PLATE COLUMN WITH PLATES DESIGNED FOR HIGH GAS-LIQUID INTERFACIAL AREA*

R. M. Counce, W. S. Groenier,
J. A. Klein, and J. J. Perona
Oak Ridge National Laboratory
Oak Ridge, Tennessee 37830

Abstract

The absorption of gaseous NO_x compounds into water and dilute HNO_3 was studied in a three-stage sieve-plate column with plates designed for high gas-liquid interfacial area. The performance of the column was measured while several operating parameters were varied. The results of the study indicate the importance of three mechanisms in the absorption of gaseous NO_x ($NO_2 + 2N_2O_4 + NO$) compounds: (1) the absorption of NO_2^* ($NO_2 + 2N_2O_4$) which results in production of liquid HNO_3 and HNO_2; (2) the dissociation of the liquid HNO_2 into HNO_3 and gaseous NO; and (3) the gas-phase oxidation of NO to NO_2. A mathematical model based on these mechanisms was developed and is presented to explain the observed phenomena.

I. Introduction

The removal of NO_x compounds from gas streams is important in the reprocessing of nuclear fuels because many of the off-gas streams in such a facility will contain these compounds in concentrations to interfere with further gas cleanup operations or exceed discharge limits. Composition of the feed-gas stream for these studies was prepared to simulate the product gas resulting from the fuel dissolution step. This product gas contains a large amount of steam as well as air and NO_x compounds. The mechanism of NO_x removal considered in this study is based on: (1) the absorption of NO_2^* ($NO_2 + 2N_2O_4$) into dilute HNO_3, which results in the production of liquid HNO_3 and HNO_2; (2) the dissociation of liquid HNO_2 into liquid HNO_3 and gaseous NO; and (3) the gas-phase oxidation of NO to NO_2. This method is attractive for the proposed application because the HNO_3 produced could be recycled for use in the plant.

Commercial NO_x scrubbing equipment, usually bubble-cap columns, is based on HNO_3-industry experience. Since the absorption reactions are exothermic, commercial scrubbers generally have cooling coils in the froth of each column stage. The absorber under development is intended for operation in a radioactive environment, and hence the design of the scrubber should be as simple as possible to facilitate maintenance. The scrubber system under investigation meets this requirement. In this system, dilute HNO_3 is recirculated through the column; the water input is provided by condensing steam from the feed gas. The column under development is designed to operate at high liquid flow rates, which eliminates the need for internal cooling. Heat associated with the absorption reactions and condensing steam is removed from the scrubber liquid in external heat exchangers.

*Research sponsored by the Nuclear Power Development Division, U.S. Department of Energy under contract W-7405-eng-26 with the Union Carbide Corporation.

II. Experimental Apparatus and Procedure

The flowsheet for the experiment is shown in Fig. 1. The NO_x scrubber is a three-stage sieve-plate column constructed of 0.076-m-ID by 0.254-m-long sections of Pyrex glass pipe. The plates and downcomers, shown in Fig. 2, are constructed of stainless steel.

The free area per plate, 0.6%, is relatively low when compared with that of a typical sieve-plate column.[1] This is because the column was designed for high ratios of liquid flow rate to gas flow rate (L/G) in an attempt to dissipate the heat generated from the absorption reactions and the condensation of the steam with increased liquid flow rates; this also provides increased gas residence time in the column.

Other equipment used in the experiment include: a scrubber liquid holdup tank, pump, rotameter, and heat exchanger; a gaseous NO_2^* supply system; and process air, steam, and water supply systems. The gas-handling equipment includes a NO_2^*-air rotameter, an effluent gas holdup tank, an infrared analyzer to determine the concentrations of NO_x in the feed and effluent gas streams, a calibration gas supply system, and an exhaust gas system.

The system is normally operated by pumping the scrubber liquid from the scrubber liquid holdup tank and metering it through heat exchangers to the column. Upon leaving the column, the effluent liquid stream flows by gravity to the return tank. Gaseous NO_2^* is supplied to the system by vaporizing commercially obtained liquid NO_2^* in a temperature-regulated water bath. Process air is metered with the NO_2^* by a rotameter and is blended with steam in a common feed stream to the column. Steam flow is controlled by maintaining a constant differential pressure across a calibrated capillary tube. The system is allowed to reach steady-state conditions before data are taken. The system is considered to be at steady state when all gas and liquid flow rates, column temperatures, and NO_x concentrations in the feed and effluent streams have shown no change over a 30-min interval. The gas stream is sampled before and after leaving each stage. The gas-sample streams, with the exception of the feed stream, are passed through a sample holdup tank to provide sufficient time for the NO_x gases to reach the NO_2^* state for analysis. The sample streams are then metered to an infrared analyzer (Lira Model 202), which is specific for NO_2^* and requires a gas with a known air-NO_2^* content for the purpose of calibration. Samples of the scrubber liquid are taken entering and leaving the column. These liquid samples are analyzed for HNO_3 and HNO_2 by standard techniques. Plate and column efficiencies are then calculated from the gas concentration differences.

III. Theoretical Development

The overall chemical reactions involved in the steady-state absorption of NO_x compounds into water or dilute HNO_3 appear to be adequately represented as follows:

$$2NO_2(g) \rightleftharpoons N_2O_4(g) , \tag{1}$$

$$N_2O_4(g) \rightleftharpoons N_2O_4(\ell) , \tag{2}$$

$$N_2O_4(\ell) + H_2O(\ell) \rightarrow HNO_3(\ell) + HNO_2(\ell) , \tag{3}$$

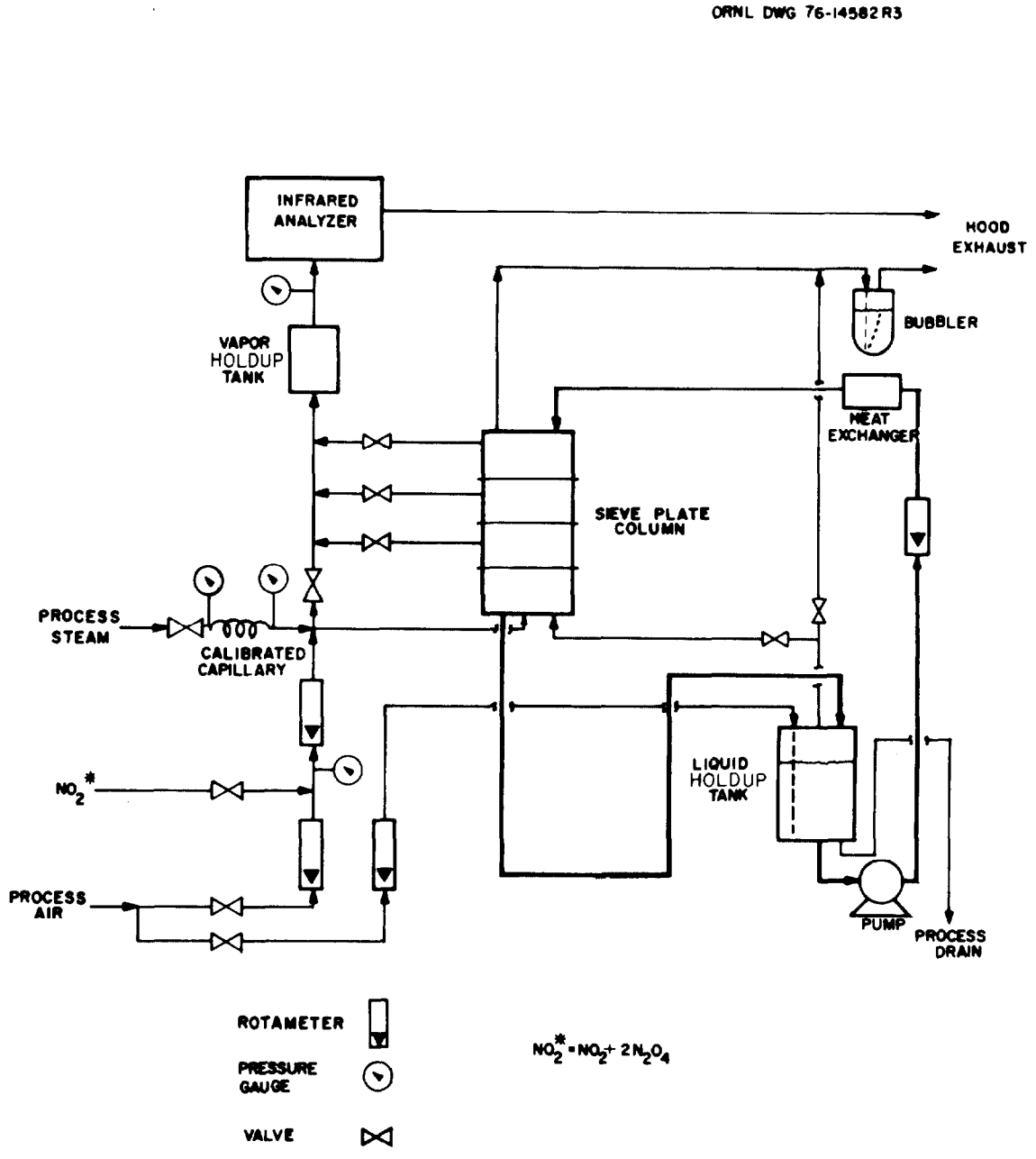

FIGURE 1
FLOWSHEET OF EQUIPMENT USED IN NO_x SCRUBBING EXPERIMENT.

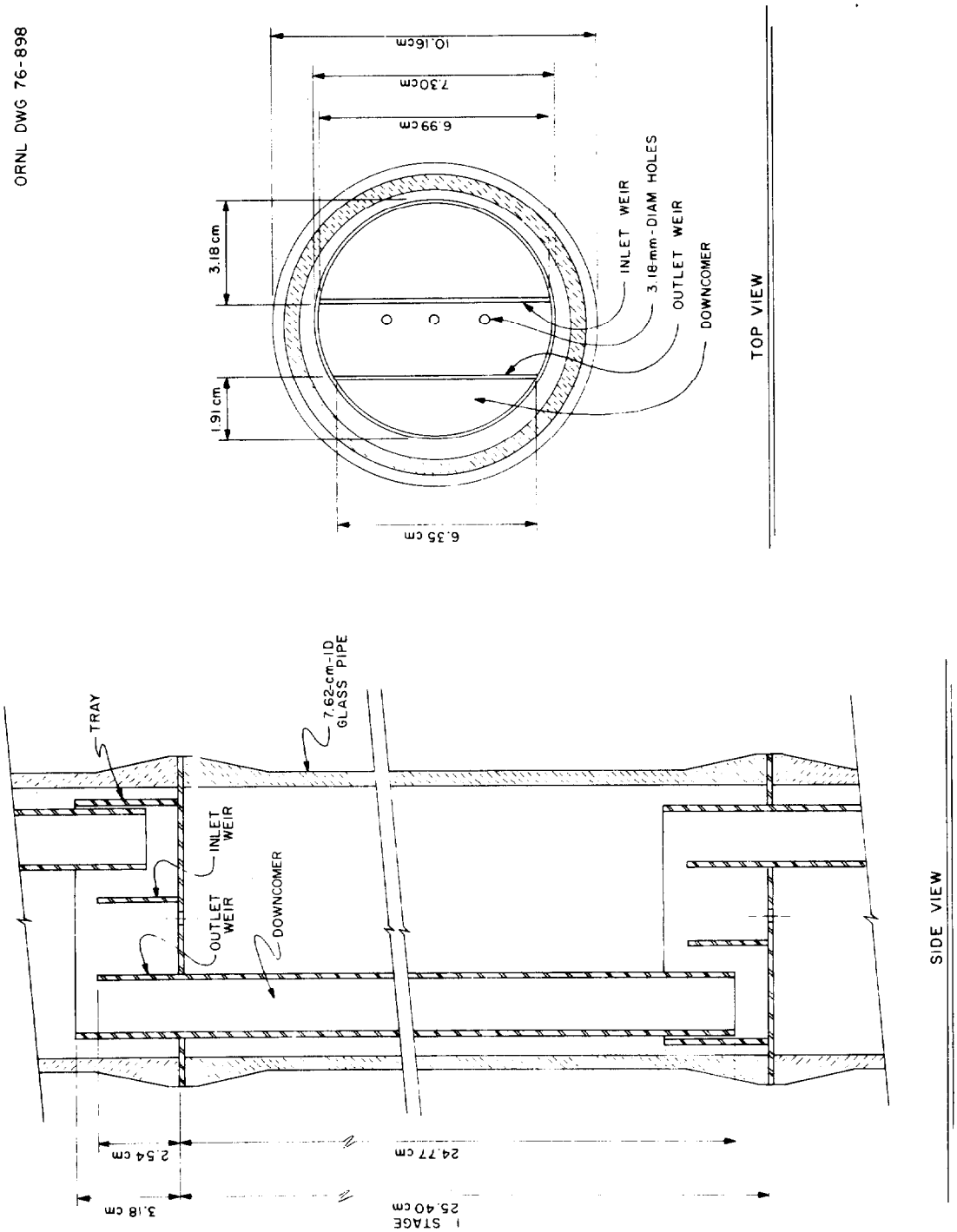

FIGURE 2
TYPICAL PLATE AND DOWNCOMER ARRANGEMENT FOR SIEVE-PLATE COLUMN.

$$3HNO_2(\ell) \rightleftarrows H_2O(\ell) + HNO_3(\ell) + 2NO(g) , \quad (4)$$

$$2NO(g) + O_2(g) \rightarrow 2NO_2(g) , \quad (5)$$

where (g) and (ℓ) indicate gas and liquid species respectively. A review of the literature indicates that the following assumptions about the overall reactions may be made:

1. The NO_2 and N_2O_4 are in continuous gas-phase equilibrium.[2-4]
2. Reaction of N_2O_4 with water proceeds by means of a fast-first-order liquid-phase reaction.[4-16] (For NO_2^* partial pressures >0.01 atm, this is the predominant absorption reaction).[17]
3. The HNO_2 decomposes exclusively by Eq. (4).[18-21]
4. Oxidation of NO occurs as an overall third-order gas-phase reaction.[22-27]

The following additional assumptions were made concerning the characteristics of the column gas and liquid phases:

1. The froth on the sieve plates is well mixed.
2. No backmixing occurs in the gas traveling through the sieve-plate froth.
3. The changes in gas flow rate through the froth and through the gas space between plates are considered to be negligible while in that particular phase.
4. The gases behave ideally.
5. The gas in the gas space between the plates is well mixed.

The NO_2-N_2O_4 equilibrium and the absorption of gaseous N_2O_4 into water or dilute HNO_3 are simulated mathematically and combined into an equation for N_2O_4 absorption in the froth on the sieve plates. The dissociation of liquid HNO_2 to gaseous NO is also treated mathematically. By using the gas-phase reaction rate for NO oxidation, a mathematical expression is developed for the extent of this reaction in the gas space between the sieve plates. These three equations are combined in an overall mathematical model for NO_x removal in a multistage-plate column.

The equilibrium between N_2O_4 and NO_2 can be defined by[2-4]

$$K_{p,1} = \frac{P^2_{NO_2}}{P_{N_2O_4}} , \quad (6)$$

where

$K_{p,1}$ = pressure equilibrium constant for reaction (1), atm;

P_{NO_2} = partial pressure of NO_2, atm; and

$P_{N_2O_4}$ = partial pressure of N_2O_4, atm.

If α represents the degree of dissociation of N_2O_4 and the partial pressures of N_2O_4 and NO_2 are expressed in terms of NO_2^* and α, then

$$P_{N_2O_4} = (1 - \alpha)P_{NO_2}^*/2 \tag{7}$$

and

$$P_{NO_2} = \alpha P_{NO_2}^* \ . \tag{8}$$

where

$$P_{NO_2}^* = P_{NO_2} + 2P_{N_2O_4}, \text{ atm.}$$

Combination and rearrangement of the above equations results in the following equation for α:

$$\alpha = \frac{-K_{p,1} + K_{p,1}\sqrt{1 + 8P_{NO_2}^*/K_{p,1}}}{4P_{NO_2}^*} \ . \tag{9}$$

The local absorption rate for NO_2^* into dilute HNO_3, neglecting gas-phase resistance, can be expressed as:

$$\bar{R}_{NO_2}^* = 2\sqrt{(D_{N_2O_4,H_2O})k_3}\ (P_{N_2O_4}/He_{N_2O_4}) \ , \tag{10}$$

where

$\bar{R}_{NO_2}^*$ = local absorption rate of NO_2^* per unit area, kg.moles/m^2 sec,

$D_{N_2O_4,\ H_2O}$ = diffusivity of N_2O_4 in H_2O, m^2/sec,

k_3 = pseudo-first-order reaction rate constant, sec^{-1}; and

$He_{N_2O_4}$ = Henry's law constant for the solution of N_2O_4 in H_2O.

Utilizing Eq. (10) a balance for NO_2^* around a differential element of froth is developed, incorporating the following definition:

$$P_{NO_2}^{*} = P_{NO_2,\,in}^{*}\,(1 - X_{NO_2}^{*}) \,, \tag{11}$$

where

$P_{NO_2}^{*}$ = partial pressure of NO_2^{*}, atm;

$P_{NO_2,\,in}^{*}$ = partial pressure of NO_2^{*} entering the froth, atm; and

$X_{NO_2}^{*}$ = conversion of NO_2^{*}, the ratio of the change in the partial pressure of NO_2^{*} to the partial pressure of NO_2^{*} entering the froth of a given plate;

and the equilibrium relationship between N_2O_4 and NO_2 into the differential NO_2^{*} balance. Integrating over the volume of froth per plate, the following equation may be obtained:

$$\frac{\phi\sqrt{(D_{N_2O_4,H_2O})k_3}\;aRTV_{FR}}{GHe_{N_2O_4}} + \frac{2}{\phi}\left[\ell n\left(\frac{\sqrt{1 + 2\phi - 2\phi X_{NO_2}^{*}} - 1}{\sqrt{1 + 2\phi} - 1}\right)\right.$$

$$\left. + \frac{\sqrt{1 + 2\phi - 2\phi X_{NO_2}^{*}} - \sqrt{1 + 2\phi}}{(\sqrt{1 + 2\phi - 2\phi X_{NO_2}^{*}} - 1)(\sqrt{1 + 2\phi} - 1)}\right] = 0 \,, \tag{12}$$

where

ϕ = $4P_{NO_2,\,in}^{*}/K_{p,1}$;

a = gas-liquid interfacial area per unit volume of froth, m^{-1};

R = gas constant, m^3 atm/kg.mole K;

T = froth temperature, K;

V_{FR} = froth volume, m^3; and

G = superficial gas volumetric flow rate, m^3/sec .

Solution of this equation involves finding the root, $X_{NO_2}^{*}$, between zero and one.

The model for the decomposition of HNO_2 in the froth on the sieve plates presumes equilibrium of Eq. (4) as indicated by:(18-21)

$$K_{p,4} = \frac{(C_{H^+})(C_{NO_3^-})(P_{NO})^2}{C^3_{HNO_2}} . \quad (13)$$

where

$K_{p,4}$ = pressure equilibrium constant for reaction (4), m^3 atm^2/kg·mole;

C_{H^+} = liquid concentration of H^+, kg·mole/m^3;

$C_{NO_3^-}$ = liquid concentration of NO_3^-, kg·mole/m^3;

P_{NO} = partial pressure of NO, atm; and

C_{HNO_2} = liquid concentration of HNO_2, kg·mole/m^3.

Because the froth is considered to be perfectly mixed,

$$C_{HNO_2} = C^*_{HNO_2, \text{ in}} (1 - X_{HNO_2}), \quad (14)$$

where

$C^*_{HNO_2, \text{ in}}$ = concentration of liquid HNO_2 resulting from the HNO_2 in the incoming liquid stream and production from absorption reactions, kg·mole/m^3; and

X_{HNO_2} = conversion of HNO_2, the concentration decomposing per plate divided by $C^*_{HNO_2, \text{ in}}$.

A mole of NO is produced for each 3/2 moles of HNO_2 decomposed; therefore, the following relationship may be used to predict the partial pressure of NO desorbed per plate:

$$\Delta P_{NO} = (2/3)(L/G)\, R\, T C^*_{HNO_2, \text{ in}} X_{HNO_2} \quad (15)$$

where

L = liquid flow rate, m^3/sec .

Because equilibrium is approached by the decomposition of liquid HNO_2, Eq. (13) may be rearranged into the following form, using relationships given in Eqs. (14) and (15):

$$K_{p,4}[C^{*}_{HNO_2,in}(1 - X_{HNO_2})]^3 - (C_{H^+})(C_{NO_3^-})[P_{NO,in} + (2/3)(L/G)RTC^{*}_{HNO_2,in}X_{HNO_2}]^2 = 0 \ , \quad (16)$$

where

$P_{NO,\ in}$ = partial pressure of NO entering the froth, atm .

The solution of the equation involves finding the positive and real root, X_{HNO_2}, of this third-degree polynomial.

The model for NO oxidation in the free volume between the sieve plates is based on the third-order gas-space reaction of NO and oxygen. The reaction rate is expressed as:

$$\bar{r}_{NO} = k_5 P^2_{NO} P_{O_2} \ , \quad (17)$$

where

$\bar{r}_{NO}$ = local reaction rate of the oxidation of NO, atm/sec;

k_5 = reaction rate constant for reaction (5), $atm^{-2}\ sec^{-1}$;

P_{NO} = partial pressure of NO, atm; and

P_{O_2} = partial pressure of O_2, atm .

Utilizing Eq. (17) in developing a NO balance around a differential element of free space between the plates, and incorporating the following definitions:

$$P_{NO} = P_{NO,\ in}\ (1 - X_{NO}) \quad (18)$$

and

$$P_{O_2} = P_{O_2,\ in}\ [\ 1 - (P_{NO,\ in}/2P_{O_2,\ in})\ X_{NO}] \ , \quad (19)$$

where

$P_{NO,\ in}$ = the partial pressure of NO entering the gas space, atm;

X_{NO} = the conversion of NO in the free space between the sieve plates, ratio of the partial pressure of NO oxidized to the partial pressure of NO entering the gas space, dimensionless; and

$P_{O_2,\ in}$ = the partial pressure of O_2 entering the gas space, atm.

Integrating over the free space between the plates yields:

$$-X_{NO} + k_5 P_{NO,in} P_{O_2,in} \left[1 - \left(\frac{P_{NO,in}}{P_{O_2,in}} + 2 \right) X_{NO} + \left(\frac{P_{NO,in}}{P_{O_2,in}} + 1 \right) X_{NO}^2 - \left(\frac{P_{NO,in}}{2P_{O_2,in}} \right) X_{NO}^3 \right] \tau = 0 \ , \qquad (20)$$

where

τ = the gas residence time between the sieve plates, sec.

The solution of this equation involves finding the real and positive root, X_{NO}, of this polynomial.

The overall model for NO_x removal is based on the mathematical simulations developed earlier for the NO_2^* absorption and HNO_2 decomposition in the froth on a sieve plate and NO oxidation in the gas spaces between the sieve plates.

The steady-state acid molarities were calculated using the conversions of NO_2^* and HNO_2 and the stoichiometry of Eqs. (1-4). For calculations involving the recycle of the scrubber liquid, the liquid feed stream to the column was equal in concentration to the effluent-scrubber liquid stream. Steady-state acid concentrations are determined through repeated iterations of the column model, beginning with initial acid concentrations of near zero. Reaching steady state in the liquid phase coincided with establishing steady state in the gas phase for the described calculations. The model allows for adjustment of the gas density upon leaving the froth and again upon leaving the gas space. The subscripts j and k are used to indicate the stage number in a column and the position of the gas in a particular stage respectively. For gas entering the froth of plate j, k = 1; for gas leaving the froth of plate j, k = 2. The partial pressures of NO_2^*, NO, nitrogen, and oxygen of a gas stream entering the froth on stage j are indicated by $P_{NO_2^*,j,\ k=1}$, $P_{NO,j,k=1}$, $P_{N_2,j,k=1}$, and $P_{O_2,j,k=1}$ respectively. The model begins at the first plate and works upward. The partial pressures of the components leaving the froth are indicated by:

$$P_{NO_2^*,j,k=2} = P_{NO_2^*,j,k=1}(1 - X_{NO_2^*})/(1 - \varepsilon'''_{k=1} X_{NO_x}) \ , \qquad (21)$$

$$P_{NO,j,k=2} = [P_{NO,j,k=1} + \Delta P_{NO,j}]/(1 - \varepsilon'''_{k=1} X_{NO_x}) \ , \qquad (22)$$

$$P_{N_2,j,k=2} = P_{N_2,j,k-1}/(1 - \varepsilon'''_{k=1} X_{NO_x}) \ , \qquad (23)$$

and

$$P_{O_2,j,k=2} = P_{O_2,j,k=1}/(1 - \varepsilon''_{k=1} X_{NO_x}) \quad , \tag{24}$$

where

X_{NO_x} = conversion of NO_x, the ratio of the change in the partial pressure of NO_x entering the froth of a given plate.

Those leaving the gas space of stage j or entering stage j+1 are indicated by:

$$P^*_{NO_2,j+1,k=1} = [P^*_{NO_2,j,k=2} + P_{NO,j,k=2} X_{NO}]/(1 - \varepsilon''_{k=2} X_{NO}) \quad , \tag{25}$$

$$P_{NO,j+1,k=1} = P_{NO,j,k=2}(1 - X_{NO})/(1 - \varepsilon''_{k=2} X_{NO}) \quad , \tag{26}$$

$$P_{N_2,j+1,k=1} = P_{N_2,j,k=2}/(1 - \varepsilon''_{k=2} X_{NO}) \quad , \tag{27}$$

and

$$P_{O_2,j+1,k=1} = P_{O_2,j,k=2}\left(1 - \frac{P_{NO,in}}{2P_{O_2,in}} X_{NO}\right)/(1 - \varepsilon''_{k=2} X_{NO}) \quad . \tag{28}$$

The partial pressures of the gas components as well as the gas flow rates are corrected for bulk removal of the gas-phase components. This correction may be made by division or multiplication by $(1 - \varepsilon'')$, where ε'' is the fractional volume change due to removal of the gas components (k = 1 for the froth and k = 2 for the gas space). The quantities $X^*_{NO_2}$, $\Delta P_{NO,j}$, and X_{NO} are found using Eqs. (12), (15), and (20). Solution of Eq. (15) requires prior solution of Eq. (16). A multistage column may be modeled by letting j assume values from one to the number of required stages, provided the basic removal mechanisms remain valid.

IV. Experimental Results

In order to calculate the column performance, it is necessary to have numerical values for the appropriate equilibrium, kinetic, and transfer constants. The values of $K_{p,1}$ used in this study were obtained from a correlation by Hoftyzer and Kwanten[4] based on the work of Verhoek and Daniels.[3] The values of $\sqrt{D_{N_2O_4,\ H_2O}\, k_3}/He_{N_2O_4}$ used to calculate the absorption of N_2O_4 were also obtained from a correlation by Hoftyzer and Kwanten.[4] Abel's equilibrium constant as a function of temperature was used to describe the decomposition of HNO_2.[18-21] The rate constant for the oxidation of NO was derived as a function of temperature from the work of Greig and Hall.[27] The gas-liquid interfacial area was determined experimentally for the case with no steam in the feed gas by utilizing

the absorption of CO_2 into NaOH solutions, as described by Danckwerts.[28] These results are summarized in Fig. 3. The interfacial area of the bottom tray for the case when steam is present in the feed gas was estimated utilizing Eq. (12), and the experimental data given in Table I for nominal run conditions.

The nominal run conditions were:

1. scrubber liquid flow rate, 0.175×10^{-4} or 0.350×10^{-4} m^3/sec;
2. combined air and NO_2^* flow rates, 2.0×10^{-4} m^3/sec;
3. steam flow rate, 3.7 kg of steam per m^3 of air and NO_2^*;
4. inlet scrubber temperature, 298 K;
5. feed gas temperature, 363 K;
6. scrubber molarity, ~2.0;
7. feed gas partial pressure of NO_2^*, 0.31 atm;
8. total pressure, 1.1 atm.

A series of experiments was performed, as shown in Table I, in which the absorption of NO_2^* was studied using a single plate in order to evaluate the validity of Eq. (11) and the selected constants. This was accomplished by measuring the partial pressure of NO_2^* in N_2 before and after it was passed through the sieve-plate froth. The scrubber liquid for these runs was water flowing in a single pass through the column. These results are given in Table I. A representative experimental series showing experimental and model-predicted NO_2^* absorption or conversion is shown for various feed partial pressures of NO_2^* in Fig. 4. In general, NO_2^* conversion increases with increased partial pressures of NO_2^* and increased liquid flow rates and decreases with increased superficial gas flow rates. The presence of steam was shown to greatly enhance the absorption of NO_2^* in these experiments, involving a single sieve plate.

The removal of gaseous NO_x compounds depends not only on the absorption of NO_2^*, but also on the desorption and subsequent gas-phase oxidation of NO. The model predictions for the three-stage column performance provide for these phenomena as indicated previously.

The buildup of HNO_2 in the liquid phase for runs involving liquid recycle is shown in Fig. 5. The attainment of steady state appears to be closely related to reaching a steady-state concentration of HNO_2 in the recirculating scrubber liquid. As the concentration of HNO_2 increases in the scrubber liquid, the overall scrubber efficiency or conversion of NO_x is shown to decrease. The model-predicted conversion of NO_x behaves similarily as shown in Fig. 6, in which other conditions were approximately as experimental run 42 given in Tables II and III.

The model-predicted gaseous NO_x profile in the column is compared with that calculated from the experimental data of run 53 in Table IV. Plates are numbered from bottom to top. There was no steam in the feed gas for this experiment. The model-predicted profiles are very close to the experimentally determined profiles.

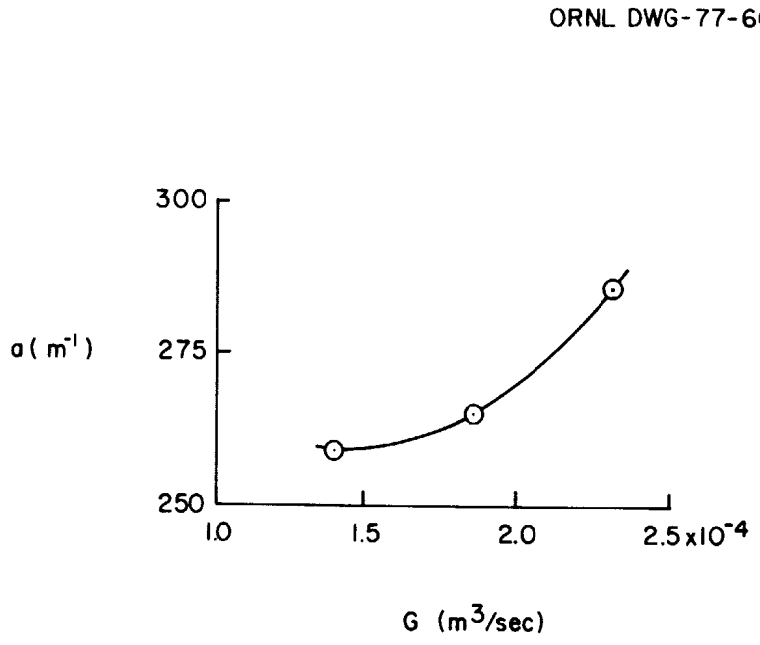

FIGURE 3
CORRELATION OF EXPERIMENTALLY DETERMINED GAS-LIQUID INTERFACIAL AREA VS GAS FLOW RATE FOR A SINGLE-STAGE SIEVE-PLATE COLUMN.

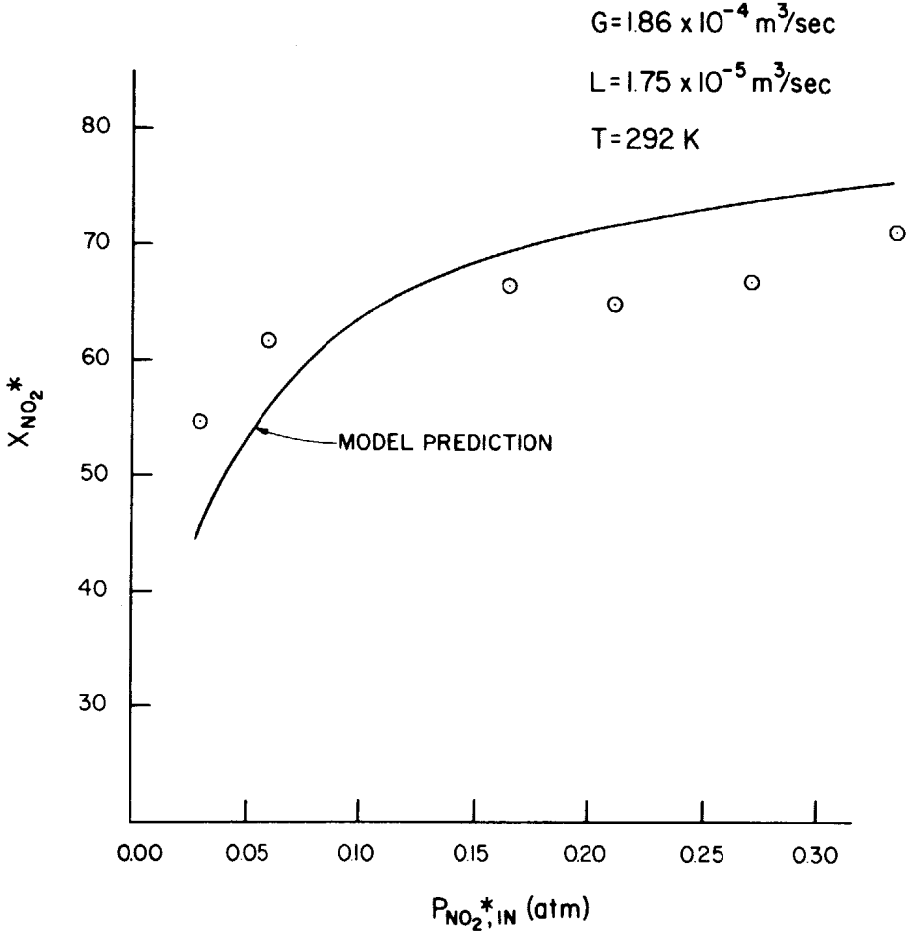

FIGURE 4
EXPERIMENTAL AND MODEL PREDICTED NO_2^* ABSORPTION VS THE PARTIAL PRESSURE OF NO_2^* ENTERING THE TRAY AT A TOTAL GAS FLOW RATE OF 1.86×10^{-4} m^3/sec IN A SINGLE-PLATE COLUMN.

Table I. Steady-state NO_2^* scrubbing data for a single sieve plate and a nonrecirculating scrubber liquid

Run No.	$P^*_{NO_2,in}$ (atm)	$P^*_{NO_2,out}$ (atm)	$T_{G,in}$ (K)	$T_{G,out}$ (K)	T_L (K)	G (std m^3/sec)	F_{STEAM} (kg/sec)	L (m^3/sec)	a (m^2/m^3)
55a	0.026	0.012	293	297	292	2.0×10^{-4}	0	1.75×10^{-5}	
55b	0.051	0.020	294	297	292	2.0×10^{-4}	0	1.75×10^{-5}	
55c	0.101	0.040	294	297	292	2.0×10^{-4}	0	1.75×10^{-5}	
55d	0.161	0.059	294	297	292	2.0×10^{-4}	0	1.75×10^{-5}	
55e	0.207	0.081	294	297	292	2.0×10^{-4}	0	1.75×10^{-5}	
55f	0.267	0.103	294	297	292	2.0×10^{-4}	0	1.75×10^{-5}	
55g	0.330	0.117	294	297	292	2.0×10^{-4}	0	1.75×10^{-5}	
56a	0.035	0.013	294	298	293	1.5×10^{-4}	0	1.75×10^{-5}	
56b	0.053	0.017	294	298	293	1.5×10^{-4}	0	1.75×10^{-5}	
56c	0.107	0.035	294	298	293	1.5×10^{-4}	0	1.75×10^{-5}	
56d	0.167	0.057	294	298	293	1.5×10^{-4}	0	1.75×10^{-5}	
56e	0.187	0.075	294	298	293	1.5×10^{-4}	0	1.75×10^{-5}	
56f	0.260	0.088	294	298	293	1.5×10^{-4}	0	1.75×10^{-5}	
56g	0.330	0.094	294	298	293	1.5×10^{-4}	0	1.75×10^{-5}	
57a	0.020	0.011	294	297	293	2.5×10^{-4}	0	1.75×10^{-5}	
57b	0.044	0.020	294	298	293	2.5×10^{-4}	0	1.75×10^{-5}	
57c	0.101	0.044	294	298	293	2.5×10^{-4}	0	1.75×10^{-5}	
57d	0.161	0.068	295	298	292	2.5×10^{-4}	0	1.75×10^{-5}	
57e	0.216	0.094	295	298	292	2.5×10^{-4}	0	1.75×10^{-5}	
57f	0.279	0.119	295	298	292	2.5×10^{-4}	0	1.75×10^{-5}	
57g	0.312	0.134	295	298	292	2.5×10^{-4}	0	1.75×10^{-5}	
58a	0.015	0.009	295	298	293	3.0×10^{-4}	0	1.75×10^{-5}	
58b	0.050	0.024	295	298	292	3.0×10^{-4}	0	1.75×10^{-5}	
58c	0.107	0.051	295	298	292	3.0×10^{-4}	0	1.75×10^{-5}	
58d	0.165	0.075	295	298	292	3.0×10^{-4}	0	1.75×10^{-5}	
58e	0.211	0.099	295	298	292	3.0×10^{-4}	0	1.75×10^{-5}	
58f	0.260	0.119	295	298	292	3.0×10^{-4}	0	1.75×10^{-5}	
59a	0.163	0.079	294	296	292	2.0×10^{-4}	0	0.44×10^{-5}	
59b	0.163	0.075	294	296	293	2.0×10^{-4}	0	0.88×10^{-5}	
59c	0.163	0.062	294	296	292	2.0×10^{-4}	0	2.60×10^{-5}	
59d	0.163	0.057	294	296	290	2.0×10^{-4}	0	3.50×10^{-5}	
63a	0.152	0.051	299	297	290	2.0×10^{-4}	0	1.75×10^{-5}	
63b	0.145	0.044	297	298	291	1.5×10^{-4}	0	1.31×10^{-5}	
63c	0.151	0.055	294	298	290	2.5×10^{-4}	0	2.19×10^{-5}	
63d	0.151	0.055	294	298	290	2.5×10^{-4}	0	2.19×10^{-5}	
64a	0.165	0.026	348	302	298	2.0×10^{-4}	1.67×10^{-4}	1.75×10^{-5}	622
64b	0.166	0.024	355	304	302	2.0×10^{-4}	3.67×10^{-4}	1.75×10^{-5}	724
64c	0.163	0.024	362	306	309	2.0×10^{-4}	7.83×10^{-4}	1.75×10^{-5}	850
64d	0.166	0.022	365	309	317	2.0×10^{-4}	11.83×10^{-4}	1.75×10^{-5}	1200
65a	0.141	0.031	368	316	337	2.0×10^{-4}	7.83×10^{-4}	0.44×10^{-5}	1650
65b	0.152	0.019	359	300	300	2.0×10^{-4}	7.83×10^{-4}	3.50×10^{-5}	781
65c	0.151	0.028	369	322	322	2.0×10^{-4}	7.83×10^{-4}	0.86×10^{-5}	1120

ORNL DWG 77-444RI

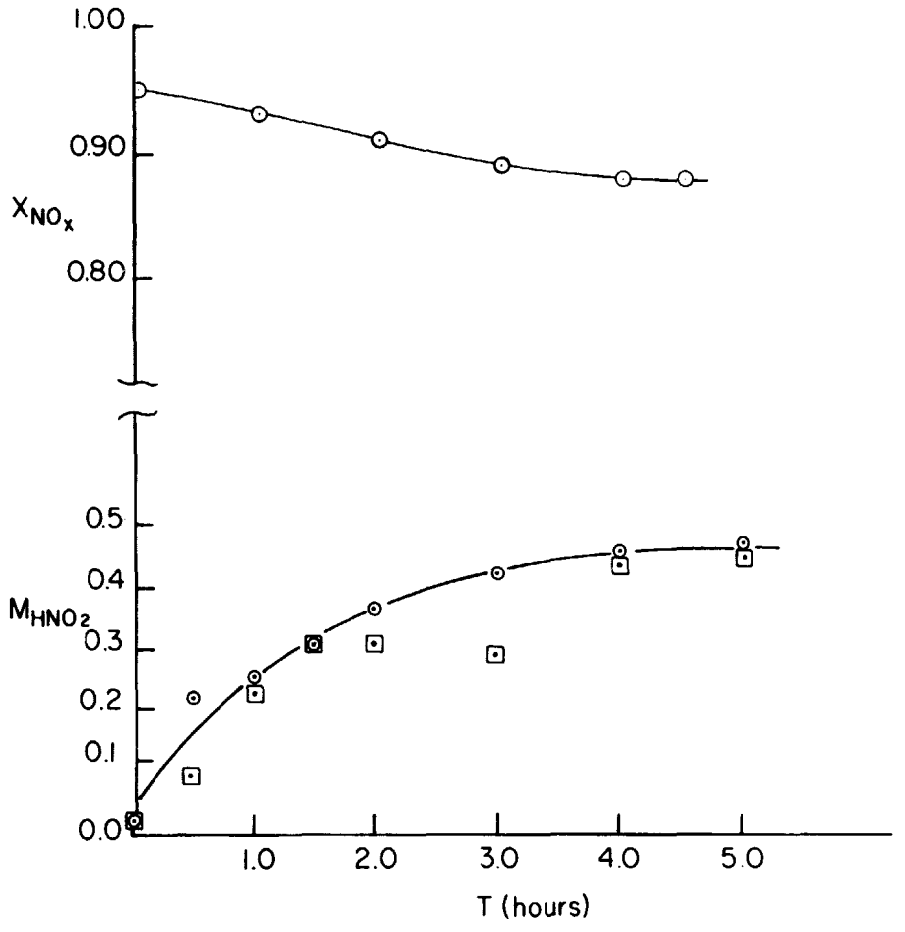

FIGURE 5
OVERALL NO_x CONVERSION IN THREE-STAGE SIEVE-PLATE COLUMN AND CONCENTRATION OF HNO_2 ($kg \cdot moles/m^3$) IN THE SCRUBBER LIQUID DURING THE APPROACH TO STEADY-STATE OPERATION (THE CIRCLE AND SQUARE DATA POINTS FOR HNO_2 CONCENTRATION ARE SCRUBBER LIQUID EFFLUENT AND FEED RESPECTIVELY).

ORNL DWG. 78-1010

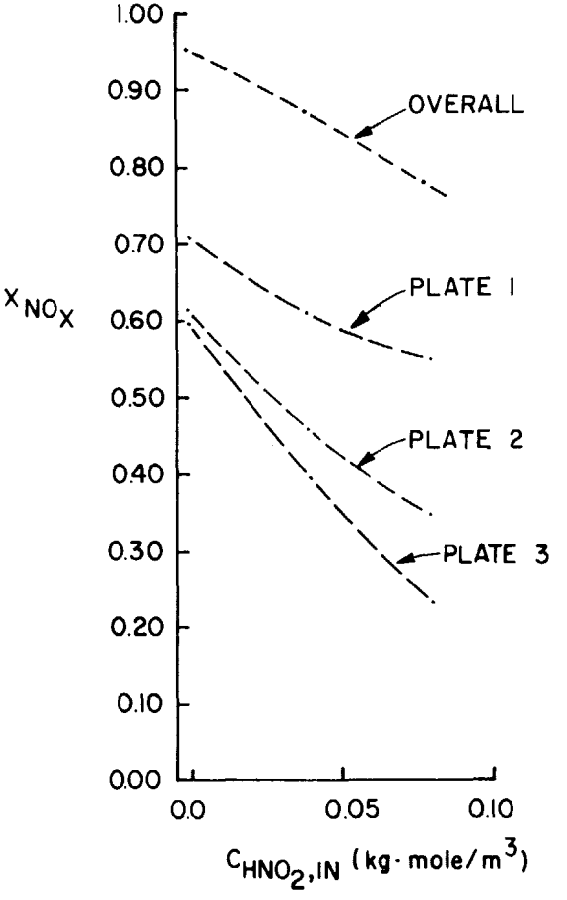

FIGURE 6
MODEL-PREDICTED CONVERSION OF NO_x FOR VARYING CONCENTRATIONS OF HNO_2 IN THE SCRUBBER LIQUID STREAM TO COLUMN AT REFERENCE CONDITIONS.

Table II. Steady-state NO_x scrubbing data for recirculating scrubber liquid

Run no.	NO_x partial pressure (atm)				Gas temperature (K)				Liquid temperature (K)		
	feed	stage 1	stage 2	stage 3	feed	stage 1	stage 2	stage 3	stage 1	stage 2	stage 3
					Recirculating scrubber liquid						
9	0.308	0.106	0.067	0.051	352	314	306	305	310	298	297
10	0.312	0.114	0.068	0.053	353	312	305	303	310	297	297
11	0.299	0.114	0.073	0.058	353	312	304	304	310	297	297
12	0.295	0.110	0.068	0.053	351	309	305	304	310	297	297
13	0.273	0.012	0.073	0.062	353	312	305	303	310	297	297
15	0.341	0.128	0.073	0.051	353	313	305	304	312	297	297
16	0.310	0.141	0.084	0.070	298	302	303	305	297	297	297
17	0.293	0.100	0.057	0.040	352	312	304	303	310	297	297
18	0.332	0.103	0.057	0.042	351	312	304	303	309	297	297
19	0.0	0.0	0.0	0.0	351	303	299	299	310	297	297
20	0.310	0.117	0.066	0.042	351	316	305	303	309	297	297
31	0.341	0.125	0.079	0.057	353	312	305	304	310	297	297
32	0.352	0.117	0.070	0.051	353	313	305	304	310	297	297
42	0.306	0.141	0.088	0.062	364	320	307	305	320	298	297
44	0.295	0.136	0.095	0.066	365	320	308	306	320	298	297
45	0.301	0.150	0.097	0.084	299	303	306	299	298	297	297
46	0.301	0.125	0.088	0.070	357	311	306	305	310	298	297
47	0.301	0.143	0.097	0.068	368	322	308	305	331	299	298
48	0.350	0.141	0.090	0.068	363	315	307	305	313	299	297
49	0.301	0.107	0.069	0.051	363	317	305	304	309	298	297
50	0.312	0.171	0.112	0.075	367	333	310	305	337	299	297
51	0.145	0.066	0.048	0.040	362	317	304	303	318	298	297
52	0.215	0.127	0.110	0.105	298	300	300	301	298	297	297
53	0.317	0.183	0.123	0.103	299	303	307	309	298	297	297
54	0.321	0.132	0.101	0.079	365	317	306	305	318	296	295
60	0.293	0.129	0.079	0.057	366	317	306	303	310	298	297
61	0.400	0.174	0.101	0.070	366	315	305	303	311	297	296
62	0.308	0.114	0.068	0.050	357	336	313	300	310	297	297

Table III. Steady-state NO_x scrubbing data
(total pressure = 1.1 atm in all runs)

Run no.	Steam feed rate[a] ($kg/sec \times 10^3$)	Air feed rate[a] ($m^3/sec \times 10^4$)	Liquid feed rate[a] ($m^3/sec \times 10^4$)	HNO_2 (M)	HNO_3 (M)	Recycle of gas from liquid holdup tank	Liquid holdup tank sparge rate ($m^3/sec \times 10^6$)	Liquid holdup volume ($m^3 \times 10^2$)
9	0.73	1.40	0.35	—	1.0	Yes	0.0	1.64
10	0.73	1.40	0.35	—	2.0	Yes	0.0	1.64
11	0.73	1.40	0.35	—	3.5	Yes	0.0	1.64
12	0.73	1.40	0.35	—	3.0	Yes	0.0	1.64
13	0.73	1.40	0.35	—	3.5	Yes	0.0	1.64
15	0.73	1.40	0.35	—	2.4	Yes	2.5	1.64
16	0.73	1.40	0.35	—	3.2	Yes	0.0	1.64
17	0.73	1.40	0.35	—	3.0	Yes	7.5	1.64
18	0.73	1.40	0.35	—	2.4	Yes	14.0	1.64
19	0.73	1.40	0.35	—	2.2	Yes	0.0	1.64
20	0.73	1.40	0.35	—	2.2	Yes	2.5	2.51
31	0.73	1.40	0.35	0.45	1.3	No	0.0	1.64
32	0.73	1.40	0.35	0.39	1.7	No	2.5	1.64
42	0.70	1.40	0.17	0.25	2.3	No	0.0	1.64
44	1.08	2.10	0.26	0.20	1.6	No	0.0	1.64
45	0.00	1.40	0.18	0.28	2.7	No	0.0	1.64
46	0.35	1.40	0.18	0.18	3.0	No	0.0	1.64
47	1.09	1.40	0.18	0.18	2.8	No	0.0	1.64
48	0.67	1.40	0.26	0.30	2.6	No	0.0	1.64
49	0.67	1.40	0.35	—	2.0	No	0.0	1.64
50	0.67	1.40	0.09	0.20	2.4	No	0.0	1.64
51	0.67	1.70	0.18	0.21	2.0	No	0.0	1.64
52	0.00	1.80	0.18	—	2.1	No	0.0	1.64
53	0.00	2.16	0.26	0.20	3.0	No	0.0	1.64
54	0.85	1.80	0.22	0.20	3.0	No	0.0	1.64
60	0.83	1.80	0.22	0.19	1.5	No	0.0	1.64
61	0.65	1.24	0.17	0.28	2.4	No	0.0	1.64
62	0.36	1.22	0.13	0.27	2.4	No	0.0	1.64

[a]The tabulated numbers in the columns have been multiplied by the indicated factor.

Table IV. A comparison of steady-state NO_x column profiles calculated from experimental data versus NO_x removal predicted by model for experiment 53

Experiment 53 (no steam in feed gas)

$P_T = 1.1$ atm

$G_{feed} = 3.07 \times 10^{-4}$ m^3/sec

$L = 2.6 \times 10^{-5}$ m^3/sec

$M_{HNO_3} = 3.0$

$M_{HNO_2} = 0.20$ (experimental), 0.13 (calculated)

NO_x Profile in Column (atm)

	Experimental	Calculated
Feed	0.317	0.317
Stage 1	0.183	0.181
Stage 2	0.123	0.134
Stage 3	0.103	0.116

Table V. Calculated partial pressures of gaseous components for stage, i, and position, j, where j = 1 entering froth and j = 2 leaving froth for experiment 53

Stage (i,j)	$P^*_{NO_2}$	P_{NO}	P_{O_2}	P_{N_2}
(1,1)	0.317	0.000	0.165	0.618
(1,2)	0.095	0.086	0.193	0.726
(2,1)	0.135	0.051	0.163	0.751
(2,2)	0.051	0.083	0.172	0.794
(3,1)	0.087	0.051	0.143	0.819
(3,2)	0.037	0.080	0.147	0.837

The steady-state HNO_2 concentration calculated by the model is slightly lower than that determined experimentally. The calculated partial pressures of the gaseous component are given for each plate (i) and for positions entering the froth (j=1) and leaving the froth (j=2) in Table V.

Experimentally determined NO_x conversions are compared with those predicted by the model in Fig. 7 for two different feed gas rates with no steam in feed gas. The NO_x conversions predicted by the model are then compared with those experimentally determined for varying scrubber liquid flow rates, feed gas flow rates, NO_x partial pressure in feed gas, and steam component in feed gas at reference conditions in Figures 8-11. In almost all cases, the model used to predict NO_x conversions in sieve plate columns is low with respect to absorption efficiencies. Consequently, the steady-state-predicted concentrations of HNO_2 (usually ~0.1 kg.mole/m^3) are always lower than the experimental values. The column overall NO_x conversion for varying HNO_3 molarities is given in Fig. 12.

Some researchers have consolidated the forward rates of Eqs. (3) and (4) producing one-third of a mole of NO for every mole of NO_2^* absorbed. No apparent difference in the revised model and the one described in this paper was detected when this mode was tested for the steady-state case involving recycle of the scrubber liquid. However, the use of this simple model does not account for the buildup of liquid HNO_2 in the system or for the reduced NO_x removal efficiency that results from its presence in the scrubber liquid. The model clearly demonstrates the observed phenomenon that the presence of HNO_2 in the scrubber liquid reduces the overall NO_x scrubbing efficiency of the system.

V. Conclusions

The following conclusions can be drawn from the results of this study:

1. The model adequately represents the experimental results for the experimental system over the range of variables studied.

2. The conversion of NO_x varies directly with the gas and liquid flow rates and the partial pressure of NO_2^*.

3. The model predicts a buildup of HNO_2 in the scrubber liquid and a corresponding decrease in scrubbing efficiency. This was verified in the experimental work.

4. These findings indicate that a method to destroy HNO_2 in the scrubber liquid before its recycle to the column will greatly increase the system NO_x removal efficiency.

5. Additional investigation will be necessary in order to verify the use of this model in predicting effluent-gas partial pressures of less than 0.01 atm.

VI. Acknowledgement

This work was performed in the Chemical Technology Division under the auspices of the Advanced Fuel Recycle Program of the Oak Ridge National Laboratory.

ORNL DWG. 78-1007

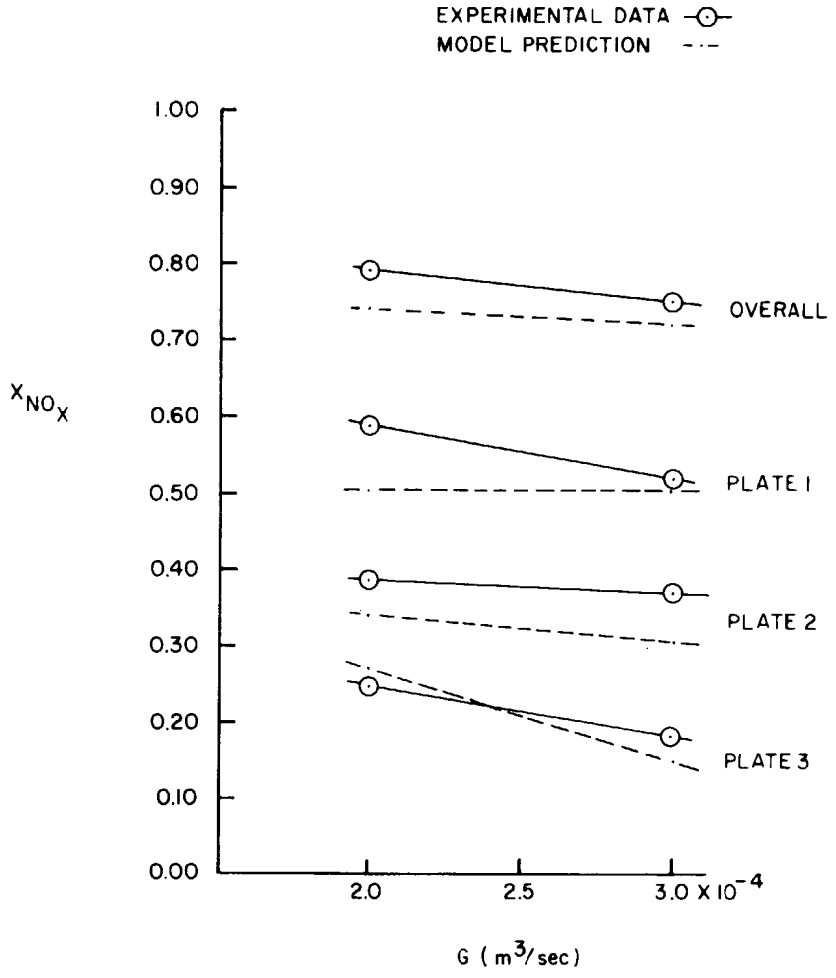

FIGURE 7
EXPERIMENTAL NO_x CONVERSIONS AND THOSE PREDICTED BY THE MODEL FOR VARYING GAS FLOW RATES WITH NO STEAM IN FEED GAS AT OTHERWISE REFERENCE CONDITIONS FOR STEADY-STATE, THREE-STAGE, SIEVE-PLATE COLUMN OPERATION.

ORNL DWG. 78-1008

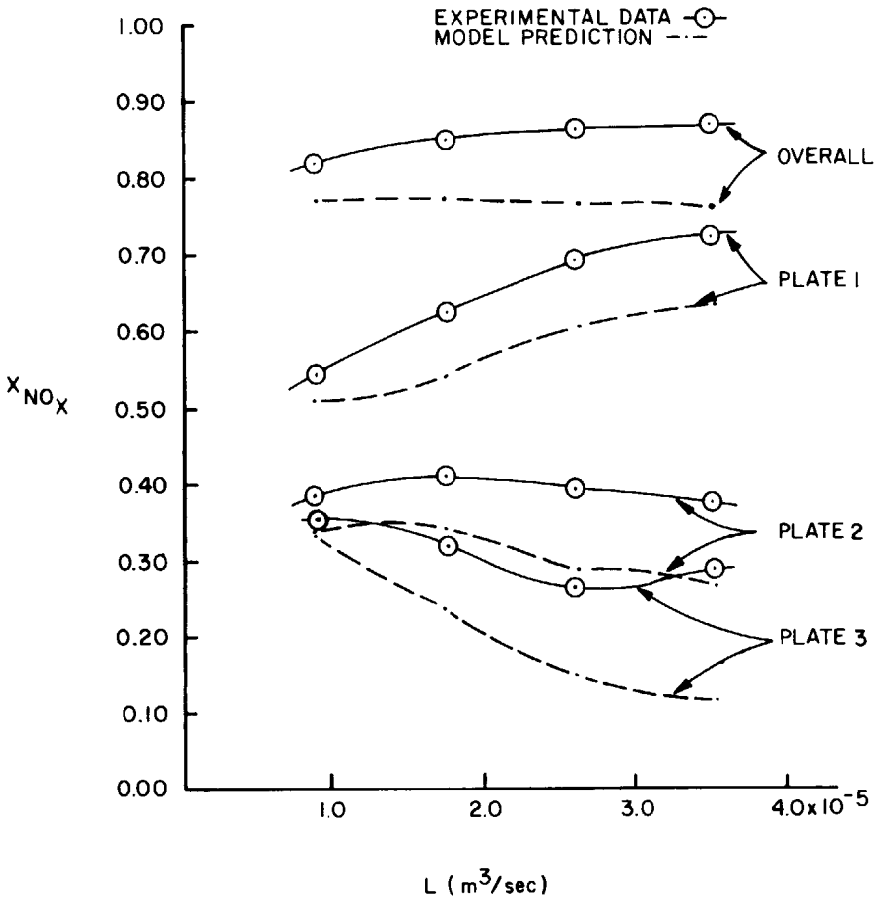

FIGURE 8
EXPERIMENTAL NO_x CONVERSIONS AND THOSE PREDICTED BY THE MODEL FOR VARYING SCRUBBER LIQUID FLOW RATES AT OTHERWISE REFERENCE CONDITIONS FOR STEADY-STATE THREE-STAGE COLUMN OPERATION.

ORNL DWG.78-1009

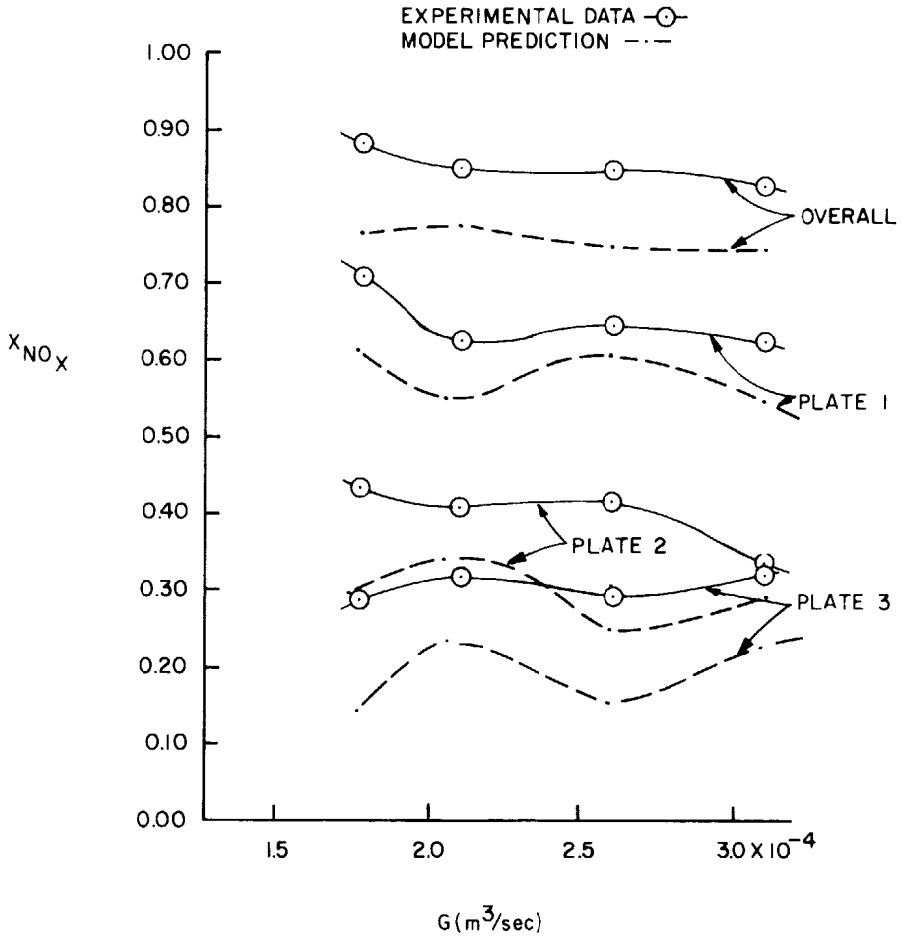

FIGURE 9
EXPERIMENTAL NO_x CONVERSIONS AND THOSE PREDICTED BY THE MODEL FOR VARYING FEED GAS FLOW RATES AT OTHERWISE REFERENCE CONDITIONS FOR STEADY-STATE THREE-STAGE COLUMN OPERATION.

ORNL DWG.78-1011

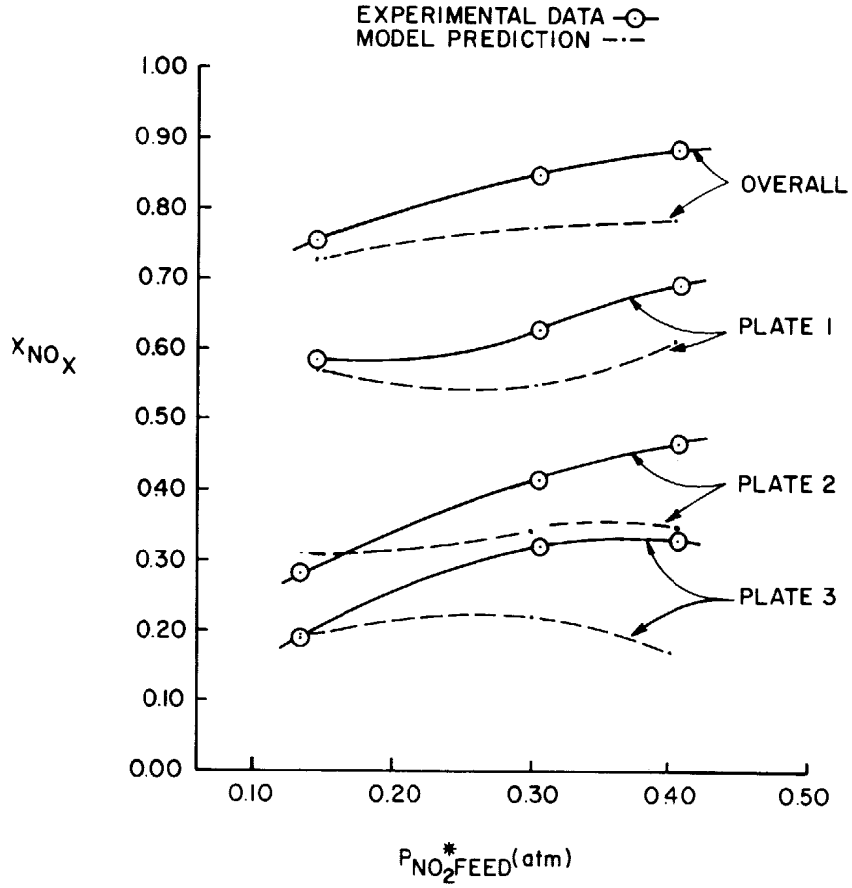

FIGURE 10
EXPERIMENTAL NO_x CONVERSIONS AND THOSE PREDICTED BY THE MODEL FOR VARYING PARTIAL PRESSURE OF NO_x IN THE FEED GAS AT OTHERWISE REFERENCE CONDITIONS FOR STEADY-STATE THREE-STAGE COLUMN OPERATION.

ORNL DWG.78-1012

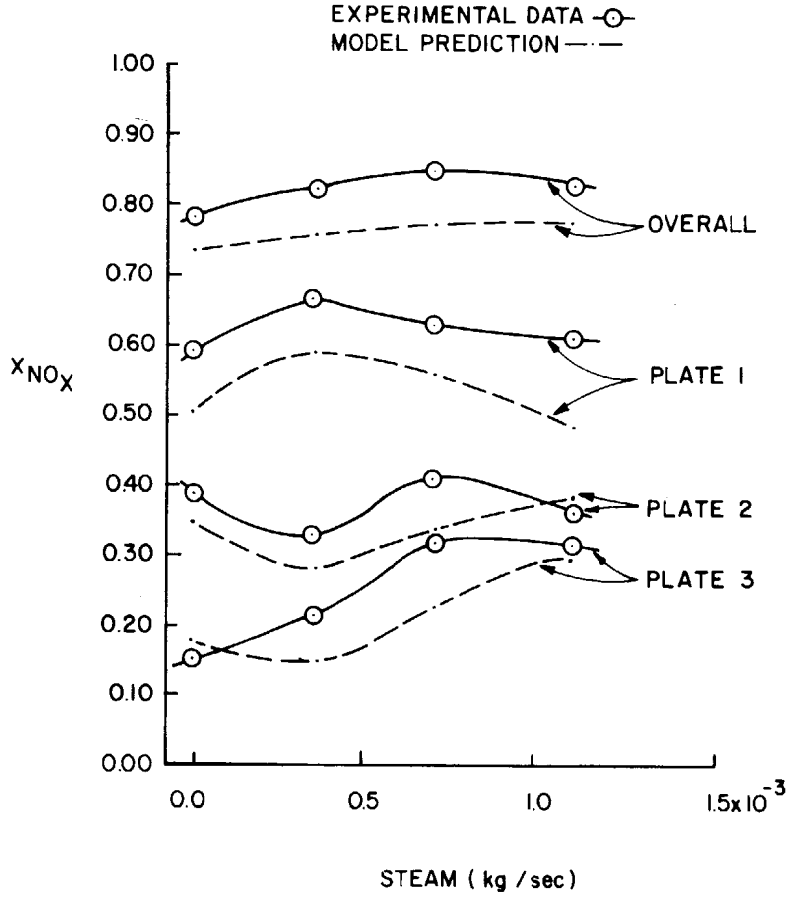

FIGURE 11
EXPERIMENTAL NO_x CONVERSIONS AND THOSE PREDICTED BY THE MODEL FOR VARYING STEAM FLOW RATES AT OTHERWISE REFERENCE CONDITIONS FOR STEADY-STATE THREE-STAGE COLUMN OPERATION.

ORNL DWG.77-443

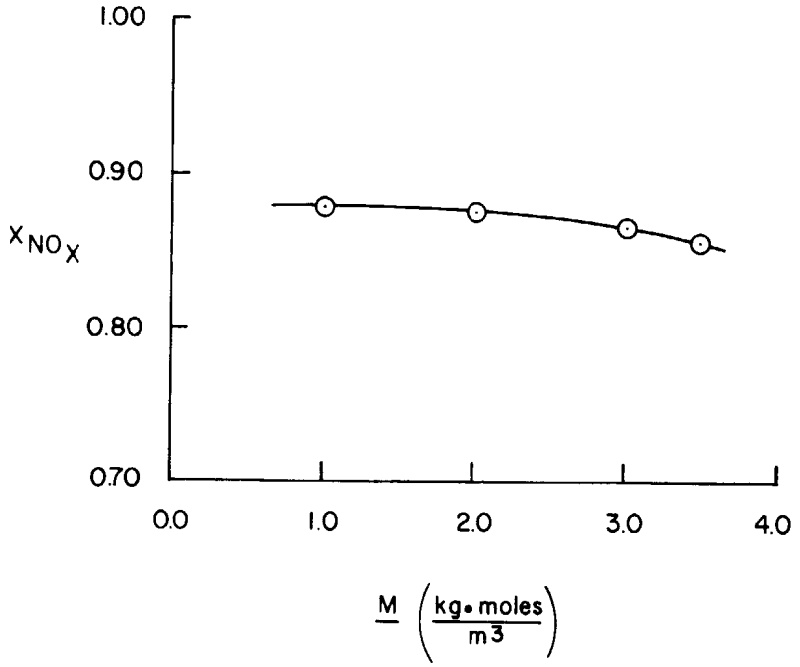

FIGURE 12
OVERALL NO_x REMOVAL IN THREE-STAGE SIEVE-PLATE COLUMN AS A FUNCTION OF ACID MOLARITY IN SCRUBBER LIQUID.

VII. List of References

1. R. H. Perry and C. H. Chilton, "Chemical engineers' handbook," 5th ed., 18-8, McGraw-Hill, New York (1973).

2. M. Bodenstein, "Formation and decomposition of nitrous oxides of high volume," Z. Elektrochem. 100: 68-123 (1922).

3. F. H. Verhoek and F. J. Daniels, "The dissociation constants of nitrogen tetroxide and of nitrogen trioxide," J. Am. Chem. Soc. 53: 1250-63 (1931).

4. P. J. Hoftyzer and F. J. G. Kwanten, "Process for air pollution control," 2nd ed., 164-87, Chemical Rubber Co., Cleveland (1972).

5. K. G. Denbigh and A. J. Prince, "Kinetics of nitrous gas absorption in aqueous nitric acid," J. Chem. Soc. 53: 790-801 (1947).

6. P. G. Caudle and K. G. Denbigh, "Kinetics of the absorption of nitrogen peroxide into water and aqueous solutions," Trans. Faraday Soc., 49: 39-52 (1953).

7. M. M. Wendel and R. L. Pigford, "Kinetics of nitrogen tetroxide absorption in water," AIChE. J. 4: 249-56 (1958).

8. M. S. Peters and J. L. Holman, "Vapor- and liquid-phase reactions between nitrogen dioxide and water," Ind. Eng. Chem. 47: 2536-39 (1955).

9. J. J. Carberry, "Some remarks on chemical equilibrium and kinetics in the nitrogen oxides-water system," Chem. Eng. Sci. 9: 189-94 (1959).

10. W. A. Dekker, E. Snoeck, and H. Kramers, "The rate of absorption of NO_2 in water," Chem. Eng. Sci. 11: 61-71 (1959).

11. E. S. Koval and M. S. Peters, "How does nitric oxide affect reactions of aqueous nitrogen dioxide?," Ind. Eng. Chem. 52: 1011-14 (1960).

12. M. J. Moll, "The rate of hydrolysis of nitrogen tetroxide," Ph.D. Dissertation, Univ. of Washington (1966).

13. J. P. Detournay and R. H. Jadot, "Determination of the reactive phase during the absorption of nitrogen oxides in water," Chem. Eng. Sci. 28: 2099-2102 (1973).

14. M. S. Peters, C. P. Ross, and J. E. Klein, "Controlling mechanisms in the aqueous absorption of nitrogen oxides," AIChE. J. 1: 105-11 (1955).

15. H. Kramers, M. P. P. Blind, and E. Snoeck, "Absorption of nitrogen tetroxide by water jets," Chem. Eng. Sci. 14: 115-23 (1961).

16. T. K. Sherwood, R. L. Pigford, and C. R. Wilke, "Mass transfer," 346-361, McGraw-Hill Book Co., New York (1975).

17. S. P. Andrews and D. Hanson, "The dynamics of nitrous gas absorption," Chem. Eng. Sci. 14: 115-23 (1961).

18. E. Abel and H. Schmid, "Kinetics of nitrous acid," Z. Phys. Chem. 132: 55-77 (1928).

19. E. Abel and H. Schmid, "Kinetics of nitrous acid: kinetics of the decomposition of nitrous acid," Z. Phys. Chem. 134: 279-300 (1928).

20. E. Abel, H. Schmid, and S. Babad, "Kinetics of nitrous acid: kinetics of the formation of nitrous acid from nitric acid and nitric oxide," Z. Phys. Chem. 136: 135-45 (1928).

21. E. Abel, H. Schmid, and S. Babad, "Kinetics of nitrous acid: kinetics of the nitrous acid-nitric acid-nitric oxide reaction," Z. Phys. Chem. 136: 419-36 (1928).

22. M. Bodenstein, "Velocity of reaction between nitric oxide and oxygen," Z. Elektrochem. 24: 183-201 (1918).

23. R. L. Hasche and W. A. Patrick, "Studies on the rate of oxidation of nitric oxide; II the velocity of the reaction between nitric oxide and oxygen at 0° and 30°," J. Am. Chem. Soc. 47: 1207-14 (1925).

24. J. C. Treacy and F. Daniels, "Kinetic study of the oxidation of nitric oxide with oxygen in the pressure range 1-20 mm," J. Am. Chem. Soc. 77: 2033-36 (1955).

25. P. G. Ashmore, M. G. Burnett, and B. J. Tyler, "Reaction of nitric oxide and oxygen," Trans. Faraday Soc. 58: 685-91 (1962).

26. M. E. Morrison, R. C. Rinker, and W. H. Corcoran, "Rate and mechanism of gas-phase oxidation of parts-per-million concentrations of nitric oxide," Ind. Eng. Chem. Fundam. 5: 175-81 (1966).

27. J. D. Greig and P. G. Hall, "Thermal oxidation of nitric oxide at low concentrations," Trans. Faraday Soc. 63: 655-61 (1967).

28. P. V. Danckwerts, "Gas-liquid reactions," 96-150, 117-118, 227, McGraw-Hill, New York (1970).

REMOVAL OF ^{14}C-CONTAMINATED CO_2 FROM SIMULATED LWR FUEL REPROCESSING OFF-GAS BY UTILIZING THE REACTION BETWEEN CO_2 AND ALKALINE HYDROXIDES IN EITHER SLURRY OR SOLID FORM

D. W. Holladay and G. L. Haag
Oak Ridge National Laboratory
Oak Ridge, Tennessee 37830

Abstract

An important consideration in the design of a LWR fuel reprocessing plant is the removal of ^{14}C-contaminated CO_2 from the process off-gas. The separation and fixation of essentially all the CO_2 from the simulated off-gas can be accomplished by reaction with alkaline slurries in agitated tank-type contactors. Based on efficacy for CO_2 removal, consideration of reactant cost, and stability of the carbonate product as related to long-term storage requirements, the two most promising slurry reactants for CO_2 removal from low CO_2-content feed gases are $Ca(OH)_2$ and $Ba(OH)_2$.

The removal of ^{14}C-contaminated CO_2 from simulated LWR off-gases was studied as a function of both operating conditions and varying sizes of bench-scale design. Parametrically, the effects on the CO_2 removal rate of feed composition (330 ppm - 4.74% CO_2), impeller speed (325-650 rpm), superficial velocity (5-80 cm/min), reactants [$Mg(OH)_2$, $Ca(OH)_2$, $Ba(OH)_2$, NaOH], contactor size (20.3 cm and 27.3 cm ID), and type of operation (semibatch or continuous slurry) were determined.

The decontamination factors (DF, i.e. moles CO_2 in/moles CO_2 out) for CO_2 removal from gases containing 0.033 to 3% CO_2, for fixed values of such parameters as gas superficial velocity, slurry temperature, and power consumption, varied directly with the solubility of the metal hydroxide employed. For 1.0 m $Ca(OH)_2$ in the 27.3-cm-ID contactor, a power consumption of 21.0 kW/m^3 (n = 650 rpm), a temperature of 15°C, and a 0.033% CO_2-air feed, DFs were 2×10^3 to 10^2 for superficial velocities of 5 to 80 cm/min. For 0.4 m $Ba(OH)_2$ in the 27.3-cm-ID contactor, a power consumption of 21.0 kW/m^3 (n = 650 rpm), a temperature of 15°C, and a 0.033% CO_2-air feed, DFs were 10^4 to 10^3 for superficial velocities of 20 to 80 cm/min. For 1.0 M NaOH in the 27.3-cm-ID contactor, a power consumption of 21.0 kW/m^3 (n = 650 rpm), a temperature of 25°C, and a 0.033% CO_2-air feed, DFs were 10^4 to 10^3 for superficial velocities of 40 to 80 cm/min. DFs obtained for CO_2 removal from 0.033% CO_2-air mixtures were about a factor of 2 larger than those obtained for CO_2 removal from 1-3% CO_2-air feed gases.

A very promising alternative process for removing CO_2 from off-gases with low CO_2 content is the reaction with solid $Ba(OH)_2$ (mono- or octahydrate) in packed or fluidized beds. Decontamination factors $>10^4$ were obtained for CO_2 removal at ambient conditions from water-saturated gas feeds containing 4.5% CO_2, and DFs of at least 10^3 were obtained for CO_2 removal from water-saturated air.

I. Introduction

Recently, the fact that ^{14}C may constitute a significant radiological hazard in the effluents from nuclear power facilities, particularly from fuel reprocessing plants, has become a matter of increasing concern. Since Bonka[1] and Magno[2] first discussed the problem posed by ^{14}C which is produced in nuclear power reactors, studies have been conducted to measure the quantity of ^{14}C released at nuclear power plants [Kunz[3]] and to predict the behavior of the ^{14}C that would be released in LWR, HTGR, and LMFBR fuel reprocessing plants [Davis[4], Croff[5], and Killough[6]]. Among the studies conducted to predict the behavior of CO_2 in the atmosphere were those of Machta[7], Killough[8], and Snider and Kay[9].

According to Davis[4], ^{14}C is formed from neutron reactions with isotopes of elements that are normal or impurity components of the cooling water, fuel, and structural materials of LWRs. The neutron-induced reactions are: (1) $^{13}C(n,\gamma)^{14}C$, (2) $^{14}N(n,p)^{14}C$, (3) $^{15}N(n,d)^{14}C$, (4) $^{16}O(n,^{3}He)^{14}C$, and (5) $^{17}O(n,\alpha)^{14}C$. Most of the ^{14}C will be formed by the fuel reactions $^{17}O(n,\alpha)^{14}C$ and $^{14}N(n,p)^{14}C$. Nitride nitrogen at a median concentration of 25 ppm was estimated to produce 14 and 15 Ci of ^{14}C/GW(e)-yr in BWR and PWR fuels, respectively, while the contribution of ^{17}O in BWR and PWR fuels would be 3.3 and 3.5 Ci of ^{14}C/GW(e)-yr, respectively. The net contribution of all the possible neutron reactions was estimated to be in the range of 400 to 2200 Ci of ^{14}C per year for a LWR fuel reprocessing plant treating 1500 metric tons of heavy metal annually with a range of 40 to 240 ppb of $^{14}CO_2$ in a reference flow of 500-scfm off-gas.

Also, Kunz et al.[2] have reported that for the BWR at Nine Mile Point [625 MW(e)], a release rate of 8 Ci of ^{14}C per year was observed. These authors also reported that 6 Ci/GW(e)-yr was measured in the emissions from Ginna, Indian Point 1, and Indian Point 2 PWRs. For the BWR, the ^{14}C was distributed as 95% CO_2, 2.5% CO, and 2.5% in the hydrocarbons, while in the PWRs more than 80% of total gaseous ^{14}C activity was contained in CH_4 and C_2H_6, with less than 5% as CO_2 and CO.

In view of the above-noted concentrations of $^{14}CO_2$ in LWR power plant and fuel reprocessing off-gases, a process evaluation was conducted to review the various technical methods for recovering $^{14}CO_2$, along with the more abundant normal CO_2, from the LWR reprocessing plant dissolver off-gas stream and for immobilizing it in a stable leach-resistant solid matrix. An initial experimental program[10] had shown that DFs of 10^2 for single-stage contacting and 10^4 for two-stage contacting in a gas-lime slurry [$Ca(OH)_2$] agitated contactor were feasible for removing CO_2 from simulated HTGR fuel reprocessing off-gases. The product $CaCO_3$, which could be easily recovered in an aqueous mixture containing 40 to 50 wt % $CaCO_3$, offered a very attractive chemical form capable of maintaining acceptable stability under requisite long-term storage conditions. However, the simulated HTGR off-gases which were studied were very rich in CO_2 ($\sim$90%) so that it was necessary to conduct additional

experiments for simulated LWR fuel reprocessing off-gases for which probable CO_2 concentrations are in the range of 0.03-1.0%.

II. Experimental Apparatus

Mechanically Agitated Gas-Alkaline Slurry Contactor

Two continuous stirred-tank contactors were utilized in the studies concerning CO_2 removal from simulated LWR fuel reprocessing off-gases. The 20.3-cm-ID contactor has been previously described in detail[10], while the 27.3-cm-ID contactor was designed to be a geometrically similar scaled-up version, by about a factor of 2, of the smaller Rushton-type contactor. However, to simplify operation during studies utilizing continuous slurry flow, the disengaging section of the larger contactor was redesigned to allow the slurry to be removed through the top flange area of the contactor. To minimize troublesome flow interruption from slurry settling during intermittent operation, two input ports for the slurry were provided in the bottom flange of the 27.3-cm-ID contactor. Additional improvements to the original contactor were replacement of the shaft seal, consisting of pressure rings and a packing gland, with a more dependable Crane mechanical seal, and introduction of a 2-to-1 gear reduction in the Gast air-motor drive to enhance torque-loading capabilities of the turbine impeller. A schematic of the experimental equipment is shown in Fig. 1.

Beds of Hydrated Barium Hydroxide

The efficient removal of CO_2 from 0.033% CO_2-air feeds was also achieved in beds of barium hydroxide at ambient conditions ($\sim$21°C). Both packed beds and fluidized beds were useful for treatment of 0.033% CO_2-air feeds; higher velocities were achieved in the fluidized bed contactor. The packed beds had dimensions of 2.54 x 15.2 cm and contained up to 62 g of $Ba(OH)_2$ (mono- or octahydrate). The fluidized beds were tapered, varying from 2.54 to 7.62 cm ID over a 91-cm length. Neither column contactor was provided with means for controlling temperature.

III. Analytical Techniques

Background

In the initial stages of this experimental program, it quickly became apparent that the employment of sensitive analytical instrumentation to detect CO_2 effluent concentrations $\leq$1 ppm would be as important to the success of the program as the development of processes to achieve effluents of that quality. Brief discussions of three different analytical techniques which were investigated and, in some cases, successfully applied to analyzing CO_2 at the $\leq$1 ppm level are presented in the paragraphs that follow.

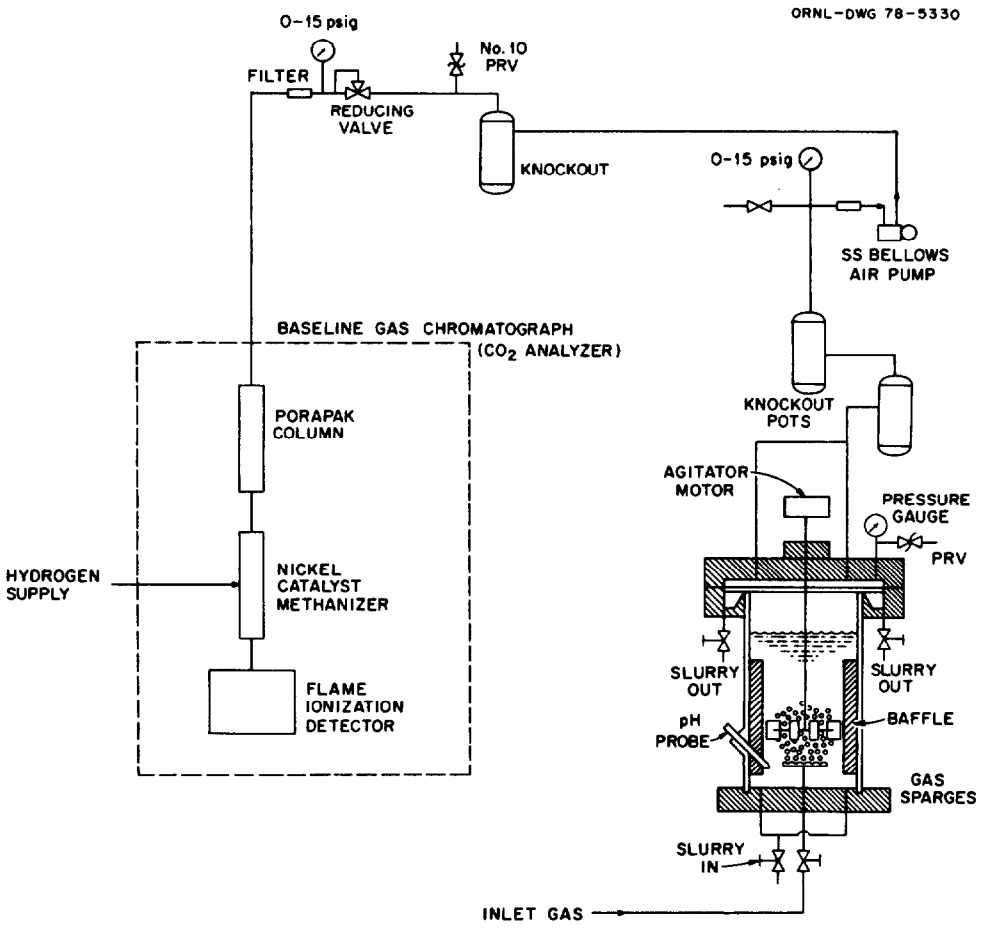

Fig. 1. Schematic of agitated-contactor experimental equipment and gas analysis system.

Liquid Scintillation Counting of Sorbed $^{14}CO_2$

In an alternative technique for measuring traces of $^{14}CO_2$ in both feed and product streams, the CO_2 can be sorbed from the appropriately sized thief-stream into a solvent capable of quantitative reaction with the CO_2. The solvent is then mixed with the appropriate scintillant, and the bound $^{14}CO_2$ is detected in a liquid scintillation counter. Among the most widely used solvents for this analytical technique are the hydroxide of hyamine, ethanolamine-cellosolve mixtures, and phenethylamine[11-13].

The continuous reaction of CO when bubbled into a stirred solvent at a low flow rate appears to be the most promising technique for $^{14}CO_2$ trapping. Of course, any ambient CO_2 that is sorbed does not interfere with the $^{14}CO_2$ counting because nonradioactive CO_2 only consumes part of the solvent, which is supplied at sufficient excess to avoid depletion. We have been able to reproducibly count $^{14}CO_2$-labeled air (330 ppm total CO_2) containing 10^6-10^7 cpm/liter and obtain an accountability of >95% of the available counts. However, a primary concern with this method has been to ensure that the continuous-bubbling organic solvent technique is capable of trapping CO_2 at levels below 1 ppm. This question has been studied by making controlled dilutions, with pure helium, of 1/100, 1/500, and 1/1000 of a 0.033% CO_2-air feed for which the $^{14}CO_2$ content is known. Thus the ability of the organic solvent to trap 3 ppm or 0.3 ppm of CO_2 can be tested. Initial results with the gas containing 3 ppm of CO_2 with $^{14}CO_2$ tracer have indicated that at least 80% of the 3 ppm can be sorbed in the organic solvent bubbler. Experiments will be continued at the ppb level. Great care must be taken to ensure that such small quantities of CO_2 are not absorbed in the piping and glassware prior to the organic solvent bubbler.

Infrared Spectroscopy

A number of manufacturers can provide infrared spectrometers which are capable of measuring CO_2 in the 1-ppm range. We are in the process of evaluating infrared (IR) instrumentation which is capable of detecting CO_2 in the 100-ppb range. Thus far in our investigation, we have utilized IR to obtain data for CO_2 effluents in the 1-ppm range.

Flame Ionization Detection

The analytical system that has provided the most reliable determinations of CO_2 effluent stream concentrations below 1 ppm involves gas chromatography (GC) with analysis by flame ionization detection. Williams et al.[14] and Eaton et al.[15] have shown that, by utilization of a methanizer in conjunction with appropriate fractionating columns and a flame ionization detector (FID), CO_2 can be measured accurately at the 100-ppb level in ideal gas mixtures containing air with a known organic component. Our most reproducible results were obtained with a specially fitted GC instrument containing the three required elements: a fractionating column, a H_2-nickel catalyst bed for carbon compound conversion to CH_4, and the

FID unit. As much as 50% uncertainty may exist in measurements at the 100-ppb level. Some developmental work may be necessary to accurately obtain CO_2 levels below 1 ppm whenever actual or accurately simulated fuel reprocessing off-gases are studied, because such gases could contain trace organics at the 1-ppm level. A schematic of the methanizer and flame ionization detection system is shown in Fig. 1.

IV. Theoretical Considerations

Juvekar and Sharma[16] have extensively discussed the mechanism for the absorption of CO_2 into a suspension of $Ca(OH)_2$ in both bubble columns and mechanically agitated contactors. They hypothesized that the overall process of carbonation of lime could be described by:

$$Ca(OH)_2(s) \rightleftarrows Ca^{2+}(aq) + 2OH^-(aq) \quad (1)$$

$$CO_2(g) \rightleftarrows CO_2(aq) \quad (2)$$

$$CO_2(aq) + OH^-(aq) \rightarrow HCO_3^-(aq) \quad (3)$$

$$HCO_3^-(aq) + OH^-(aq) \rightarrow H_2O + CO_3^{2-}(aq) \quad (4)$$

$$Ca^{2+}(aq) + CO_3^{2-}(aq) \rightarrow CaCO_3(s) \quad (5)$$

Because reactions (4) and (5) are instantaneous, the controlling mechanism is in reaction (1), (2), or (3). The gas-phase diffusional resistance could become important only for gases containing low concentrations of CO_2. After consideration of the rate equations for transport of CO_2 through the gas film, for the rate of dissolution of $Ca(OH)_2$, and for the rate of transport of CO_2 into the liquid and the reaction of CO_2 with hydroxyl ions, Juvekar derived the following rate expression:

$$R_a = \frac{a H p_g [D_A k_2 (OH^-)_s + k_L^2]^{0.5}}{1 + \dfrac{a H [D_A k_2 (OH^-)_s + k_L^2]^{0.5}}{k_G a}}, \quad (6)$$

where

R = specific rate of absorption of CO_2, g-mole/sec-cm^2 dispersion,
a = gas-liquid interfacial area, cm^2/cm^3 dispersion,
p_g = partial pressure of CO_2 in the bulk gas, atm,
D_A^g = diffusivity of CO_2 in aqueous solution, cm^2/sec,
k_2 = rate constant for the reaction between CO_2 and OH^- ions, cm^3/(g-mole-sec),
$(OH^-)_s$ = saturation concentration of OH^- ions in aqueous solution in equilibrium with solid $Ca(OH)_2$, g-ion/cm^3,
k_L = liquid-side mass transfer coefficient in the absence of chemical reaction, cm/sec,

$k_G a$ = gas-side mass transfer coefficient, g-mole/(cm^3 · dispersion-sec-atm),
H = Henry's coefficient of solubility, g-mole/(cm^3-atm).

This expression applies to about 80% of the reaction time (for semi-batch operation), which is called the "constant rate period" wherein hydroxyl concentration remains constant. Another expression is necessary to describe the "falling rate period" (in which the OH^- concentration and the rate of CO_2 reaction decrease). Operation of the process with continuous slurry flow allows for OH^- stabilization and thus eliminates the falling rate period.

Because the contactor design and operating conditions of this study were similar to those used by Juvekar and Sharma, we may adopt their value of $\sim 10^{-4}$ g-mole/(cm^3-sec-atm) for $k_G a$ (gas-side mass transfer coefficient for gas-phase control in an agitated contactor). In order for the gas-side resistance to contribute significantly to the overall mass transfer resistance, the following relationship should be satisfied:

$$\frac{aHp_g[D_A k_2 (OH^-)_s + k_L^2]^{0.5}}{k_G a} \geq 1 \ . \qquad (7)$$

Condition 7 is not satisfied for feed gases containing 1-5% CO_2 or 0.033% CO in air, so that the rate expression for CO_2 absorption in a lime suspension in the mechanically agitated contactor becomes:

$$Ra = aHp_{DF}[D_A k_2 (OH^-)_s + k_L^2]^{0.5} \ , \qquad (8)$$

or, for dilute CO_2-air feed gases,

$$[\ln DF]\ Ra \cong aH(p_i - p_o)[D_A k_2 (OH^-)_s + k_L^2]^{0.5} \ . \qquad (8a)$$

The rate expression given in Eq. 8 is generally assumed to be applicable at any point in the agitated contactor and thus the specific rate Ra can be directly related to the overall mass transfer rate for the total dispersed volume in the contactor. The proper form of the pressure term p_{DF} for the agitated contactor appears to be dependent on the nature of the solution or suspension in the contactor. The log-mean pressure was shown by Juvekar for dilute CO_2-air mixtures to be the proper form for the pressure driving force for the CO_2-$Ca(OH)_2$ reaction under the following conditions: (1) CO_2 reacting with a $Ca(OH)_2$ slurry; (2) CO_2 concentrations in air of about 10%; (3) a 12.5-cm-ID agitated contactor; (4) impeller speeds, n, of 1000 to 2000 rpm; and (5) gas superficial velocities, Q_s, of 2.2 to 4.6 cm/sec. For these conditions [(1) through (5)], utilization of the log-mean (based on natural log) form for pressure resulted in more "reasonable" values for the interfacial area than those calculated from the backmix model because the latter model would predict the illogical trend that the area increased as the flow rate decreased.

It is interesting to note that, for similar contactor design, operating conditions, and feed gas compositions, previous studies

(Mehta and Sharma[17], Hanhart et al.[18]) have shown that both gas and liquid phases in an agitated gas-liquid dispersion are almost completely mixed when the speed of agitation exceeds a certain critical value. However, for CO_2 sorption into a slurry, several studies (Holladay[10], Morris and Woodburn[19], Juvekar and Sharma[16]) have shown that the system appears to be better represented by a plug flow model than by a backmix assumption. It is believed that the presence of the fine solids alters the coalescence behavior and flow pattern of the gas bubbles.

The data of this study differ from those of Juvekar and Sharma in two key respects: (1) a considerable number of the experiments were conducted with feed gas containing only 0.033% CO_2; (2) in order to achieve the primary goal of these studies, which was a high CO_2 removal efficiency, it was necessary to use superficial gas feed rates considerably lower than those studied by Juvekar. With regard to point 1, the similarity between DFs obtained for feed gases containing 0.033% CO_2 or 1-5% CO_2 in air would appear to eliminate the concern that there were different mass transfer control regimes for the two feed concentrations. However, the variation in flow rates is a major factor in the interpretation of our data with the model of Eq. 8. Whereas Juvekar noted no variation in interfacial area with superficial velocity, calculations of interfacial area a based on our studies indicate a very strong dependence of a on Q_S, even for agitation speeds well in excess of n_O (as defined by Westerterp et al.[20]). The log-mean model resulted in calculation of values of a from 0.2 to 2.0 cm^2/cm^3, while the backmix model predicted values from 30 to 50 cm^2/cm^3. The log-mean values of a varied directly with Q_S up to $Q_S \cong 2$ cm/sec and then appeared to level off in agreement with Juvekar's work.

Thus, Eq. 8 can be utilized to formulate qualitative predictions about the effects of such operating parameters as temperature, impeller speed, and gas superficial velocity on the rate, and more importantly the DF, which can be obtained for CO_2 removal in agitated contactors. Because the dissolution of $Ba(OH)_2$ and subsequent reaction with CO_2 in a sparged, agitated tank should follow the same reaction scheme as proposed in Eqs. 1-5, the same form of Eq. 8 should be relevant to the predictions of CO_2 reaction with $Ba(OH)_2$ slurries. The reaction between CO_2 and the NaOH solution should also be described by Eq. 8, with the backmix pressure term.

So in general for fixed H, D_A, k_2, (OH^-), and k_L, it is predicted by Eq. 8 that the DF will vary inversely with gas superficial velocity Q_S (because of the direct variation of Ra with Q_S) and directly with impeller speeds above the critical speed (because of the direct variation of interfacial area with n). DF will also vary directly with temperature for suspensions in which the solubility of the solids increases with temperature. The temperature variation occurs because the effects of the increase in rate constant and hydroxyl solubility are larger than the effect of the decrease in CO_2 solubility in aqueous solutions. Because of the inverse variation of $Ca(OH)_2$ solubility with temperature, Eq. 8 sometimes predicts a reduction in DF for an elevation in temperature for $Ca(OH)_2$ slurries for the log-mean case.

Yet the question remains concerning the precise form of Eq. 8 for application to the removal of CO_2 from 0.033% CO_2--air at low superficial velocities and high impeller speeds. The precise form of the residence time is unclear for the CO_2 in transit through the suspension; hence uncertainty remains about the proper form for the pressure driving force. The DFs predicted by the log-mean model for a $Ba(OH)_2$ slurry when compared to the DFs for a $Ca(OH)_2$ slurry under the same feed and operating conditions are higher than the actual measured data (it was assumed that a, H, T, D_A, and k_2 were held constant). The DFs predicted by the backmix model are lower than those obtained experimentally. Perhaps the ultimate solution to this quandary is to describe the DF by an expression which links both the kinetics as expressed in Eq. 8 and the effects of physical parameters such as power input, superficial velocity, impeller design, solution density, and viscosity through a multiparameter empirical model.

V. Experimental Results

Comparison of Decontamination Factors Obtained for CO_2 Removal in the 20.3- and 27.3-cm-ID Contactors

Two comparisons of the experimental data for removal of CO_2 from air containing 0.033% and 1-5% CO_2 are shown in Fig. 2. First, results were obtained for air feeds to the 20.3- and 27.3-cm-ID contactors to provide initial information concerning scale-up of the process. Second, the results for removal of CO_2 from air containing 0.033% or 1-5% CO_2 were obtained to determine the effect of two orders of magnitude of feed gas dilution on the efficiency of the process. The CO_2 contents in the contactor gaseous effluents were determined by GC with methanization and flame ionization detection for concentrations less than $\sim$1 ppm and by IR spectroscopy and GC with thermal conductivity detection for concentrations $\geq$1 ppm. As indicated in Fig. 2, a few of the high DF values at low superficial velocities were also corroborated by analysis utilizing sorption of $^{14}CO_2$ tracer from 0.033%--air feeds into organic solvents (ethanolamine-Cellosolve mixture) and subsequent counting by beta scintillation detection. The temperature of the suspension and solutions in the contactor was controlled in the range of 15-25°C.

The useful similarity between the DF curves for removing CO_2 from 0.033% CO_2-air or from 1-5% CO_2-air is apparent in Fig. 2. It is also evident from the data of Fig. 2 that there is reasonable agreement between the DF values obtained in the 20.3- and 27.3-cm-ID contactors for the same feed gas compositions, superficial velocities operating temperatures, and impeller speeds. All the DF curves appear to follow the same general pattern as a function of gas superficial velocity; that is, at low velocities, they tend to pinch toward asymptotically increasing values of DF. For gas superficial velocities in the range of 10-60 cm/min, the DF curves become essentially exponential functions of Q_S. At high superficial velocities, all curves appear to level off toward values which are probably associated with a rapid plug flow transit through the

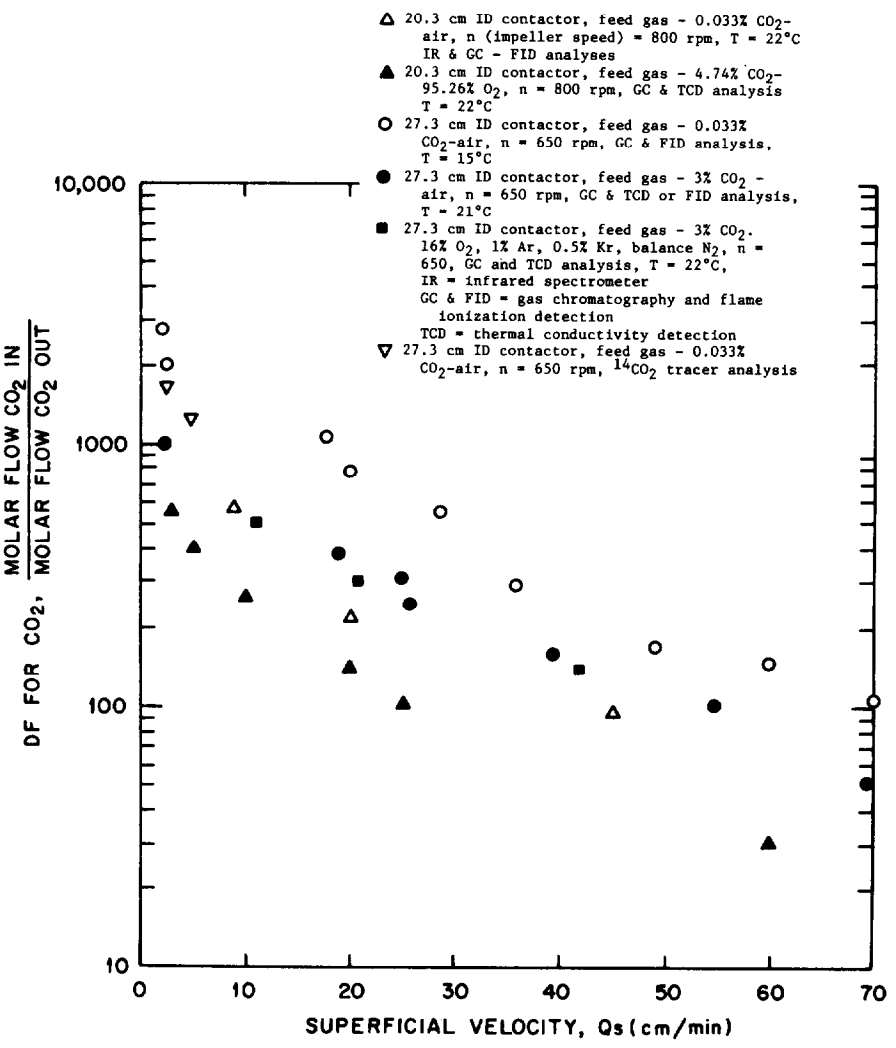

Fig. 2. Comparison of DFs for CO_2 removal from dilute gas streams utilizing a 1.0 m $Ca(OH)_2$ slurry in 20.3- and 27.3-cm-ID agitated contactors.

contactor. It is not clear whether all curves would tend to approach the same value at high superficial velocities. Further studies may be desirable at very high superficial velocities.

When a 0.033% CO_2--air feed was reacted with a 1.0 m $Ca(OH)_2$ slurry in the 27.3-cm-ID contactor, the DFs varied from 10^3 to 10^2 as the superficial velocity was increased from 5 to 70 cm/min. In general, the DF values obtained for CO_2 removal from 1-5% CO_2--air were somewhat lower (about a factor of 2) than those obtained for 0.033% CO_2--air for similar operating conditions (i.e., equal impeller speed, slurry concentration and temperature, superficial velocity, and contactor size).

The higher DFs obtained in the 27.3-cm-ID contactor may have been due to a slightly better design which resulted in more efficient mixing and higher interfacial area and mass transfer for that contactor. The volumes of the two contactors were too similar to allow us to determine whether the most appropriate criterion for contactor scale-up should be maintenance of constant superficial velocity or constant retention time. Either case would require additional scaling criteria such as maintenance of constant interfacial area, maintenance of the constant $nD_I/D_T^{0.5}$ (D_I = impeller diameter, D_T = contactor diameter) [proposed by Westerterp(20,21)], or maintenance of constant power input per volume of contactor. The data obtained at this time for constant power inputs did appear to show more similarity when compared for equal residence times rather than for equal superficial velocities. However, the question of proper scaling factor remains to be solved at a larger scale of contactor design.

It is also apparent from the results of Fig. 2 that the presence of 0.5% krypton in the feed gas had no effect on removal of CO_2 from air streams containing 1-5% CO_2. Further studies are now being conducted with ^{85}Kr-traced feed gases to determine the distribution of krypton between the gas and slurry phases. If the distribution is such that only a very low level (e.g., krypton in slurry = 0.0001 krypton in gas) of krypton is included in the slurry, the CO_2 removal process could be placed upstream of the krypton removal operation during off-gas processing.

When CO_2 was removed from 0.033% CO_2-air with a 1.0 m $Ca(OH)_2$ slurry in a 27.3-cm-ID contactor for no mechanical agitation (n = 0), the DFs ranged from 10 to 1 as the gas superficial velocity was increased from 5 to 70 cm/min.

For most of the experiments in this study, DFs were obtained for removal of CO_2 from dilute CO_2-air feeds with semibatch operation of the agitated contactor (no slurry flow). For semibatch operation with 1.0 m $Ca(OH)_2$, gas flow was maintained through the agitated contactor until the pH began to drop below the 12.4-12.6 range (dependent on operating slurry temperature). The time at which the pH begin to fall coincided with about 90% conversion of the $Ca(OH)_2$. Semibatch operation with $Ba(OH)_2$ slurries was obtained in a similar manner, but the pH range was different. Semibatch operation with NaOH solution was obtained for only a small decrease in pH due to excess capacity of the solution relative to a feed gas containing

only 3% CO_2. In a few experiments, for the same operating conditions (that is, gas flow rate, slurry temperature, impeller speed, etc) in both modes of operation, it was shown that there was little difference in DFs obtained for CO_2 removal for either semibatch or continuous slurry operation. Because the feed gases studied were dilute in CO_2, only a very slow continuous flow of 1.0 m $Ca(OH)_2$ was needed to replace the $Ca(OH)_2$ depleted by reaction with CO_2.

Comparison of Decontaminated Factors Obtained for CO_2 Removal from 0.033% CO_2--Air and 1% CO_2--Air Feeds with Slurries of $Ca(OH)_2$ and $Ba(OH)_2$ or Solutions of NaOH

Figure 3 shows experimental results which indicate the effects of varying the metal hydroxide composition or the power input on the removal of CO_2 from dilute CO_2--air feed gases in the 27.3-cm-ID agitated contactor. The theoretical nonsparged power inputs in the 27.3-cm-ID contactor for impeller speeds of 325 and 650 rpm, for impeller diameters one-half the contactor diameter, are about 2.6 and 21.0 kW/m^3 (0.1 and 0.8 hp/ft^3), respectively. Although the DF values are presented as a function of gas superficial velocity, the latter variable can be converted to nominal residence time by reciprocation after division by the appropriate dispersed-phase height (32-34 cm). The quiescent slurry volume was about 17 liters, while the agitated dispersed volume was typically 19 to 20 liters.

According to Eq. 8, at fixed values of superficial gas velocity, temperature (H and k_2 fixed), and impeller speed, the pressure driving term should vary inversely with hydroxyl ion concentration, according to the particular metal hydroxide employed. Conversely, the process DF should vary directly with $[OH^-]$. For fixed operating conditions, an increase in $[OH^-]$ should result in an increase in R_a but a decrease in p_{DF}. However, for operating conditions which result in DFs in excess of 10^2, the rate R_a becomes relatively constant, as there is little difference in 0.99 N_{CD}, 0.999 N_{CD}, or 0.9999 N_{CD} (where N_{CD} is CO_2 molar flow rate). Thus an increase in $[OH^-]$ concentration is manifested in a concomitant decrease in p_{DF} (and an increase in DF). Also, as previously discussed in Section IV, the process DF is predicted by Eq. 8 to vary inversely with superficial velocity, directly with impeller speed, and in most cases directly with slurry temperature. All of these predicted functional relationships are supported by the results in Fig. 3.

Under standard operating conditions of $T \cong 20°C$ and n = 650 rpm, the lowest DFs obtained for CO_2 removal in the 27.3-cm-ID contactor were for 1.0 m $Mg(OH)_2$ suspensions. With fixed gas velocities, the DFs increased according to the solubilities of the hydroxyl species, varying in the order $DF(NaOH) > DF(Ba(OH)_2) > DF(Ca(OH)_2)$. The DFs obtained for $Ba(OH)_2$ and NaOH systems varied directly with temperature, while for $Ca(OH)_2$ the dependence was less due to an inverse relationship between $Ca(OH)_2$ solubility and temperature.

Doubling the impeller speed at fixed operating conditions resulted in a sizable increase in the DF for CO_2 removal, regardless

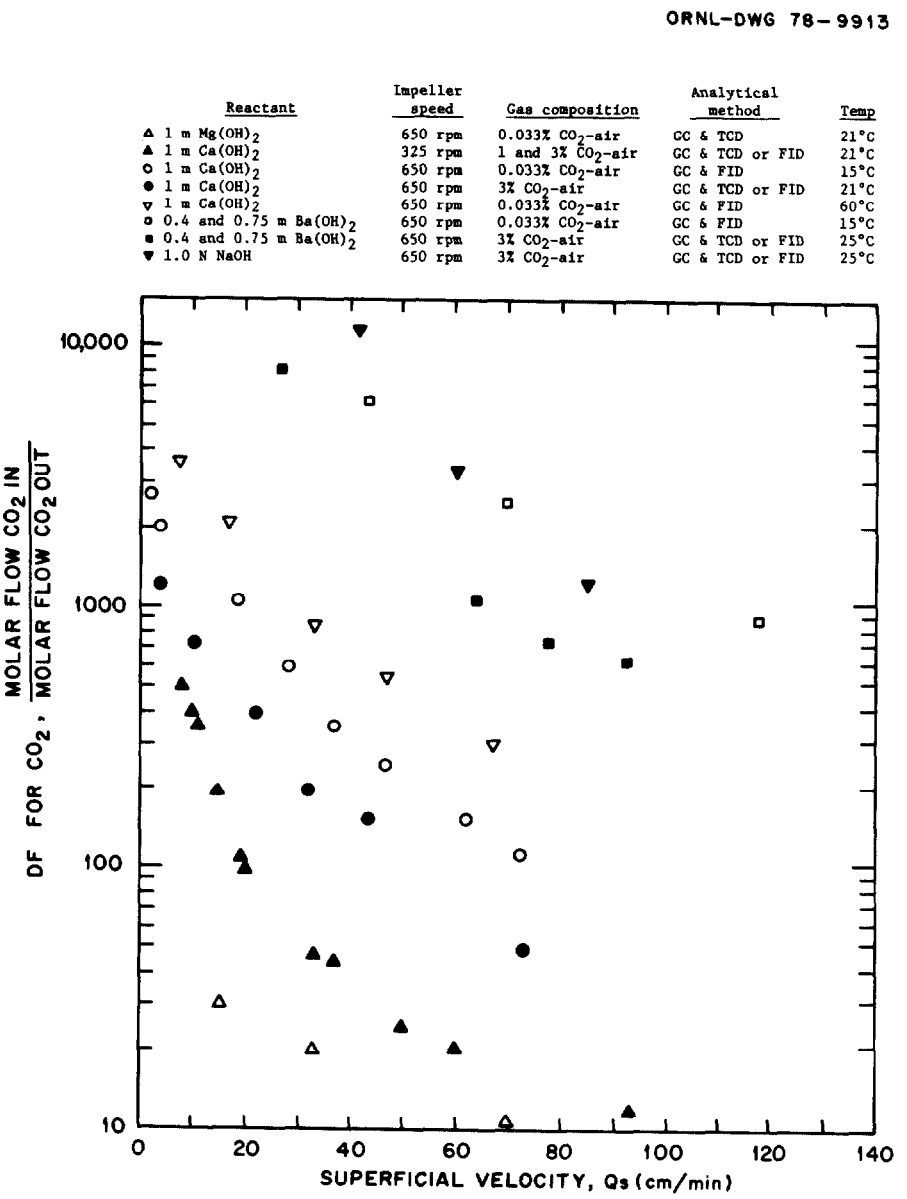

Fig. 3. DFs for CO_2 removal obtained for different metal hydroxide slurries at various impeller speeds, superficial velocities, and temperatures in the 27.3-cm-ID contactor.

of which metal hydroxide was used. Unfortunately, the improvement in process DF was accompanied by a penalty of about an eightfold increase in power input.

The similarity in the DFs obtained for CO_2 removal from feeds containing 0.033% CO_2--air and 1-5% CO_2--air is shown for both $Ba(OH)_2$ and $Ca(OH)_2$ suspensions. However, the DFs appear to be consistently higher for removal of CO_2 from the more dilute feed gas. Determination of DFs for CO_2 removal from gases containing 1-5% CO_2 was made for two reasons: (1) a need for treating a reprocessing off-gas containing as much as 1-5% CO_2 may arise in the future, (2) the similarity between DFs obtained for 0.033% and 1-5% CO_2 was useful because, even with the GC-flame ionization detection system, the practical lower limit for CO_2 detection was ∿100 ppb. When such concentrations occurred in effluents from the contactor for 0.033% CO_2--air feeds at low gas velocities, approximate DF values for the 0.033% CO_2-air feed could be readily estimated from the effluents from the contactor for feed gases containing 1% CO_2. In that case, an effluent of 100 ppb corresponded to a DF of 10^5.

Examination of the results of Fig. 3 indicates that there could be an advantage in utilizing a combination of NaOH solution with a $Ca(OH)_2$ or $Ba(OH)_2$ slurry to enhance the scrubbing efficiency for CO_2 removal from feed gases either dilute or rich in CO_2. Although no experiments have yet been conducted with this promising system, one might expect a set of reactions such as the following:

$$2NaOH + CO_2 \rightarrow Na_2CO_3 + H_2O \quad (9)$$

$$Ca(OH)_2 + CO_2 \rightarrow CaCO_3 + H_2O \quad (10)$$

$$Na_2CO_3 + Ca(OH)_2 \rightarrow 2NaOH + CaCO_3 \quad (11)$$

The total process could be conducted in one stirred contactor. Reactions 9 and 10 would be competing; however, the $CaCO_3$ would be a desirable end-product as it is for the CO_2-$Ca(OH)_2$ reaction alone. Any Na_2CO_3 formed by reaction 9 would react as in Eq. 11, resulting in the release of NaOH as an autocatalyst. The product would be filtered, the cake would be washed to remove any soluble salts, and the liquor containing primarily NaOH (with makeup $Ca(OH)_2$ added) could be recycled to the initial contactor operated in a continuous-flow mode.

Examination of the Group 2 elements in the periodic chart reveals that the metal hydroxide solubility increases, and the carbonate solubility decreases, with increasing atomic weight. However, when both cost and carbonate solubility are considered, $Ba(OH)_2$ appears to be the only other Group 2 hydroxide which could actually be competitive with slurried $Ca(OH)_2$.

CO_2 Removal from 0.033% CO_2--Air and 1-5% CO_2--Air Utilizing Fixed Beds and Fluidized Beds of Dry Hydrated Barium Hydroxides

Background. The efficacy of hydrated barium hydroxide in reacting with CO_2 at ambient conditions appears to have been ignored

in the search for techniques which serve to remove CO_2 from dilute CO_2--air streams and simultaneously provide a product amenable to the extended storage time which is necessitated by the long half-life of ^{14}C. It has been known for years[22] that LiOH as a solid bed possessed excellent CO_2 removal characteristics. Although the solid Li_2CO_3 product would be quite resistant to thermal decomposition, it would be too soluble to qualify as a candidate for long-term storage. Holladay[10] and Engel et al.[23] have shown previously that solid $Ca(OH)_2$ does not readily react with CO_2 at ambient conditions; significant rates are achieved only by adding heat at approximately 400°C. Also, CO_2 does not readily react with CaO or BaO at ambient conditions because of rate limitations which arise from diffusional resistance produced by formation of carbonates on the surface of CaO or BaO particles.

The gas-solid carbonation reaction between CO_2 and CaO has been the subject of numerous studies. Depending on the experimental conditions used, the conversion of CaO and $CaCO_3$ has ranged from 10 to 80%. The rate of solid carbonation was enhanced by ensuring the presence of water vapor, by increasing the temperature in the range of 300-800°C, and by increasing the pressure at the higher temperatures. It has been reported that BaO reacts with CO_2 faster at lower temperatures than does CaO. The interested reader should consult the review conducted by Swanson[24], who has compiled a list of 71 references concerning the reaction between CO_2 and solid alkaline oxides, hydrated alkaline hydroxides, alkaline slurries, and other substances.

Experimental Results

The studies that have been performed to date for removing CO_2 at ambient conditions from dilute CO_2--air feed gases with $Ba(OH)_2$ hydrates in fixed and fluidized beds have been of a preliminary and scoping nature. Thus, only general information and process trends will be discussed. Much more in-depth information must be obtained before the process can be discussed from a mechanistic or theoretical perspective.

In initial experimental studies with $Ba(OH)_2 \cdot 8H_2O$ reactant at room temperature, DFs in excess of 300 were obtained for CO_2 removal from 0.033% CO_2-air with the reactant in both fixed and fluidized beds (DFs >300 could not be analytically detected in preliminary experiments). Results of these early studies showed that the DFs for CO_2 removal from 0.033% CO_2--air were considerably enhanced when the feed gases were presaturated with water vapor. Therefore, all subsequent experiments were performed with water-saturated feed gases.

For the removal of CO_2 from feed gases containing 0.033%, 4.7%, and 88% CO_2 (balance as air), the highest DFs and bed conversions (routinely >95%) were obtained with the $Ba(OH)_2 \cdot H_2O$ species. A typical CO_2 sorption profile for a feed gas of 0.033% CO_2--air contacted at room temperature with $Ba(OH)_2 \cdot 8H_2O$ in a 2.54 x 15 cm glass column is shown in Fig. 4. For the initial 1 hr of contact time, DFs in excess of 3000 were obtained (100 ppb was the lower limit at which CO_2 could be accurately detected with the FID system). The DF then

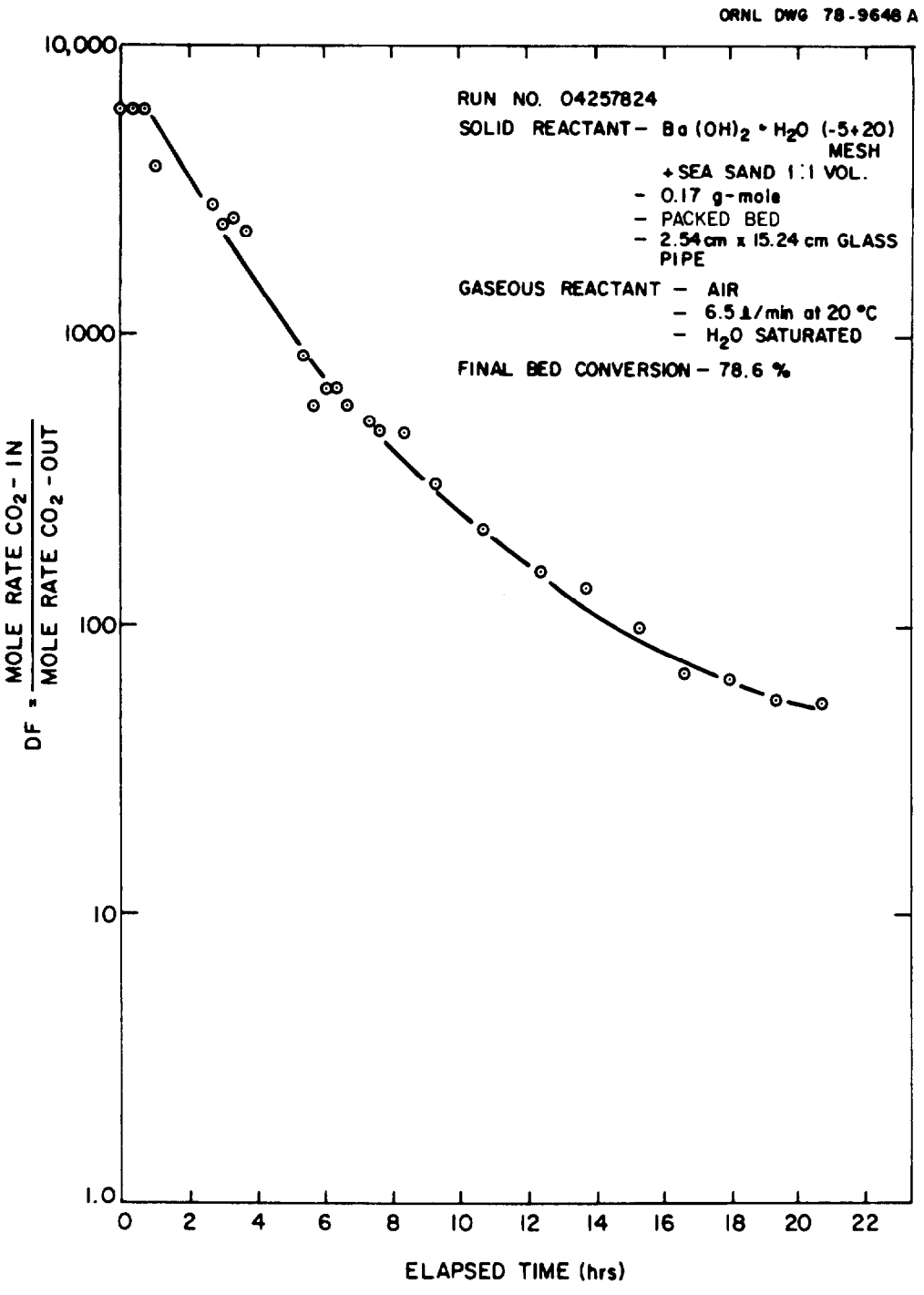

Fig. 4. Carbon dioxide removal capability of $Ba(OH)_2 \cdot H_2O$ in a fixed bed for treating a water-saturated feedstream containing 0.033% CO_2-air.

decreased gradually as indicated, although a value of 10^2 could be obtained for 13 hr of operation or until about 40% of the bed had been converted. After 25 hr of operation, the bed conversion was 78%. The DFs for CO_2 removal from very dilute feed gases appear to be dependent on the movement of a mass transfer zone through the bed. Further studies will be necessary to characterize this mass transfer mechanism and, in particular, its dependence on such parameters as flow rate, feed gas composition, $Ba(OH)_2$ species, and column design.

For the removal of CO_2 from a 4.78% CO_2-air feed, the highest DFs and bed conversions were obtained with the $Ba(OH)_2 \cdot H_2O$ species. The results of typical experiments for sorption of CO_2 from a 4.78% CO_2-air feed at room temperature in packed beds of the three barium hydroxide species are shown in Fig. 5. DFs as high as 3×10^4 were obtained for 75% of the run time in the $Ba(OH)_2 \cdot H_2O$ packed bed. Final bed conversion for processing 4.74% CO_2-air was as much as 85%; however, in the latter portion of the operation, process DFs rapidly decreased below 10^3 as complete bed conversion was approached. When barium hydroxide hydrates are used for CO_2 removal, a common operational problem is an increase in pressure which results from the production of $BaCO_3$ fines. However, this effect can be at least partially reduced, if not eliminated, by increasing bed porosity with such measures as adding solids such as fly ash or sand to the bed or forming the $Ba(OH)_2 \cdot H_2O$ into small pellets.

Fixed-bed treatments of 88% CO_2--air feeds have been successful only for $Ba(OH)_2 \cdot H_2O$ reactants. Conditions for a typical run consisted of processing 0.23 std liters/min of 88% CO_2--air through 0.2 g-mole of $Ba(OH)_2 \cdot H_2O$ in a 2.54 x 15 cm glass column. The maximum DF for a representative run was in excess of 10^5. Conversion at the base of the bed was 95%. Because of the fast rate of reaction, sufficient heat was generated to increase the column temperature to >70°C, which caused the $Ba(OH)_2 \cdot H_2O$ in the upper portions of the bed to melt. The product formed in the presence of this high temperature was a hard solid which complicated product removal. The various heat-related process problems that occurred for treatment of the 88% CO_2--air feed were alleviated when sand was added to the $Ba(OH)_2 \cdot H_2O$. The presence of the sand changed the character of the product to a free-flowing solid. The DFs for removing CO_2 from 88% CO_2--air feeds with $Ba(OH)_2 \cdot 5H_2O$ and $Ba(OH)_2 \cdot 8H_2O$ have been much lower than those obtained with $Ba(OH)_2 \cdot H_2O$.

Based on the initial experimental studies with very dilute CO_2--air feeds, the removal and permanent fixation of CO_2 from 0.033% CO_2-air with $Ba(OH)_2 \cdot H_2O$ in fluidized beds appear to be very promising. DFs in excess of 300 have been obtained at gas velocities considerably in excess of the minimum fluidization velocity (as much as five times the flow rate for the same DF in a packed bed). However, operation of the fluidized bed at the minimum fluidization velocity may sufficiently restrict the time and degree of gas-solid contact so as to produce poor overall mass transfer. Initial scoping data on laboratory-scale equipment have indicated that this may occur for a feed gas with 5% CO_2 concentration when it is contacted with 25-50 mesh $Ba(OH)_2 \cdot H_2O$ in a tapered fluidized bed. Although entrainment of fines has cuased operational difficulties, it is likely that

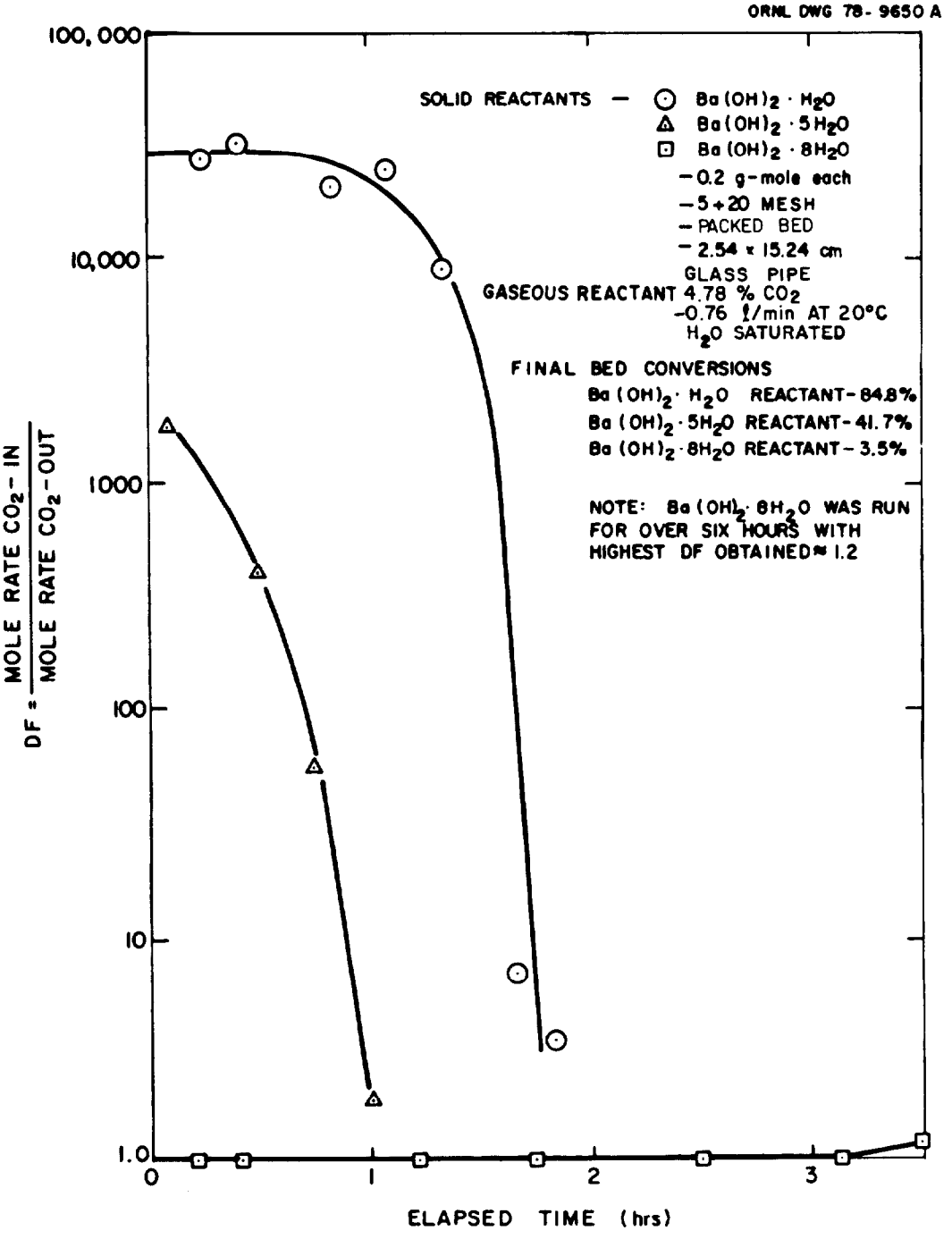

Fig. 5. Carbon dioxide removal capability of $Ba(OH)_2 \cdot H_2O$ in a fixed bed for treating a water-saturated feedstream containing 4.78% CO_2-air.

this problem can be resolved in larger-scale equipment through the use of cyclones and/or blowback filters.

The use of solid $Ba(OH)_2$ offered possibilities of an operationally simpler and less expensive process than the $Ca(OH)_2$ slurry contactor with its ancillary $CaCO_3$ recovery equipment. However, a distinct disadvantage of $Ba(OH)_2$ was the expense relative to $Ca(OH)_2$. Because reagent-grade $Ba(OH)_2 \cdot 8H_2O$ was found to cost in excess of $3.00/lb, a search for commercial suppliers of $Ba(OH)_2$ was made. Discussions have been conducted with two vendors who will supply $Ba(OH)_2$ in bulk quantities. Source I quoted $Ba(OH)_2 \cdot 8H_2O$ in truckload quantities at $0.50/lb (as of November 1977). Source 2 quoted truckload quantities of $Ba(OH)_2 \cdot H_2O$, $Ba(OH)_2 \cdot 5H_2O$, and $Ba(OH)_2 \cdot 8H_2O$ at $0.34, $0.28, and $0.235/lb, respectively (as of December 1977). Bulk $Ca(OH)_2$ may be purchased at $0.015/lb (as of May 1978). The various hydrates of $Ba(OH)_2$ have been obtained from both vendors and are now being studied in fixed-bed experiments to ascertain their relative efficiencies in reacting with feed gases containing low concentrations of CO_2.

VI. Conclusions

The removal of CO_2 from simulated LWR fuel reprocessing off-gases containing 0.033% CO_2--air and 1-5% CO_2--air has been shown to be feasible for gas processing with both alkaline slurries in agitated contactors and hydrated barium hydroxides in packed beds. It appears feasible to obtain CO_2 DFs of 10^2 to 10^3 for tractable sizes of equipment and operating conditions. However, the gas feeds that have been studied are those which simulate the composition of LWR fuel reprocessing off-gases as they would occur at the end of the off-gas processing train where I_2, NO_x's, and krypton would already have been removed. Thus, further experiments will be conducted to determine the effect of placing the CO_2 removal processes at optional sites in the off-gas processing train where such contaminants as I_2 and NO_x's could complicate the operation and to determine the proper scaling factors for increasing the size of the agitated contactor process. Additional experiments will be conducted with $Ba(OH)_2 \cdot xH_2O$ beds to optimize the parametric relationships among the following factors: degree of barium hydroxide hydration, bed particle size, bed temperature, gas flow rate, column design, and bed conversion and bed DF for CO_2 removal.

VII. References

1. H. Bonka et al., "Contamination of the Environment by Carbon-14 Produced in High Temperature Reactors," Kerntechnik 15(7), 297 (1973).

2. P. J. Magno, C. B. Nelson, and W. H. Ellett, "A Consideration of the Significance of Carbon-14 Discharges from the Nuclear Power Industry," p. 1047 in Proceedings of the Thirteenth AEC Air Cleaning Conference, San Francisco, Calif., CONF-740807 (August 12-15, 1974).

3. C. O. Kunz, W. E. Mahoney, and T. W. Miller, "Carbon-14 Gaseous Effluents from Boiling Water Reactors," Trans. Am. Nucl. Soc. 21, 91 (1975).

4. W. Davis, Jr., "Carbon-14 Production in Nuclear Reactors," ORNL/NUREG/TM-12 (February 1977).

5. A. G. Croff, "An Evaluation of Options Relative to the Fixation and Disposal of ^{14}C-Contaminated CO_2 as $CaCO_3$," ORNL/TM-5171 (April 1976).

6. G. G. Killough et al., "Progress Report on Evaluation of Potential Impact of ^{14}C Releases from an HTGR Reprocessing Facility," ORNL/TM-5284 (July 1976).

7. L. Machta, "Prediction of CO_2 in the Atmosphere," Carbon and the Biosphere, G. M. Woodwell and E. V. Pecan, Eds., Technical Information Center, Office of Information Services, U.S. Atomic Energy Commission (August 1973).

8. G. G. Killough, "A Diffusion-Type Model of the Global Carbon Cycle for the Estimation of Dose to the World Population from Releases of Carbon-14 to the Atmosphere," ORNL/TM-5269 (1977).

9. J. W. Snider and S. V. Kaye, "Process Behavior and Environmental Assessment of ^{14}C Releases from an HTGR Fuel Reprocessing Facility," Proceedings of the ANS-AIChE Topical Meeting, Sun Valley, Idaho, August 5-6, 1976.

10. D. W. Holladay, "Experiments with a Lime Slurry in a Stirred Tank for the Fixation of Carbon-14 Contaminated CO_2 from Simulated HTGR Fuel Reprocessing Off-Gas," ORNL/TM-5757 (1978).

11. E. Rapkin, "Hydroxide of Hyamine 10-X," Packard Technical Bulletin, revised 1961.

12. H. Jeffay and J. Alvarez, "Liquid Scintillation Counting of Carbon-14; Use of Ethanolamine-Ethylene Glycol Monomethyl Ether-Toluene," Anal. Chem. 33, 612 (1961).

13. F. H. Woeller, "Liquid Scintillation Counting of $^{14}CO_2$ with Phenethylamine," Anal. Biochem. 2, 508 (1961).

14. F. W. Williams, F. J. Woods, and M. E. Umstead, "Determination of Carbon Dioxide in the Parts-Per-Million Range with Gas Chromatography," J. Chromat. Sci. 10, 570 (1972).

15. H. G. Eaton, M. E. Umstead, and W. D. Smith, "A Total Hydrocarbon Analyzer for Use in Nuclear Submarines and Other Closed Environments," J. Chromat. Sci., 11, 275 (1973).

16. V. A. Juvekar and M. M. Sharma, "Absorption of CO_2 in a Suspension of Lime," Chem. Eng. Sci., 28, 825 (1973).

17. V. D. Mehta and M. M. Sharma, "Mass Transfer in Mechanically Agitated Gas-Liquid Contactors," Chem. Eng. Sci., 26, 461 (1971).

18. J. Hanhart, H. Kramers, and K. R. Westerterp, "The Residence Time Distribution of the Gas in an Agitated Gas-Liquid Contactor," Chem. Eng. Sci., 18, 503 (1963).

19. R. M. Morris and E. T. Woodburn, "Testing of Certain Design Equations for Predicting the Performance of a Calcium Hydroxide Carbonation Reactor, Part I: Gas Bubble Dynamics and Interfacial Areas in a Stirred Tank," South African Chem. Proc. (June-July 1967); "Part II: The Constant Rate Period," South African Chem. Proc. (August-September 1967); "Part III: The Falling Rate Period," South African Chem. Proc. (October-November 1967).

20. K. R. Westerterp, L. L. Van Dierendonck, and J. A. De Kraa, "Interfacial Areas in Agitated Gas-Liquid Contactors," Chem. Eng. Sci., 18, 157 (1963).

21. K. R. Westerterp, "Design of Agitators for Gas-Liquid Contacting," Chem. Eng. Sci., 18, 495 (1963).

22. R. M. Wright, J. M. Ruder, V. B. Dunn, and K. C. Hwang, "Development of Design Information for Molecular-Sieve Type Regenerative CO_2-Removal Systems," NASA-CR-2277, prepared by Airresearch Man. Co. (July 1973).

23. R. Engel, V. Decken, and B. Claus (Brown Boveri/Krupp Reaktorbau G.m.b.H.), "Method of Removing CO_2 and H_2O from a Gas Stream," U.S. Patent 3,519,384, granted July 7, 1970.

24. R. R. Swanson, "Literature Survey, Reaction of CO_2 with Solid CaO," Idaho Chemical Programs Operational Office, RRSW (October 1976).

DISCUSSION

KABAT: Have you tested the absorbent at higher temperatures and what is the maximum operational temperature you recommend for $Ba(OH)_2$?

HAAG: Temperature is not a variable of significant importance as the reaction is kinetically feasible under ambient conditions. We are restricted to upper temperatures of 105°C for the $Ba(OH)_2 \cdot H_2O$ and 78°C for the $Ba(OH)_2 \cdot 8H_2O$, as these are melting points.

KABAT: It means that the temperature limit for this reaction would be roughly 100°C?

HAAG: That would be the upper limit. We had been obtaining data at ambient conditions, i.e., 25°C, and this is the temperature I recommend for the process.

VAN BRUNT: Have you considered spouted beds and slowly moving beds?

HAAG: We have considered them. I should point out that the bulk of this work has been performed during the past nine months, and has been of an exploratory nature. Fluidized bed work has been put off primarily because of the problems we're having with entrainment of fines. The spouted bed looks good but we see some funny things, e.g., the minimum fluidization velocity seems to change and the bed conversion changes. Operation of a spouted fluidized bed could very definitely be an alternative in reducing the fines entrainment problem and we will examine it with further process development.

VAN BRUNT: You would expect the fines problem to be minimized at minimum fluidization.

HAAG: Yes.

BROWN: Do the advantages of the solid-state reactions appear large enough to justify halting the work on the aqueous system?

HAAG: This is difficult to answer at this time due to the different stages of development of the slurry and packed bed processes. I must point out that we have not conducted an in-depth examination of the effects of possible off-gas constituents, e.g. NO_x, I_2, CH_3I, Kr, on the two systems. Furthermore, the location of this process in the overall offgas flowsheet is subject to change. This will affect the feed gas. Packed beds of $Ba(OH)_2$ hydrates look very promising but they are in the initial stages of development. Based upon the expertise which we have developed with respect to the slurry system and its present stage of development, a nominal effort will complete the study. My choice, at this time, would be the packed bed approach but with the reservation that more data are required before a firm decision can be made. The size of a stirred tank reactor to treat 500 cfm would be excessive and the power input would be high.

BROWN: Would the disadvantage of handling the aqueous system and the subsequent clean-up be prohibitive?

HAAG: You are exactly right.

McDONALD: The authors should be aware that the Navy has been using LiOH canisters for several years to remove CO_2 from contained atmospheres. It is possible that these commercial systems have applicability in airborne nuclear wastes. At any rate, advantage may be taken of a large technical literature pertaining to the research and development and commercialization of these systems.

HAAG: I am aware of the open literature work of Dietz, Umstead, et al. at the Naval Research Lab that pertains to submarine environments and I would gladly welcome any information which would be beneficial in our process development. I understand LiOH was used by NASA in the early Mercury space flights for CO_2 removal from spacecraft environments and was eventually discontinued and replaced by molecular sieves due to weight limitation problems. Incidentally, our present analytical system, conversion of CO_2 to CH_4 over a nickel catalyst and subsequent FID analysis of the methane, may be referenced to some excellent work performed at NRL by Williams, Eaton, Umstead, et al.

MEASUREMENT OF RADIOACTIVE GASEOUS EFFLUENTS FROM VOLOXIDATION AND DISSOLUTION OF SPENT NUCLEAR FUEL*

J. A. Stone and D. R. Johnson
Savannah River Laboratory
E. I. du Pont de Nemours & Co.
Aiken, South Carolina 29801

Abstract

Laboratory-scale tests gave data on the release of tritium, ^{14}C, ^{85}Kr, and ^{129}I as radioactive gases from spent nuclear fuels during voloxidation and dissolution. Voloxidation, a proposed reprocessing step, is intended to remove tritium from fuel by oxidation of UO_2 to U_3O_8 prior to dissolution of the fuel with nitric acid. ^{14}C, ^{85}Kr, and ^{129}I may be evolved in both steps. Quantitative data from the tests may be used in designing off-gas treatment processes and equipment. The tests were performed in a shielded cell with a combination voloxidizer-dissolver. With a recirculating off-gas system, tritium and ^{14}C were trapped on molecular sieves; ^{129}I was trapped on silver-exchanged zeolite. ^{85}Kr was measured by online gamma-ray counting. Zircaloy-clad UO_2 fuels from H. B. Robinson-2, Oconee-1, and Saxton reactors, with burnups from ~100 to ~28,000 MWD/MTHM, were tested. The results confirm that voloxidation released most of the tritium but only small fractions of the ^{14}C, ^{85}Kr, and ^{129}I; the remainder of these radioactive gases evolved when the voloxidized fuels were dissolved. Voloxidation off-gases typically contained >99.8% of the tritium, 17 to 22% of the ^{14}C, 7 to 17% of the ^{85}Kr, and <8% of the ^{129}I. Tritium evolved as HTO, with <0.1% as HT.

Introduction

In processing spent nuclear fuel to recover fissile material, volatile radionuclides such as tritium, ^{14}C, ^{85}Kr, and ^{129}I evolve into the off-gas system. Technology is available for trapping the gaseous radioactive species to prevent release to the environment.(1-3) However, proper design of off-gas facilities requires quantitative data on amounts evolved in each process step.

A reference flowsheet for head-end processing steps is shown in Figure 1. The spent fuel rods are sheared into short pieces, and then a voloxidation step drives tritium out of the fuel. The oxidized fuel is dissolved with nitric acid, and the clarified solution is fed to solvent-extraction steps. Most of the gaseous radionuclides enter the off-gas system during the voloxidation and dissolution steps.

* The information contained in this article was developed during the course of work under Contract No. AT(07-2)-1 with the U. S. Department of Energy.

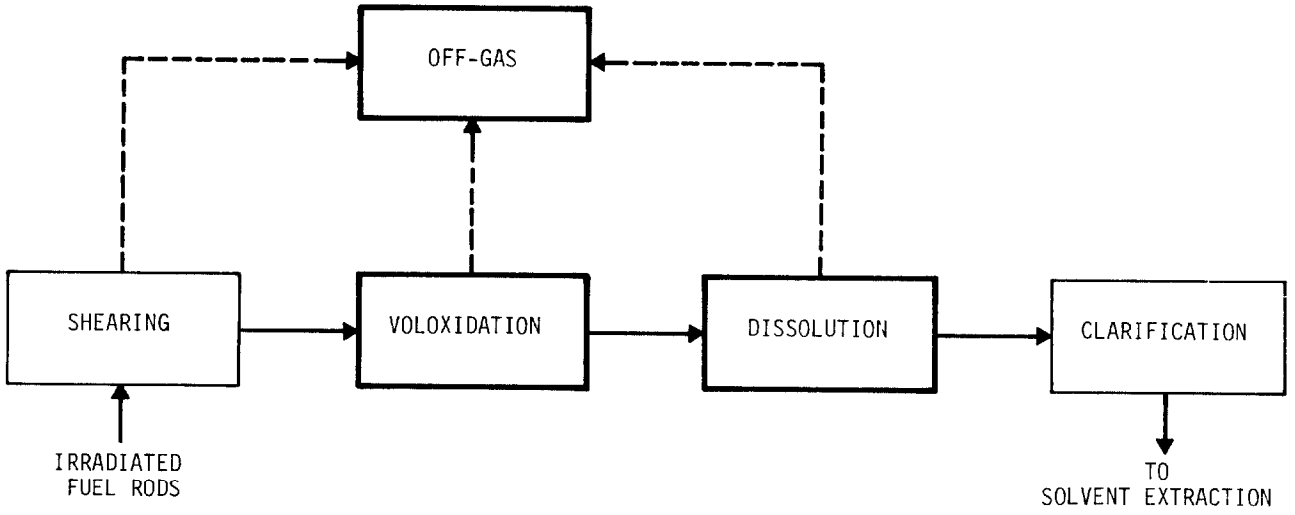

Figure 1. Head-end process operations.

In voloxidation, first developed at Oak Ridge National Laboratory,[4] UO_2 fuel oxidizes to U_3O_8 at about 490°C, promoting evolution of tritium as HTO (water vapor). During oxidation, the fuel expands, disintegrates into fine powder, and separates from the cladding. Tritium removal before fuel dissolution is desirable to avoid extensive isotopic dilution by nontritiated water. Previous studies[4,5] showed that even though tritium evolved quantitatively during voloxidation, species such as ^{85}Kr and ^{129}I evolved incompletely.

In this paper, new laboratory-scale measurements of tritium, ^{14}C, ^{85}Kr, and ^{129}I evolved during voloxidation and dissolution of irradiated power-reactor fuels are reported. We confirm the quantitative evolution of tritium during voloxidation and report the distribution of the other species between voloxidation and dissolution.

Experimental Procedure

Apparatus

Voloxidizer-Dissolver. A stainless-steel reaction vessel, shown in Figure 2, serves for both voloxidation and dissolution of irradiated fuel. The apparatus is in a shielded cell for remote operation and is connected to off-gas collection facilities. The voloxidizer-dissolver is a 2-liter reaction chamber equipped with numerous heaters, thermocouples, cooling coils, a rotary agitator, and orifices for off-gases. The reaction chamber rotates on a horizontal axis to provide two operating positions: 1) tilted as shown in Figure 2 for voloxidation or 2) vertically upright for dissolving. Gases emerge through a reflux condenser during dissolving or through another orifice during voloxidation.

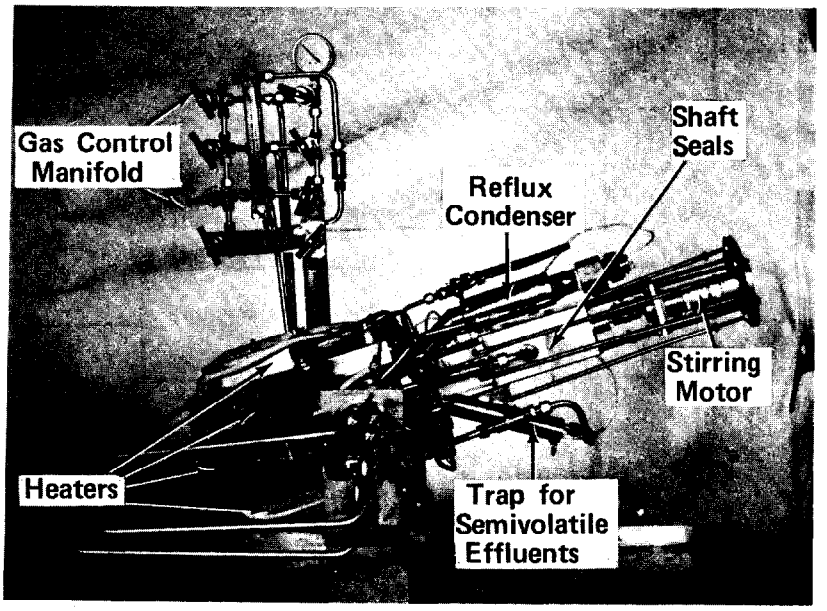

Figure 2. Voloxidizer-dissolver.

Off-Gas System. The voloxidizer-dissolver is coupled to laboratory-scale off-gas equipment both inside and outside the shielded cell; the arrangement for voloxidation is shown schematically in Figure 3. A small pump recirculates helium carrier gas through the closed system. Oxygen consumed in the system is replaced to maintain constant oxygen content in the recirculating gas. ^{85}Kr is measured by online gamma-ray counting; tritium, ^{14}C, and ^{129}I are collected on a series of molecular sieve traps for later analyses. The off-gas system was tested and calibrated with tracer amounts of radioactive gases.

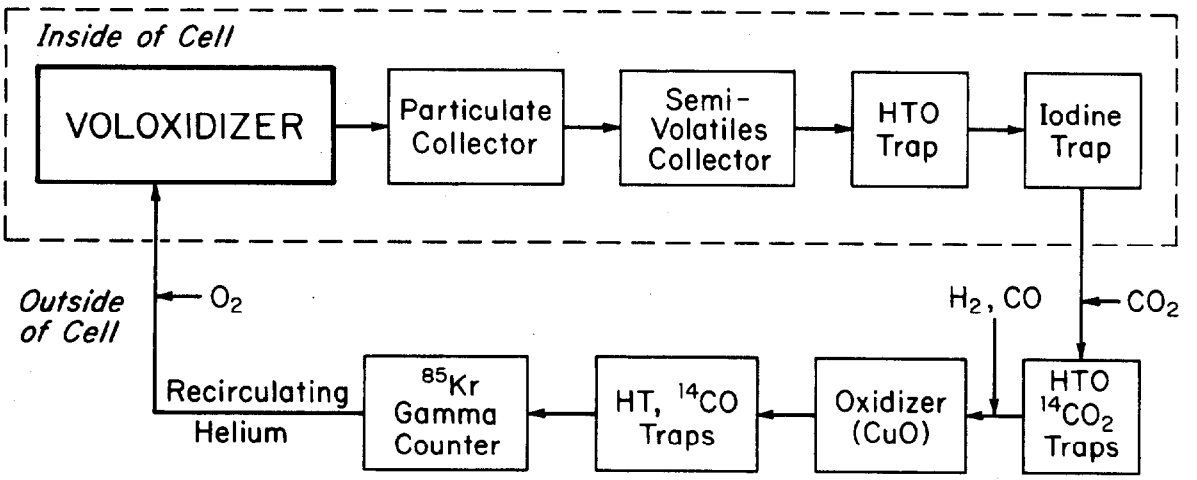

Figure 3. Off-gas system.

Particulates in the off-gas are collected on impacter plates at the mouth of the voloxidizer. Semivolatile elements such as cesium, antimony, and ruthenium may plate out along a temperature-gradient tube following the particulate collector. Data on particulates and semivolatiles are not discussed in this paper.

Three Type 3A molecular sieve traps collect tritium as HTO. One trap closely coupled to the voloxidizer collects evolved HTO quantitatively. Water vapor introduced into the off-gas recirculation line carries the HTO. The other two traps are in a hood outside the shielded cell, one upstream and one downstream from an oxidizing bed of CuO at 300°C. The upstream trap is a backup for collecting residual HTO, whereas the downstream trap collects HTO converted from HT in the off-gas. Hydrogen gas introduced upstream from the CuO bed carries any HT.

Two Type 13X molecular sieve traps collect ^{14}C as $^{14}CO_2$. These traps are also outside the shielded cell, one on each side of the heated CuO bed. Any ^{14}CO in the off-gas is oxidized to $^{14}CO_2$ and collected in the second trap. Carrier CO_2 is added before the first trap, and carrier CO is added before the CuO bed. As discussed in the following section, separation of CO and CO_2 in this system is not entirely satisfactory.

The off-gas circulates through a calibrated chamber for counting the 514-keV gamma ray of ^{85}Kr with a high-resolution Ge-Li detector. These rapid online measurements allowed the course of voloxidation and dissolution reactions to be monitored.

A bed of silver-exchanged zeolite (Ag^0-X) at 180°C traps iodine in the off-gas. During voloxidation, the iodine trap, although near the voloxidizer in the shielded cell, is downstream from the tritium trap. Because any ^{129}I that deposited in the upstream lines or in the tritium trap would not have been detected, the measured ^{129}I is possibly less than the total amount evolved.

The arrangement of the off-gas system for dissolution is similar to that shown in Figure 3. Equipment outside the shielded cell is identical. In the cell, dissolver off-gases pass through a reflux condenser directly to an iodine trap.

Analytical Methods

After each voloxidation or dissolution test, tritium, ^{14}C, and ^{129}I are removed from their primary sorbents by a heat treatment. The methods used are summarized in Table I. HTO and $^{14}CO_2$ are desorbed from molecular sieve pellets to obtain forms suitable for liquid scintillation beta-counting. Used pellets are discarded.

Because silver interferes with neutron-activation analysis for ^{129}I, the iodine is removed from silver zeolite as HI and resorbed on lead zeolite, which does not interfere. This method was adapted from the work of Staples, Murphy, and Thomas.[6,7] The regenerated silver-zeolite traps are reused.

Table I. Analyses for gaseous radioactive species.

Radionuclide	Primary Sorbent	Bakeout[a]	Carrier Gas	Secondary Trap	Analytical Method
^{3}H	3A	Yes	H_2O	Cold trap[b]	β counting
^{14}C	13X	Yes	CO_2	CO_2mMET[c,d]	β counting
^{85}Kr	-	-	He	-	Online γ counting
^{129}I	Ag^0-X	Yes[e]	H_2	Pb-X(150°C)	Neutron activation

a. Heat treatment at 500°C for 8 to 16 hours.

b. Refrigerated to -50°C.

c. Trademark of Amersham/Searle carbon dioxide trapping agent.

d. Preceded by cold trap for H_2O.

e. Heated at 500°C with flowing hydrogen gas.

Irradiated Fuels

Representative fuels with a wide range of burnups from three different light-water reactors, listed in Table II, were used for the tests described in this paper. Each of these fuels was UO_2 and was originally clad with Zircaloy. Fuels from H. B. Robinson-2 and Oconee-1 reactors were from single rods. Saxton fuel was contained in four rods with different irradiation histories.[8]

Similar unirradiated UO_2 fuel was tested in a control experiment to establish lower limits of detection for the gaseous radioactive species.

Table II. Characteristics of Zircaloy-clad UO_2 fuel rods.

Reactor	Rod[a]	Burnup, MWD/MTHM	Cooling Period, yr	Initial ^{235}U Enrichment, %
H. B. Robinson-2	-	∿28,000	3	2.55
Oconee-1	-	∿11,000	3	2.0
Saxton	A	∿6,000	5	12.5
	B	∿3,000	5	12.5
	C	∿3,000	5	12.5
	D	∿100	5	12.5

a. Arbitrary designations.

Test Conditions

Voloxidation. About 200 g of irradiated UO_2 fuel in cladding and/or as loose fragments was charged to the voloxidizer. Cladding pieces were from 2.5 to 3.8 cm long. The fuel was heated for 4 hours at 490°C and was tumbled with the rotary agitator at 3.5 rpm. Oxygen content of the recirculating gas was monitored periodically with an inline oxygen analyzer and was held at a nominal 20% in most tests, by adding oxygen as needed. Eleven tests were run with irradiated fuels. Control tests were run with unirradiated fuel and without fuel.

Figure 4 shows the behavior of a typical voloxidation test. Reaction temperature, incremental oxygen additions, and ^{85}Kr evolution were measured as a function of time. In this example, for Saxton fuel, the reaction appeared to be complete after one hour at 490°C. Part of the added oxygen was consumed in the off-gas system by reactions in the heated CuO bed; this fraction was determined in a separate blank experiment and was subtracted from the data to obtain the amount of oxygen consumed by voloxidation.

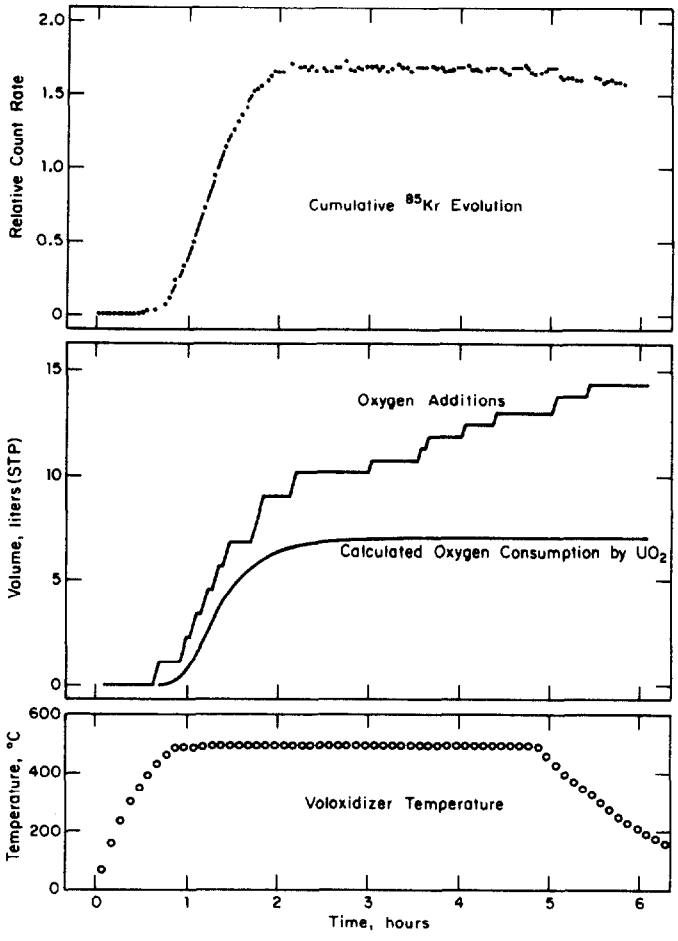

Figure 4. Typical voloxidation behavior (Saxton fuel).

Dissolution. Fuel dissolution was initiated at ambient temperature with a batch quantity of 1 to 3M HNO_3. As the dissolution proceeded, 10M HNO_3 was metered in over 60 to 75 minutes, to slowly increase acid concentration. Ninety minutes after the initial acid charge, the solution temperature was increased to 90°C to complete the dissolution. Gas circulated through the dissolver and off-gas system, and radioactive species were trapped as with voloxidation. Additional steps included leaching the spent cladding hulls and any undissolved residue with 10M HNO_3 and then rinsing with 1 to 3M HNO_3.

Figure 5 shows the behavior of a typical dissolution test. Dissolved uranium concentration and ^{85}Kr evolution were measured as a function of time. The data show that total dissolution time was about 200 minutes and that ^{85}Kr evolution correlated well with the fuel dissolution rate.

Each batch of voloxidized fuel (11 irradiated and 1 unirradiated) and single batches of unvoloxidized Robinson and Oconee fuels were dissolved. A few experiments[5] in a glass apparatus with less complete off-gas facilities are reported for comparison. In a blank experiment, dissolving operations without fuel were also performed.

Dissolver solutions were analyzed for tritium, ^{14}C, and ^{129}I. Negligible ^{14}C or ^{129}I was found in solution. The tritium decontamination factor (DF) for voloxidation was calculated from the amount of tritium in the dissolver solution.

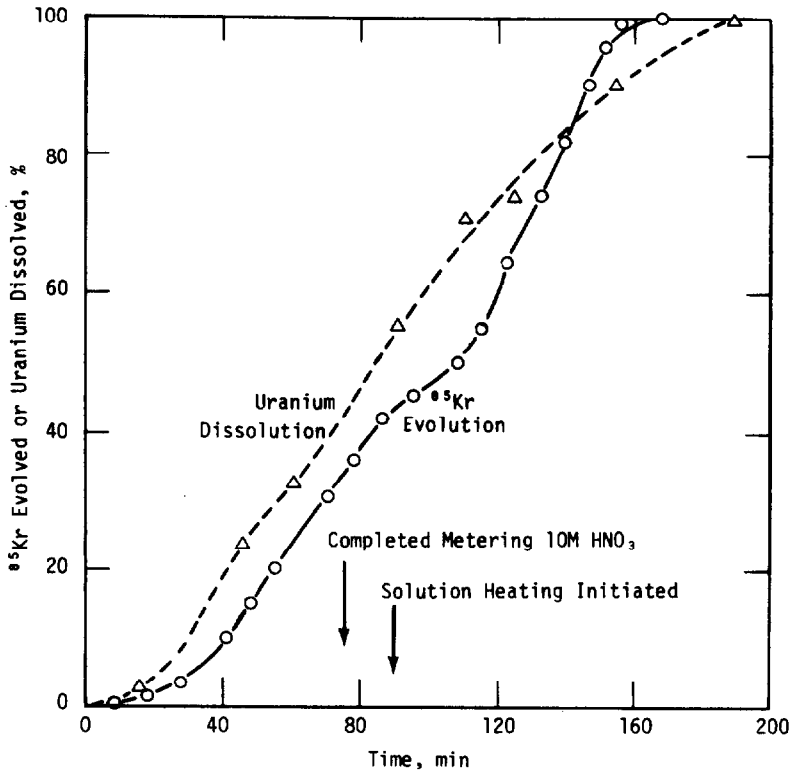

Figure 5. Typical dissolution behavior (Saxton fuel).

Results and Discussion

Tritium

Table III shows, for the cases studied, that nearly all of the tritium in spent fuel evolved during voloxidation, thus confirming the effectiveness of voloxidation for tritium removal. In most of the tests, >99.8% of tritium in the fuel was removed by voloxidation. The small amount of tritium remaining in the fuel after voloxidation was not released to off-gas by dissolution; it was found as HTO in the dissolver solution.

In two tests, the fraction of tritium evolved during voloxidation was somewhat low (87 and 98% released). Conversion of UO_2 to U_3O_8 was incomplete in both tests. In every test with complete conversion to U_3O_8, the tritium DF exceeded 650.

The total amount of tritium for each test is the sum of amounts found in all off-gas traps and in the dissolver solution. Most of the total in each test was found in the trap nearest the voloxidizer, as expected. Duplicate tests with Saxton rods gave good reproducibility. Total tritium from Robinson and Saxton fuels appears to be correlated with burnup, but tritium from Oconee fuel is less than that expected on the basis of burnup.

Table III. Tritium distribution.

	Tritium, Ci/MTU			Voloxidation		
Fuel	Voloxidizer Off-gas	Dissolver Solution	Total	Tritium DF	Tritium, % of Total	HT, %[a]
Robinson	133	0.004	133	33,150	>99.9	0.03
	b,c	250	250	-	-	-
Oconee	6	0.91	7	8[d]	87.5	0.05
	16	0.002	16	6,560	>99.9	0.02
	27	0.013	27	2,170	>99.9	0.01
	7	0.035	7	195	99.5	0.07
	b	35	35	-	-	-
	b,c	7	7	-	-	-
Saxton						
A	31	0.57	32	55[d]	98.2	0.01
B	25	0.027	25	925	99.9	0.1
B	29	0.044	29	665	99.8	0.1
C	28	0.003	28	8,450	>99.9	0.05
C	28	0.007	28	4,150	>99.9	0.03
D	10	0.012	10	805	99.9	0.02
Unirradiated	0.2	0.033	0.2	-	-	-
Blank	1.2	0.008	1.2	-	-	-

a. Upper limit.

b. Unvoloxidized UO_2 fuel.

c. Dissolved in glass apparatus (Reference 5).

d. Incomplete oxidation.

Tritium in irradiated fuel arises principally from ternary fission and activation of ^{6}Li impurities. Thus, total tritium will depend upon the lithium impurity level and upon irradiation history of the fuel. A calculation with the ORIGEN code[9] for Robinson fuel predicted about 470 Ci/MTU of tritium from fission and a comparable amount from activation. Observed amounts are less. Possible sources of variation in the results include: loss of tritium in earlier operations, such as shearing and storage; differences in burnup along a fuel rod; migration of tritium within a rod, because of thermal gradients; tritium trapped in the cladding.

Carbon-14

From 17 to 22% of the total ^{14}C in the fuels evolved during voloxidation in most of the tests (Table IV). The remainder of the ^{14}C was released to the off-gas system during dissolution. The amounts found were 1000 times greater than the limit of detection for ^{14}C, as determined by the control experiments. Duplicate tests with Saxton fuel showed that the measurements were reproducible.

Somewhat less than the typical ∿20% of the ^{14}C evolved during the two voloxidation tests with incomplete conversion to U_3O_8; about 9% was released in these tests. Saxton fuel with very low burnup was another exception, evolving only 2% during voloxidation.

Table IV. Carbon-14 distribution.

Fuel	^{14}C, Ci/MTU			Voloxidation		Dissolution
	Voloxidizer Off-gas	Dissolver Off-Gas	Total	^{14}C, % of Total	^{14}CO, %[a]	^{14}CO, %[a]
Robinson	0.066	0.243	0.309	21.3	59	0.04
Oconee	0.010	0.104	0.114	9.1[b]	22	72
	0.025	0.124	0.149	16.8	27	65
	0.024	0.104	0.128	18.7	2	31
	0.035	0.141	0.176	19.7	51	24
	c	0.081	0.081	-	-	0.2
Saxton						
A	0.0037	0.0389	0.0426	8.7[b]	0.07	0.14
B	0.0055	0.0235	0.0290	19.1	75	29
B	0.0068	0.0234	0.0302	22.4	51	58
C	0.0053	0.0216	0.0269	19.7	64	29
C	0.0047	d	d	d	69	d
D	0.00001	0.0005	0.0005	2.0	76	4
Unirradiated	0.000005	0.00005	0.00005	-	50	55
Blank	0.000005	0.00003	0.00003	-	50	20

a. Upper limit (see text).

b. Incomplete oxidation.

c. Unvoloxidized UO_2 fuel.

d. Not determined.

^{14}C in irradiated fuels is formed primarily by the $^{14}N(n,p)^{14}C$ reaction on nitrogen impurities in the fuel and secondarily by the $^{17}O(n,\alpha)^{14}C$ reaction. Thus, the amount of ^{14}C produced depends upon the amount of nitrogen impurity and upon fuel burnup. A typical calculated value is 0.5 Ci/MTU for fuel with 20-ppm nitrogen irradiated to about 30,000 MWD/MTHM. The amounts of ^{14}C measured in Robinson, Oconee, and Saxton fuels are correlated with the burnups and are in the range expected for 10 to 20 ppm nitrogen in the fuels.

Krypton-85

Table V shows that, in most of the tests, 7 to 17% of the total ^{85}Kr in the fuels evolved during voloxidation. The dissolution tests confirmed that the major fraction of ^{85}Kr remained in voloxidized fuel but was totally released by dissolving. Duplicate tests with Saxton fuel agreed well. Again, somewhat lower results (4 to 6% released during voloxidation) were obtained for the two tests with incomplete conversion to U_3O_8.

The small fraction of ^{85}Kr from voloxidation agrees with results of other workers with different fuels.[4] Apparently, krypton from fission is dispersed throughout the fuel as individual atoms rather than accumulated as bubbles at the grain boundaries. Oxidation of UO_2 does not release much of the krypton from the matrix, even though a very fine U_3O_8 powder is formed. Since tritium is released completely under the same conditions, the results imply that krypton diffuses much slower than tritium in the U_3O_8 crystal lattice.

Table V. Krypton-85 distribution.

Fuel	^{85}Kr, Ci/MTU: Voloxidizer Off-Gas	^{85}Kr, Ci/MTU: Dissolver Off-Gas	^{85}Kr, Ci/MTU: Total	Voloxidation ^{85}Kr, % of Total
Robinson	137	1651	1788	7.7
Oconee	41	969	1010	4.1[a]
	123	1087	1210	10.2
	77	1011	1088	7.1
	115	1058	1173	9.8
	b	1070	1070	-
Saxton				
A	62	944	1006	6.2[a]
B	75	377	452	16.6
B	62	396	458	13.5
C	60	388	448	13.4
C	61	c	c	c
D	0.7	5.1	5.8	11.3
Unirradiated	0.07	1.00	1.07	-
Blank	0.07	0.08	0.15	-

a. Incomplete oxidation.

b. Unvoloxidized UO_2 fuel.

c. Not determined.

Total ^{85}Kr in fuel is related to burnup, cooling period, and perhaps previous thermal history. A calculation with the ORIGEN code predicted about 7000 Ci/MTU of ^{85}Kr for the Robinson fuel. The amounts of ^{85}Kr measured in Robinson, Oconee, and Saxton fuels correlate well with burnups but are somewhat lower than calculated values. An unknown amount of krypton may have been released on initial puncture of the rods and subsequent storage of the fuel.

Iodine-129

Table VI gives results for ^{129}I collected during voloxidation and/or dissolution of the fuels. The data are less consistent than for the other radioactive gases, possibly because of experimental difficulties. We conclude from our experience with these tests that separate experiments designed specifically to measure iodine will yield more accurate results.

In all of the tests, very little ^{129}I (from 0.02 to 1.7 g/MTU) was collected during voloxidation. These amounts also were small fractions of total ^{129}I found, ranging from 0.1 to 7.9% evolved during most of the voloxidation tests. In two tests, the fractions from voloxidation were 59 and 84%; however, material balances for iodine in these two tests did not agree well with amounts expected.

Table VI. Iodine-129 distribution.

Fuel	^{129}I, g/MTU Voloxidizer Off-gas	^{129}I, g/MTU Dissolver Off-gas	^{129}I, g/MTU Total	Voloxidation ^{129}I, % of Total
Robinson	0.18	58	58	0.3
	a,b	171	171	-
Oconee	0.03	27	27	0.1
	0.76	31	32	2.4
	1.7	20	22	7.9
	a,b	104	104	-
	a,c	102	c	c
Saxton				
A	1.5	27	28	5.4
B	0.16	0.03	0.19	84
C	0.03	c	c	c
C	0.02	c	c	c
D	1.1	0.8	1.9	59
Unirradiated	0.007	0.016	0.023	-
Blank	0.014	0.009	0.023	-

a. Dissolved in glass apparatus (Reference 5).

b. Unvoloxidized UO_2 fuel.

c. Not determined.

Also shown in Table VI are previously reported results[5] for Robinson and Oconee fuels dissolved in a glass apparatus; the iodine was collected in an NaOH off-gas scrubber. About three times more ^{129}I was obtained with the glass apparatus than with the metal equipment used in this work. Reasons for the difference have not been determined, although results from the glass apparatus are believed to be more accurate. The earlier work showed little difference in ^{129}I evolved during dissolution of voloxidized or unvoloxidized Oconee fuel; this is consistent with the fraction of ^{129}I evolved during voloxidation being small.

Total ^{129}I should be proportional to burnup only. A typical calculated value for Robinson fuel is 187 g/MTU.

Chemical Species

Upper limits on the amounts of tritium evolved as HT and ^{14}C evolved as ^{14}CO were determined from tritium or ^{14}C found in the traps downstream from the oxidizing bed of CuO. Table III gives the fraction of tritium from voloxidation found in the downstream tritium trap. Table IV gives similar information for ^{14}C from both voloxidation and dissolution.

The results show that nearly all of the tritium from voloxidation was in the form of HTO, as expected. Less than 0.1% could have been in the form of HT. Although these amounts are 10 to 100 times greater than the background level of the system, they are within the range of possible leakage from upstream traps and therefore should be regarded as upper limits for HT. From dissolution of voloxidized fuel, no tritium as HT was observed; only background levels of tritium were found in the downstream trap.

The distribution between $^{14}CO_2$ and ^{14}CO is uncertain. During the required conditions of prolonged flow, some CO_2 desorbed from the upstream trap and collected in the downstream trap. This effect was shown in a calibration test with $^{14}CO_2$; the ^{14}C was found equally distributed between the two traps even though no ^{14}CO was in the system. In voloxidation tests, up to 76% (in a test with Saxton fuel) of the ^{14}C was found in the downstream trap. In dissolution tests, up to 72% (in a test with Oconee fuel) of the ^{14}C was found in the downstream trap. Because an unknown part of the ^{14}C on this trap was originally $^{14}CO_2$ and not ^{14}CO, the values shown represent only upper limits on ^{14}CO; the actual amounts could have been much less. In one test with Saxton fuel, only about 0.1% of the ^{14}C from either voloxidation or dissolution appeared as ^{14}CO. Total ^{14}C evolved was accurately measured because the total capacity of the upstream and downstream traps for CO_2 was adequate for the quantities involved.

Conclusions

From the data of Tables III - VI, we conclude the following:

- Voloxidation of spent nuclear fuel releases tritium to the off-gas system quantitatively but releases only small fractions of the ^{14}C, ^{85}Kr, and ^{129}I in the fuel.
- Dissolution of voloxidized fuel in nitric acid releases the remaining ^{14}C, ^{85}Kr, and ^{129}I to the off-gas system.
- Typical values for the fractions evolved during voloxidation are >99.8% of the tritium, 17 to 22% of the ^{14}C, 7 to 17% of the ^{85}Kr, and <8% of the ^{129}I.
- Tritium is evolved as HTO during voloxidation; less than 0.1% is HT.

References

1. Proceedings - Controlling Airborne Effluents from Fuel Cycle Plants, Sun Valley, Idaho, August 5-6, 1976. American Nuclear Society (1976).

2. R. A. Brown, Ed. "Volatile radioisotope recovery and off-gas treatment." Alternatives for Managing Wastes from Reactors and Post-Fission Operations in the LWR Fuel Cycle. USERDA Report ERDA-76-43, Chapter 13, Vol. 2, pp 13.1-13.68, Washington, DC (1976).

3. O. O. Yarbro, F. E. Harrington, and D. S. Joy. Effluent Control in Fuel Reprocessing Plants. USAEC Report ORNL-TM-3899, Oak Ridge National Laboratory, Oak Ridge, TN (1974).

4. J. H. Goode, Ed. Voloxidation – Removal of Volatile Fission Products from Spent LMFBR Fuels. USAEC Report ORNL-TM-3723, Oak Ridge National Laboratory, Oak Ridge, TN (1973).

5. D. R. Johnson and J. A. Stone. "Light water reactor fuel reprocessing: dissolution studies of voloxidized fuel." Paper presented at ANS Topical Meeting on the Back End of the LWR Fuel Cycle, Savannah, GA, March 19-22, 1978.

6. B. A. Staples, L. P. Murphy, and T. R. Thomas. "Airborne elemental iodine loading capacities of metal zeolites and a dry method for recycling silver zeolite." Proceedings of the Fourteenth ERDA Air Cleaning Conference, Sun Valley, Idaho, August 2-4, 1976. USERDA Report CONF-760822, pp 363-379 (1977).

7. T. R. Thomas, B. A. Staples, L. P. Murphy, and J. T. Nichols. Airborne Elemental Iodine Loading Capacities of Metal Zeolites and a Method for Recycling Silver Zeolite. USERDA Report ICP-1119, Idaho National Engineering Laboratory, Idaho Falls, ID (1977).

8. G. W. Gibson, et al. Characteristics of UO_2-Zircaloy Fuel Rod Materials from the Saxton Reactor for Use in Power Burst Facility. USNRC Report ANCR-NUREG-1321, Aerojet Nuclear Co., Idaho Falls, ID (1976).

9. M. J. Bell. ORIGEN – The ORNL Isotope Generation and Depletion Code. USAEC Report ORNL-4628, Oak Ridge National Laboratory, Oak Ridge, TN (1973).

DISCUSSION

EVANS: The amount of ^{129}I and ^{85}Kr released during the voloxidation step seems quite small compared to the assumed releases for DBA melt-down for reactors. Do you believe your numbers could be used as valid source terms for future accident analysis work?

STONE: The absolute quantities reported represent data for the fuels as received. Unknown amounts of gases may have been released in the prior history of the fuel, as, for example, in the initial puncture of the fuel rods and during their storage. The relative amounts released would probably be valid in air at the quoted temperature, 490°C. There are literature data that suggest that ^{85}Kr and ^{129}I will be completely released at higher temperatures (say, 1000°C).

LAMBERGER: You stated that more than 99.8% of the tritium in the fuel was released by voloxidation. Does this include tritium in cladding, in the gas plenum, or in the getter (if any)?

STONE: No, the fraction quoted is of total tritium found in the offgas system after voloxidation and dissolution, and in the dissolver solution.

LAMBERGER: Do you have any data on tritium distribution in clad, fuel, gas, and getter?

STONE: No.

SCHINDLER: In the dissolution step, did you look at the distribution of the iodine and the carbon-14 with respect to the offgas and the liquid? Did it all go out in the offgas or did some remain in the liquid?

STONE: Within the limits of our detection it all went out in the offgas. That is, greater than 98%. We don't know if a small amount was left that was beyond the limit of detection.

INVESTIGATION OF AIR CLEANING PROCESSES FOR REMOVING TRIBUTYL PHOSPHATE VAPORS FROM FUEL REPROCESSING OFF-GAS STREAMS*

Graham B. Parker
Lysle C. Schwendiman

Pacific Northwest Laboratory
Richland, Washington

Abstract

Tributyl Phosphate (TBP) is used as an extractant in combination with the solvent dodecane in the dissolution process in a conventional nuclear fuel reprocessing plant. When recycled acid is used in the process, the dissolver off-gas (DOG) may contain small amounts of TBP and dodecane vapor. The vessel off-gas (VOG) will also contain TBP vapors in even higher fractions. Under some conditions, TBP vapor in these gas streams adversely affects the performance of silver-loaded solid sorbent beds used in the treatment of these streams to remove iodine and organic iodide compounds. This study is investigating the use of inorganic solid sorbent beds located upstream of the silver-loaded sorbent beds to remove TBP and extend the useful life of the silver beds.

Laboratory scale experiments have been conducted using selected inorganic solid sorbent materials which have specific properties indicating their effectiveness for removing TBP or similar organic compounds. Screening studies of short duration were run using several materials to select the most promising materials for further parametric testing. Twelve materials (10 inorganic and 2 organic based) designated A through M were used in these initial studies. The materials were packed in a bed 2.5 cm diameter by 5 cm deep. Typical TBP concentrations ranged from 4×10^{-4} to 1×10^{-3} g/ℓ in air flowing at 172 mℓ/min. Results indicated 4 inorganic materials (D, H, K, L) would retain greater than 95% of inlet TBP over a 3-hour run time.

These four materials are being tested in a small packed glass column arrangement using variations in TBP concentration, face velocity and column temperature. As a part of this work, a sensitive quantitative analysis technique was developed enabling continuous real time analysis of TBP vapor concentrations, as low as 1×10^{-7} g/ℓ, so that breakthrough progression can be measured.

Of the three materials examined to date in parametric experiments (D, H and L), material H shows the highest retention efficiency for TBP. Material H will retain 15 times more TBP before detectable breakthrough than the next most efficient material. Concentrations of TBP in these experiments ranged from 6×10^{-5} to 4.5×10^{-4} g/ℓ in air flowing at 0.45-2ℓ/min.

*Work performed under DOE Contract EY-76-C-1830

Material H will be used in further laboratory experiments to demonstrate TBP removal in a simulated process stream. The materials selected for this experiment will be used as protective beds upstream of iodine sorbent beds and iodine retention for protected and unprotected beds will be a measure of the effectiveness of the beds to remove TBP.

I. Introduction

Tributyl phosphate ($C_{12}H_{27}PO_4$) diluted with dodecane (or normal paraffin hydrocarbon, NPH) is the solvent used in the PUREX process to separate uranium and plutonium from fission products in spent LWR fuel. Most PUREX flow sheets used to date and those proposed for future reprocessing plants incorporate acid recycle. When the acid is recycled, small amounts of NPH and TBP vapor will be present in the dissolver off-gas and vessel off-gas. Both of these gas streams will contain other airborne fission products released during the reprocessing steps which must be removed by gas cleaning processes.

Iodine and organic iodides are major radioactive constituents of these gas streams. Current treatment methods proposed involve the use of silver-loaded inorganic sorbents to remove iodine. Laboratory and pilot plant studies have shown that the presence of TBP vapor in these gas streams reduce the capacity of the silver beds to remove iodine, thus resulting in more frequent replacement of the beds.(1)

Little work addressing the problem has been done in the United States. The presence of TBP/NPH in the off-gas streams has been recognized as a possibility since the PUREX flow sheets were prepared and plants built at Hanford and Savannah River to reprocess spent fuel. The potential deleterious effect of TBP on silver sorbents has not been fully explored. Work has been done in this area in West Germany in conjunction with research involved in iodine removal from DOG and VOG streams using the Karlsruhe Reprocessing Pilot Plant (WAK).(1) Airborne TBP in concentrations of $\sim 6 \times 10^{-3}$ g/ℓ significantly reduced iodine sorption capacity of AC 6120 material. Removal efficiency of AC 6120, however, could be restored by introducing NO_2 in the air stream. Dodecane was found to have no deleterious effect.

Use of NO_2 to reduce the effect of TBP contamination may be a viable option for AC 6120 silver-impregnated material because of its unique chemical composition. If materials such as silver-substituted zeolites (faujasite) or mordenites are used as iodine sorbents, this may not be feasible. Work with silver mordenites and silver zeolites has shown that the presence of NO_2 significantly reduces the loading of iodine.(2) If off-gas treatment includes using silver zeolites or silver mordenites, then TBP must be removed prior to iodine removal to assure efficient use of the silver.

II. General Approach

A literature survey was conducted to identify possible inorganic sorbents having properties indicating their effectiveness to remove TBP or similar organic compounds. The required material would have a surface area of less than 500 m^2/g to minimize the water sorption, a

pore diameter greater than ~50 Å to accept a molecule the size of tributyl phosphate and must be able to be used at temperatures up to 170°C. Materials showing an affinity to "fix" phosphates such as alumina or iron-containing materials were considered. Candidate material selected for study include silica gels, aluminas, acid treated clays and zeolite molecular sieves.

Before any laboratory work could begin, a sensitive quantitative analysis technique for measuring very low concentrations of TBP was to be developed. Gas chromatography was successful for analysis of liquid TBP.[3] The use of a gas chromatograph for direct vapor injections of airborne TBP was not successful in the current study. A continuous real time monitoring instrument was most desirable due to the nature of the planned experiments. A search for the best available analysis method was initiated.

A series of laboratory and pilot plant experiments was developed. Initial screening studies in the laboratory using packed beds of small amounts of material in short term TBP loading experiments were designed to identify promising materials for future work. The candidate material would be used in parametric experiments using only TBP in an air stream to identify the most promising material for further laboratory experiments. Tests using variations in flow rate, TBP loading rate, and bed temperature would be conducted. Final laboratory experiments would be conducted using a simulated reprocessing off-gas stream containing major constituents found in actual reprocessing streams.

The final phase of the study involves demonstrating the selected air cleaning system in the Nuclear Waste Vitrification pilot plant at PNL which can operate as a fuel reprocessing pilot plant. Part of this work will be to measure the typical TBP vapor concentrations found in off-gas streams. The demonstrated TBP removal system will be installed in an off-gas stream at an operating fuel reprocessing plant such as at Savannah River or Hanford to assess its effectiveness under actual operating conditions. Part of this task would also involve measuring TBP vapor concentrations under the various operating conditions.

III. Analysis Methods

Laboratory work was initiated to develop a sensitive method to quantitatively analyze low concentrations of TBP vapor (10^{-5} g/ℓ). One method explored was to trap TBP vapor on charcoal-impregnated filter papers and analyze for the phosphorus by x-ray fluorescence. A series of experiments were conducted by placing charcoal filters in series in an air stream containing TBP vapor. The filters were analyzed to determine TBP trapping efficiency. A lower detection limit of 0.1 mg P/filter sample was established.

A phosphorus gradient on the filter papers from front to back was identified by the analyses. The amount of phosphorus detected was also inconsistent from one run to another. An attempt was made to macerate and homogenize the paper and press it into a suitable size for analysis to give a uniform phosphorus distribution. The sample preparation was not found to be suitable for x-ray analysis and consequently the effort was terminated.

An analysis method for organic phosphates outlined in the NIOSH standard procedures was explored for TBP analysis since TBP has many of the same chemical characteristics as the organophosphate pesticides.[4][5]. This method involves collection of airborne TBP vapor in ethylene glycol using an impinger system. The TBP is extracted from the glycol into hexane and concentrated. The liquid concentrate is analyzed by a gas chromatograph equipped with a flame ionization phosphorus detector. The detector limit was 0.005 μℓ TBP. This method was successful for samples <10 mg TBP/50 mℓ glycol and was used in the initial laboratory screening experiments. This method was modified later in the experiments to eliminate the glycol by sparging the TBP laden air directly into hexane in a cold trap.

Direct injection of TBP vapor samples into a gas chromatograph was explored in an attempt to eliminate the hexane cold trap and give a faster turnaround time and a semicontinuous analysis. A Hewlett-Packard 5730 gas chromatograph with an N_2/P sensitive flame ionization detector and associated integrator was used. Optimum conditions for TBP liquid analysis were established in the chromatograph and highly reproducible results were obtained. Repeated TBP vapor injections gave a good response, however, they were not reproducible. TBP vapor pressure is very low (0.09 mm at 60°C) which may account for the difficulty in analysis.[6]

A continuous real time instrument for vapor phase phosphorus analysis was subsequently identified with the capability to detect phosphorus near 10^{-7} g/ℓ. The instrument, a Meloy Laboratories, Inc. PA-460*, uses a patented flame photometric detector. The instrument was found suitable for TBP vapor analysis after slight modification. TBP was found to adsorb onto and degrade the teflon tubing used in the internals of the instrument. The pathway the TBP followed to the detector was altered to pass only through specially treated chromatographic grade stainless steel tubing. This instrument was used in the long term experiments to measure TBP retention of selected sorbents.

IV. Experimental Runs and Results

Initial Screening Studies

Several commercially available sorber materials identified through manufacturer's literature and known applications were obtained for use in the initial screening studies to evaluate TBP retention. The materials selected were either silicon oxide, aluminum oxide or combination of magnesium, silicon, alumina and iron oxides. Other materials (A and B) were either carbon based or contained activated charcoal and were used as a reference material for comparison with the other materials. These short studies were run at one set of conditions and were designed to identify sorbents showing a high TBP retention for use in further parametric long term loading experiments.

*Meloy Laboratories, Inc., Springfield, Virginia

The analyses of TBP in these experiments were performed using the NIOSH method. The reproducibility of the overall methods of generation, sampling and measurement were evaluated as part of these studies. A schematic of the experimental apparatus is shown in Figure 1.

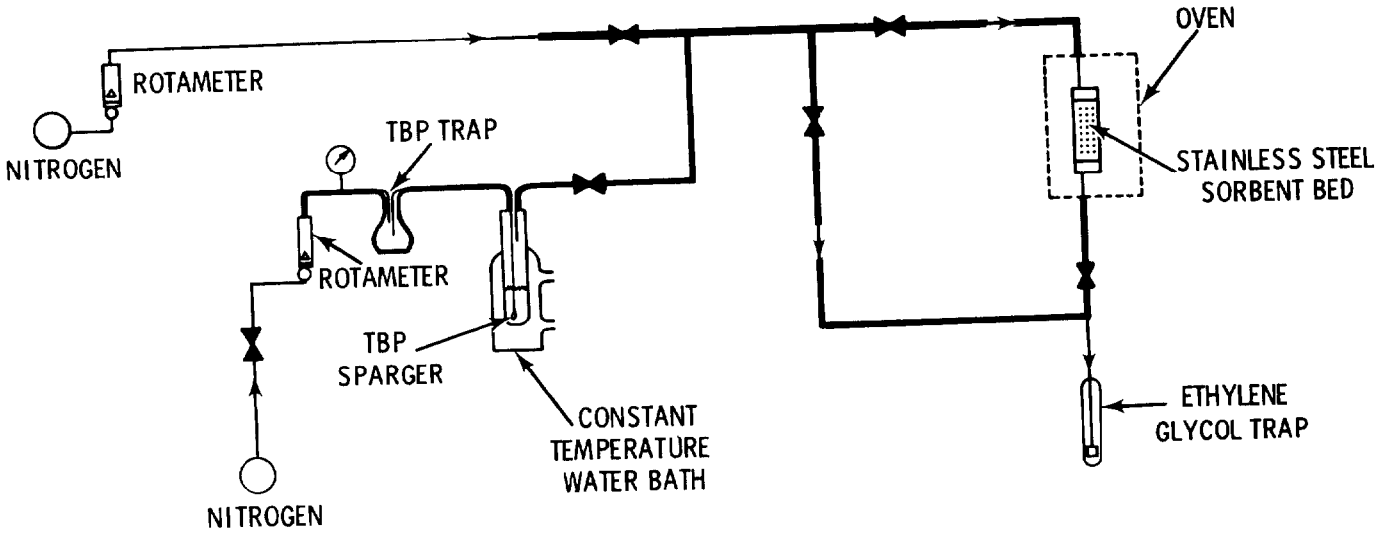

FIGURE 1
SCHEMATIC DIAGRAM OF APPARATUS USED IN
INITIAL SCREENING STUDIES OF TBP REMOVAL

Sorbents were packed into a 5 cm deep by 2.5 cm diameter stainless steel column which was placed in an oven maintained at 100°C. The feed stream to the column consisted of TBP vapor in dry nitrogen flowing at 172 mℓ/min. TBP vapor was generated by sparging the nitrogen at 72 mℓ/min through TBP liquid kept at a constant temperature. The constant temperature was set at a point between 80° and 90°C. A side stream of dry nitrogen flowing at 100 mℓ/min combined with the sparger stream to make up the feed stream. All feed lines in the system were standard grade stainless steel and heated where necessary to prevent condensation. Temperature and pressure were continuously monitored.

Prior to each experiment, samples were taken of the bed inlet feed stream by sparging the total stream through ethylene glycol to establish the inlet TBP concentration. Measured TBP concentration ranged from 4×10^{-4} to 1×10^{-3} g/ℓ. Experiments were started by diverting the feed stream to the bed. The effluent from the bed was passed through the glycol. Samples were taken in 1 hour increments continuously for a total of 3 hours. In several test runs, a sample was also taken of the carrier gas (N_2) alone which was passed through the bed material for 1 hour at the end of the test run to measure any TBP eluting from the bed. Each ethylene glycol sample was analyzed for TBP. Efficiency of the material to remove TBP was determined by calculating the retained percentage of the total TBP metered to the bed. Table I is a summary of the results.

Table I Tributyl phosphate removal by sorbents. Airflow 172 cc/min, bed temperature 100°C, bed 5 cm deep by 2.5 cm diameter.

Material	Inlet TBP, mg	Outlet TBP 1st hr, mg	2nd hr, mg	3rd hr, mg	Total, mg	TBP in N_2 for 1 hr Flush Following Run, mg	% TBP Retention
Charcoal(a)	1.8	0.119	0.031	0.005	0.155	0.008	91.4
A	1.8	<0.005	<0.005	<0.005	<0.015	<0.005	>99
B	2.6	--	--	--	0.22(b)	--	91.5
	1.9	0.14	0.008	0.808	0.156	0.008	91.8
C	1.4	0.071	(c)	0.008	--	0.008	--
D	1.5	0.015	<0.005	<0.005	<0.025	<0.005	>98.3
E	2.6	0.14	0.01	<0.005	<0.155	<0.005	>94
F	2.0	0.16	0.064	<0.005	<0.229	0.005	>89
G	1.9	0.34	0.089	0.20	0.579	0.005	70
H	1.6	0.006	<0.005	<0.005	<0.016	<0.005	>99
J	2.4	0.16	0.038	0.019	0.217	0.006	91
K	19.8	0.67	0.069	0.041	0.77	--	96.1
L	19.8	0.37	0.061	0.029	0.47	--	97.7
M	9.6	0.52	0.099	0.035	0.654	0.018	93.2

(a) Coconut base
(b) Total of 4.5 hr run time
(c) Sample lost

The indicated inlet concentration of TBP in this series of experiments extending over a period of about 4 months had a standard deviation of 26% at the 95% confidence level. The reproducibility is largely determined by the errors in the extraction step and the gas chromatographic analyses. Furthermore, each screening test was performed over a relatively short time period during which more nearly constant conditions could be maintained. Thus, the bed removal efficiencies are more accurate than represented by the standard deviation determined over the full range of these experiments.

Parametric Studies

The most promising inorganic sorbents for TBP removal identified in the initial screening studies were selected for further experimentation. These experiments involve longer TBP loading at flow conditions more nearly approaching those likely to be found in actual reprocessing off-gas streams. These experiments were designed to evaluate materials under various operating conditions of temperature, flow and TBP concentration. The best material as determined early in these experiments will be used in experiments in the laboratory demonstration unit using a simulated process stream. The apparatus in use in these experiments is shown in Figure 2.

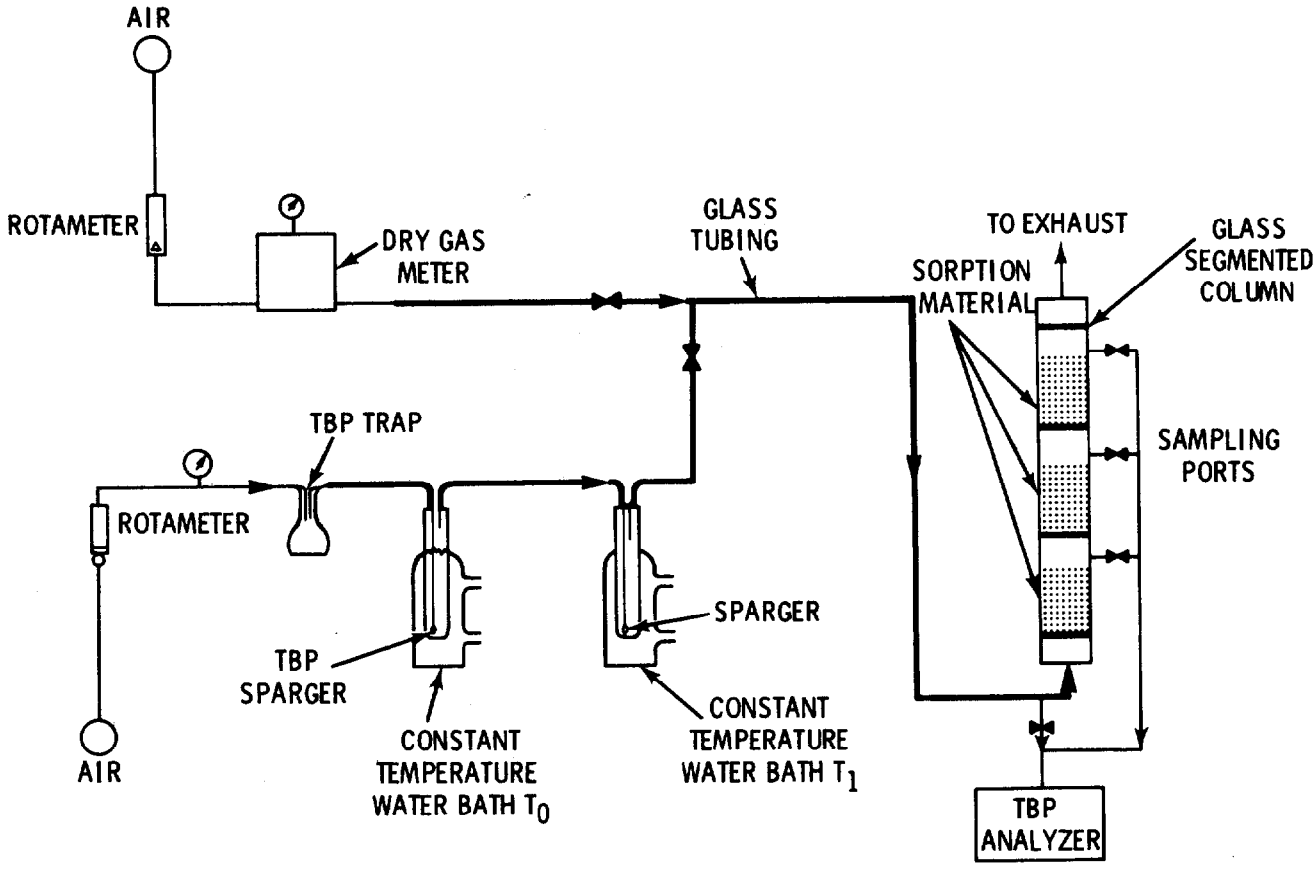

FIGURE 2
SCHEMATIC DIAGRAM OF APPARATUS USED IN PARAMETRIC EXPERIMENTS USING SELECTED SORBENT MATERIALS FOR TBP REMOVAL

TBP vapor is generated by sparging air at a low flow through two temperature controlled gas washing bottles in series. The first bottle is at 95°C and the second at 60°C. In this manner a saturated air stream containing a known TBP vapor concentration is reproducibly generated at 60°C. This configuration was necessary due to the low TBP vapor pressure. The TBP vapor stream is mixed with air which has passed through a dry gas meter. The flows are regulated by rotameters to obtain the desired airborne TBP feed concentration. After mixing, the feed stream flows through 6 mm glass tubing to the bed of material which is packed in glass column segments. Glass is used in the system because in early attempts to calibrate the PA-460 phosphorus analyzer using clean commercial grade stainless steel it was found that TBP adsorbed on the walls of the stainless steel tubing. Experiments showed no significant TBP adsorption on the glass tubing.

The material to be loaded with TBP is packed into the 2.5 cm diameter glass column shown in Figure 3.

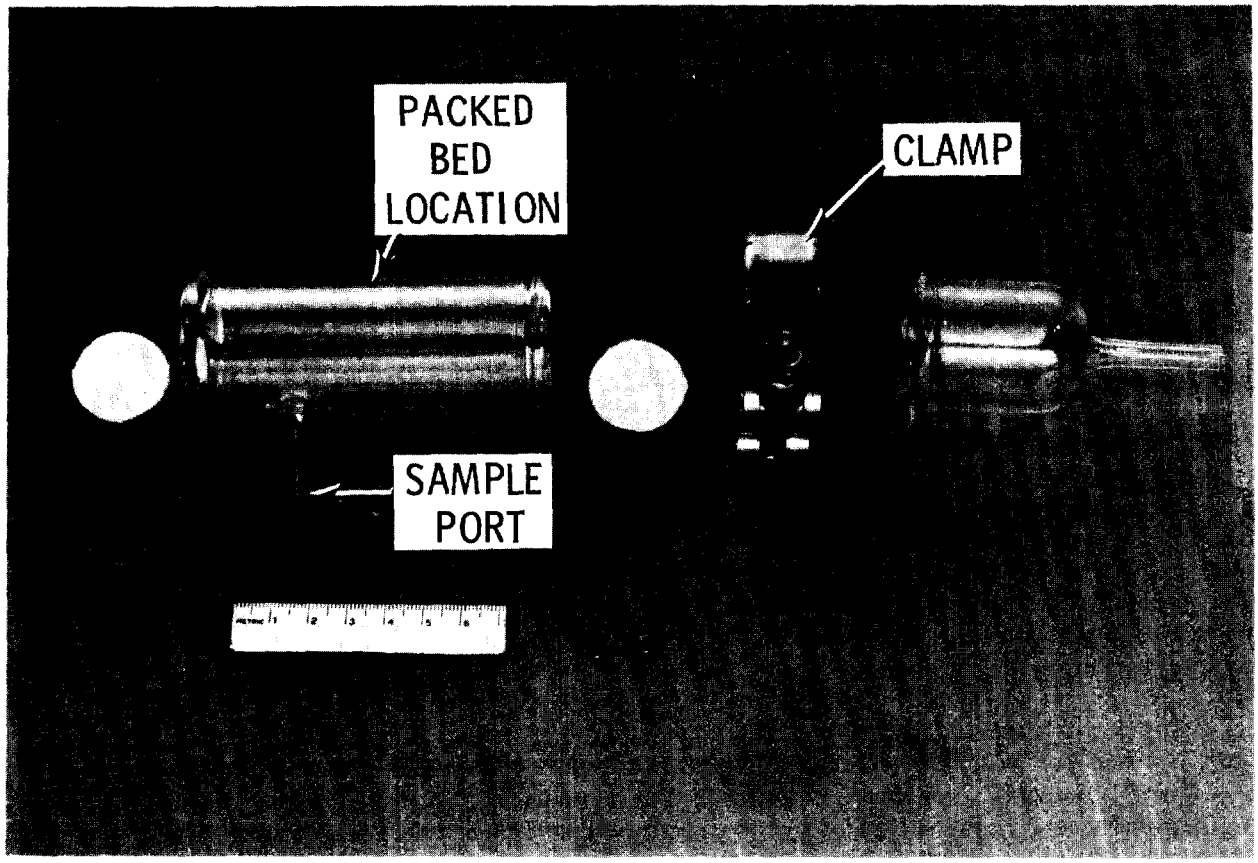

FIGURE 3
GLASS COLUMN ARRANGEMENT FOR HOLDING MATERIAL
IN PARAMETRIC STUDIES OF TBP REMOVAL

Approximately 3.8 cm of material is held in place by Gelman Type G glass fiber filters placed in front of stainless steel screens and snap rings to retain any fines purged from the material. A 1/4 inch sample port located just downstream of the material is used to sample the airstream leaving the bed segment. Airflow is upward through the system. As many as three column segments can be loaded with TBP during an experiment.

During an experimental run, TBP entering the inlet to the column is sampled via the sampling line to the PA-460. The PA-460 draws a portion of the total feed stream at 200 cc/min into the instrument. This inlet concentration (C_o) is sampled periodically. Samples of the airstream leaving each column segment are taken continuously to measure TBP concentration (C) breaking through the material: Sampling concentrates on the first column segment until significant breakthrough is measured. Subsequent samples are taken of each column segment as necessary to follow breakthrough progression through the entire column. A ratio of C/C_o is calculated as a measure of breakthrough. The calculated standard deviation in breakthrough calculations is ±25% at a 95% confidence level. Largest

contributing errors in these calculations occur in instrument calibration in combination with the analysis of the inlet and outlet stream during experimentation.

Experiments with sorbent H. From the initial screening studies, sorbent H, an 8x14 mesh granular activated alumina material had the highest retention of the noncarbonaceous materials tested (material A contained an activated charcoal mix), and was selected for further parametric study. Three column segments containing 20 g of material H in each segment were loaded with TBP. The following conditions were employed.

Bed temperature: 100°C
Average airflow: 0.45 ℓ/min
TBP concentration: $1x10^{-4}$ - 2.4×10^{-4} g/ℓ
Preconditioning with air: 2.5 hours

After more than 277 hours of run time and 1.8 grams TBP metered to the columns, a breakthrough of C/C_o = 0.02% in the first column segment was measured. No breakthrough in the other two column segments was detected. The concentration of TBP entering the columns was increased during the test run from $1x10^{-4}$ g/ℓ to accelerate loading and breakthrough.

A second experiment using material H was prepared. A single column segment was packed with 19.1 g of material and loaded with TBP. Airflow was increased by a factor of 4 to assess the effect of this parameter. The following conditions were employed.

Bed temperature: 100°C
Average airflow: 1.9 ℓ/min
TBP concentration: $1x10^{-4}$ - 4.5×10^{-4} g/ℓ
Preconditioning with air: 2 hours

The material was loaded with 2.9 g TBP before any breakthrough (>0.01%) was measured. A total of 8.96 g TBP was metered to the material over a period of 331.6 hours before the run was terminated. Breakthrough measured at the end of the run was ~100%. The complete breakthrough curve is shown in Figure 4.

The capacity of the material to retain TBP was calculated from the breakthrough curve to be 377 mg TBP/g material. Because of the high TBP retention of material H in these experiments, it was decided to use the material in laboratory experiments run under simulated offgas stream conditions.

Experiments with sorbent D. TBP loading of 4x8 mesh spherical catalyst material D was initiated in late February 1978. A single column segment of material weighing 14.6 g was used in this first experiment. The following conditions were employed:

Bed temperature: 100°C
Average airflow: 1.9 ℓ/min
TBP concentration: $1x10^{-4}$ g/ℓ
Preconditioning with air: 2 hours

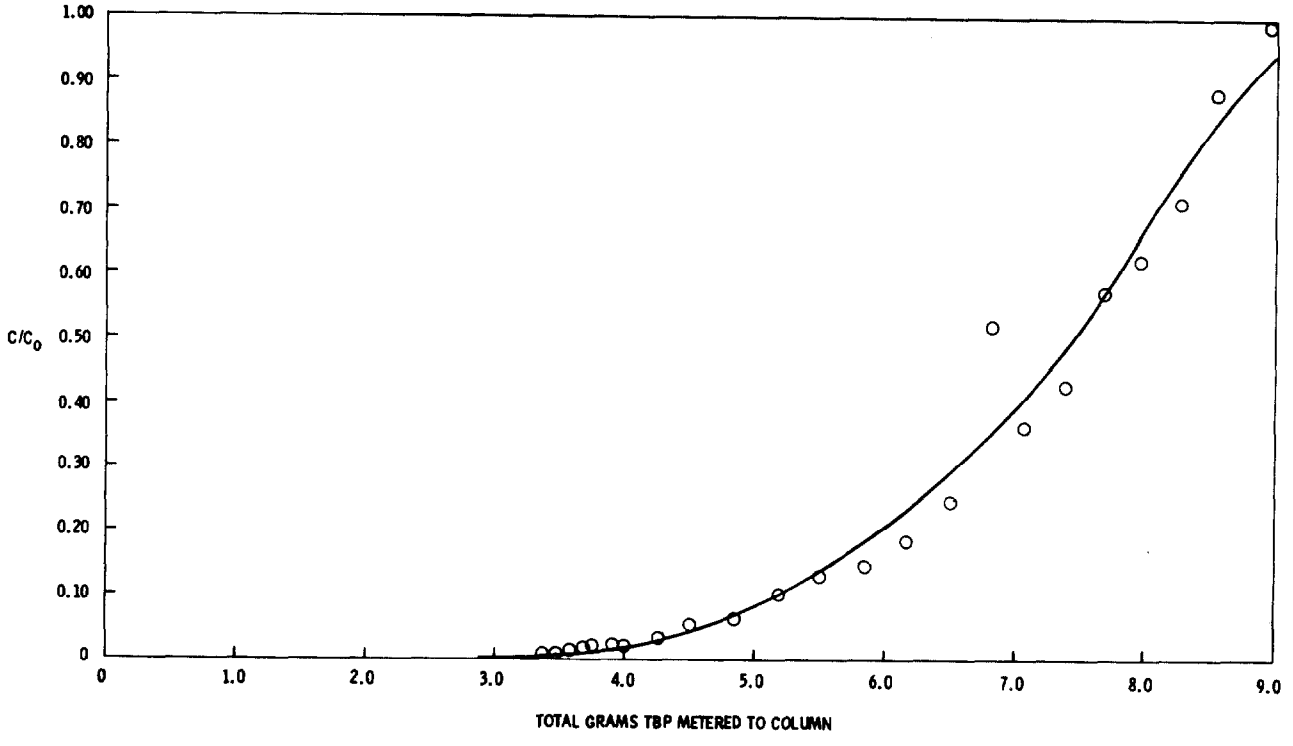

FIGURE 4
BREAKTHROUGH HISTORY FOR TBP LOADING OF MATERIAL H. AIRFLOW 1.9 ℓ/MIN, BED TEMPERATURE 100°C, TBP CONCENTRATION 1-4.5x10^{-4} g/ℓ

Nearly instantaneous breakthrough was measured and 100% breakthrough was achieved after 37.6 hours of run time and 0.45 g TBP metered to the material. From the breakthrough curve in Figure 5, the capacity of the spherical material to retain TBP was calculated to be 11 mg TBP/g material, which is considerably less than the granular material H tested under nearly identical conditions.

This spherical material was crushed to 6x14 mesh in an effort to increase the surface area for reaction. The crushed material weighing 15.1 g was packed into a single glass column and TBP was loaded onto the material under identical conditions as those used for the spherical form of the material.

As in the experiment using the spherical form of material D, nearly instantaneous breakthrough was measured. The run was terminated after metering 0.97 g TBP to the material in 73.1 hours. The breakthrough curve for this material is shown in Figure 6. Calculated TBP retention of the crushed material is 39 mg TBP/g material.

Even though TBP retention was increased by 3.5, retention is significantly lower than that achieved with material H. Further experimentation with material D is not considered due to the very low TBP retention.

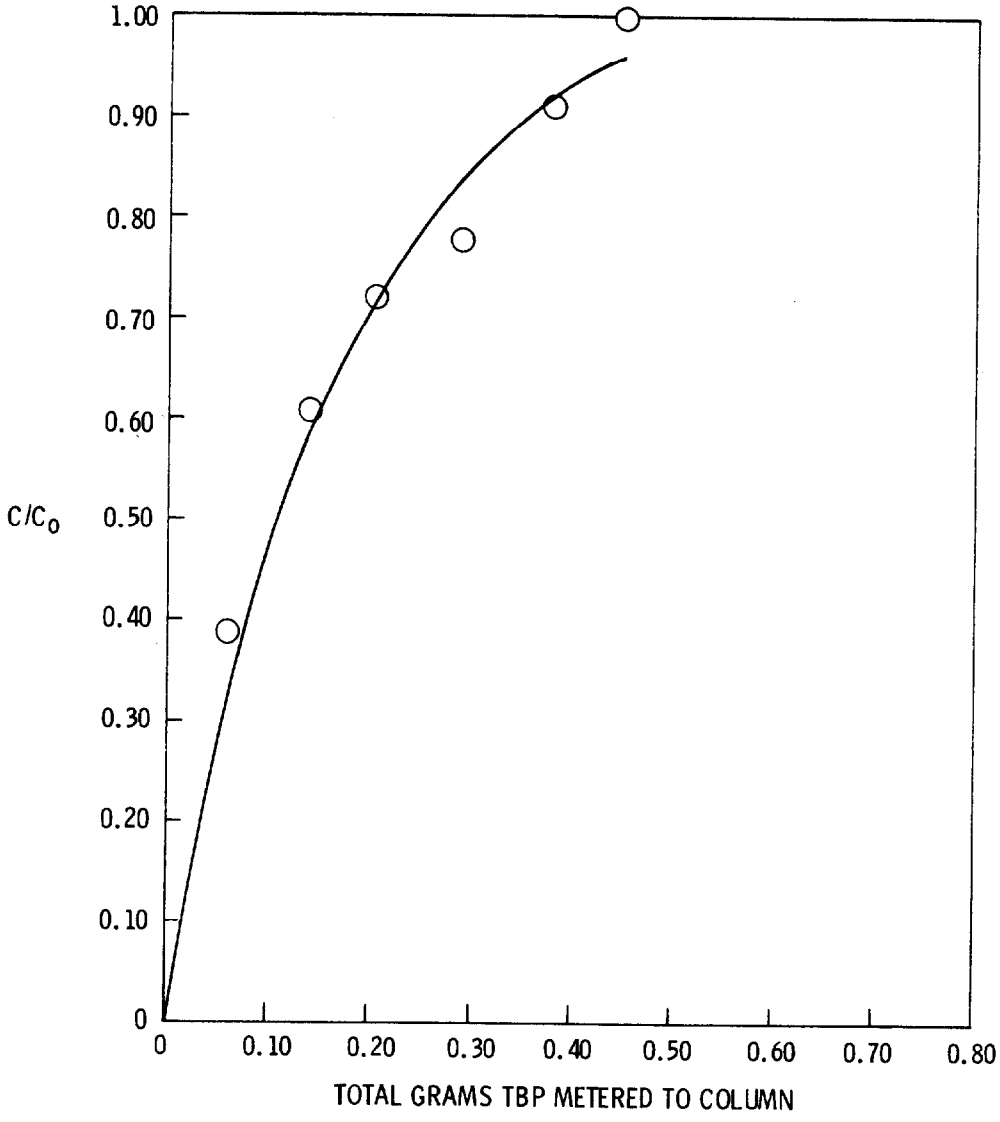

FIGURE 5
BREAKTHROUGH HISTORY FOR TBP LOADING ONTO MATERIAL D (4x8 MESH SPHERICAL). BED TEMPERATURE 100°C, AIRFLOW 1.9 ℓ/MIN, TBP CONCENTRATION 1×10^{-4} g/ℓ

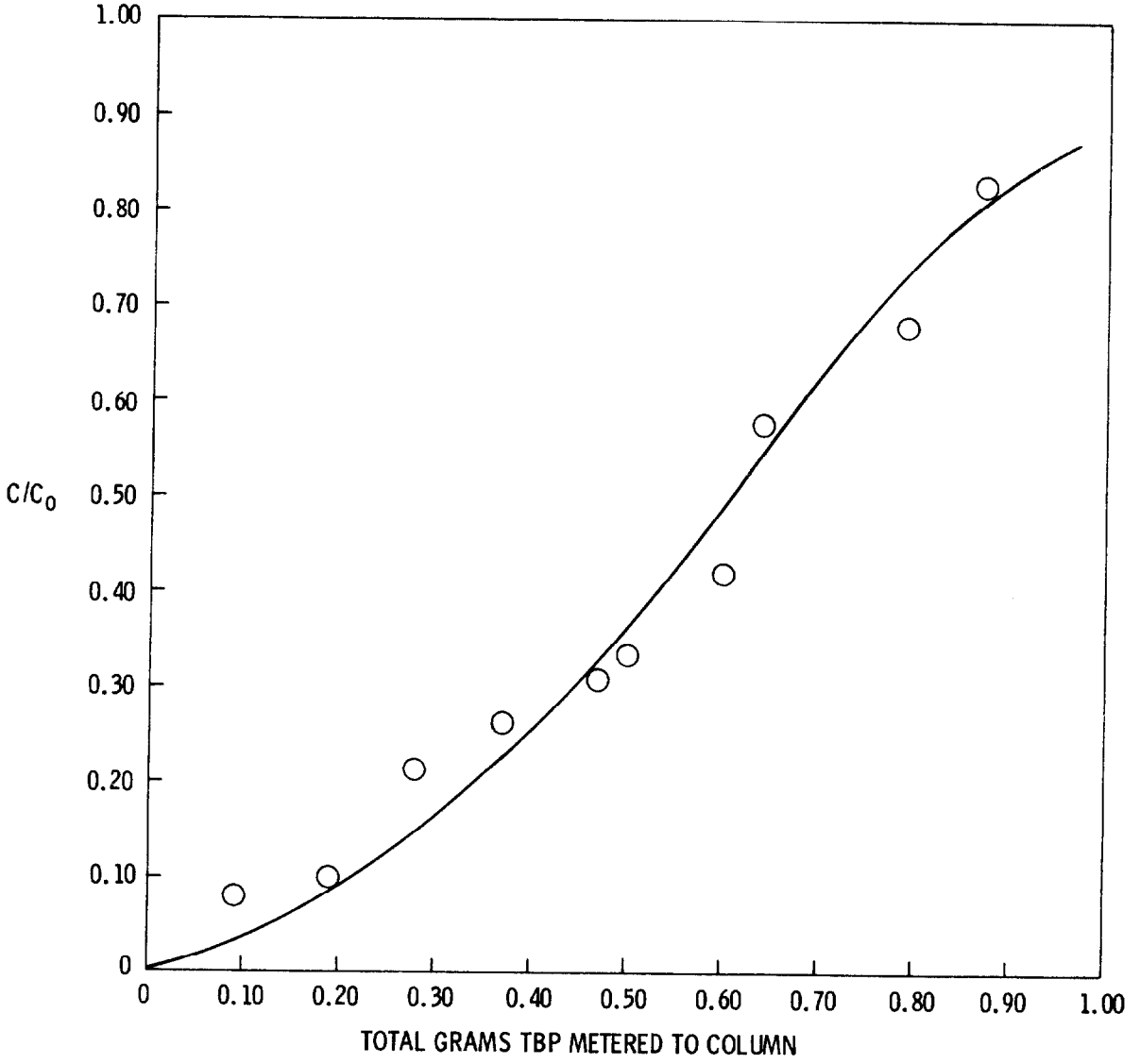

FIGURE 6
BREAKTHROUGH HISTORY FOR TBP LOADING ONTO MATERIAL D (6x14 MESH GRANULAR). BED TEMPERATURE 100°C, AIRFLOW 1.9ℓ /MIN, TBP CONCENTRATION $1x10^{-4}$ g/ℓ

Experiments with sorbent L. The next material used in these experiments was sorbent L, an 8 x 30 mesh granular, silica, alumina, magnesia sorptive clay, which indicated the third highest TBP retention of the noncarbonaceous materials in the screening studies. Two 3.8 cm x 2.5 cm glass column segments were packed with material L and prepared for loading with TBP. Segment 1 contained 13.6 g and segment 2 contained 14.0 g. The following conditions were employed.

Bed temperature: 100°C
Average airflow: 2.0 ℓ/min
TBP concentration: $6x10^{-5}$ g/ℓ
Preconditioning with air: 2 hours

A breakthrough of 0.6% in segment 1 was measured after metering 0.19 TBP to the column. After metering 0.94 g of TBP to the material a breakthrough of 54% was measured in the first column segment at which time the run was terminated. No breakthrough was measured in the second column segment. The breakthrough curve for the first column segment is found in Figure 7.

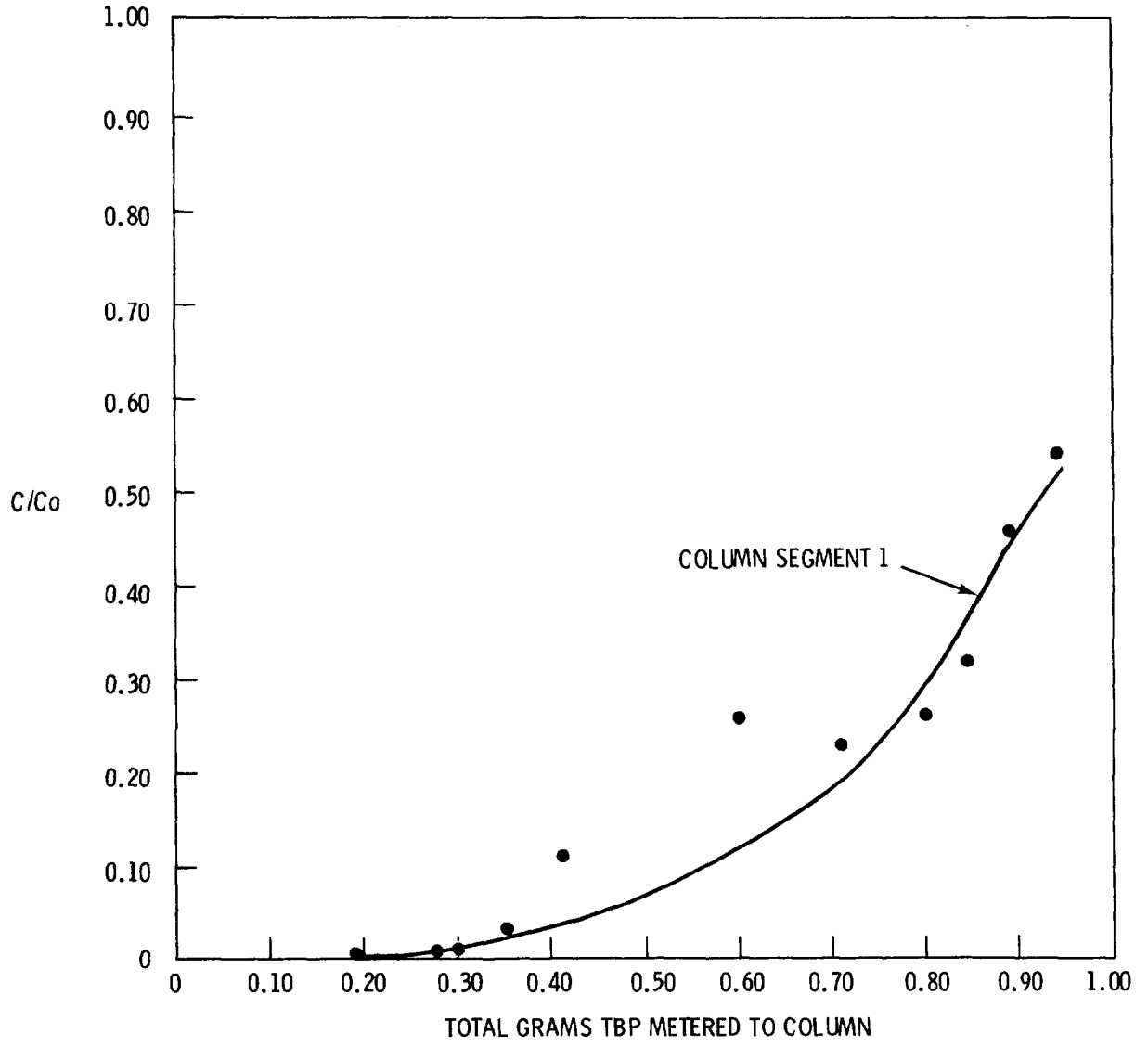

FIGURE 7
BREAKTHROUGH HISTORY FOR TBP LOADING ONTO MATERIAL L. BED TEMPERATURE 100°C, AIRFLOW 2.0 ℓ/MIN, TBP CONCENTRATION 6×10^{-5} g/ℓ

Even though breakthrough was not followed to 100%, total capacity of the material can be estimated from the available breakthrough data. Approximated capacity of the material extrapolated to 100% breakthrough is 70 mg/g material which is greater than material D but considerably less than material H.

V Future Work

Material H will be used in laboratory demonstration experiments to determine the effectiveness of the material to remove TBP vapor and protect iodine sorbent beds downstream. The measure of effectiveness for TBP removal will be iodine retention of the iodine sorbent material. The experiments will be conducted using an air stream containing TBP, water vapor and other constituents likely to be present. Other candidate materials will be used in this demonstration unit as they are identified in the parametric experiments.

An alternative method to quantitatively measure TBP vapor using a remote optoacoustic laser analysis technique is being explored. The feasibility of such an analysis method is being studied by first examining the possible constituents present in the off-gas that could cause interference in this analysis method.

VI Summary and Conclusion

- It has been demonstrated that it is possible to quantitatively analyze low concentrations of airborne TBP using a modified real time continuous instrument. Based on vapor pressure calculations, concentrations as low as 1×10^{-7} g TBP/ℓ air have been measured using this instrument.

- Several inorganic sorbents identified through literature have shown promise to retain TBP vapors in low flow, short duration sorption experiments. Four of the inorganic materials gave greater than 95% TBP retention and one of the four gave greater than 99% retention.

- Long duration parametric experiments have shown material H to be the most efficient sorbent for TBP removal. The first experiment at an airflow of 0.45 ℓ/min gave a detectable TBP breakthrough after metering 1.8 g TBP to the material. Increasing the airflow by a factor of 4 increased TBP retention before measurable breakthrough by a factor of 1.6.

- No other material tested in nearly identical long duration experiments has shown as efficient TBP retention as material H. Material L, the next most efficient material showed a measurable TBP breakthrough in 3.8 cm of material after metering less than 0.19 g TBP. This is 1/15 the TBP which was metered to material H before measurable breakthrough in a nearly identical experiment.

References

(1) Wilhelm, J. G. and J. Furrer, "Head-end iodine removal from a reprocessing plant with a solid sorbent," Proceedings of the 14th ERDA Air Cleaning Conference," CONF 760822 (1976).

(2) Thomas, T. R., L. P. Murphy, B. A. Staples and J. T. Nichol, "Airborne iodine loading capacities of metal zeolites and a method for recycling silver zeolite," ERDA, Idaho Operations Office, ICP-1119, (1977).

(3) Horton, A. D., "Gas chromatographic determination of trimethyl phosphate, dimethyl phosphate, methyldibutyl phosphate and tributyl phosphate," Journal of Chromatographic Science, 10:125 (1972).

(4) NIOSH Method P&CAM 158, "Parathion in air," revised (1973).

(5) EHS Procedure P-3, "Pesticide analysis of plant tissue" (1973).

(6) Burger, L. L., "The chemistry of tributyl phosphate a review," HW-40910, U.S. A.E.C., Hanford Atomic Products Operation, Richland, Washington

DISCUSSION

VAN BRUNT: Have you performed experiments with other solvent constituents such as TDP or n-decane?

PARKER: Yes. In the bench scale experiment designed for testing the TBP sorbents as protective beds for iodine sorbents, TBP is used in combination with dodecane (NPH) in the field stream. I do not expect any deleterious effect from the dodecane, however.

VAN BRUNT: Do you expect that the TBP vapor from a knockout pot following the dissolver and from the VOG to be near your experimental conditions, i.e. at 100°C? I would expect a conservative temperature to be closer to 60°C.

PARKER: True, the TBP vapor temperature would be closer to 60°C than 100°C. But TBP removal beds can be operated at temperatures above 60°C (up to 150°C) if they are placed in the system in the same manner as the iodine sorbent beds. These TBP sorbent beds seem to operate more efficiently at the higher temperatures.

VAN BRUNT: Wouldn't you expect the TDP vapor pressure to be very low after a knock-out pot?

PARKER: TDP vapor pressure is just low, but some is still going to get into the air stream even at 50 or 60°C.

WILHELM: Did you try cold adsorption of elementary iodine on your material? I find it quite interesting and I would be happy if this material could be used in front of a silver adsorption bed. But you may have iodine adsorption on it

and you may not be able to desorb the iodine again. Because iodine is not in a chemical compound with no, or low, pressure, it may desorb slowly. This may generate a contamination and place restrictions on where you put the material which you use to remove tributyl phosphate.

PARKER: You're saying that possibly iodine could be adsorbed in a TBP adsorbent, also?

WILHELM: Yes.

PARKER: For the laboratory tests that we're running now with methyl iodide, the results are in the April, May, June quarterly report to the Department of Energy. The question you asked would be answered in that report but I can't answer it here because it's a limited distribution.

WILHELM: What about elemental iodine?

PARKER: Yes, I'd say there's a good possibility it could happen with elemental iodine. It would be something to explore. Of course, elemental iodine will plate out on just about everything in the world.

A REVIEW OF SOME U.K.A.E.A. WORK ON GAS CLEANING IN FUEL REPROCESSING PLANT

M.N. Elliot (UKAEA, Harwell)
E. Lilleyman (UKAEA, Dounreay)

Abstract

The efficiency of air cleaning systems for fuel reprocessing plant is of prime importance and present systems based upon HEPA filtration have proved very satisfactory in this respect. However, with the larger installations the associated handling and storage procedures are less attractive and new approaches are being developed for the changing levels of radioactivity and plant throughput. This paper presents an interim report of the work.

Improvements can be obtained from a reduction in the size or number of filter installations, an increase in filter life, and from simpler handling and storage procedures. Alternative schemes which can reduce the ventilation load or the number of separate filter installations are discussed. Prefiltration techniques can extend filter life and work on a condensation technique and electrostatic precipitation is described. Methods of volume reduction for storage or disposal of spent filters (by compaction, dismantling and incineration) are being examined and progress to date is reported. Filter sealing and change mechanisms vary with application and have some features in common with more conventional posting systems. Techniques in use or being considered for α and $\beta\gamma$ -active applications are discussed.

I. Introduction

An unconventional design approach is as necessary for the ventilation and filtration systems as for other sections of nuclear fuel reprocessing plant. However until comparatively recently this has not been fully acknowledged and conventional technology, modified to suit the process conditions, has largely been used.

The ideal gas cleaning system should:

(a) guarantee highly efficient removal of radioactive particulates under both normal and incident conditions,

(b) minimise handling operations and penetration of containment,

(c) minimise the treatment and storage of contaminated filters.

Present well-sealed systems satisfy criterion (a) but the handling and storage procedures are cumbersome and costly. As the industry expands, filtration plant employing improved techniques will be required, and dealing with the 'back-end' of the system presents challenging development problems.

Many gas cleaning systems throughout the world are based upon once-through ventilation and HEPA filtration. For U.K. applications a filter efficiency of at least 99.95% is specified, the filters must be capable of continuous operation at 200°C and show an efficiency of 98% after exposure to 500°C for ten minutes. Steel cases are used and the pleated glass fibre medium is sealed by a layer of glass fibre wadding.

The filters are reproducibly highly efficient when correctly installed. However a single installation may contain some tens of individual 1700m^3/h (1,000 cfm) units and a complete plant may require many such installations, grouped according to the plant layout and including primary, secondary and stand-by filter banks. The handling, particularly by remote means, of the large number of individual units is time-consuming and costly. Since approximately 75% of the unit volume is virtually void, storage and disposal of unprocessed filters is costly and wasteful.

Improvements seem possible in three main areas:

(a) reduced installation size,

(b) increased filter life,

(c) improved handling and storage/disposal procedures.

This paper contains an interim report of some work in these areas, carried out within the UKAEA. However, before considering the three headings in detail, it is worthwhile completing the discussion of future trends.

Gas cleaning systems based upon sand beds have been successfully used at the Savannah River site for some years[1][2]. The avoidance of regular filter-changing procedures is very attractive but there is some uncertainty about their eventual decommissioning. A sealed, loaded sand bed does not conform strictly to the definition of a retrievable store and some provision for bed transfer may be necessary to satisfy the regulations. Thus whilst the application of such systems is under consideration, no firm conclusion has been reached.

II. Reduced Installation Size

A reduction in the ventilation load and hence in size of filter installation is an important objective of any design exercise. For example, the once-through air flow can be reduced by improving the leak-tightness of containment structures and penetrations and/or matching ventilation rates to specific process operations rather than to some general air change criterion. Such principles have been applied to the conversion of the Dounreay fast reactor (DFR) fuel reprocessing plant to prototype fast reactor (PFR) reprocessing, where it has proved possible to reduce the combined extracts from the fuel breakdown cave, process cell and vessel vents from the original design value of approximately 20,000m^3/h (12,000cfm) to a normal operating flowrate of 1,700m^3/h (1,000cfm).

However the size of an installation may be dictated by other factors which must be included in the design studies. For example, the rating is sometimes controlled by the forecast emergency situation and in this case

an assessment of procedures which might ease the burden of such a restriction is important. A fairly common example is the design of access arrangements to avoid the high air flows which result when the criterion of 1m/sec linear velocity through an opening is applied. Fluidic devices can be used to carefully control the pressure drop between contamination zones and to respond, but not over-react, to the emergency condition. By such measures the flowrate under incident conditions has been limited, in the case above, to approximately double the normal value.

Recirculating systems, already used for inert atmosphere glove-boxes can, in principle, be applied more widely. An example is the new fuel handling cave associated with the PFR reprocessing plant, designed to contain some hundreds of tons of liquid sodium and provided with a nitrogen blanket gas system including purification using a by-pass low temperature plant. The cave has a volume of 850m^3 and a leak-rate of 0.05 volume % per hour has been achieved at the 13mm w.g. ($\frac{1}{2}$") working pressure differential. This despite many envelope penetrations including an 18m^2 area shielded access door (fitted with an inflatable seal).

Closed cycle ventilation using a condensible gas is now being studied experimentally at Dounreay[3] and would seem most suitable for use on the head-end sections of a reprocessing plant. The concept offers the potential for greatly eased fission product gas removal and particulate removal but the early state of development excludes a more detailed discussion at present.

III. Increased Filter Life

The HEPA Filter is not a high dust-capacity device and even in moderate dust-loading situations the use of a prefilter is desirable. Although it has been shown that removal of the larger particulates results in a more rapid increase of pressure drop with dust loading, and hence in reduced dust capacity[4], the filter life is very significantly increased because of the reduced incident aerosol concentration.

This is of clear benefit provided that the handling and storage problems are not greatly increased. Conventional prefilters do tend to present additional complications, however, and ideally devices which can be cleaned and maintained in-situ by remote means are required.

A technique which could be applied to the water-saturated air flows characteristic of scrubbed vessel vent streams has been studied at the laboratory scale (10m^3/h total air flow)[5]. The process involves the condensation of water onto the particulate nuclei, followed by removal of the grown droplets using a wire mesh demister. In the laboratory, condensation was promoted by mixing saturated air at 45°C with chilled air at 5°C, and removal efficiences > 90% were measured for naturally occurring airborne particulates larger than 0.3 μm.

As has been noted by others[6], the process is not economically competitive if steam injection is necessary to form a saturated air stream. However humid vessel vent streams, saturated at approximately 45°C, present special problems due to the impingement of water droplets and condensation at the HEPA filter, and dehumidification by cooling is being investigated

for their protection. The recycle of part of the chilled air to promote condensation appears feasible and is to be tested, in conjunction with the dehumidification work, on the 2,000m^3/h scale.

The demisting operation should be essentially self-cleaning but some spray wash could be incorporated if necessary to ensure remote functioning and cleaning.

Electrostatic precipitation is another technique which promises reliable remote operation for long periods and has a wider application. The satisfactory experience with the special electrostatic filters on the highly active storage tank off-gas systems at Windscale[7] is encouraging.

A compact reliable unit is required which can be cleaned remotely and be easily removed in modules for maintenance. Ignition of solvent vapours which might be present must be avoided.

The present work is in two parts. Firstly a commercial unit is being installed in an inactive process area to obtain first-hand experience of reliability and cleaning methods with particulates similar to those of cell and cave extract streams. Electrical design parameters are also being examined to design a compact reliable multi-stage unit, using a spark energy limitation technique to avoid solvent ignition problems, as described by other workers[8][9]. Filled, fibre reinforced laminates appear well-suited for use in the collection section.

IV. Improved Handling and Storage Procedures

4.1 Handling

The Dounreay experience of filter sealing and change systems associated with enriched uranium fuel reprocessing[10], coupled with the move to a plutonium fuel cycle and a policy of minimising plastic waste generation called for a critical review of techniques. As a consequence, the following criteria have been applied to the design of filter housings for the PFR reprocessing plant:

(1) the system should guarantee plutonium containment standards at all times and external radiation levels at the housing surface should not exceed 0.5 mrem/h during normal operation and filter change. Isolation during the filter change must therefore ensure no by-pass to the downstream ductwork.

(2) secondary waste production should be minimised and (because of radiolytic production of HCl in retrievable storage), PVC bagging procedures should be excluded. Used filters should be packaged for delivery to a disposal facility or storage in an externally clean container.

(3) provision for inspection and maintenance of the permanent sealing faces should be included.

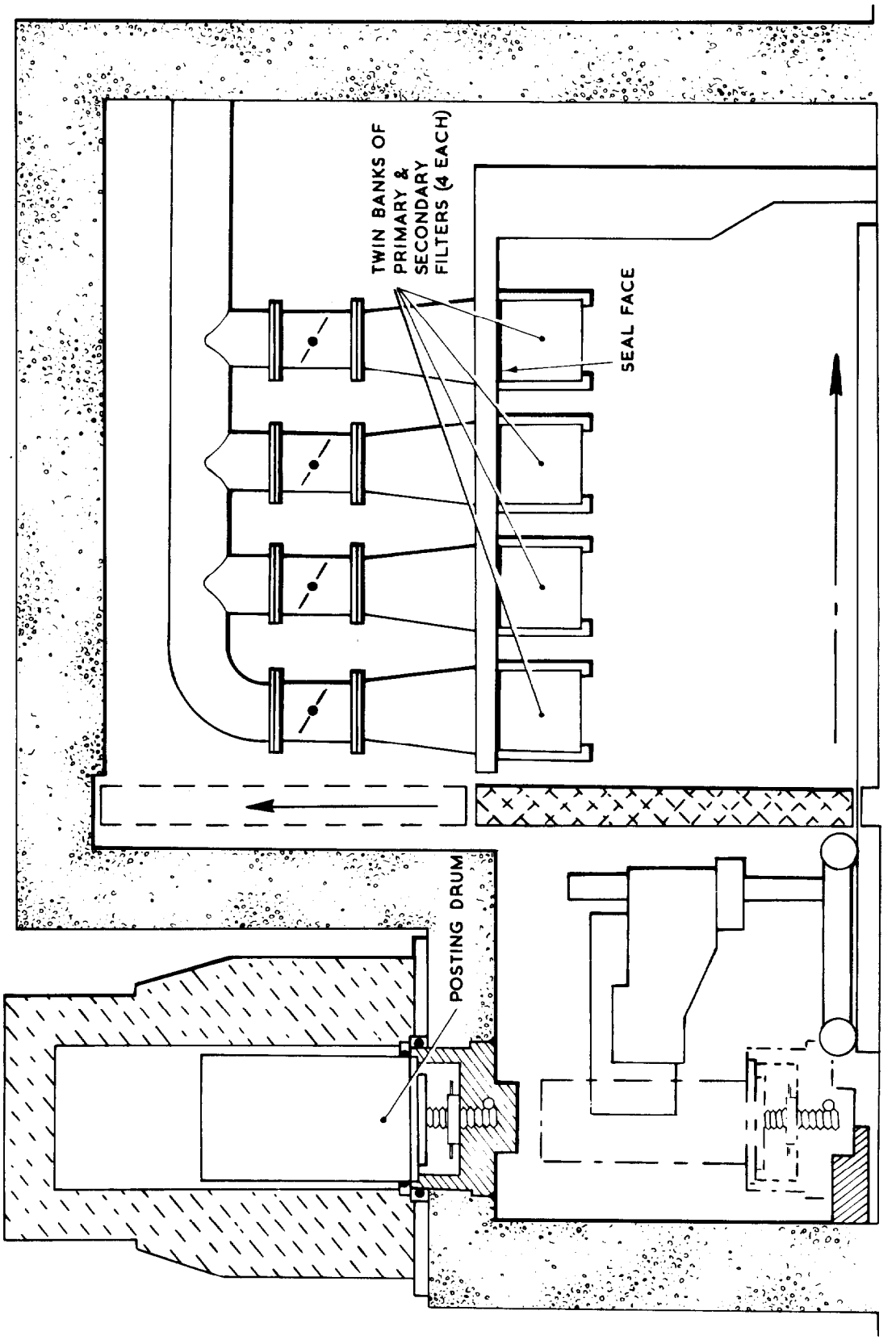

FIG I REMOTE ROBOT FILTER CHANGE SYSTEM

The first system designed to these criteria handles the combined extracts from the PFR reprocessing plant (figure 1). The primary and secondary filter banks, rated at 4000m^3/h (2,400fm) each, contain four filter units, installed in the same shielded enclosure. The filters are sealed to the cell roof and arranged with downflow through the primaries, upflow through the secondaries.

Clean and used filters are transferred in 200 litre posting drums contained in a shielded flask. The drum lid locates with the shield plug of the posting port to protect the external surfaces from contamination, as with other double door systems, of which the La Calhene posting system is an example. Similar posting facilities are provided at the waste handling and storage facility. Transfers between the posting and filter cells are carried out using a robot, and, once they are located, sealing pressure is applied to the filters by a separate remotely operated system. The operating sequence is then as follows:

1. Position posting drum containing new filter, locate lid and shield plug, lower the lid assembly and filter into the posting cell.

2. Transfer the filter to a stand-by position.

3. Transfer the robot (via a shielded access door) to the filter cell and engage with the used filter.

4. Release the sealing pressure and locate the sealing clamps in the filter withdrawal position.

5. Lower the used filter, transfer to the posting cell and insert with the lid assembly into the posting drum.

6. Transfer the clean filter, locate, actuate sealing clamps and withdraw robot.

Valves rather than dampers are used for isolation during the changing operation and a chemical to fix loose contamination can be sprayed onto the used filter before removal.

The design satisfies the criteria but is mechanically rather complex. For the waste handling facilities a filter change system has been developed which again uses the double door principle, but with operations carried out manually by means of rods through the shielding (figure 2)[11]. The unit comprises three filters, rated at 425m^3/h (250fcm) each, one in use with two on permanent standby.

The rectangular filters are fitted with circular end pieces sealed by plugs which engage with corresponding plugs in the filter cell ducts. After sealing by manual lever, duct and filter plugs are engaged by rotation and then by further rotation are released so that both can be withdrawn to a parking position. Air is then free to pass through the filter.

For filter removal the filter and duct plugs are re-located, the former containing radioactive particulate within the filter and the latter isolating the filter cell from the inlet and outlet ducts. A high standard

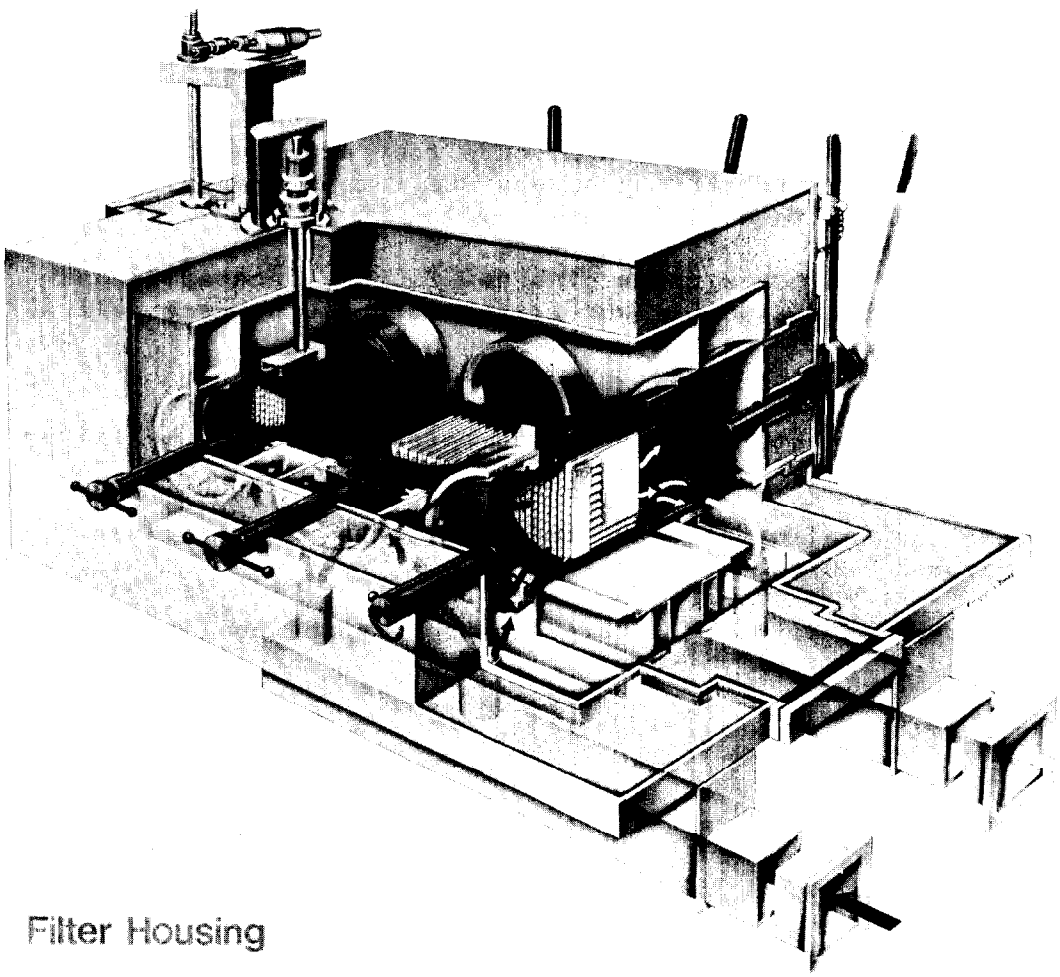

FIGURE 2
MANUALLY OPERATED SHIELDED FILTER CHANGE SYSTEM

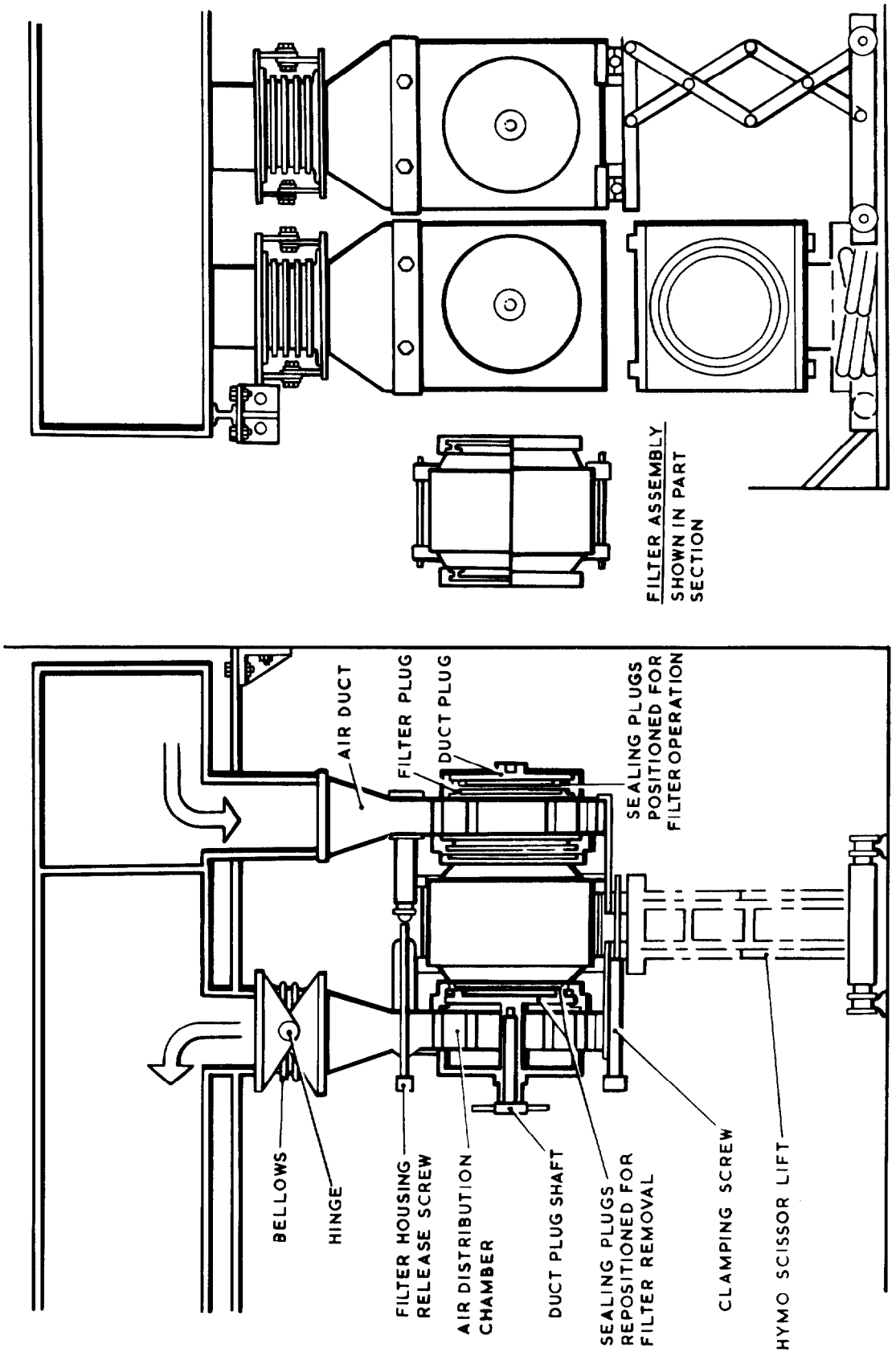

FIGURE 3
HIGH α LOW $\beta\gamma$ FILTER INSTALLATION

of containment can thus be obtained. Further, the use of both inlet and outlet sealing faces ensures a pressure differential between the cell and filter/ducting which avoids by-passing of the filter, irrespective of the condition of the seal faces.

A similar principle has been applied to unshielded systems, handling 1700m^3/h filters, to avoid the conventional bagging procedures and to provide good isolation during filter changes. A prototype unit is illustrated in figure 3 and an installation rated at 51,000m^3/h is being manufactured.

4.2 Storage or Disposal

The volume reduction of filters for retrievable storage or disposal is patently beneficial. Compression techniques such as baling are being evaluated elsewhere[12][13] but the handling and contamination problems can be quite formidable, and two alternatives which promise fewer remote handling problems are being studied at Harwell.

Firstly, for conventional metal-cased dry-sealed units, techniques based upon dismantling are being examined. Cases of riveted or bolted construction can be opened using power tools but their use is inconvenient and time-consuming and only suited for low levels of radioactivity. To facilitate rapid dismantling by either direct or remote handling, a method of construction using proprietary quick-release fasteners has been developed in conjunction with Vokes Ltd. A prototype filter is illustrated in figure 4. The filter efficiency is unimpaired by this method of construction and in-service testing of prototypes is planned. As an alternative, the use of carefully positioned, easily sheared rivets is being examined for the 425m^3/h units used with the shielded filter change system described previously.

In the simplest case, if the filter pack can be removed by hand, it can be readily processed without heavy engineering equipment. Recycle of the case appears feasible.

At higher levels of radioactivity, frogsuit or glove box manipulations may be restricted or shielded operations required, and for these situations mechanical removal of the paper is being developed[14].

The technique is illustrated in figure 5. This involves removing one side of the case and the associated wadding to expose one edge of the pleated pack of glass fibre paper. The exposed edge is located in a driven spool which withdraws the paper, forming a tightly coiled roll which is easily handled even when removed from the spool. Spacers are separated during coiling and collected in trays on both sides of the machine. The separated fractions can be treated as required. Plutonium recovery from the paper is possible and it appears that the glass fibre and aluminium can readily be compacted or melted.

Using a laboratory model or the prototype machine shown in figure 6, over 20 inactive or slightly contaminated filters from installations at Harwell have been treated. The machines were installed in a PVC tent to monitor airborne contamination and this has proved to be very low. Some

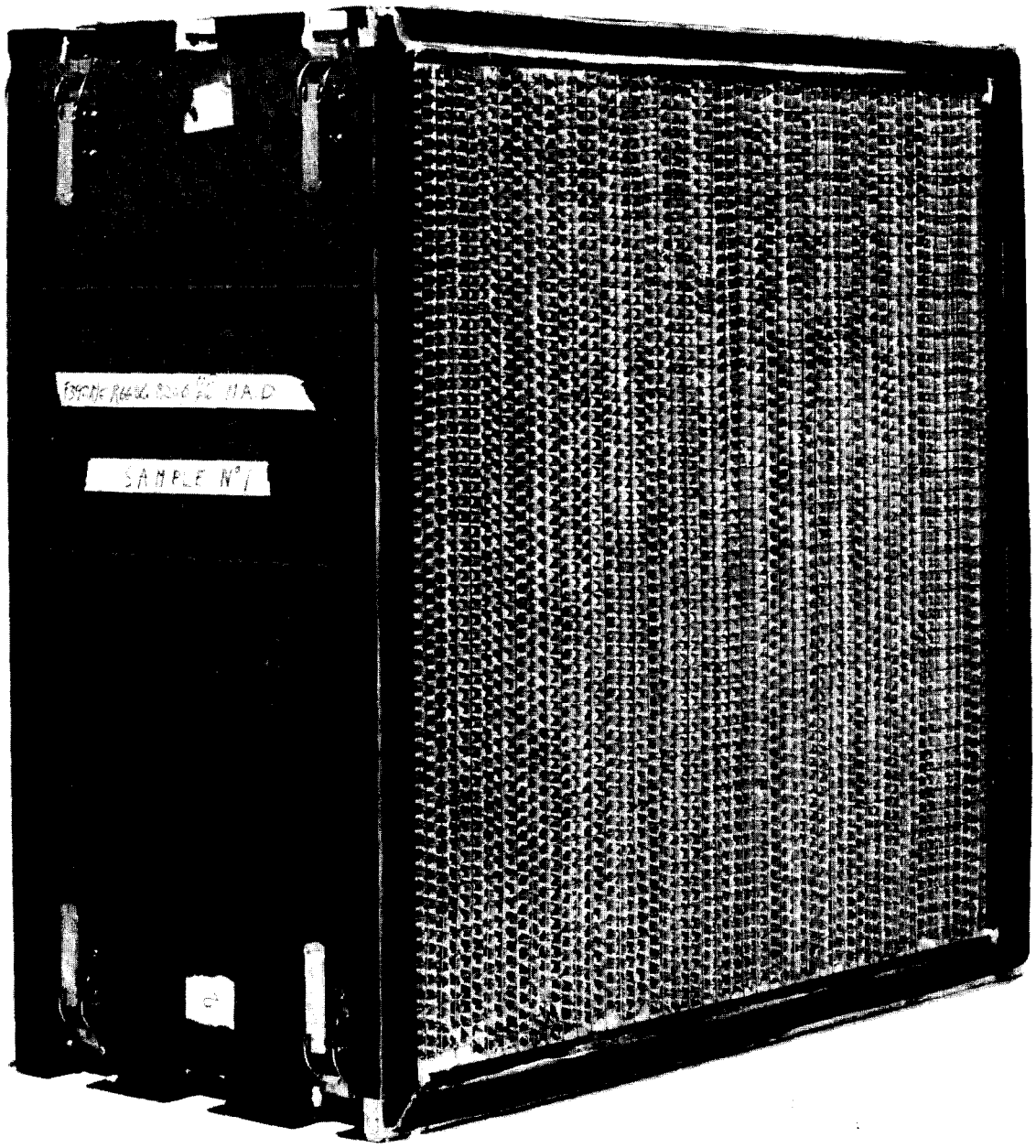

FIGURE 4
MODIFIED HEPA FILTER

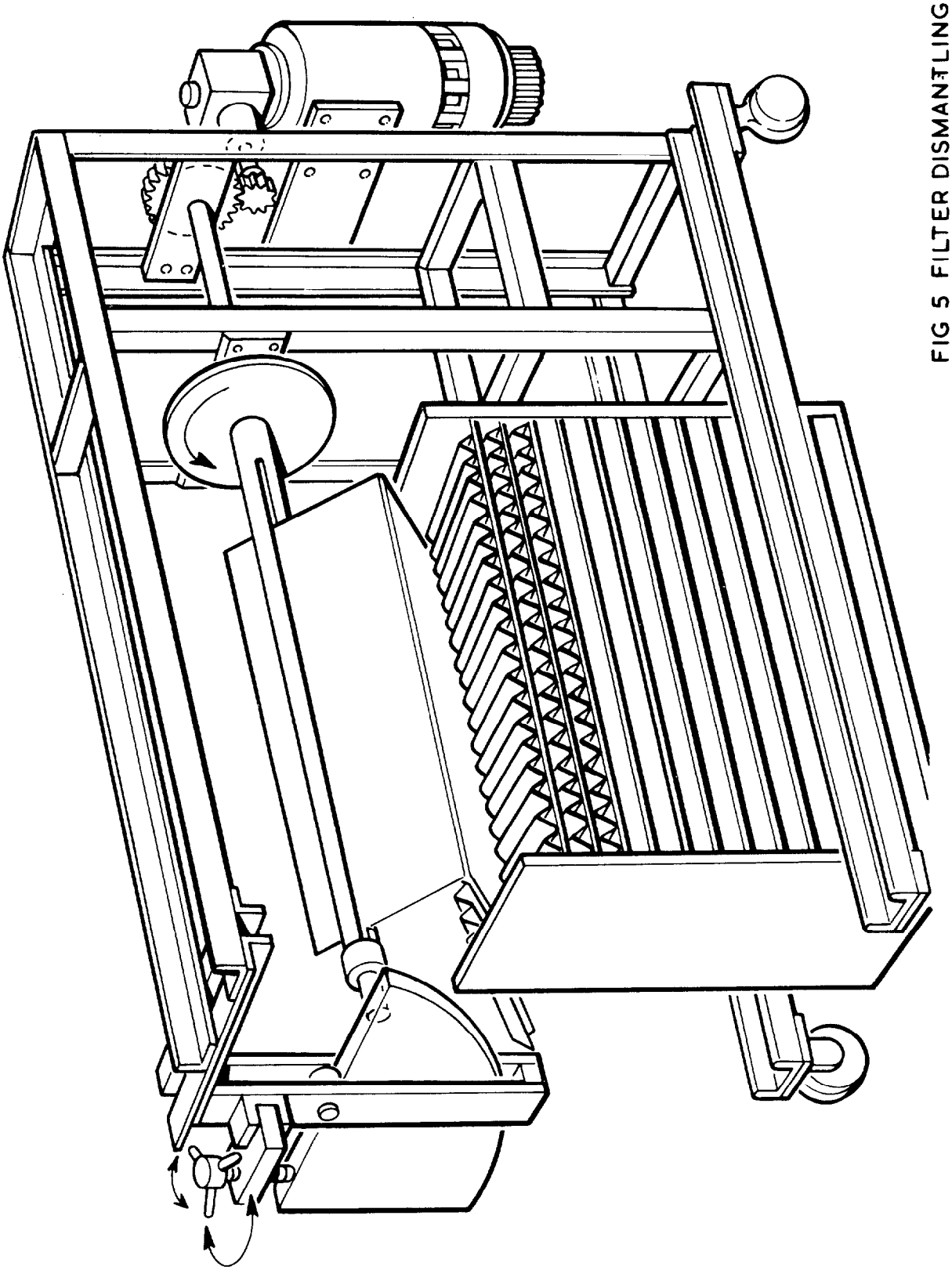

FIG 5 FILTER DISMANTLING MACHINE

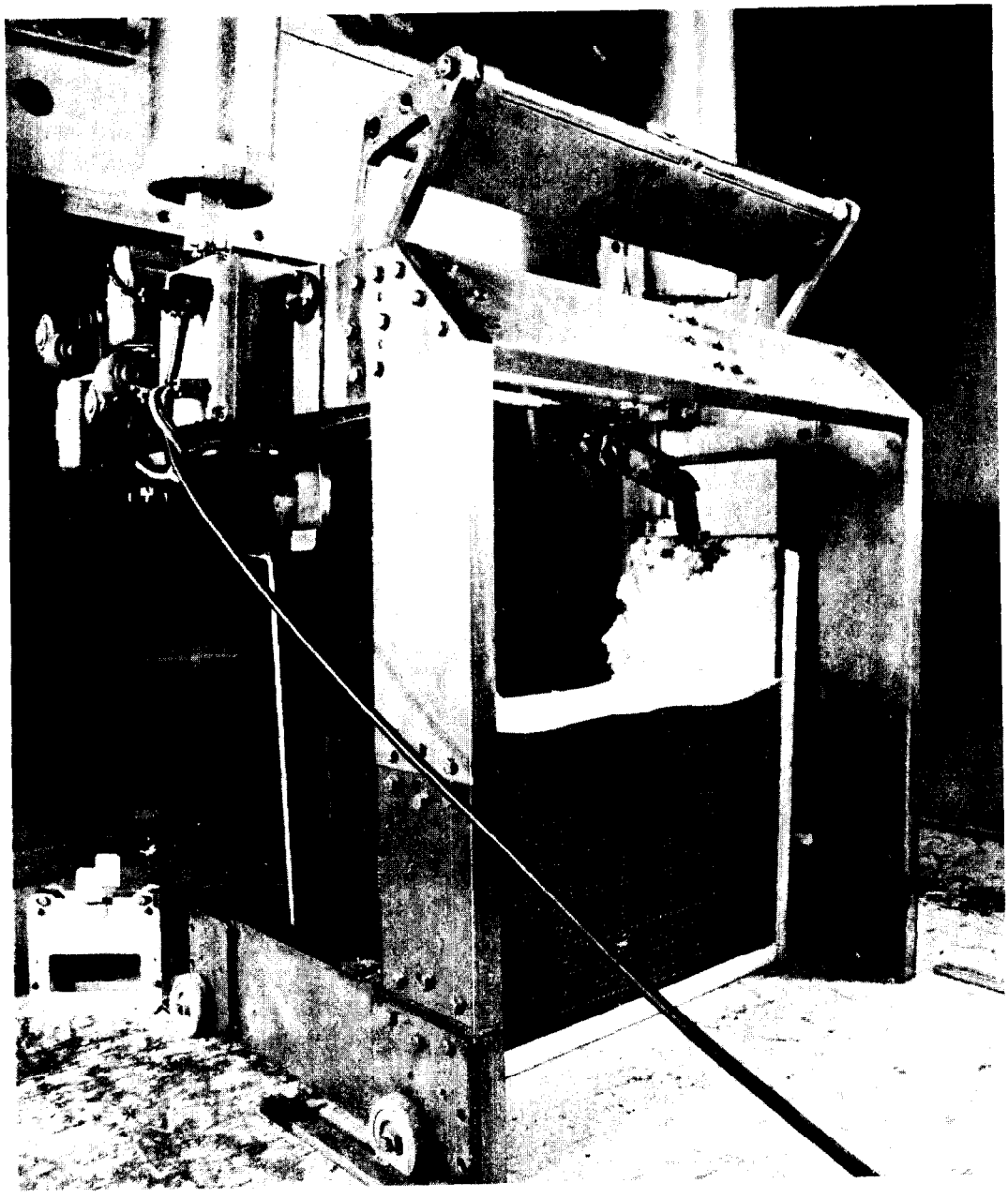

FIGURE 6
PROTOTYPE DISMANTLING MACHINE

surface contamination, in the form of agglomerated dust, has been observed but this is not readily dispersed. Used filters in good condition have been processed without difficulty but trouble was experienced with plenum filters from an office building. These were of indeterminate age and were found to be coated with a black deposit, possibly derived from vehicle exhaust, which caused the spacers to adhere very firmly to the filter paper. A prototype machine has also been installed at Dounreay for evaluation under radioactive conditions, and again the success of the technique has been found to depend upon the condition of the filter. In some cases badly corroded aluminium spacers, with the residue adhering to the paper, made coiling difficult, whilst in others the paper tore when coiling tension was applied. These weaknesses appeared to result from exposure to wet nitric acid vapours.

Evidence to date is that the technique is quite satisfactory for filters in reasonable condition. In radioactive service, actions should be taken to prevent the arising of heavily contaminated or badly deteriorated filters, and thus the requirement for easy dismantling is in line with good filter practice.

As a longer-term and perhaps more speculative alternative to dismantling, materials of construction are being examined at Harwell which, whilst satisfying the temperature performance criteria described in section 1, can be reduced in bulk by incineration or pyrolysis[15]. The materials properties specification is quite demanding and a survey of fibrous materials concluded that a replacement for the glass fibre paper was unlikely to be found. However, three promising resins have been identified which can be used with glass fibre reinforcement for the case and spacers. Preliminary costings show, not surprisingly, a considerable increase in the unit cost of filters and a response from potential users will be obtained before further work to fabricate and test prototypes is carried out.

V. Conclusions

An unconventional design and development approach is required for the ventilation and filtration systems of highly radioactive plant, particularly when due attention is given to the handling and storage procedures. Certain aspects of UKAEA work in this field have been reviewed in the paper, and some of these advances, necessary for heavier-duty plants and operations, will inevitably increase the immediate unit cost of installations. This will be balanced to some extent by reductions in the installation size and perhaps by savings in the waste management operations associated with discarded filters. The overall effect on fuel cycle costs will be insignificant but the influence on the acceptability of certain types of reprocessing and fuel fabrication operations could be quite important.

References

1. Sykes, G.H. and Harper, J.A. (1968) I.A.E.A. Symposium on the Treatment of Airborne Radioactive Wastes.

2. Moyer, R.A., Crawford, J.H. and Tatum, R.E. (1974) Proceedings of the 13th A.E.C. Air Cleaning Conference.

3. Williams, J.A. and Jackson, R.F. (1976) Unpublished study.

4. Adley, F.E. and Wisehart, D.E. (1961) Proceedings of the 7th A.E.C. Air Cleaning Conference.

5. Horsley, D.M.C. (A.E.R.E. Harwell), 1978, Unpublished work.

6. Davis, R.J. and Truitt, J. (1971) ORNL-4654.

7. Warner, B.F. (1967) Kerntechnik, 9, 249.

8. Thompson, J.K., Clark, R.C. and Fielding, G.H. (1976), Proceedings of the 14th U.S. E.R.D.A. Air Cleaning Conference.

9. Clark, R.C., Fielding, G.H., and Thompson, J.K. (1976). Proceedings of the Seminar on High Efficiency Aerosol Filtration, Aix-en-Provence, 605.

10. Bristow, H.A.S. and Lilleyman, E. (1976), Ibid, 483.

11. U.K. Patent Application No. 26336/78. Changing and storing of active filters.

12. Mallek, H. (1976). Proceedings of the Seminar on High Efficiency Aerosol Filtration, Aix-en-Provence, 495.

13. Sinhuber, D., Stiehl, H.H., and Schroth, W. (1976). Ibid 503.

14. Powell, R.M. (A.E.R.E. Harwell), 1978, Private Communication.

15. Macphail, I. (A.E.R.E. Harwell), 1978, Private Communication.

DISCUSSION

LOO: How will the robot used for filter changeout be maintained? I take it that the robot will be highly contaminated after a few filter changeouts in a real operating condition.

DYMENT: The robot is designed to work in the contaminated atmosphere, although it's the filters, themselves, which bear the vast quantity of the contamination that presents an external hazard. Maintenance will be carried out in an active servicing area which is shielded from the external radiation hazard in the filter cell. The robot would normally not be in the filter cell. It can be maintained there by a staff who can go into the active area without very much in the way of external radiation. The whole concept is to be as reliable as possible, but, of course, it is accepted that nothing is 100% reliable these days.

ELIMINATION OF NO_x BY SELECTIVE REDUCTION WITH NH_3

A. Bruggeman, L. Meynendonckx, W.R.A. Goossens
S.C.K./C.E.N., Mol, Belgium

Abstract

In nuclear reprocessing plants the nitrogen oxides generated during the dissolution of the fuel are only partially removed in the primary off-gas treatments. Further reduction to the ppm level is necessary as a preliminary step to the cryogenic retention and separation of the noble gases. If simultaneous oxygen removal is not required, selective reduction of NO (and NO_2) to N_2 and H_2O by NH_3 is a preferable method.

The feasibility of this method was investigated on a laboratory scale at atmospheric pressure. Since excess NH_3 has to be destroyed to get a suitable method, not only the catalytic NO reduction by NH_3 in air was studied, but also the catalytic destruction of NH_3 by the oxygen of the air. Hydrogen mordenite was used as catalyst in a packed bed with an internal diameter of 4.15 cm. At temperatures between 350 and 500 °C, NH_3 showed to react preferentially with NO rather than with oxygen. To drop the NO inlet concentration (up to 5,000 ppm v/v in air) to less than 1 ppm v/v at the reactor outlet, a residence time as low as 0.2 s was sufficient when the NH_3 inlet concentration was at least 1.5 times the NO influent concentration. Hence, the NH_3 oxidation in air being slower than the NO reduction by NH_3, the design of the catalytic reactor has to be based on the NH_3 oxidation rate. The experimental study proved that the NH_3 oxidation is a pseudo first order reaction with an Arrhenius activation energy of $2.4.10^5$ J mol^{-1}.

Although some physical decrepitation of the catalyst occurred, the catalytic activity was not observed to decrease during the experiments. No poisoning of the catalyst could be demonstrated when iodine was added to the process stream. In the absence of O_2 however, the reaction between NO and NH_3 slowed down extremely.

Based on these laboratory results a pilot denitro-unit has been designed and constructed as part of an integrated reprocessing off-gas purification test loop. The working pressure of this unit is 8.10^5 Pa, the flow rate 25 m^3 h^{-1} and the maximum concentration 1 % v/v. Demonstration tests with this pilot unit are planned for the second half of 1978.

I. Introduction

In nuclear reprocessing plants the dissolver off-gas contains rather large amounts of nitrogen oxides generated during the dissolution of the fuel in nitric acid. Provided oxygen is present in excess these nitrogen oxides are partially removed in the wet primary off-gas treatments. Complete elimination is precluded due to the slow oxidation of nitric oxide at low concentrations and its reiterative formation from the reaction of nitrogen dioxide with water. The residual nitric oxide content of the off-gas is expected to be of the order of 0.1 to 1 % v/v.

If cryogenic processes are used to trap the noble gases from the off-gas, the residual concentration of nitrogen oxides has to be further reduced to the ppm level, probably by catalytic reduction to nitrogen. In the non selective reduction with hydrogen, where oxygen reacts first and the excess hydrogen is used for the reduction of nitric oxide, the high oxygen concentration consumes large quantities of hydrogen and excessive capacities of heat exchange are required. If simultaneous oxygen removal is not necessary the selective reduction of nitric oxide to nitrogen is the preferable method for economical as well as for safety reasons.

With proper temperature control and when ammonia is used as the reductant selective catalytic reduction of nitric oxide in the presence of oxygen is possible.[1] In this case the reaction between NH_3 and NO in air has to be faster than the oxidation of NH_3 by the oxygen of the air. The latter reaction however should preferably still be fast enough since excess NH_3 has to be destroyed. Thomas and Pence have reported favourable performances with hydrogen mordenite, an acid resistant molecular sieve, as a catalyst.[2,3] Recently an evaluation of this method was published.[4]

II. Laboratory experiments and conclusions

Experimental Set Up

The laboratory loop built to investigate the feasibility of the elimination of NO in air by selective reduction with NH_3 at atmospheric pressure is schematically shown in Figure 1. The feeding part comprised pressure regulators, rotameters and regulating valves for the carrier gas, NO, NH_3 and interfering gas. An iodine generator made it possible to add continuously 1 g I_2 per hour to the carrier gas. For this purpose a smal flow of 0.027 m^3 (at 20 °C and 1 bar) h^{-1} N_2 was almost saturated with I_2 by passing it through a first column filled with I_2 crystals and thermostated at 61 °C. Further stabilization of the I_2 flow rate was obtained by crystallization and sublimation in a second column thermostated at 55 °C. To prevent crystallization the I_2 containing N_2 flow was then further heated before being added to the carrier gas.

If not otherwise stated, purified plant air with a water content of about 0.5 % v/v (atmospheric dew point of -1 °C) was used as the carrier gas at flow rates of 1 to 5 m^3 (at 20 °C and 1 bar) h^{-1}. The nitric oxide concentrations were of the order of 0.1 to 0.5 % v/v. The nitric oxide used had a purity of 99.85 % but some oxidation during the addition to the carrier air was observed.

Before entering the reactor the air - NO(NO_x) mixture was preheated to the desired operating temperature in an externally heated electric preheater. Behind the preheater and close to the reactor NH_3 was added to this gas mixture. A cylindrical stainless steel reactor with an inner diameter of 41.5 mm and a height of 300 mm contained the catalyst. The reactor walls were also heated to the operating temperature. After leaving the reactor the hot gases were cooled consecutively by air and water.

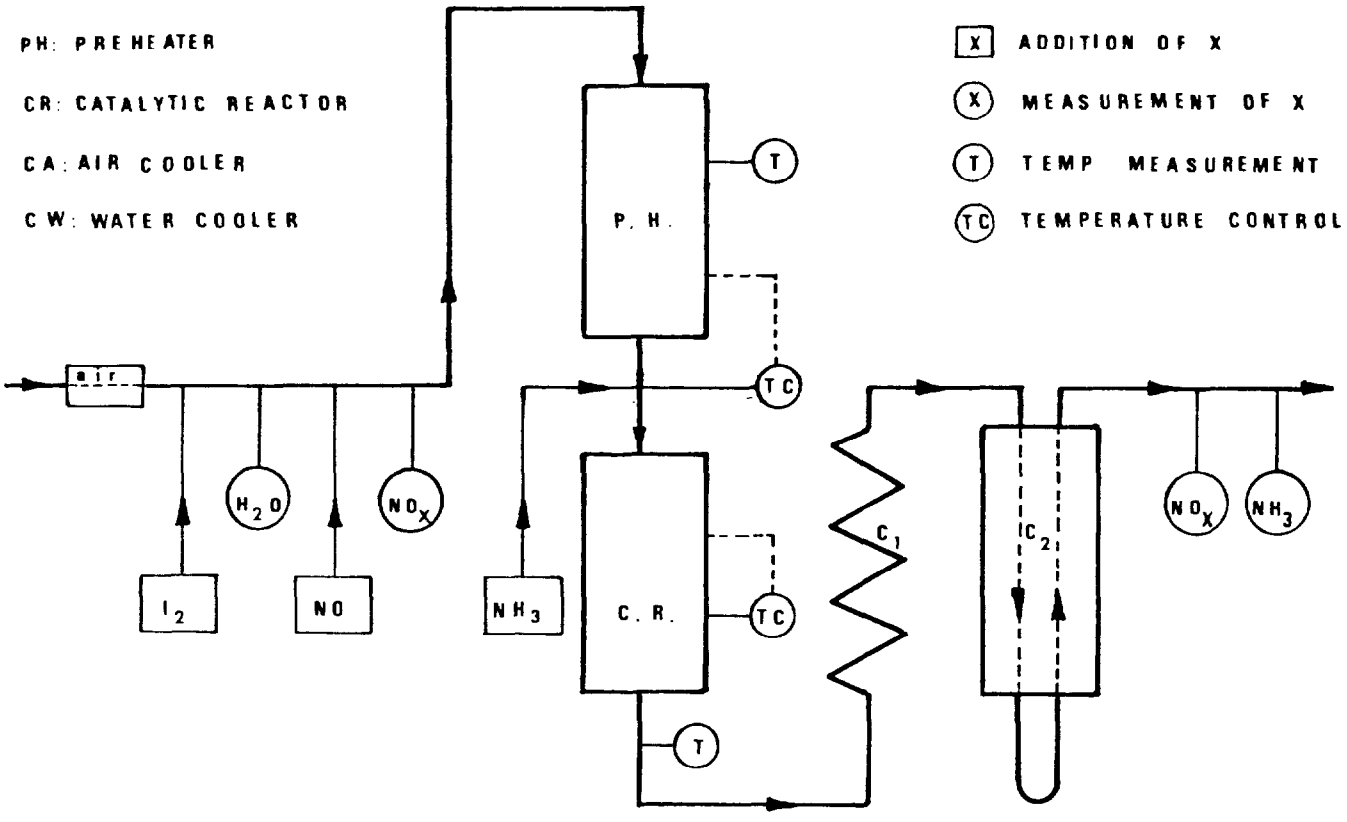

FIGURE 1
SIMPLIFIED DIAGRAM OF EXPERIMENTAL LABORATORY APPARATUS

Sample ports were provided before the preheater and behind the water cooler. Some samples were also taken between preheater and reactor. Influent and effluent NO_x concentrations were measured with a calibrated chemiluminescence monitor (calibration range 0.01 to 5 ppm v/v) after appropriate dilution, if required. After absorption in 0.01 N H_2SO_4 the effluent NH_3 concentrations were determined colorimetrically by the indophenol method.(5) For large NH_3 concentrations and when no NO_2 interferences were present, back titration with 0.01 N NaOH gave comparable results.

Catalyst

Fe_2O_3-Cr_2O_3-C, Pd on Al_2O_3, Al_2O_3 and sodium mordenite catalysts were tested, but selective reduction of NO to the ppm level was only achieved with synthetic hydrogen mordenite. All the experiments reported below were carried out with 1.6 mm extrudates of hydrogen mordenite.

For the first experiments hydrogen mordenite was prepared by treating the available commercial sodium mordenite with HCl 2 M. After an exchange period of 2 hours the hydrogen mordenite was washed with distilled water until no more Cl^- ions could be detected in the wash water. After drying at 110 °C, further drying was carried out dynamically in the reactor. A second amount was prepared in nearly the same way but instead of HCl 2 M a warm 2 M solution of NH_4Cl was

used. After washing and drying this catalyst was loaded into the reactor and NH_3 was further expelled by heating. For the last experiments commercial hydrogen mordenite was used (Zeolon 900 H, manufactured by Norton Chemical Company). Some physical and chemical characteristics of this material, as given by the manufacturer are represented in Table I.[6]

Table I. Physical and chemical characteristics of Zeolon 900 H[6]

Chemical composition	$H_8 Al_8 Si_{40} O_{96} . 24 H_2O$
Effective pore diameter	0.8 - 0.9 nm
Surface area	450 $m^2 g^{-1}$
Physical form	extrudates 1.6 mm diam.
Equivalent particle diameter	2.8 mm
Bulk packing density	720 kg m^{-3}
Static H_2O capacity	11 wt %

Results and discussion

Selective reduction of NO with NH_3. The selective reduction of NO in air with NH_3 over hydrogen mordenite was investigated at temperatures between 300 and 500 °C, at space times between 0.2 and 1 s and at inlet NH_3 concentrations between 1 and 2 times the inlet NO concentration. As stated earlier the inlet NO concentration was varied between 1000 and 5000 ppm v/v.

In not any experiment a difference in catalytic activity between the 3 badges of hydrogen mordenite could be observed. The NO conversion increased with increasing NH_3/NO inlet ratio until the latter value was about 1.5. When the added NH_3 concentration was 1.5 times the inlet NO concentration or higher and when the reactor temperature was 400 °C or higher, the effluent NO_x concentration was always measured to be smaller than 1 ppm v/v, whereas the effluent NH_3 concentration decreased with decreasing excess of NH_3 used and with increasing temperature. It could thus be concluded that with hydrogen mordenite as a catalyst and under the conditions mentionned the reaction between NH_3 and NO in air is much faster than the oxidation of NH_3 by the oxygen of the air.

Oxidation of NH_3 in air. As not only NO_x but preferably also the NH_3 added has to be eliminated to the ppm level over the same hydrogen mordenite catalyst, the oxidation rate of the excess NH_3 determines the required reactor dimensions. The oxidation of NH_3 in air was thus studied in the conditions to be used for the selective reduction of NO with NH_3. Therefore the breakthrough of NH_3 was measured as a function of the inlet NH_3 concentration.

As shown for two series of experiments at a superficial velocity of 80 cm s^{-1} and a temperature of respectively 350 °C and 400 °C in Figure 2, the data obtained in these experiments indicated a pseudo first-order irreversible reaction :

$$r = k_1 C_{NH_3} \quad (1)$$

where r is the reaction rate, C_{NH_3} the concentration of NH_3 and k_1 the apparent reaction rate constant.

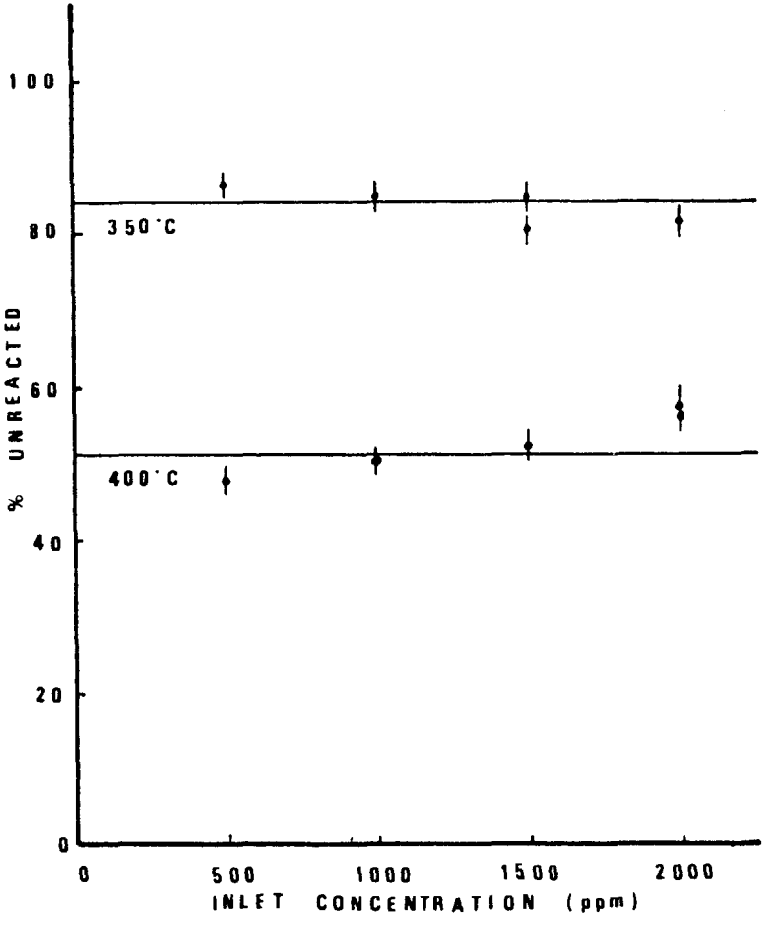

FIGURE 2
REACTION OF NH_3 IN AIR ON HYDROGEN MORDENITE : UNREACTED NH_3 VS INLET CONCENTRATION

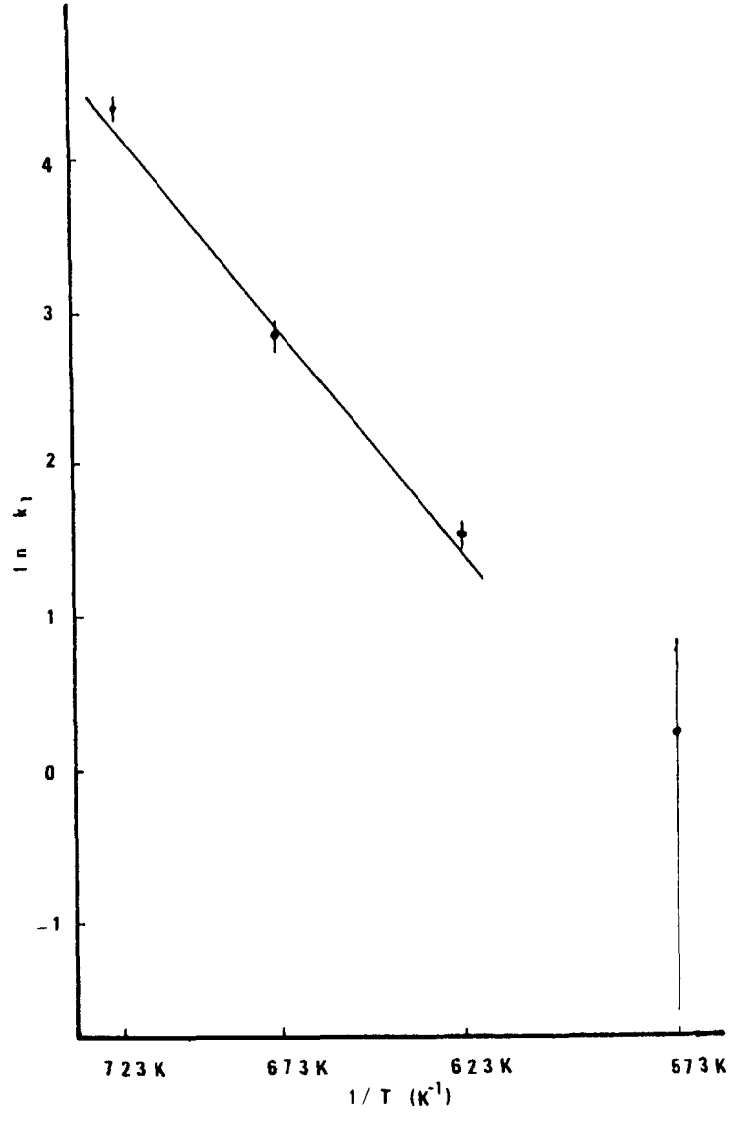

FIGURE 3
REACTION OF NH_3 IN AIR ON HYDROGEN MORDENITE : TEMPERATURE DEPENDENCE OF THE REACTION RATE

Especially at higher temperature the apparent reaction rate constant was observed to decrease with decreasing linear velocity. A linear regression analysis yielded :

$k_1 \sim G^{0.54}$ at 450 °C, $k_1 \sim G^{0.43}$ at 400 °C and $k_1 \sim G^{0.21}$ at 350 °C, where G is the total flow rate. This behaviour suggested that the reaction rate was partially controlled by extragranular material transport, but even at 450 °C and 20 cm s^{-1} a material balance for the hydrodynamic boundary layer around the catalyst pellets yielded a concentration gradient of only 1.2 %. In any case the expression for the reaction rate mentionned above is only an empirical first approximation.

Neglecting their variation with flow rate the apparent reaction rate constants (in m^3 per hour and per kg catalyst) at each temperature were averaged. The natural logarithms of these mean values are plotted in Figure 3. When one does not take into account the values at 300 °C, where the experimental failures are too large, a linear regression according to the equation :

$$\ln k_1 = \ln K_A - \frac{E_A}{RT} , \qquad (2)$$

where R is the universal gas constant, yields an Arrhenius activation energy, E_A, of 2.4 10^5 J mol^{-1}.

As a first approximation the weight W (kg) of 1.6 mm extrudates of hydrogen mordenite needed to obtain under atmospheric pressure and in air with a water content of 0.5 % v/v a given conversion of NH_3 at a given temperature can thus be calculated from the well known expression for a first-order irreversible reaction in a fixed bed reactor with plug flow :

$$W = \frac{G}{k_1} \ln \frac{C_i}{C_f} , \qquad (3)$$

where C_i and C_f are the inlet and outlet concentrations of NH_3. The value of k_1 at the temperature T can be found from Figure 3.

Deterioration of the catalyst. With a new catalyst load the pressure drop over the catalyst bed increased during the first experiments but stabilized later on. When the reactor was unloaded some physical decrepitation of the catalyst was visible and the sieve was clearly more white than before. Porosity measurements revealed that both unused and used catalyst pellets contained practically no meso- or macropores and that the total microporous volume was almost unchanged(7). The fine powder formed was insoluble in water or acids.

An analogous decripitation of Norton Zeolon was observed when it was refluxed in HNO_3 4 M. In this last case X-ray powder patterns of the untreated extrudate, of the powder removed by the refluxing and of the extrudates that had been refluxed indicated that in no case any structural changes had taken place(8).

During the experiments the catalytic activity was not observed to decrease. After one month working at 450 °C the hydrogen mordenite catalyst still performed well.

Interference by iodine. Although I_2 will normally be eliminated from the dissolver off-gas before the NO_x abatement, the influence of I_2 on the selective reduction of NO in air with NH_3 over hydrogen mordenite was controlled by adding 0.33 g m^{-3} (at 20 °C and 1 bar) of I_2 to the proces gas during 18 days. Even with such large amounts of I_2 only a very small increase of the effluent NO_x and NH_3 concentrations was observed, as represented in Figure 4.

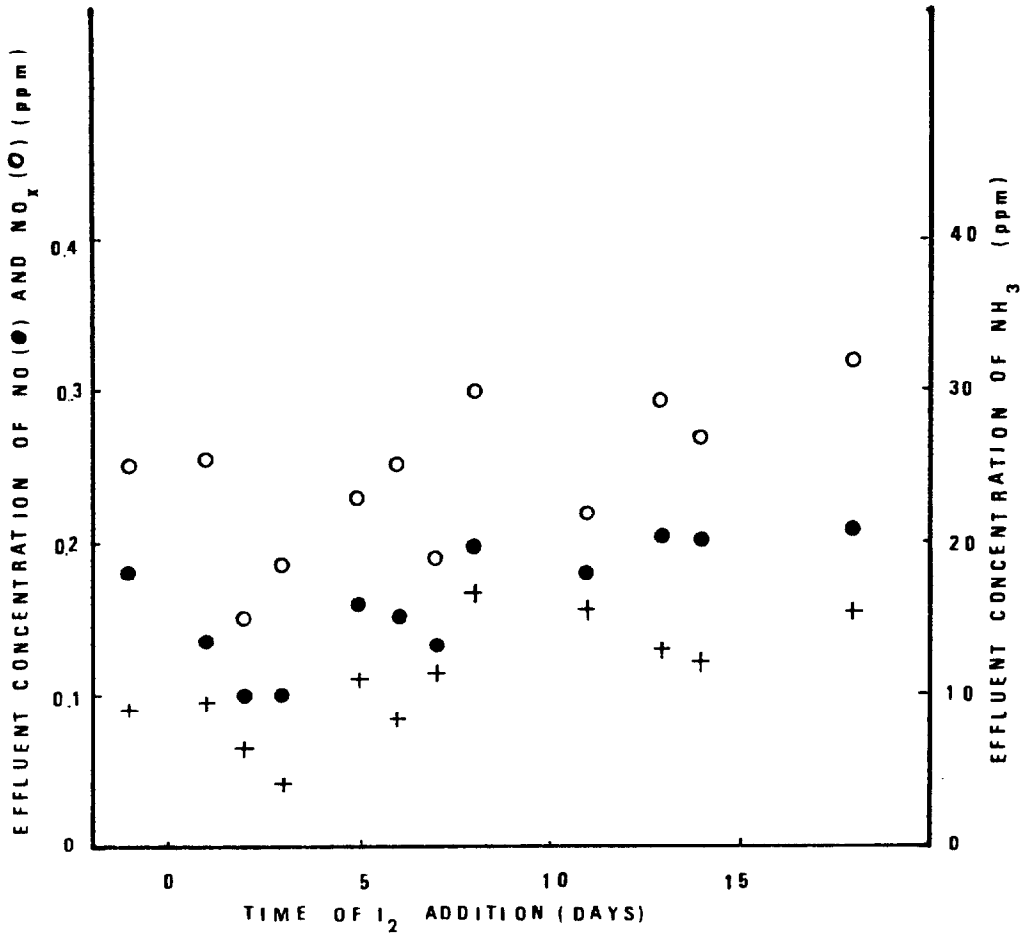

FIGURE 4
SELECTIVE REDUCTION OF NO IN AIR WITH NH_3 :
IODINE INTERFERENCE

Influence of oxygen. The influence of O_2 on the reaction of NO with NH_3 was not studied in detail but a few experiments were carried out with dry N_2, wet N_2 and a mixture of 80 % v/v dry N_2 and 20 % v/v dry O_2 as the carrier gas. The results obtained with the mixture of N_2 and O_2 corresponded completely with the air results but in the absence of O_2 no reduction of NO by NH_3 could be demonstrated. The rate of the reaction of NO with NH_3 over hydrogen mordenite is thus strongly decreased by the absence of O_2.

III. Design and construction of a pilot denitro-unit

Object

Based on the laboratory results discussed above, a pilot denitro-unit has been designed and constructed as part of an integrated reprocessing off-gas purification test loop. After fuel dissolution, nitric acid recovery, aerosol and iodine capture in the wet section of the integrated gas purification loop "Gaston", the off-gas is further purified in the conditioning section before being sent to the cryogenic distillation unit for the separation of krypton and xenon. The object of the denitro installation, which is part of the conditioning section, is the selective elimination beyond the ppm level of the nitrogen oxides from the oxygen containing off-gas, in which they are present for maximum 1 %.

Description

The denitro-unit is shown in Figure 5 and the flow sheet is represented in Figure 6. After compression to 8.10^5 Pa and after passing a cooler condensor and a demister the off-gas with a flow rate of about 25 m^3 (at 20 °C and 1 bar) h^{-1} and with a maximum NO_x concentration of 1 % v/v is first heated from about 25 °C to about 275 °C

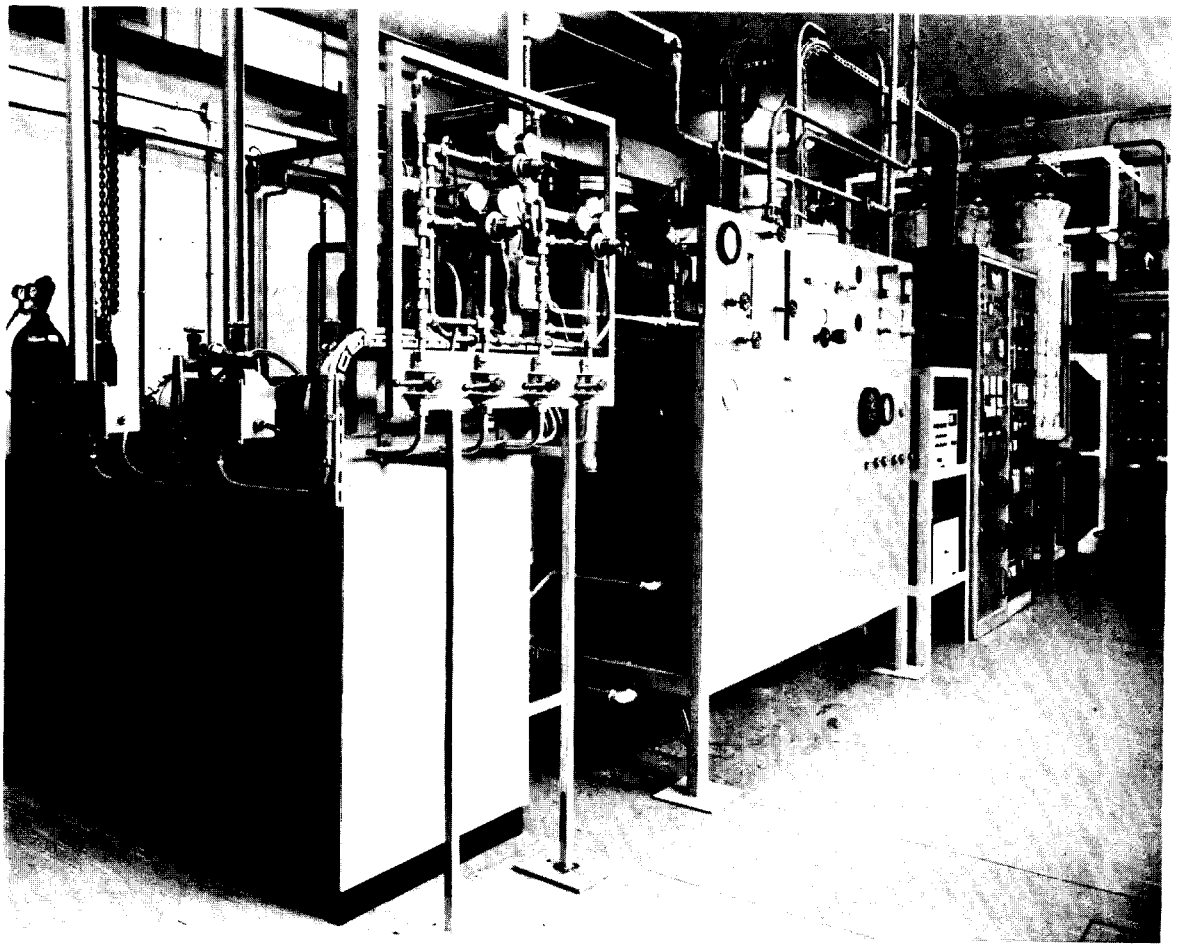

FIGURE 5
VIEW OF THE DENITRO INSTALLATION

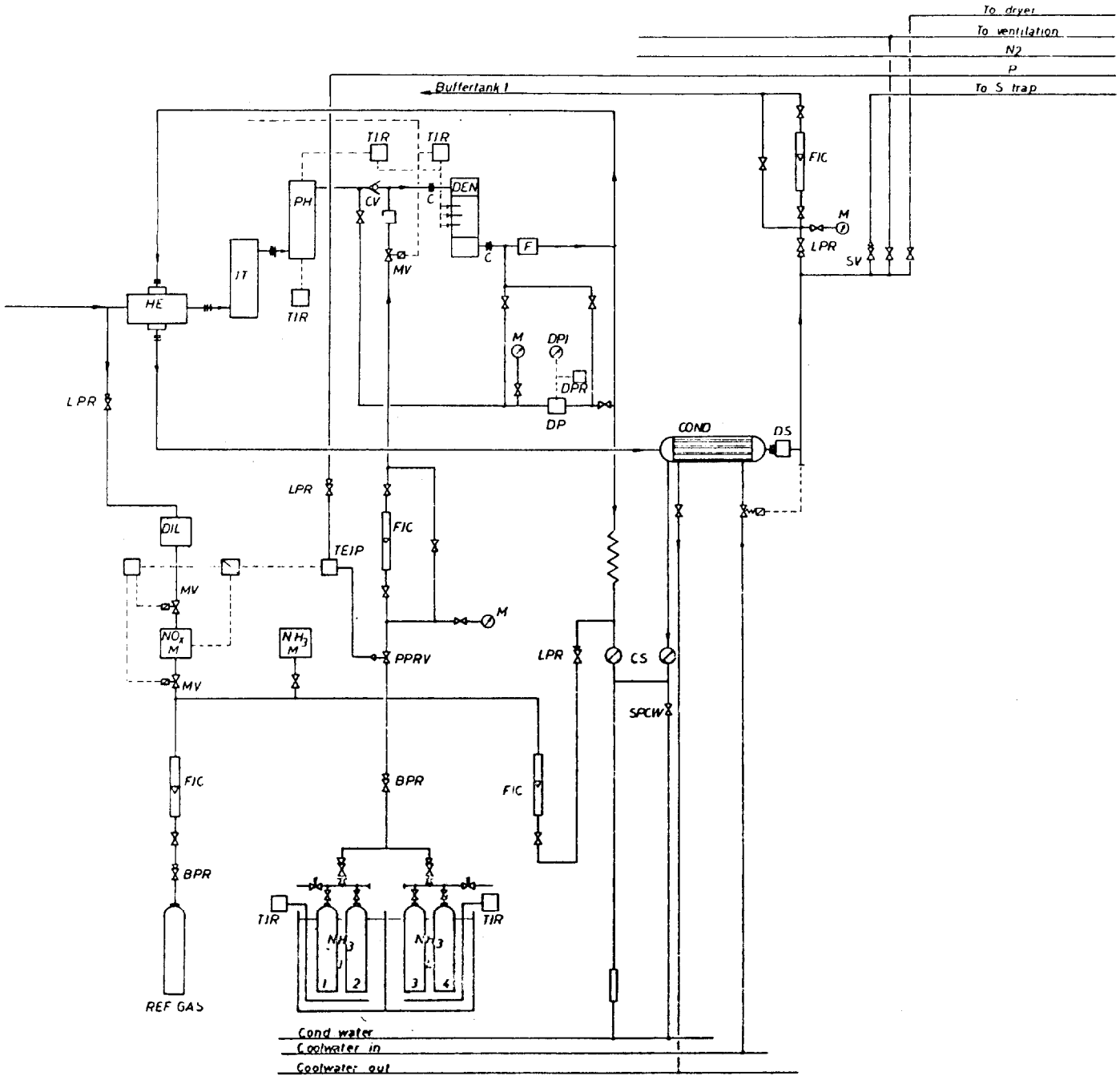

FIGURE 6
FLOW SHEET OF THE DENITRO INSTALLATION

by heat recuperation in a compact helix type heat exchanger. The warm gas passes through a final iodine trap filled with silver impregnated molecular sieves and is then further heated in an electric preheater.

After the preheater and just before the reactor NH_3 gas is added to the off-gas in an amount of 1.5 times the initial NO_X concentration. The addition of NH_3 is regulated by a valve, actuated in function of the NO_X concentration measured at the inlet of the installation. A semi-automatic manifold provides a continuous addition of NH_3. The

high pressure resisting NH_3 bottles are kept at a pressure of 15.5 . 10^5 Pa, by heating them in a thermostated water bath at 40 °C.

The hot process gas mixed with NH_3 enters the denitro reactor which is filled with the hydrogen mordenite catalyst Zeolon 900 H, 1.6 mm extrudates. Here NO_x and the excess NH_3 have to be reduced to less than 1 ppm by conversion to N_2 and H_2O. The working temperature of the reactor is chosen at 500 °C. To reduce heat losses from the reactor, the reactor wall is also heated at 500 °C. The temperature in the reactor is measured and in spite of the varying NO_x (and thus also NH_3) concentration, this temperature is kept within a narrow range by a temperature regulator, which drives the preheater. To avoid the formation of dangerous NH_4NO_3 at too low temperatures and damage to the installation at too high temperatures, the NO_x containing off-gas from the wet section is automatically replaced by plant air when the reactor temperature is lower than 300 °C or when it rises above 600 °C.

A filter which collects dust particles larger than 10 μm has been placed after the reactor. A pressure drop measurement is possible over the reactor, over the filter and over both. After the dust filter a sampling system for NH_3 and NO_x determination is provided. The filtered hot gas leaving the denitro reactor is cooled from 500 °C to about 250 °C in the previously mentioned heat exchanger and the heat is recuperated by the incoming gas. In the water cooler condensor the gas is further cooled to about 20 °C. The cooling feed water is automatically adjusted by a regulation valve which is actuated in function of the temperature of the gas leaving the cooler condensor. The condens water can be sampled.

Finally the proces gas passes through a drop separator and can be sent either to a drying installation or to the vent. It is also possible to recycle a part of the gas over a pressure regulator and a rotameter before the compressor to dilute the incoming gas or to reduce the consumption of compressed air when the denitro installation works as a separate unit. A safety relief valve is placed in parallel on the exit line and will open at a pressure of 10.5 . 10^5 Pa, releasing the gas to the ventilation.

The mechanical and electrical construction of the pilot unit is completed and demonstration tests are planned for the following months.

IV. Conclusion

Laboratory experiments have confirmed the feasibility of eliminating NO from air beyond the ppm level by adding NH_3 over a hydrogen mordenite catalyst. At atmospheric pressure and with air (water content 0.5 % v/v) as a carrier gas selective catalytic reduction of NO to N_2 is easily achieved at temperatures up to 500 °C. Under the same conditions dimensioning of the reactor for destruction of the excess NH_3 by the O_2 of the air is made possible. The activity of the catalyst remains rather constant even when large concentrations of I_2 are present. On the basis of the laboratory results a pilot installation has been designed and constructed which will demonstrate the process in an integrated gas purification loop at a pressure of 8.10^5 Pa during the next months.

Acknowledgements

The authors are very indebted to Dr. D.T. Pence of Science Applications Inc. and to Dr. L.H. Baetslé and Ir. G. Collard, for helpful discussions. The technical assistance of D. Smets, J. Van Dooren, E. Ooms and J. Boons was greatly appreciated.

References

1. H.C. Andersen, W.J. Green and D.R. Steele,
"Catalytic treatment of nitric acid plant tail gas"
Ind. Eng. Chem. vol. 53, no. 3, pp 199 (1961).

2. D.T. Pence and T.R. Thomas,
"NO_x abatement at nuclear processing plants",
Proceedings of the Second AEC Environmental Protection Conference,
WASH-1332(74) (April 1974).

3. T.R. Thomas and D.T. Pence,
"Reduction of NO_x with ammonia over zeolite catalyst",
Proceedings of the 67th Annual Meeting of the Air Pollution Control Association, paper no. 75-258 (June 1974).

4. T.R. Thomas and D.H. Munger,
"An evaluation of NO_x abatement by NH_3 over hydrogen mordenite for nuclear fuel reprocessing plants",
ICP-1133 (January 1978).

5. Z. Marczenko,
"Spectrophotometric determination of elements" pp. 392,
Ellis Horwood Ltd, Chichester (1976).

6. Norton Chemical Process Products Division,
"Zeolon acid resistant molecular sieves",
Bulletin Z-50.

7. P. Henrion,
S.C.K./C.E.N., personnal communication.

8. L.C. Lewis
"Evaluation of adsorbents for purification of noble gases in dissolver off-gas"
IN-1402 (July 1970).

DISCUSSION

T. R. THOMAS: What was the dewpoint of your test gas and what was the effluent concentration of ammonia from your bed?

BRUGGEMAN: The dewpoint of the test gas was $-1^{\circ}C$, corresponding to about 0.5 volume-% of water. The concentration of ammonia was dependent on the working conditions, but the final working conditions were such that the ammonia concentration was below one part per million at the outlet of the reactor. These conditions do not seem difficult to fulfill, at least in the range of working conditions we have tested.

T. R. THOMAS: That agrees very well with our work. But, when the gas streams are wet, excess ammonia seems to come roaring through.

BRUGGEMAN: We didn't do experiments with wet gases. We used dry gases and then very dry gases and the results didn't change.

T. R. THOMAS: You mean you didn't get ammonia coming through with the wet gas?

BRUGGEMAN: No. We used gases that were drier. We used mixtures of dry oxygen and dry nitrogen and we used air with a dewpoint of $-1^{o}C$. We didn't use gases with a higher dewpoint.

T. R. THOMAS: What was the temperature gradient in your bed and were you able to measure the inlet-outlet temperature?

BRUGGEMAN: In the laboratory experiments, we had no means to measure the temperature gradient. We will have them in the pilot unit.

T. R. THOMAS: Is your rate constant based on the outlet or inlet temperature of the bed? I always had a gradient of $40-50^{o}$ across the bed when I ran my tests.

BRUGGEMAN: In our low NO and NH_3 inlet experiments, the temperature at the inlet and the outlet was about the same because we heated the walls of the catalytic reactor to keep it at the same working temperature as the incoming gases from the preheater. At higher concentrations, temperature gradients are hard to avoid.

T. R. THOMAS: Have you looked at NO_2 in this reaction?

BRUGGEMAN: We measured NO_2 but we didn't use NO_2 at the inlet. We always used nitric oxide. We have seen some oxidation of nitric oxide, about 20% in some cases. In the preheater, we had a small reduction. At higher temperatures, we had a reduction of nitrogen dioxide to nitric oxide, so the first oxidation was opposite to the reduction in the preheater. We think that, at most, we had 10% nitrogen dioxide at the inlet of the reactor.

COWAN: Did you check to see if there's any N_2O in the offgas from the reaction of the ammonia and oxides of nitrogen?

BRUGGEMAN: We didn't measure N_2O because we used only a chemiluminescence monitor. The formation of N_2O in this reaction is possible, but we do not expect formation of N_2O at temperatures as high as $500^{o}C$.

T. R. THOMAS: I'd like to make a comment on this topic. We looked at that particular reaction very closely, and, in no case, could we find N_2O when only NO was introduced into the feed gas. It only occurs in the presence of NO_2. There was very little NO_2 from this reaction. When starting with 5000 ppm NO, possibly 10% went to NO_2 but I never saw N_2O when only NO was introduced upstream of the reactor.